Quercetin és chrysin konjugátumok farmakokinetikai kölcsönhatásainak *in vitro* vizsgálata

Doktori (PhD) - értekezés

Dr. Mohos Violetta Karolin

Gyógyszertudományok Doktori Iskola
A gyógyszerterápia optimalizálásának lehetőségei Program

Doktori iskola vezető: **Prof. Dr. Pintér Erika**
Programvezető: **Prof. Dr. Botz Lajos**
Témavezető: **Dr. Poór Miklós**

Pécsi Tudományegyetem
Gyógyszerésztudományi Kar
Gyógyszerhatástani Tanszék
OGYDHT

Pécs, 2021.

Tartalomjegyzék

Rövidítések jegyzéke

4’-OH-diclofenac	4’-hydroxydiclofenac
4-OH-mephenytoin	4-hydroxymephenytoin
6β-OH-testosteron	6β-hydroxytestosteron
6-MP	6-mercaptopurin
AMP	adenozin-monofoszfát
APU	allopurinol
BCRP	breast cancer resistance protein
CHR	chrysin
COMT	catechol-*O*-metil-transzferáz
CYP	citokróm P450
C7G	chrysin-7-glükuronid
C7S	chrysin-7-szulfát
FDA	U.S. Food and Drug Administration
DMSO	dimetil-szulfoxid
G6P	glükóz-6-foszfát
GMP	guanozin-monofoszfát
HPLC	nagyhatékonyságú folyadékkromatográfia
HSA	humán szérum albumin
IMP	inozin-monofoszfát
IR	isorhamnetin
I3G	isorhamnetin-3-glükuronid
Keap1	kelch-like ECH-associated protein 1
QUI	quinidin
MRP	multi-drug-resistance associated protein
NAD^+/NADH	nikotinamid-adenin-dinukleotid
$NADP^+$/NADPH	nikotinamid-adenin-dinukleotid-foszfát
NAP	naproxen
Nrf2	nuclear factor erythroid 2-related factor 2
OAT	szerves anion transzporter
OATP	szerves anionokat transzportáló polipetid
OXI	oxipurinol

PBS	phosphate buffered saline
P-gp	P-glikoprotein
Q	quercetin
Q3’S	quercetin-3’-szulfát
Q3G	quercetin-3-glükuronid
SGLT1	Na^+-függő glükóz transzporter 1
SULF	sulfaphenazol
SULT	szulfotranszferáz
TAM	tamarixetin
TIC	ticlopidin
UGT	uridin-difoszfát glükuronil-transzferáz
WAR	warfarin
XMP	xantozin-monofoszfát
XO	xantin-oxidáz

I. Bevezetés

A chrysin és a quercetin a természetben gyakran előforduló flavonoid aglikonok melyek számos növényben, gyümölcsben és zöldségben előfordulnak, emellett több étrend-kiegészítőben is extrém magas mennyiségben megtalálhatók. Mint a legtöbb flavonoid esetében, a chrysin és a quercetin orális biohasznosulása alacsony, ami a vegyületek alacsony vízoldhatóságával, valamint jelentős preszisztémás eliminációjával magyarázható. A chrysin biotranszformációja során főként szulfát és glükuronid metabolitok, míg a quercetin esetén metil származékok is képződnek. A normál étrenddel a flavonoidok és konjugátumaik együttes plazmakoncentrációja a nmol/L-es skálán mozog, de extrém bevitel esetén akár a több μmol/L-es értéket is elérhetik. A szakirodalom alapján a chrysin és a quercetin számos fehérjével (pl. szérum albumin, biotranszformációs enzimek, transzporterek) képesek kölcsönhatásba lépni. Azonban a metabolitok kapcsán – melyek jellemzően jóval magasabb koncentrációkat érnek el a szisztémás keringésben az anyavegyülethez képest – viszonylag kevés információ áll rendelkezésre. Ezért doktori képzésem során a chrysin és a quercetin fő konjugált metabolitjainak interakcióit vizsgáltam humán szérum albuminnal, valamint citokróm P450 és xantin-oxidáz enzimekkel. Kutatási eredményeink rávilágítanak, hogy nemcsak az aglikonok, de konjugált metabolitjaik is képesek kölcsönhatásba lépni albuminnal és biotranszformációs enzimekkel. Mivel a chrysin és/vagy a quercetin extrém magas bevitele befolyásolhatja az együttesen szedett gyógyszerek farmakokinetikai tulajdonságait, a magas flavonoid tartalmú étrend-kiegészítők gyógyszerekkel történő együttes alkalmazása fokozott elővigyázatosságot igényel.

II. Irodalmi áttekintés

II.1. Humán szérum albumin

A humán szérum albumin (HSA) a keringésben legnagyobb mennyiségben megtalálható plazmaprotein (Yamasaki és mtsai., 2013). A HSA egy 585 aminosavból felépülő, kb. 66,5 kDa móltömegű, nem glikozilált egyláncú polipeptid (***1. ábra***; Yamasaki és mtsai., 2013), amely három szerkezetileg hasonló α-hélix doménből épül fel (I, II, III), melyek további két-két aldoménre (A és B) oszthatók (Carter és Ho, 1994; Curry és mtsai., 1998). A szervezetben a HSA fontos szerepet játszik a plazma onkotikus nyomásának fenntartásában, valamint számos endogén anyag (pl. zsírsavak, aminosavak, epesavak, hormonok, bilirubin és egyes fémionok) megkötéséért és keringésben történő szállításáért is felelős (Kragh-Hansen és mtsai., 2002; Simard és mtsai., 2005; Fanali és mtsai., 2012). A HSA ezen kívül exogén vegyületek (pl. gyógyszerek, toxinok) szállítófehérjéjeként is funkcionál, befolyásolva ezek farmakokinetikai és toxikokinetikai sajátságait és ezáltal egyes gyógyszerek farmakológiai hatásának nagyságát és/vagy időtartamát (Meyer és Guttman, 1968; Jusko és Gretch, 1976; Vallner, 1977; Fanali és mtsai., 2012). Emellett az albumin ún. pszeudo-enzimatikus és antioxidáns tulajdonságokkal is rendelkezik (Fanali és mtsai., 2012). A HSA egy negatív akutfázis fehérje, melynek koncentrációja egyes patológiás állapotokban (pl. daganatos megbetegedések, reumatoid artritisz, iszkémia) csökken (Ritchie és mtsai., 1999; Gupta és Lis, 2010; Sbarouni és mtsai, 2011; Fanali és mtsai., 2012). Ezenkívül a HSA-t a klinikumban számos betegség, pl. hipoalbuminémia, hipovolémia, égési sérülések, sokk, akut respiratórikus distressz szindróma, hemodialízis, akut májelégtelenség és krónikus májbetegségek kezelésére is alkalmazzák (Fanali és mtsai., 2012).

A HSA-on számos kötőhely található, melyek közül a gyógyszerek főként a IIA aldoménen elhelyezkedő Sudlow's Site I (másnéven „Site I" vagy „acidic drug binding site"), valamint a IIIA aldoménen található Sudlow's Site II (másnéven „Site II" vagy „benzodiazepine binding site") régióhoz kötődnek (Fanali és mtsai., 2012; Yamasaki és mtsai., 2013). Újabb vizsgálatok alapján az IB aldoménen elhelyezkedő FA1 (másnéven a „hem kötőhely") régió is fontos szerepet tölt be egyes gyógyszerek (pl. camptothecin, doxorubicin, dicoumarol) albumin-kötődésében (Zsila, 2013). A Site I kötőhely, melyet warfarin kötőhelynek is neveznek, egy nagy és flexibilis, alacsony sztereoszelektivitású régió, amely számos különböző ligandummal képes kölcsönhatásba lépni, sőt egy időben

akár több molekula befogadására is képes (Kragh-Hansen, 1988; Yamasaki és mtsai., 2013). A főként bázikus oldalláncú aminosavakból felépülő kötőhely apoláros jellegű, ezért az ide kapcsolódó ligandumok nagyrészt a régió apoláros kompartmentjeit elfoglalva hidrogénhíd-kötést alakítanak ki a kötőhely egy tirozin aminosavának hidroxilcsoportjával (Ascenzi és Fasano, 2010). A Site I kötőhelyhez általában dikarbonsavak és/vagy nagyméretű negatív töltéssel rendelkező heterociklusos vegyületek kapcsolódnak (Kragh-Hansen és mtsai., 2002; Otagiri, 2005; Yamasaki és mtsai., 2013). A HSA-on a Site I régióhoz kötődik pl. a warfarin, a phenylbutazon, az indometacin, a tolbutamid, a iodipamid és a furosemid (Anton, 1973; Vallner, 1977; Montero és mtsai., 1986; Yamasaki és mtsai., 1996; Takamura és mtsai., 2005). A Site II kötőhely a Site I-hez képest kisebb és szűkebb, kevésbé flexibilis, valamint jelentős sztereoszelektivitást mutat, ami az ide kapcsoló ligandumok kismértékű szerkezeti változásaira is rendkívül érzékeny (Kragh-Hansen és mtsai., 2002; Ghuman és mtsai., 2005). Például az *(R)*-ibuprofen az *(S)*-enantiomerhez képest 2,3-szor magasabb affinitással kötődik a Site II kötőhelyhez (Itoh és mtsai., 1997). A Site II régió egy apoláros üreg, melynek egyetlen poláros része a kötőhely bejárata közelében található (Curry, 2009). A Site II-höz kötődő vegyületek főként aromás karbonsav szerkezetűek (pl. diazepam, ibuprofen, diclofenac, naproxen), (Honoré és Brodersen, 1984; Yamasaki és mtsai., 1996; Setoguchi és mtsai., 2013), amelyek a kötődéskor hidrofil molekularészletükkel egy tirozin aminosav hidroxilcsoportjával alakítanak ki kölcsönhatást, de a kötődésben arginin és szerin aminosavak is közreműködnek hidrogénhíd-kötések és sóhidak kialakítása révén (Ascenzi és Fasano, 2010).

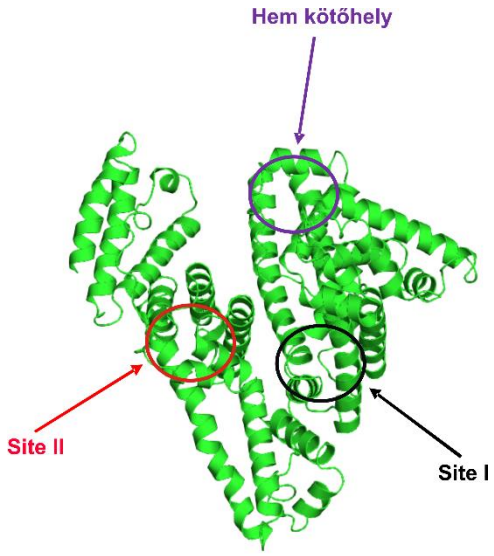

1. ábra: A humán szérum albumin (HSA) szerkezete és fő gyógyszerkötőhelyei.

Az erős albuminkötődés ún. „depot" hatást okoz: csak a szabad (nem albuminkötött) molekulák képesek passzív diffúzióval vagy specializált transzporttal áthaladni a biológiai membránokon (így elérve a szöveti targetet, ami a farmakodinámiás hatás kifejlődését eredményezheti), valamint szintén csak a nem plazmafehérjekötött gyógyszermolekulák képesek a szövetekben biotranszformálódni vagy a szervezetből exkrécióval távozni (Koch-Weser és Sellers, 1976; Smith és mtsai., 2010). Ebből adódóan, a gyógyszerek albuminkötődése és annak megváltozása hatást gyakorolhat egyes farmakokinetikai paramétereikre és farmakológiai hatásukra (Meyer és Guttman, 1968; Vallner, 1977; Otagiri, 2005). A HSA-hoz nagymértékben kötődő vegyületek képesek lehetnek leszorítani az albuminhoz szintén nagymértékben kötődő egyéb anyagokat (pl. gyógyszereket). A leszorítás lehet kompetitív kölcsönhatás eredménye, de bekövetkezhet a kötőhely konformációváltozása miatt is alloszterikus interakció eredményeként (Kragh-Hansen és mtsai., 2002; Otagiri, 2005). Kompetíció esetén, az adott gyógyszer leszorítóképessége függ a szer kötődési affinitásától, valamint a leszorító és a leszorított vegyületek egymáshoz viszonyított koncentrációitól (Fanali és mtsai., 2012). Leszorításos interakciók kialakulása elsősorban a nagymértékben albuminhoz kötődő, szűk terápiás ablakkal jellemezhető, alacsony megoszlási térfogatú és klírenszű hatóanyagok (pl. phenytoin, warfarin, tolbutamid) esetében lehet leginkább klinikailag is releváns (Christensen és mtsai., 2006). A HSA-ról történő leszorítás az adott szer megnövekedett szabad plazmakoncentrációját eredményezi, de jelentős kölcsönhatást általában abban az esetben okoz, ha egyéb tényezők (pl. csökkent metabolizmus vagy

exkréció) is fennállnak (Fanali és mtsai., 2012). A gyógyszerek albuminkötődésének mértéke bizonyos patológiás állapotokban (pl. analbuminémia, hipoalbuminémia) és egyes betegségekben a fehérje csökkent képződése (pl. krónikus májbetegség) vagy fokozott vesztése (pl. nefrózis szindróma, égési sérülés) következtében is változhat (Vallner, 1977; Grandison és Boudinot, 2000; Kragh-Hansen és mtsai., 2002).

II.2. Citokróm P450 enzimek

A citokróm P450 (CYP) enzimek egy szupercsaládot alkotó, hem tartalmú enzimfehérjék, melyek a legtöbb élőlényben (pl. baktériumok, növények, emlősök) megtalálhatóak (Meunier és mtsai., 2004; De Montellano, 2010). A hemet tartalmazó CYP enzimek prosztetikus csoportjában egy Fe^{3+} vas-protoporfirin IX-ként (hem) kovalensen kötődik a fehérje egy cisztein aminosavának kénatomjához (Meunier és mtsai., 2004). A CYP450 enzimcsalád nevét onnan kapta, hogy a prosztetikus csoport vasionjának redukált formája képes szén-monoxidot megkötni és az így képződött komplex 450 nm-en képes jelentős fényt abszorbeálni (Nebert és Russell, 2002). A különböző élő szervezetekben előforduló CYP enzimek más-más funkciókat töltenek be: pl. a prokariótákban antibiotikum bioszintézisért, a növényekben többek között fitohormonok és pigmentek előállításáért, míg emlősökben különböző endogén és exogén vegyületek biotranszformációjáért felelősek (Danielson, 2002).

A humán CYP enzimek (***2. ábra***) kiemelkedő szereppel bírnak a szteroidogenezisben, a zsírsavak metabolizmusában, számos gyógyszer és xenobiotikum oxidatív biotranszformációjában, valamint prokarcinogén és promutagén ágensek potenciális karcinogénné történő átalakításában is (Danielson, 2002). A több mint 50 gén által kódolt humán CYP enzimeket 18 különböző családba és a családokon belül 44 alcsaládba sorolják (Zanger és Schwab, 2013). Azok az enzimek, amelyek aminosav szekvenciája legalább 40%-ban vagy ennél nagyobb mértékben egyezik egy családba, míg azok, amelyeknél ez az érték 55% fölötti, egy alcsaládba tartoznak (Nebert és Russel, 2002; Bibi, 2008; De Montellano, 2010). Az azonos családokat a CYP rövidítés után egy arab számmal jelöljük (pl. CYP1, CYP2, CYP3), ami után az alcsaládot jelölő latin betű (pl. CYP1A, CYP2D, CYP3A) következik (Nebert és Russel, 2002; Bibi, 2008; McDonnell és Dang, 2013). A rövidítés legutolsó tagja szintén egy arab szám, mely az adott alcsaládon belüli izoenzimet jelöli (pl. CYP1A2, CYP2D6, CYP3A4) (Nebert és

Russel, 2002; McDonnell és Dang, 2013). Az enzimfehérjéket kódoló CYP gének különböző alléljait az adott enzimet kódoló gén nevét követő csillaggal és egy arab számmal (pl. CYP2D6*1) vagy egy arab szám és egy latin betű kombinációjával jelöljük (pl. CYP2D6*1A) (Daly és mtsai., 1996). A CYP enzimek legnagyobb része a májban expresszálódik, de megtalálhatóak egyéb szövetekben is, mint pl. a vékonybélben, a tüdőben, a vesében és az agyban (Preissner és mtsai., 2013; Zanger és Schwab, 2013).

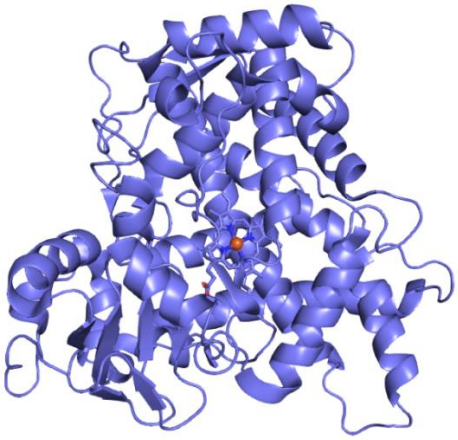

2. ábra: A CYP2C9 enzim 3 dimenziós szerkezete.

A CYP enzimek által katalizált reakciók közé tartozik a hidroxiláció, oxigenáció, epoxidáció, dealkiláció, deamináció, deszulfuráció, dehalogenáció és a dehidrogenáció, de olykor redukciót is katalizálhatnak egyes képviselőik (Jurva és mtsai., 2003). Az oxigenáció során a CYP enzimek a molekuláris oxigén atomjait felhasználva az egyik oxigénatomot az oxigenált metabolitba építik, miközben a másik oxigén redukciója egy víz molekula képződéséhez vezet (Meunier és mtsai., 2004; De Montellano, 2010; Guengerich, 2018). Az oxigenálásnak két fő típusát különböztetjük meg: az egyik során az oxigénatom beépítése egy stabil metabolit képződését eredményezi, míg a másik esetében egy instabil intermedier metabolitét, mely ezt követően spontán módon két termékre hasad (Guengerich, 2001). Mivel alapvetően a molekuláris oxigén egyik oxigénatomja épül be a szubsztrátba, a CYP enzimeket gyakorta nevezik monooxigenázoknak is (Meunier és mtsai., 2004). CYP enzimek katalizálta reakciókhoz a nikotinamid-adenin-dinukleotid-foszfát (NADPH)-függő CYP reduktáz működésére is szükség van, amely az elektronok CYP-re történő szállításáért felelős (Laursen és mtsai., 2011).

Mindössze az első három CYP család (CYP1-3) tagjai vesznek részt a xenobiotikumok biotranszformációjában, a többi CYP enzim az endogén vegyületek metabolizmusáért felelős (Sim és Ingelman-Sundber, 2010). A terápiában alkalmazott gyógyszerek kb. 90%-ának oxidatív biotranszformációjáért a CYP1A2, CYP2C9, CYP2C19, CYP2D6, CYP2E1, CYP3A4 és CYP3A5 enzimek felelősek (***3. ábra***) (Bibi, 2008; Saha, 2018). Ezek közül a CYP3A4/5 enzimek a gyógyszerek 37%-ának, a CYP2C9 17%-ának, a CYP2D6 15%-ának, a CYP2C19 10%-ának, a CYP1A2 9%-ának, míg a CYP2E1 kb. 2%-ának biotranszformációjában vesznek részt (Zanger és mtsai., 2008). Fontos kiemelni, hogy számos gyógyszer több CYP enzim közreműködésével metabolizálódik (Preissner és mtsai., 2013). A CYP1A2 enzim pl. a theophyllin, coffein, duloxetin, tizanidin és a paracetamol metabolizmusában vesz részt (Eichelbaum és Gross, 1990; Granfors és mtsai., 2004; Lobo és mtsai., 2008). A CYP2C9 enzim többek között a warfarin, számos nemszteroid gyulladáscsökkentő, a tolbutamid, a phenytoin és a losartan biotranszformációját katalizálja, a CYP2C19 enzim szubsztrátjai közé pl. a diazepam, a fluoxetin, a sertralin, az omeprazol, a propranolol és az amitriptylin sorolható (Leemann és mtsai., 1993; Kaminsky és Zhang, 1997; Yasumori és mtsai., 1999; Äbelö és mtsai., 2000; Hiemke és Härtter 2000; Wilkinson, 2005; Bibi, 2008; Zanger és mtsai., 2008). A CYP2D6 enzim számos központi idegrendszerre ható szer (pl. triciklusos antidepresszánsok és antipszichotikumok) metabolizmusáért felelős, de egyes antiaritmiás szerek (pl. flecainid, propafenon) és néhány bétablokkoló (pl. metoprolol, timolol, carvedilol) biotranszformációjában is érintett (Otton és mtsai., 1988; Ghahramani és mtsai., 1997; Wilkinson, 2005; Hendset és mtsai., 2007; Bibi, 2008; Zanger és mtsai., 2008). A CYP3A alcsalád tagjai a legnagyobb mennyiségben előforduló CYP enzimek, melyek a májban az összes izoforma közel 30%-át, míg a vékonybélben közel 70%-át teszik ki (Slaughter és Edwards, 1995). A CYP3A4 enzim szubsztrátjai pl. a fluticason, az alprazolam, az atorvastatin, a lovastatin, az erythromycin, a clindamycin, a buspiron, a fentanyl, a buprenorphin és a tadalafil (Greenblatt és mtsai., 1993; Feierman és Lasker, 1996; Kivistö és mtsai., 1997; Wynalda és mtsai., 2003; Elkader és Sproule, 2005; Neuvonen és mtsai., 2006; Pearce és Leeder 2006; Zanger és mtsai., 2008). A CYP2E1 enzim pedig többek között a szén-tetraklorid, a halothan, a chloroform és az isofluran metabolizmusában vesz részt (Gillum és mtsai., 1993; Bibi, 2008).

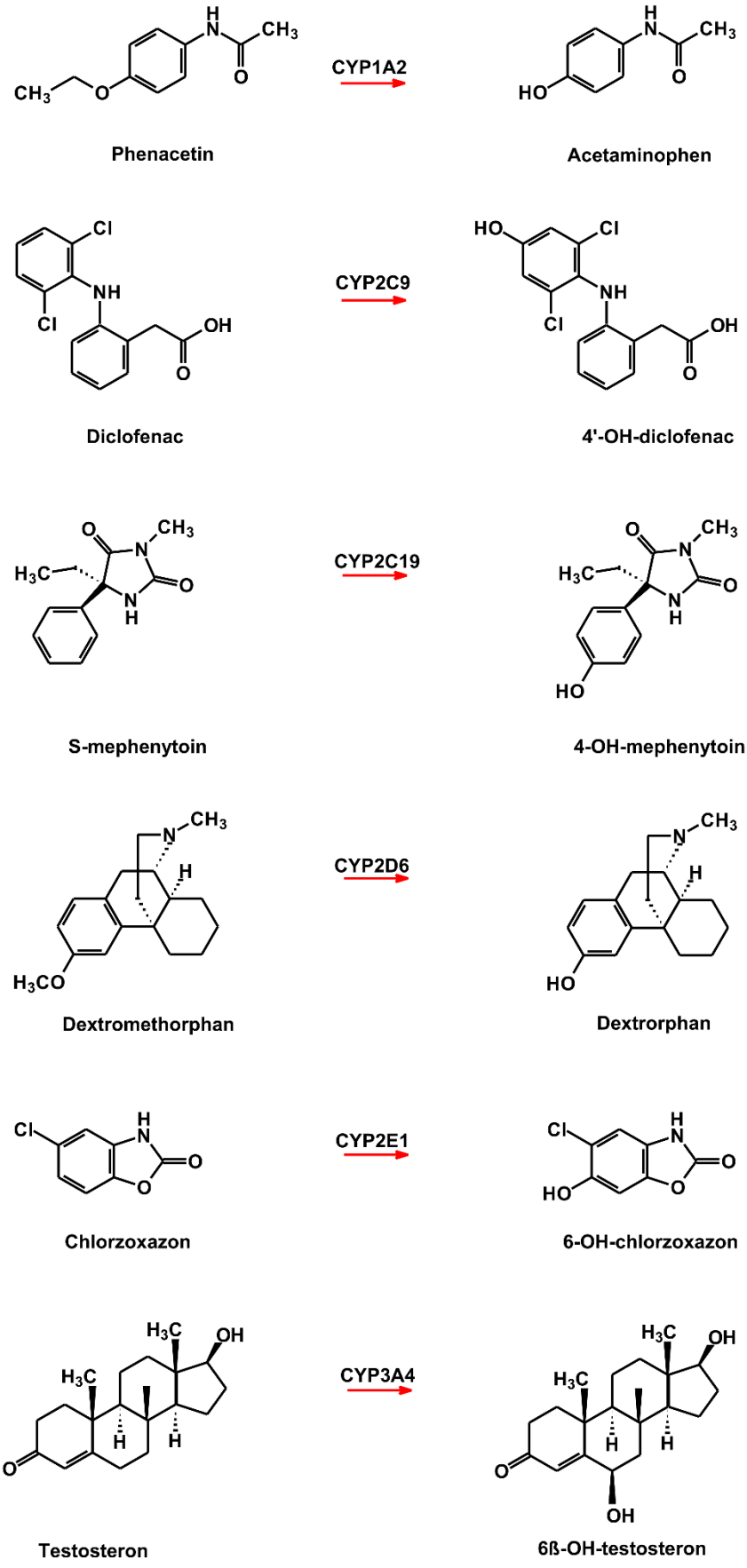

3. ábra: Példák a főbb CYP enzimek által katalizált biotranszformációs reakciókra.

Fontos kiemelni, hogy olykor a CYP enzimek nemcsak detoxikálásért, hanem egyes toxikálási folyamatok katalizálásáért is felelősek, pl. az *Aspergillus* gombafajok által termelt aflatoxin B1 mikotoxin különböző CYP enzimek katalizálta reakcióban képezi erős DNS-károsító toxikus epoxid metabolitját (Neal, 1995). De megemlíthető még a CYP2E1 enzim szerepe pl. a chloroform, a szén-tetraklorid vagy a paracetamol toxikoaktivációjában is (Raucy és mtsai., 1989; Patten és mtsai., 1993; Novak és Woodcroft, 2000; Gonzalez, 2005; Trafalis és mtsai., 2010).

Egyes CYP enzimek (pl. CYP2C9, CYP2C19, CYP2D6) metabolikus aktivitása kapcsán jelentős különbségeket tapasztaltak a humán populációban (Preissner és mtsai., 2013). A különböző enzimaktivitású formák kialakulásáért főként a fehérjéket kódoló gének egypontos nukleotid polimorfizmusait tartják felelősnek (Preissner és mtsai., 2013). Emellett a gyógyszerek metabolizmusában megjelenő eltéréseket egyéb faktorok is befolyásolják, pl. a nem, az életkor vagy az általános egészségi állapot (Scandlyn és mtsai., 2008; Zanger és Schwab, 2013).

A gyógyszerek mellett egyes növényekben és élelmiszerekben megtalálható nutriensek is képesek befolyásolni (gátolni/indukálni) a CYP enzimek működését, olykor klinikailag releváns kölcsönhatásokat eredményezve (Lynch és Price, 2007). Az interakciók lehetnek enyhék, de okozhatnak akár súlyos hatásokat/mellékhatásokat is (Dresser és mtsai, 2000; Siddoway, 2003). Például az egyes CYP3A4 gátló gyógyszerek (pl. clarithromycin, erythromycin, diltiazem, itraconazol, ketoconazol) terfenadinnal, cisapriddel vagy pimoziddal együtt alkalmazva gátolják az utóbbiak CYP3A4 általi eliminációját, ami a szerek megnövekedett plazmakoncentrációját eredményezve akár súlyos aritmiát is eredményezhet (Dresser és mtsai, 2000). Emellett, az amiodaron gátolja a warfarin CYP2C9-katalizált metabolizmusát, ami fokozott antikoaguláns hatást okoz (Sanoski és Bauman; 2002; Siddoway, 2003). Egy másik tanulmány szerint a diphenhydramin gyors metabolizálókban képes gátolni a metoprolol CYP2D6 általi biotranszformációját, ami jelentősen megnövelheti a metoprolol negatív krono- és inotróp hatásait (Hamelin és mtsai., 2000). A CYP enzimek nemcsak gátolhatóak, de indukálhatóak is egyes szerek által. A rifampicin az egyik legpotensebb CYP induktor gyógyszer, amely számos CYP (CYP2C9, CYP2C19, CYP3A4) működését képes befolyásolni (Niemi és mtsai., 2003). A rifampicin klinikailag releváns interakciói közé tartozik pl. az *(S)*-warfarin CYP2C9- és a ciclosporin CYP3A4-katalizált metabolizmusának indukálása (Niemi és mtsai., 2003). Mindemellett a rifampicin számos gyógyszer (pl. propranolol, nifedipin, alprazolam, methadon, tolbutamid, diazepam,

doxycyclin, sanquinavir) biotranszformációját is képes indukálni (Syvalahti és mtsai., 1976; Herman és mtsai., 1983; Ohnhaus és mtsai., 1987; Ndanusa és mtsai., 1997; Schmider és mtsai., 1999; Grub és mtsai., 2001; Niemi és mtsai., 2003). A rifampicin mellett többek között a phenobarbital, a phenytoin és a carbamazepin is potens CYP induktornak számítanak (Riva és mtsai., 1996; Lin és Lu, 1998). A phenobarbital pl. a warfarin CYP2C9 általi biotranszformációját, míg a carbamazepin és a phenytoin pl. a midazolam CYP3A4-katalizált metabolizmusát fokozhatják (Backman és mtsai., 1996; Cropp és Bussey, 1997).

A gyógyszerek mellett egyes növények (pl. *Hypericum perforatum*, *Ginkgo biloba*) hatóanyagai is kölcsönhatásba lépnek CYP enzimekkel (Zhou és mtsai., 2004; Kupiec és Raj, 2005). Az orbáncfű (*Hypericum perforatum*) képes indukálni a CYP3A4 enzim működését, így csökkentve pl. az ethinylestradiol hatását (ez nemkívánt terhességet eredményezhet) (Zhou és mtsai., 2004; Borrelli és Izzo, 2009; Russo és mtsai., 2014), de számos egyéb gyógyszer (pl. theophyllin, nifedipin, omeprazol, dexamethason, voriconazol, midazolam) kapcsán is fontos lehet ez az interakció (Wang és mtsai., 2004; Zhou és mtsai., 2004; Wang és mtsai., 2007; Borrelli és Izzo, 2009; Chen és mtsai., 2012; Russo és mtsai., 2014). Emellett a CYP2C19 enzim indukcióját is leírták *Ginkgo biloba* tartalmú étrend-kiegészítő fogyasztása kapcsán, ami az együttesen alkalmazott phenytoin és nátrium-valproát fokozott metabolizmusához vezetett (Kupiec és Raj, 2005).

A grapefruitban előforduló furanokumarinok és flavonoidok, mint a bergamottin és a naringenin képesek gátolni a simvastatin OATP- (szerves anionokat transzportáló polipetid) mediált felvételét a hepatocitákba, valamint a szer CYP3A4-katalizált eliminációját (Pirmohamed, 2013). Ebből adódóan, a simvastatin és a grapefruitlé együttes fogyasztása nagyságrendileg növeli a simvastatin koncentrációját a keringésben és az extrahepatikus szövetekben, ami rabdomiolízishez és következményesen veseelégtelenséghez vezethet (Pirmohamed, 2013).

II.3. Xantin-oxidáz enzim

A humán szervezetben a purin nukleotid bázisok lebontásának utolsó két lépését a xantin-oxidoreduktáz enzim katalizálja (Harrison, 2004). A xantin-oxidoreduktáz a hipoxantint előbb xantinná, majd a xantint húgysavvá oxidálja, miközben az enzim molibdén atomja redukálódik (Berry és Hare, 2004). Az emberi szervezetben a purin nukleotidok katabolizmusának végterméke a húgysav, ami alacsonyabb rendű emlősökben az urát-oxidáz által katalizált reakcióban vízoldékony allantoinná oxidálódik (Usuda és mtsai., 1988).

A xantin-oxidoreduktáz enzimnek kétféle egymásba átalakulni képes formája létezik: a xantin-oxidáz (XO, ***4. ábra***) és a xantin-dehidrogenáz (Stirpe és Della Corte, 1969; Kang és Ha, 2014). A XO és a xantin-dehidrogenáz metallo-flavoproteinek, amelyek ugyanazon gén termékének alternatív formái (Hille és Nishino, 1995). E két forma két azonos, de katalitikusan független alegységből épül fel, melyek egy C-terminális molibdénprotein-kötő domént, egy N-terminális vaskötő domént (Fe_2-S_2) és egy központi flavin-adenin-dinukleotid domént tartalmaznak (Hille és Nishino, 1995; Enroth és mtsai., 2000). Habár, a xantin-oxidoreduktáz többnyire xantin-dehidrogenáz formában van jelen *in vivo* (Della Corte és mtsai., 1969; Stirpe és Della Corte, 1969), reverzibilis oxidációs reakciók vagy irreverzibilis proteolitikus hasítások eredményeként XO-zá alakul (Enroth és mtsai., 2000; Berry és Hare, 2004; Kang és Ha, 2014).

4. ábra: A xantin-oxidáz (XO) enzim 3 dimenziós szerkezete.

A hipoxantin és a xantin oxidációját a XO és a xantin-dehidrogenáz is katalizálhatja (Hille és Nishino, 1995), ugyanakkor a mellékreakcióban az oxidáz forma csak a molekuláris oxigént redukálja, míg a dehidrogenáz az oxigént és a nikotinamid-adenin-dinukleotidot (NAD^+) is képes redukálni (***5. ábra***), de affinitása az utóbbihoz jóval nagyobb (Waud és Rajagopalan, 1976; Hille és Nishino, 1995). A XO-katalizált oxidáció során az enzim a molekuláris oxigént elektronakceptorként használva melléktermékként szuperoxid gyökanion, hidrogén-peroxid és egyéb reaktív oxigéngyökök képződését eredményezi, azonban a xantin-dehidrogenáz a NAD^+ redukciójával NADH-t képez (Berry és Hare, 2004; Kang és Ha, 2014). Mivel a szakirodalom szerint a reaktív oxigéngyökök szerepet játszhatnak iszkémiás reperfúziós károsodással járó patológiás folyamatokban, a XO enzimet gyakran egyes kórképek (pl. szívroham, agyvérzés, hipoxiás szövetkárosodás, ateroszklerózis, gyulladás, metabolikus betegségek, magas vérnyomás) kialakulásával is összefüggésbe hozzák (McCord, 1985; Dawson és mtsai., 2006; Pacher és mtsai., 2006).

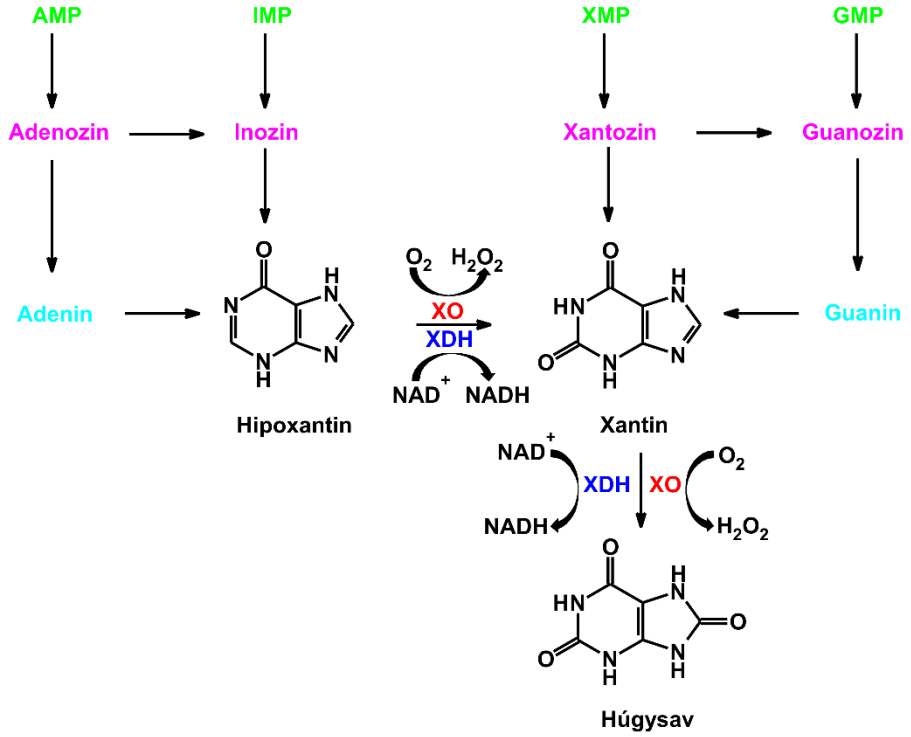

5. ábra: A purin bázisok lebontása (AMP: adenozin-monofoszfát, IMP: inozin-monofoszfát, XMP: xantozin-monofoszfát, GMP: guanozin-monofoszfát, XO: xantin-oxidáz, XDH: xantin-dehidrogenáz, NAD^+/NADH: nikotinamid-adenin-dinukleotid; *forrás:* Litwack, 2018).

A XO szöveti expressziójával kapcsolatban ellentmondásos információkat olvashatunk a szakirodalomban (Pritsos, 2000). Ami biztosnak tűnik, hogy a máj és a bélrendszer rendelkezik a legnagyobb XO aktivitással (Pritsos, 2000). Habár egyes kutatások szerint az agy-, a szív- és a vázizomszövetekben nem mutatható ki XO (Sarnesto és mtsai., 1996; Sakela és mtsai., 1998), egy korábbi tanulmány relatíve magas XO aktivitást detektált humán posztmortem agy- és szívszövetekben, sőt bizonyos mértékű enzimaktivitás a vese, vázizom, lép és mellékvese esetében is mérhető volt (Wajner és Harkness, 1989). Továbbá e tanulmányok szintén ellentmondásban állnak egymással a XO feltételezett szerepéről a különböző szövetek (pl. agy, szív, vese, tüdő) iszkémiás reperfúziós károsodásában (Chambers és mtsai., 1985; Adkins és Taylor, 1990; Linas és mtsai., 1990; Terada és mtsai., 1991).

A hiperurikémia a vér emelkedett húgysavszintjét jelenti (Harris és mtsai., 1999). A normálisnál magasabb húgysavszint kialakulásának oka lehet a megnövekedett húgysavtermelés, a csökkent kiválasztás vagy a kettő tényező együttes hatása (George és Minter, 2020). Megnövekedett húgysavtermeléssel kell számolni az alábbi patológiás kórképekben: tumorlízis, hemolízis, rabdomiolízis, míg pl. a veseelégtelenség és a metabolikus acidózis, bizonyos gyógyszerek (pyrazinamid, ethambutol, ciclosporin) illetve toxikus anyagok (alkohol, berillium, ólom) a húgysav csökkent kiválasztását eredményezik (Dong és mtsai., 2017; George és Minter, 2020). Továbbá, a szérum húgysav szintjének emelkedése különböző betegségek (diabetes mellitus, metabolikus szindróma, kardiovaszkuláris betegségek, krónikus vesebetegségek) markereként is szolgál (Barkas és mtsai., 2018). A húgysav fokozott termelődését a purin bázisokban gazdag ételek, italok túlzott mértékű fogyasztása is kiválthatja, ilyenek pl. a vörös húsok, kagylófélék és egyes alkoholos italok (Schlesinger, 2005). A húgysav egy gyenge sav, amely fiziológiás pH-n főként ionizált formában, urát anionként van jelen (Choi és mtsai., 2005). Ha a testfolyadékokban nő a húgysav szintje, az urát bizonyos koncentráció felett kicsapódik, a képződött mononátrium-urát kristályok pedig az ízületekben lerakódva gyulladást, köszvényt indukálnak (Shipley, 2011).

Napjainkban az allopurinol (APU) az egyik leggyakrabban alkalmazott gyógyszer hiperurikémia kezelésében és akut köszvényes rohamok megelőzésében (Day és mtsai., 2007). Az APU-t ugyan a XO gátlószereként fejlesztették ki, de eredetileg nem a húgysav képződésének mérséklésére, hanem egyes antineoplasztikus hatóanyagok (pl. 6-mercaptopurin) XO-katalizált inaktiválásának gátlására alkalmazták (Rundles, 1982; Day és mtsai., 1994). Azonban a későbbiekben kiderült, hogy APU képes csökkenteni a

szérum urát szintet és ennek következtében az akut köszvényes rohamok gyakoriságát is. Az APU egy hipoxantin analóg, amely szubsztrátja és gátlószere is a XO enzimnek (Murrell és Rapeport, 1986). Az APU-ból az aldehid-oxidáz és a XO által katalizált oxidáció során oxipurinol (másnéven alloxantin) képződik, amely mint egy aktív metabolit, szintén potens gátlószere a XO enzimnek (Day és mtsai., 2007). Az APU farmakológiai hatásáért tehát az anyavegyület és a metabolit együttesen felelősek (Murrell és Rapeport, 1986; Day és mtsai., 2007). Az APU egyrészt kompetitíve gátolja a XO által katalizált xantin oxidációt, közben az enzim szubsztrátjaként oxipurinollá oxidálódik (utóbbi az enzim redukált állapotú molibdén atomjához kapcsolódva szintén gátolja annak működését) (Day és mtsai., 2007). Az oxidált termék és a redukált enzim nagyon erős komplexet képez, ezért az oxipurinolt gyakran a XO „pszeudo-irreverzibilis" gátlószerének nevezik (Spector, 1977; Galbusera és mtsai., 2006; Day és mtsai., 2007). Továbbá, az APU és az oxipurinol a *de novo* purin szintézist is képesek gátolni, mivel a húgysavszint csökkenésének következményeként nő a hipoxantin és a xantin koncentrációja, amely növeli a hipoxantin inozinná, inozin-monofoszfáttá, valamint adenozin- és guanozin-monofoszfáttá történő visszaalakulását, ami negatív feedback révén a *de novo* purin szintézis sebességmeghatározó lépését katalizáló amidofoszforibozil-transzferázt gátolja (Choi és mtsai., 2005; Day és mtsai., 2007). Ezenfelül, az APU és az oxipurinol szerepe a húgysav képződés gátlása mellett, a reaktív oxigéngyökök képződésének csökkentése kapcsán is előnyös lehet (Berry és Hare, 2004; Galbusera és mtsai., 2006).

A XO enzim egyes gyógyszerek biotranszformációját is katalizálja, pl. a tiopurinokét és a metilxantinokét (Guerciolini és mtsai., 1991). Az antitumor vagy immunszupresszáns szerként alkalmazott purin analóg gyógyszer, a 6-mercaptopurin (6-MP) inaktív 6-thiohúgysavvá történő átalakulását is a XO katalizálja (***6. ábra***) (Dubinsky és mtsai., 2000; Leong és mtsai., 2008). Mivel az APU gátolja a XO enzimet, köztudott, hogy az APU és a 6-MP vagy az azathioprin (a 6-MP prodrugja) együttes alkalmazása a 6-MP oxidációjának gátlása révén lassítja az antitumor gyógyszer eliminációját, ami súlyos, akár fatális kimenetelű mieloszupressziót is okozhat (McLeod, 1998). E farmakokinetikai interakció elkerülése végett az APU és a 6-MP vagy az azathioprin együttes alkalmazása során az utóbbi gyógyszerek dózisát legalább egyharmadára kell csökkenteni (Leong és mtsai., 2008).

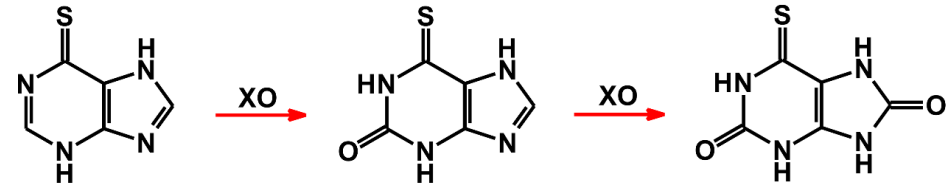

6. ábra: A 6-mercaptopurin (6-MP) inaktív 6-thiohúgysavvá alakulása a XO által katalizált reakcióban.

II.4. Flavonoidok

II.4.1. A flavonoidok általános jellemzése

A flavonoidok a polifenolok csoportjába tartozó természetes vegyületek, melyek megtalálhatóak számos növényben (orbáncfű, kamilla), gyümölcsökben (narancs, grapefruit) és zöldségekben (hagyma, brokkoli), valamint egyes italokban (tea, vörösbor) is (Hollman és mtsai., 1996; Butterweck és mtsai., 2000; Pietta, 2000; Mckay és Blumberg, 2006; Toh és mtsai., 2013). A flavonoidok fenil-kromon származékoknak tekinthetők, melyeknél két benzol gyűrű (A és B gyűrű) egy heterociklusos *O*-atomot tartalmazó pirán gyűrűn (C gyűrű) keresztül kapcsolódik (***7. ábra***) (Cook és Saman, 1996; Wang és mtsai., 2018). A flavonoidok különböző csoportokra oszthatók a C gyűrű telítettsége és szubsztitúciója alapján, illetve attól függően, hogy a B gyűrű a C gyűrű melyik szénatomjához kapcsolódik (***7. ábra***) (Beecher, 2003; Kumar és Pandey, 2013; Panche és mtsai., 2016). Az izoflavonoidoknál a B gyűrű a C gyűrű hármas szénatomjához kapcsolódik, míg a neoflavonoidoknál a B gyűrű a C négyes szénatomjához kapcsoltan helyezkedik el (***7. ábra***) (Beecher, 2003; Panche és mtsai., 2016). Az ún. normál flavonoidok esetében a B gyűrű a C gyűrű második szénatomjához kötődik, itt további alcsoportokat különböztethetünk meg (pl. flavonok, flavonolok, flavanonok, flavanonolok, katechinek, antocianidinek és kalkonok) (***7. ábra***) (Beecher, 2003; Tapas és mtsai., 2008; Kumar és Pandey, 2013; Panche és mtsai., 2016). A flavonoidok a növényekben fenilalaninból szintetizálódnak (Wink, 2010) és legtöbbször glikozidok formájában vannak jelen (Tapas és mtsai., 2008; Vukics és Guttmann, 2010). Az *O*-glikozidoknál a cukormolekula az aglikon egyik (általában a hármas vagy hetes pozícióban elhelyezkedő) hidroxilcsoportjához kapcsolódik, míg a *C*-glikozidoknál a cukor rész szén-szén kötésen keresztül kapcsolódik az aglikonhoz, többnyire a váz hatos

vagy nyolcas szénatomján (Viskupičová és mtsai., 2008; Vukics és Guttmann, 2010). A flavonoid glikozidok cukorkomponensei leggyakrabban a D-glükóz és az L-ramnóz, ritkábban pedig xilóz, arabinóz és glükuronsav (Tapas és mtsai., 2008; Vukics és Guttmann, 2010).

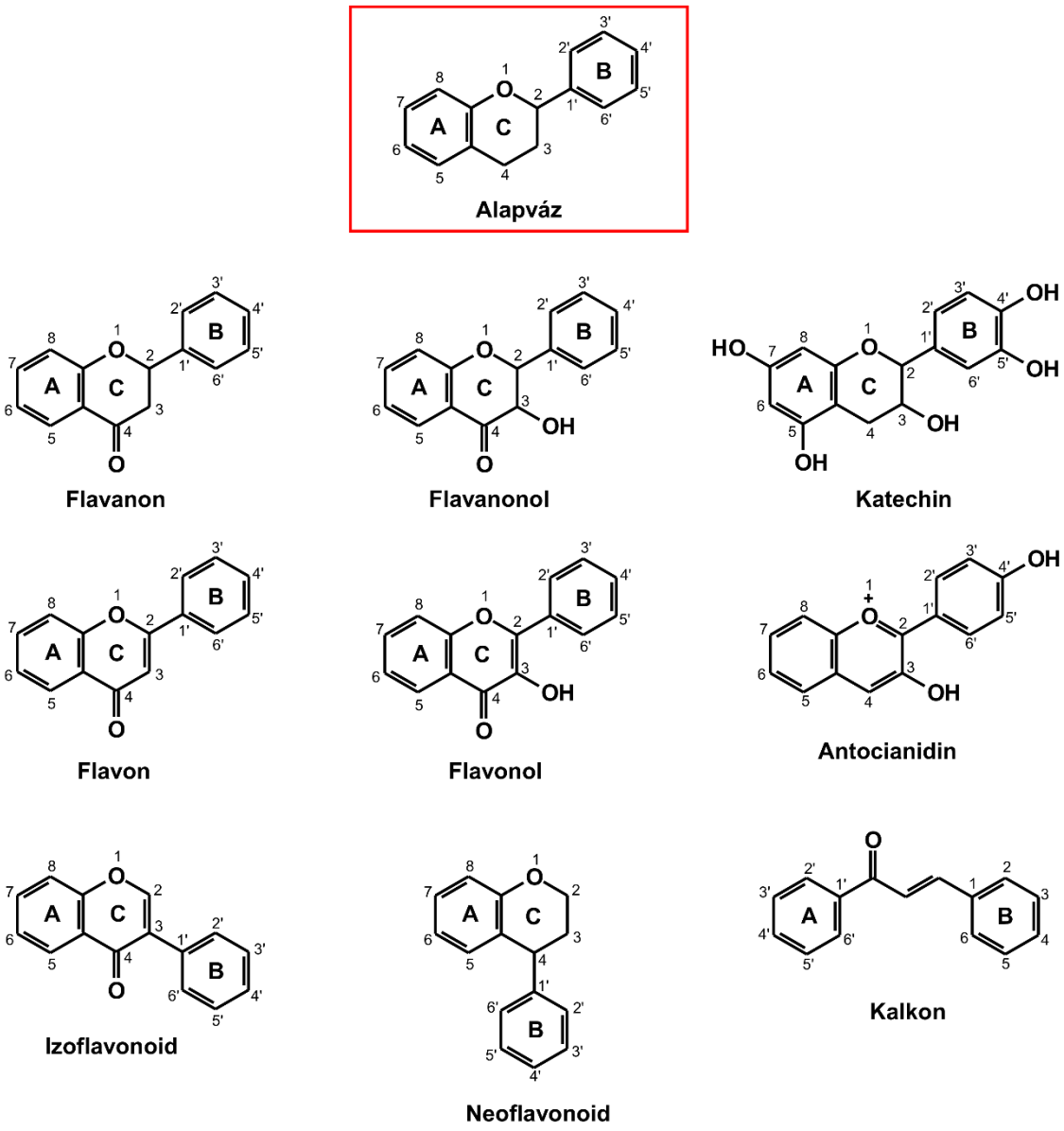

7. ábra: A flavonoidok fő csoportjainak kémiai szerkezete.

A flavonoidok a növényi metabolizmus másodlagos anyagcseretermékei melyek szerepet játszanak a növények színének és aromájának kialakításában, részt vesznek a növény növekedésében és fejlődésében, valamint kiemelkedő szerepük van a különböző abiotikus és biotikus tényezőkkel szembeni és UV-B sugárzás elleni védekezésben is (Di Carlo és mtsai., 1999; Samanta és mtsai., 2011). A flavonoidok eloszlása a növényekben,

gyümölcsökben és zöldségekben eltérő és számos tényező befolyásolja (pl. fényexpozíció mértéke, csapadék mennyisége, egyéb környezeti faktorok, genetikai eltérések) (Yao és mtsai., 2004). Például a flavanonok jellemzően citrusfélékben, az izoflavonoidok hüvelyesekben, a flavonok gyógynövényekben, a katechinek pedig különböző teákban fordulnak elő (Hollman és Katan, 1999; Yao és mtsai., 2004). A flavonoidokat az emberi szervezet nem képes előállítani (Cook és Samman, 1996), bevitelük ezért csak külső forrásból lehetséges (pl. gyümölcsök, zöldségek, étrend-kiegészítők, gyógyszerek). A normál humán étrend legnagyobb mennyiségben izoflavonoidokat (pl. genistein, daidzein), flavonolokat (pl. quercetin, myricetin, kaempferol) és flavonokat (pl. luteolin, apigenin) tartalmaz (Zand és mtsai, 2002). Az átlagos flavonol és flavon tartalom pl. spenótban, őszibarackban és egyes gombákban viszonylag alacsony (<10 mg/kg), vörösborokban és különböző teákban közepesnek mondható (<50 mg/kg vagy 50 mg/L), míg pl. a brokkoli és a különféle hagymák viszonylag magas mennyiségben tartalmaznak flavonolokat és flavonokat (>50 mg/kg) (Hollman és Katan, 1999). Tekintettel arra, hogy az emberek által elfogyasztott flavonoidok mennyisége, valamint az egyes források flavonoid tartalma és eloszlása különböző lehet, az átlagos napi flavonoid bevitel nagy eltéréseket mutat. Ezt az értéket Finnországban 6 mg/nap, az Egyesült Államokban 13 mg/nap, Olaszországban 27 mg/nap, Hollandiában 33 mg/nap, Japánban pedig 64 mg/nap mennyiségre becsülik (Ali és mtsai., 2017).

A flavonoidok részét képezik a mindennapi étrendnek és sok tanulmány számol be a szervezetre gyakorolt jótékony hatásaikról (Rogerio és mtsai., 2010; Zhu és mtsai., 2017; Chen és mtsai., 2019). Ennek hatására napjainkban egyre több magas flavonoid tartalmú étrend-kiegészítő kerül forgalomba, melyek akár 1000 mg hatóanyagot is tartalmazhatnak kiszerelési egységenként (pl. tabletta, kapszula) és a gyártók által javasolt napi bevitel egyes esetekben a 4000 mg-ot is elérheti (Martin és Appel, 2010; Vida és mtsai., 2019). Emellett flavonoidok és flavonoid származékok egyes gyógyszerekben is előfordulhatnak (pl. *Detralex 500 mg filmtabletta:* diosmin, hesperidin; *Dimotec 1000 mg filmtabletta:* diosmin; *Rutascorbin 20 mg/50 mg tabletta:* rutosid).

Annak ellenére, hogy a flavonoidok egészségre gyakorolt pozitív hatásai kapcsán viszonylag kevés evidencia áll rendelkezésre, a szakirodalomban megannyi tanulmányban a flavonoidok antioxidáns és szabadgyökfogó (Seyoum és mtsai., 2006; Li és mtsai. 2016; Chen és mtsai., 2019), antiproliferatív (Huang és mtsai., 1994; Scambia és mtsai., 1996; Braganhol és mtsai., 2006), gyulladáscsökkentő (Lee és mtsai., 2010;

Rogerio és mtsai., 2010; Devi és mtsai., 2015), antiaszmatikus (Kimata és mtsai., 2000; Gao és mtsai., 2012; Masuda és mtsai., 2014), antidiabetikus (Li és mtsai., 2014; Unnikrishnan és mtsai, 2014; Ghorbani, 2017), antihiperlipidémiás (Srinivasan és Pari, 2013; Unnikrishnan és mtsai, 2014) és kardioprotektív (Ravishankar és mtsai., 2017; Zhang és mtsai., 2017; Zhu és mtsai., 2017) hatásairól olvashatunk. Ezek többsége azonban *in vitro* rendszerekben vagy állatkísérletek során megfigyelt eredmények, a humán vizsgálatok eredményei ezzel szemben gyakran ellentmondásosak.

II.4.2. A flavonoidok farmakokinetikája

A flavonoidok jellemzően alacsony orális biohasznosulással rendelkeznek, melynek oka a vegyületek alacsony vízoldhatósága és jelentős preszisztémás eliminációja; emellett a különböző flavonoidok abszorpciójának mértéke és orális biohasznosulása számottevő eltéréseket mutathat (Viskupičová és mtsai., 2008; Akhlaghi és Foshati, 2017). Az izoflavonoidok felszívódása a legjobb, a katechinek, a flavanonok és a flavonolok abszorpciója közepesnek módható, míg a felszívódás az antocianidinek esetén a legrosszabb a flavonoidok körében (Viskupičová és mtsai., 2008). Emellett a különböző flavonoidok abszorpciójának mértékét egyéb tényezők is befolyásolják, mint az adott étel minőségi összetétele, az alapvázhoz kapcsolódó funkciós csoportok, valamint a fogyasztók közötti individuális különbségek (Heimm és mtsai., 2002). Továbbá a flavonoidok felszívódását egyes efflux transzporterek (pl. P-glikoprotein: P-gp, Multi-drug restistance-associated protein: MRP, Breast cancer resistance protein: BCRP) is limitálhatják (Brand és mtsai., 2006).

Az orálisan bevitt flavonoid glikozidoknak a vékonybélben előbb deglikozilálódnia kell, mivel legtöbbször csak az aglikon forma képes (passzív diffúzióval) felszívódni (Depeint és mtsai., 2002; Arts és mtsai., 2004). A cukor komponens hidrolíziséért pl. β-glükozidáz enzimek felelősek (Day és mtsai., 2003; Cermak és mtsai., 2004). Ugyanakkor egyes esetekben a glikozidok is képesek felszívódni a Na^+-függő glükóz transzporterek (pl. SGLT1) segítségével (Gee és mtsai., 2000), melyeket ezt követően az enterociták hidrolizálnak az intracelluláris enzimeik által (Manach és Donovan, 2004). Ezt követően az aglikonok egy része a portális vénán keresztül a májba kerül. Az enterocitákban és a hepatocitákban a flavonoidok nagyrésze konjugációs reakciókon megy keresztül (pl. glükuronidáció, szulfatáció, metiláció) (***8. ábra***), a képződött metabolitok pedig a májból az epébe exkretálódnak vagy a szisztémás keringésbe jutnak (Rice-Evans és mtsai., 2000;

Manach és Donovan 2004). Fontos kiemelni, hogy legtöbbször a konjugátumok a keringésben jóval magasabb koncentrációkban jelennek meg, mint az aglikon (Mullen és mtsai., 2006). A konjugált metabolitok innen a vesén keresztül, a vizelettel ürülnek (Rice-Evans, 2001; Manach és Donovan 2004).

Az oxidáció, redukció, hidrolízis és a különböző konjugációs reakciók képezik a flavonoidok fő metabolikus útvonalait, melyek közül a szulfát és a glükuronsav konjugáció a flavonoidok biotranszformációjának leggyakoribb típusai (Rice-Evans, 2001; Viskupičová és mtsai., 2008). A flavonoidok glükuronidációja főként a vékonybélben és/vagy a májban megy végbe, melyet az uridin-difoszfát glükuronil-transzferáz (UGT) katalizál. Az UGT szupercsalád számos szubsztrát glükuronsavval történő konjugációját végzi, melyek közül főként az UGT1A család enzimei felelősek a flavonoidok biotranszformációjáért (Meech és mtsai., 1997; Otake és mtsai., 2002). A flavonoidok szulfát konjugációját és metilációját a szulfotranszferáz (SULT) és catechol-*O*-metil-transzferáz (COMT) enzimek katalizálják (Manach és mtsai., 2004; Viskupičová és mtsai., 2008). A COMT enzimek a katechol szerkezeti egységet hordozó polifenolok *O*-metilezéséért felelősek, pl. a katechinek, epikatechinek, epigallokatechinek, a luteolin és a quercetin metilcsoporttal történő konjugációját katalizálják (Inoue-Choi és mtsai., 2010). Noha a COMT enzim főleg a katechol szerkezeti egység 3'-*O*-metilálását preferálja (pl. katecholaminok, fisetin és quercetin esetében) (Tsao és mtsai., 2011), a luteolinnál a 4'-hidroxil csoport metilálása a domináns (Cao és mtsai., 2014).

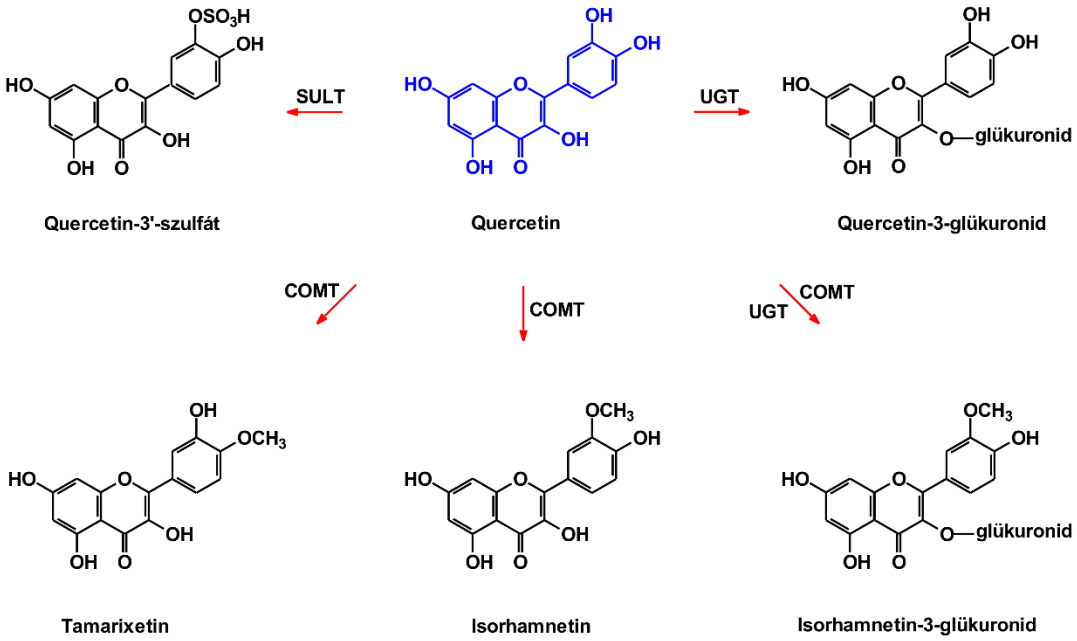

8. ábra: A flavonoidok konjugációs reakciói a quercetin példáján bemutatva (COMT: catechol-*O*-metil-transzferáz, SULT: szulfotranszferáz, UGT: uridin-difoszfát glükuronil-transzferáz).

Nagyobb mennyiségű flavonoid bevitelt követően a vegyületek (jelentős mértékű) fel nem szívódott frakciója kerül a vastagbélbe, ahol a colon mikroflóra baktériumai a heterociklusos gyűrűt hasítva kisebb molekulatömegű fenolos vegyületekre bontják az aglikonokat (Rechner és mtsai., 2002; Aura, 2008; Serra és mtsai., 2012; Del Rio és mtsai., 2013). A képződő mikrobiális metabolitok szintén felszívódhatnak, ezek szerkezetüket tekintve lehetnek hidroxi-benzolok, hidroxi-benzoesavak, hidroxi-ecetsavak vagy hidroxi-fahéjsavak (Rechner és mtsai., 2002; Aura, 2008; Serra és mtsai., 2012; Del Rio és mtsai., 2013).

II.4.3. A chrysin és a quercetin

A chrysin (CHR; ***9. ábra***) egy a flavonok csoportjába tartozó flavonoid aglikon, melynek *O*- (pl. chrysin-7-*O*-glükopiranozid, chrysin-7-*O*-gentiobiozid) és *C*-glikozidjai (pl. chrysin-6-glükopiranozil-8-arabinopiranozid) is megtalálhatóak a természetben (Yan és mtsai., 2011; Pereira és mtsai., 2012). A CHR főként a mézben (0,10-5,3 mg/kg) és a propoliszban (0,013-0,045 mg/kg) fordul elő, de megtalálható egyes növényekben (*Passiflora incarnata, Oroxylum indicum*) és bizonyos gombákban (0,17-0,37 mg/kg) is (Siess és mtsai., 1996; Kalogeropoulos és mtsai., 2013; Nabavi és mtsai., 2015).

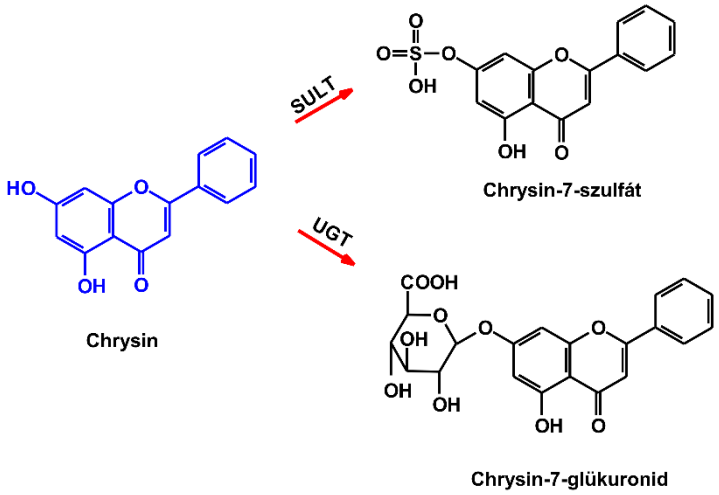

9. ábra: A chrysin biotranszformációja és fő metabolitjai (SULT: szulfotranszferáz, UGT: uridin-difoszfát glükuronil-transzferáz).

In vitro adatok alapján a CHR képes gátolni az aromatáz enzimet, amely az androstendion estronná és a testosteron estradiollá történő átalakulását katalizálja, ezért a CHR-t étrend-kiegészítőként gyakran a testosteron szint fenttartása/növelése érdekében javasolják (Kao és mtsai., 1998; Moon és mtsai., 2006). Az *in vivo* hatásosság kapcsán azonban nem áll rendelkezésre meggyőző klinikai vizsgálat. Mindemellett állatkísérletek alapján, a CHR neuroprotektív hatású, képes csökkenteni a neuronális gyulladást, valamint antidepresszáns hatással is rendelkezik (Nabavi és mtsai., 2015; Filho és mtsai., 2016). Továbbá patkányokban gyulladáscsökkentő, antioxidáns és antidiabetikus hatásokat is leírtak (Cho és mtsai., 2004; Pushpavalli és mtsai., 2010; Xiao és mtsai., 2014; Satyanarayana és mtsai., 2015). Annak ellenére, hogy a CHR pozitív hatásaival kapcsolatban nincs szilárdnak tekinthető humán evidencia, a CHR-tartalmú étrend-kiegészítőket a testosteron szint normalizáló hatás mellett szorongás, gyulladásos állapotok, köszvény, erektilis diszfunkció, kopaszodás, sőt még különböző daganatos megbetegedések kezelésére is ajánlják (Mohos és mtsai., 2018a).

A CHR jelentős mértékben biotranszformálódik a szervezetben, melynek során elsősorban chrysin-7-szulfát (C7S) és chrysin-7-glükuronid (C7G) képződik (***9. ábra***) (Walle és mtsai., 2001). Habár a metabolitok és az anyavegyület plazmakoncentrációival kapcsolatban kevés információ áll rendelkezésre, az *in vivo* vizsgálatok alapján a C7S és a C7G jóval magasabb koncentrációt érnek el az anyavegyülethez képest (Ge és mtsai., 2015; Noh és mtsai., 2016; Dong és mtsai., 2017). Például egerekben 20 mg/kg CHR orális beadását követően a C7S (C_{max} = 130 nmol/L) és a C7G (C_{max} = 160 nmol/L) több

mint 10-szer magasabb koncentrációit figyelték meg a keringésben az anyavegyülethez viszonyítva (C_{max} = 10 nmol/L) (Ge és mtsai., 2015). Patkányokban pedig 30 és 100 mg/kg CHR *per os* alkalmazása a C7G megközelítőleg 750-850 nmol/L koncentrációját eredményezte (Noh és mtsai., 2016; Dong és mtsai., 2017). Emellett egészséges önkénteseknek *per os* beadott CHR (400 mg) bevételét követően az anyavegyület csúcs plazmakoncentrációja 12-64 nmol/L volt, míg a szulfát konjugátum ennél jóval magasabb koncentrációkat (400-800 nmol/L) ért el (Walle és mtsai., 2001).

A quercetin (Q) a természetben leggyakrabban előforduló flavonoidok egyike (***8. ábra***), amely főként glikozidjai formájában található meg (Wach és mtsai., 2007; Kelly, 2011). Az aglikonhoz kapcsolódó cukorkomponens (leggyakrabban glükóz, galaktóz vagy ramnóz) általában a váz hármas pozíciójú hidroxilcsoportjához kapcsolódik (Murota és Terao, 2003; Wach és mtsai., 2007). A természetben eddig több mint száz különböző glikozidot azonosítottak, melyek közül a rutin (quercetin-3-*O*-rutinozid) az egyik leggyakoribb, de az isoquercetin (quercetin-3-*O*-β-glükozid), a quercitrin (quercetin-3-*O*-ramnozid), a hyperosid (quercetin-3-*O*-galaktozid), a quercetin-4′-*O*-β-glükozid és a quercetin-3,4′-*O*-β-diglükozid is nagy gyakorisággal jelennek meg (Hollman és Arts, 2000; Lee és Mitchell, 2012). A hagymában a quercetin-4′-*O*-β-glükozid és a quercetin-3,4′-*O*-β-diglükozid, a teában a quercetin-3-*O*-rutinozid, míg az almában a quercetin-3-*O*-galaktozid, a quercetin-3-*O*-glükozid és a quercetin-3-*O*-ramnozid a domináns quercetin glikozidok (Hollman és mtsai., 1995; Lee és Mitchell, 2012). A normál humán étrendben megtalálható fő Q források a gyümölcsök, zöldségek és egyes italok (Hollman és Arts, 2000; Aherne és O'Brien, 2002). A zöldségek közül a hagyma (180-540 mg/kg), kelkáposzta (12-110 mg/kg) és paradicsom (4-430 mg/kg), a gyümölcsök között az alma (20-260 mg/kg), a fekete áfonya (105-160 mg/kg) és a fekete ribizli (33-68 mg/kg), míg az italok esetében a vörösbor (2-15 mg/L), a fekete tea (10-25 mg/L) és a narancslé (35-57 mg/L) fontos Q forrásoknak számítanak (Hollman és Arts, 2000; Aherne és O'Brien, 2002). Az átlagos napi Q bevitelt 10-30 mg/nap-ra becsülik (Cao és mtsai., 2010; Egert és mtsai., 2008; Thilakarathna és Rupasinghe, 2013). A Q természetes forrásain kívül, számos étrend-kiegészítőben is megtalálható (Andres és mtsai, 2018; Vida és mtsai., 2019). E termékek Q-tartalma kiszerelési egységenként általában 200-1000 mg között mozog, az ajánlott napi dózisa pedig jellemzően 250 és 4000 mg között változik, amely akár több mint százszorosa is lehet a normál napi bevitelnek (Vida és mtsai., 2019).

A szakirodalom szerint a Q potens *in vitro* antioxidáns/gyökfogó hatást mutat, sőt több tanulmány a flavonoid gyulladáscsökkentő, antiproliferatív, antivirális,

antiaszmatikus, kardio- és gasztroprotektív hatásait taglalja (Knekt és mtsai., 2002; Boots és mtsai., 2008; Kelly 2011). Egyes kutatások szerint a Q antioxidáns tulajdonsága a flavonoid Nrf2 (nuclear factor erythroid 2-related factor 2) transzkripciós faktorra kifejtett hatásán alapszik (Tanigawa és mtsai., 2007; Kimura és mtsai., 2009; Li és mtsai., 2016). Az Nrf2 a citoplazmában a Keap1 (Kelch-like ECH-associated protein 1) fehérjéhez kötötten helyezkedik el, de oxidatív stressz hatására a Keap1 fehérje konformációváltozásának eredményeként arról leválva a sejtmagba transzlokálódik (Itoh és mtsai., 2004; Inami és mtsai., 2011). Ezt követően az Nrf2 transzkripciós faktor révén az ARE (antioxidant response element) szekvenciát hordozó gének transzkripcióját serkenti, amelyek olyan fehérjéket kódolnak, melyek kiemelkedő szereppel bírnak a sejtek oxidatív stressz elleni védekezésében (pl. peroxiredoxin, glutation-S-transzferáz, NADPH-kinon-oxidoreduktáz) (Ishii és mtsai., 2000; Kimura és mtsai., 2009). Egyes kutatások szerint a Q az Nrf2-höz kötött Keap1 fehérje expresszióját csökkenti, mely a transzkripciós faktor megkötéséért, citoplazmában tartásáért és degradációjának elősegítéséért felelős (Kimura és mtsai., 2009).

Per os adagolást követően a Q egy része a vékonybél- és májsejtekben biotranszformálódik, melynek eredményeként metil (3'-*O*-metil-quercetin: isorhamnetin, IR; 4'-*O*-metil-quercetin: tamarixetin, TAM), szulfát (quercetin-3'-szulfát: Q3'S) és glükuronid (quercetin-3-glükuronid: Q3G; isorhamnetin-3-glükuronid: I3G) konjugátumok képződnek (***8. ábra***) (Kelly, 2011; Del Rio és mtsai., 2013), melyek közül a Q3'S, a Q3G és az I3G a domináns metabolitok a humán keringésben (Mullen és mtsai., 2006). Az átlagos étrenddel a Q és metabolitjainak együttes plazmakoncentrációja a nmol/L-es koncentrációtartományban van, azonban a magas Q-tartalmú étrend-kiegészítők fogyasztását követően (pl. 1000 mg/nap) a Q és metabolitjainak összkoncentrációja több μmol/L-es nagyságrendű (Conquer és mtsai., 1998; Kelly, 2011; Del Rio és mtsai., 2013).

II.4.4. A chrysin és quercetin farmakokinetikai interakciói

Napjainkban a flavonoidokat a szakirodalomban leírt lehetséges pozitív hatásaik révén fokozott érdeklődés övezi, habár fontos kiemelni, hogy a flavonoidok a gyógyszerek farmakokinetikai folyamataiban nagy szerepet játszó fehérjékkel, mint pl. a HSA, különböző biotranszformációs enzimek és transzporterek is képesek kölcsönhatásba lépni (Pal és Saha, 2014; Korobkova, 2015; Miron és mtsai., 2017).

A CHR és a Q interakcióit HSA-nal több közlemény is taglalja (Sengupta és Sengupta, 2002; Xiao és mtsai., 2010; Xiao és mtsai., 2011), melyek alapján mindkét flavonoid nagy affinitással (K = 10^5-10^6 L/mol) képes kötődni az albuminhoz (Sengupta és Sengupta, 2002; Xiao és mtsai., 2010; Xiao és mtsai., 2011; Tu és mtsai., 2015; Tan és mtsai., 2019). A Q kötőhelye a HSA Site I régiójában található (Dufour és Dangles, 2005; Pal és Saha, 2014), míg a CHR esetében a Site I és II régiók is felmerültek lehetséges kötőhelyként (Tu és mtsai., 2015; Sarmah és mtsai., 2020). Mivel a flavonoidok orális bevitelét követően főként a konjugátumok jelennek meg a szisztémás keringésben, munkacsoportunk korábban a konjugált Q metabolitok albumin kölcsönhatásait is megvizsgálta (Poór és mtsai., 2017). Az eredmények rávilágítottak arra, hogy nemcsak a Q, de konjugátumai is képesek stabil komplexet kialakítani HSA-nal. Habár a glükuronid konjugátumok (Q3G és I3G) albumin iránti affinitása alacsonyabb az Q-hez viszonyítva, a Q3'S és a metil származékok (IR és TAM) még az anyavegyületnél is stabilabb komplexeket alakítottak ki a fehérjével (Poór és mtsai., 2017). Emellett a Q konjugátumok jelentős mértékben képesek voltak leszorítani albuminról a Site I marker warfarint.

A CHR és a Q biotranszformációs enzimek működését is képesek befolyásolni (Korobkova, 2015; Miron et al., 2017). *In vitro* vizsgálatok alapján a CHR és a Q potens gátlószerei több CYP enzimnek (pl. CYP1A1, CYP1A2, CYP1B1, CYP2C9, CYP2E1 és CYP3A4) (Ho és Saville, 2001; He és mtsai., 2010; Kimura és mtsai., 2010; Shimada és mtsai., 2010; Korobkova, 2015; Miron és mtsai., 2017; Östlund és mtsai., 2017; Pingili és mtsai., 2019). Fontos kiemelni, hogy egyes Q konjugátumok esetében is leírtak CYP gátló hatásokat. A Q3'S, IR és TAM hasonló mértékben gátolták a CYP2C9-katalizált 4'-hydroxydiclofenac képződést, mint a Q (Poór és mtsai., 2017). Más *in vitro* vizsgálatokban az IR gátló hatásait demonstrálták CYP1A1, CY1A2, CYP1B1, CYP2C9, és CYP3A4 enzimeken (Chang és mtsai., 2006; Kimura és mtsai., 2010; Takemura és mtsai., 2010). Állatkísérletek is alátámasztják, hogy a CHR és a Q képesek befolyásolni egyes gyógyszerek CYP-mediált biotranszformációját. Például patkányoknak orális adott CHR és Q szignifikánsan növelte a paracetamol AUC és C_{max} értékeit, valószínűleg a paracetamol CYP2E1-mediált biotranszformációjának gátlása révén (Pingili és mtsai., 2015; Pingili és mtsai., 2019). Továbbá, a *per os* adagolt CHR a CYP2E1, az alkohol-dehidrogenáz és a XO enzimek gátlását eredményezte patkányokban (Tahir és Sultana, 2011). Annak ellenére, hogy a CHR a CYP1A enzimek potens *in vitro* inhibitorának bizonyult, patkányokban a coffein CYP1A2-mediált biotranszformációját nem

befolyásolta (Noh és mtsai., 2016). Emellett, a *per os* adott Q szignifikánsan növelte patkányokban a ranolazin (Babu és mtsai., 2013), a valsartan (Challa és mtsai., 2013), a tamoxifen (Shin és mtsai., 2006) és a pioglitazon (Umathe és mtsai., 2008); nyulakban pedig a diltiazem (Choi és Li, 2005) és a verapamil (Choi és Han, 2004) plazmakoncentrációit és AUC értékeit, valószínűleg a CYP3A4 és a P-gp gátlásának eredményeként. Továbbá egészséges humán önkéntesekben a Q növelte a midazolam metabolizmusát a CYP3A enzimek indukciója révén (Duan és mtsai., 2012; Nguyen és mtsai., 2015). Míg más klinikai vizsgálatokban a *per os* adott Q szignifikánsan növelte a diclofenac (Bedada és Neerati, 2018a) és a chlorzoxazon (Bedada és Neerati, 2018b) plazmakoncentrációját, feltehetőleg a CYP2C9 és a CYP2E1 enzimek gátlása által.

Számos *in vitro* vizsgálatban demonstrálták, hogy a CHR és a Q a XO által katalizált xantin oxidáció erős gátlószerei (Cos és mtsai., 1998; Nagao és mtsai., 1999; Lin és mtsai., 2015a, b). Egyes közleményekben a CHR és a Q a pozitív kontrollként alkalmazott APU-hoz képest gyengébb (Iio és mtsai., 1985; Cos és mtsai., 1998; Lin és mtsai., 2002), míg más vizsgálatokban erősebb (Van Hoorn és mtsai., 2002; Lin és mtsai., 2015a, b) gátlószereknek bizonyultak. Emellett a flavonoidok *in vivo* xantin oxidációt gátló hatása a jelenlegi információk alapján kérdéses (Zhu és mtsai., 2004; Sarawek és mtsai., 2008; Huang és mtsai., 2011).

A CHR és a Q import és export transzporterekkel is kölcsönhatásba lépnek (Alvarez és mtsai., 2010; Miron és mtsai., 2017). Például a CHR szubsztrátja lehet egyes transzportereknek, mint az MRP2 és a BCRP (Walle, 2007; Ge és mtsai., 2015), továbbá patkányokban képes gátolni a nitrofurantoin és a topotecan BCRP-mediált transzportját (Alvarez és mtsai., 2010). Egyes kutatási eredmények alapján pedig az is feltételezhető, hogy a CHR konjugátumok is szubsztrátjai lehetnek az MRP2 és/vagy BCRP transzportereknek (Walle és mtsai., 1999; Ge és mtsai., 2015; Walle, 2007; Li és mtsai., 2015). Továbbá, a Q az OATP transzporterek számos típusát képes gátolni (Wu és mtsai., 2011; Mandery és mtsai., 2014), míg a Q3'S és a Q3G a szerves anion transzporterek (OAT) erős *in vitro* gátlószereinek bizonyultak (Wong és mtsai., 2011; Li és mtsai., 2012; Miron és mtsai., 2017). Korábbi vizsgálatok alapján a Q szubsztrátja és gátlószere is a BCRP és az MRP2 transzportereknek (Sesink és mtsai., 2005; Alvarez és mtsai., 2010; An és mtsai., 2011) és gátló hatását a P-gp transzporter kapcsán is leírták (Morris és Zhang, 2006; Shin és mtsai., 2006).

III. Célkitűzések

A CHR és a Q farmakokinetikai interakcióit számos közlemény taglalja, azonban konjugált metabolitjaik kapcsán csak kevés információ áll rendelkezésre. Ez azért is fontos, mert a konjugátumok – a CHR és a Q jelentős preszisztémás eliminációja révén – jóval magasabb koncentrációkat érhetnek el a keringésben (és feltehetőleg egyes szövetekben is) anyavegyületükhöz képest. Kísérleteim során ezért célul tűztem ki, hogy:

1. Megvizsgáljam a CHR konjugátumok kölcsönhatásait HSA-nal, beleértve a kötési állandók meghatározását, valamint a különböző site markerekkel szembeni leszorítóképességüket.

2. Beállítsak és optimalizáljak különböző *in vitro* CYP enzim esszéket és megvizsgáljam a CHR és a Q konjugátumok kölcsönhatásait CYP2C9, CYP2C19, CYP2D6 és CYP3A4 enzimekkel.

3. Beállítsak és optimalizáljak *in vitro* enzim esszéket a XO enzim gátlásának vizsgálatához 6-MP, xantin és hipoxantin szubsztrátokkal. Továbbá ezekkel a módszerekkel teszteljem a CHR és a Q konjugátumok XO enzimre kifejtett hatásait.

IV. Anyagok és módszerek

IV.1. Reagensek

In vitro kísérleteink során minden esetben analitikai vagy spektroszkópiai tisztaságú vegyszereket alkalmaztunk. A chrysint (CHR), a quercetint (Q), a humán szérum albumint (HSA), a warfarint, a naproxent, a xantin-oxidáz enzimet (XO), a CypExpress^{TM} humán enzim kiteket (2C9, 2C19, 2D6 és 3A4), a hipoxantint, a xantint, a húgysavat, az oxipurinolt, a 6-mercaptopurint (6-MP), az allopurinolt (APU), a testosteront, a 6β-hydroxytestosteront, a ticlopidin-hydrochloridot, a ketoconazolt és a quinidint a Sigma-Aldrich Kft-től (St. Louis, Missouri, Amerikai Egyesült Államok) vásároltuk. A chrysin-7-glükuronid (C7G), a diclofenac, a 4'-hydroxydiclofenac, az *S*-mephenytoin, a 4-hydroxymephenytoin, a sulfaphenazol, a dextromethorphan, a dextrorphan, és a 6-thiohúgysav beszerzése a Carbosynth-től (Berkshire, Egyesült Királyság) történt, míg a 6-thioxantint az 5A Pharmatech-től (Wuhan Hubei, Kína) vásároltuk. A glükóz-6-foszfátot (G6P) és nikotinamid-adenin-dinukleotid-foszfátot ($NADP^+$) a Reanal Laborvegyszer Kereskedelmi Kft.-től (Budapest, Magyarország) szereztük be. A quercetin-3'-szulfát (Q3'S), a quercetin-3-glükuronid (Q3G) és az isorhamnetin-3-glükuronid (I3G) szintézise a korábbiakban közölt módszer alapján történt (Needs és Kroon, 2006). Az isorhamnetint (IR) és a tamarixetint (TAM) az Extrasynthestől (Genay Cedex, Franciaország) vásároltuk. A chrysin-7-szulfát (C7S) szintézise a korábban közölt módszer alapján történt (Huang és mtsai., 2006; Mohos és mtsai., 2018a). A flavonoidokat és metabolitjaikat dimetil-szulfoxidban oldottuk (DMSO) és -20 °C-on, fénytől védve tároltuk.

IV.2. Spektroszkópiai mérések

A fluoreszcencia spektroszkópiai méréseinkhez egy Hitachi F-4500 fluorimétert (Tokió, Japán) használtunk. Méréseinket PBS pufferben (phosphate buffered saline; pH 7,4) szobahőmérsékleten végeztük. A tesztelt flavonoidok abszorpciós spektrumait is felvettük, melynek során egy HALO DB-20 UV-Vis spektrofotométert (Dynamica, London, Egyesült Királyság) használtunk. Mivel a flavonoidok belső szűrő hatása/effektusa csökkenheti az albumin fluoreszcencia emissziós jelét, a fluoreszcenciás spektrumokat az alábbi egyenlettel korrigáltuk (Larsson és mtsai., 2007):

$$I_{korr} = I_m \times e^{(A_{ex}+A_{em})/2} \qquad (1)$$

ahol I_{korr} a korrigált, I_m pedig a mért fluoreszcencia emissziós intenzitás, míg az A_{ex} és az A_{em} a tesztvegyületek abszorbancia értékeit jelöli az alkalmazott excitációs és emissziós hullámhosszokon.

Az albumin-ligandum kölcsönhatások tesztelésére fluoreszcencia kioltás típusú vizsgálatokat alkalmaztunk (Poór és mtsai, 2018a). Ennek során standard mennyiségű albuminhoz (2 μM) a flavonoidok emelkedő mennyiségeit (0; 0,5; 1,0; 2,0; 3,0; 4,0 és 5,0 μM) adtuk, majd a mintákat 295 nm-en gerjesztve, felvettük az albumin emissziós spektrumát. Az értékelést a 340 nm-en mért fluoreszcencia emissziós intenzitások alapján végeztük.

A flavonoid-albumin interakciók kiértékelése a Stern-Volmer egyenlet segítségével történt (Poór és mtsai., 2018a):

$$\frac{I_0}{I} = 1 + K_{SV} \times [Q] \qquad (2)$$

ahol I_0 az albumin fluoreszcencia emissziós intenzitása 340 nm-en (flavonoidok nélkül), míg I a fehérje 340 nm-en mért emissziós intenzitása flavonoidok jelenlétében. A K_{SV} a Stern-Volmer kioltási konstans (L/mol), a *[Q]* pedig a flavonoidok moláris koncentrációja (mol/L). Az albumin-ligandum komplexek kötési állandóit (*K*) nem-lineáris illesztéssel a Hyperquad2006 szoftver segítségével határoztuk meg (Poór és mtsai., 2018a).

A flavonoidok warfarinnal (Site I marker) szembeni leszorítóképességét a korábban közölt módszerrel végeztük (Poór és mtsai., 2017). A warfarin-HSA (1,0 μM warfarin és 3,5 μM HSA) komplex fluoreszcencia emissziós intenzitását mértük (λ_{ex} = 317 nm, λ_{em} = 379 nm) a flavonoidok emelkedő mennyiségei (0,0; 0,5; 1,0; 2,0; 3,0; 5,0 és 10 μM) mellett PBS pufferben (pH 7,4).

A warfarinnal szembeni leszorítóképesség tesztelésére fluoreszcencia anizotrópiai vizsgálatokat is alkalmaztunk (Poór és mtsai., 2018b). Kísérleteink során, a warfarin és a HSA standard mennyiségéhez (1,0 μM warfarin és 2,0 μM HSA) a flavonoidok emelkedő mennyiségeit (0,0; 1,0; 2,0; 5,0 és 10 μM) adtuk, majd meghatároztuk a fluoreszcencia anizotrópia értékeket (λ_{ex} = 317 nm, λ_{em} = 379 nm) az alábbi egyenlet alapján (Poór és mtsai., 2018b):

$$r = \frac{(I_{VV} - G \times I_{VH})}{(I_{VV} + 2 \times G \times I_{VH})} \qquad (3)$$

ahol az I_{VV} a minta előtti és utáni vertikális pozíciójú, míg az I_{VH} a minta előtti vertikális és a minta utáni horizontális pozíciójú polarizátorral mért emissziós intenzitás, a *G* pedig a műszer korrekciós faktora.

IV.3. Ultraszűrés

A flavonoidok leszorítóképességét Site I (warfarin) és Site II (naproxen) markerekkel szemben ultraszűréssel vizsgáltuk (Mohos és mtsai., 2018b). Kísérleteinkben 30 kDa cut-off értékű Pall Microsep™ (Pall Corporation, Ann Arbor, Michigan, Amerikai Egyesült Államok) centrifugacsöveket használtunk. A vizsgálat során a minták 1,0 µM warfarint és 5,0 µM HSA-t vagy 1,0 µM naproxent és 1,7 µM albumint tartalmaztak, flavonoidok nélkül vagy azok jelenlétében (10 µM vagy 20 µM) PBS-ben (pH 7,4). Centrifugálás előtt a filtereket egyszer 3 mL desztillált vízzel és kétszer 3 mL PBS-sel mostuk. Ezután a mintákat (2,5 mL) 10 percig 25 °C-on centrifugálással (7500 g) szűrtük. A szűrlet naproxen és warfarin tartalmát HPLC (nagyhatékonyságú folyadékkromatográfia) módszerrel határoztuk meg (lásd a pontos részleteket a IV.6. pontban).

IV.4. Xantin-oxidáz esszék

IV.4.1. Xantin-oxidáz esszé 6-mercaptopurin szubsztráttal

A CHR és a Q, valamint konjugált metabolitjaik hatásait először a gyógyszer szubsztráttal szemben vizsgáltuk (***10. ábra***). Az enzimkatalizált reakció során 5 µM 6-MP-t és 0,01 U/mL XO enzimet inkubáltunk a flavonoidok emelkedő koncentrációjának jelenlétében vagy anélkül (0-20 µM) termomixerben (700 rpm, 37 °C). Az *in vitro* közegben lejátszódó reakció során a 6-MP-ból előbb 6-thioxantin, majd 6-thiohúgysav képződik (***6. ábra***). Kísérleteink során APU-t alkalmaztunk pozitív kontrollként. A minták (500 µL) inkubálását 0,05 M nátrium-foszfát pufferben (pH 7,5) a XO enzim hozzáadásával indítottuk, majd 20, 40 és 60 perces inkubációkat követően 30 µL 6 M-os perklórsavval állítottuk le. A mintákat ezt követően alaposan vortexeltük, majd szobahőmérsékleten 5 percig centrifugáltuk (14.000 g). A centrifugálás végeztével minden mintáról 300 µL felülúszót távolítottunk el, melyhez 36 µL 1 M-os kálium-hidroxid oldatot adtunk. Ezt követően a mintákat 4 °C-ra hűtöttük (a $KClO_4$ kicsapódásának elősegítésére), majd 5 percig 4°C-on centrifugáltuk (14.000 g). A

felülúszóban a szubsztrát és a termékek kvantifikálása HPLC-UV módszerrel történt (lásd a IV.6. pontban). A kromatográfiás analízis során csak a 6-MP és a 6-thiohúgysav volt detektálható, amely valószínűleg azzal magyarázható, hogy a 6-thioxantin nem vagy csak alig disszociál le az enzimről a második oxidációs lépés előtt (Kudo és mtsai., 2010).

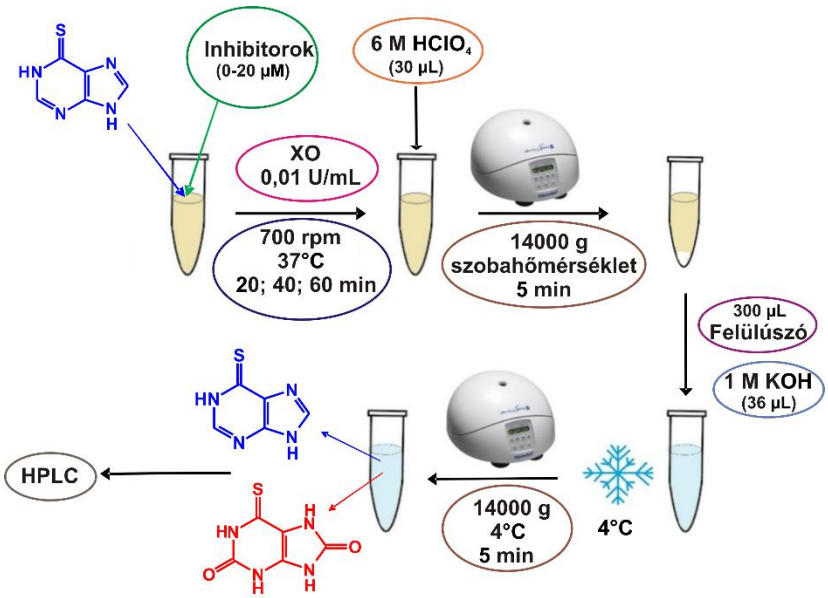

10. ábra: A XO esszé sematikus bemutatása 6-MP szubsztrát esetében.

IV.4.2. Xantin-oxidáz esszé xantin szubsztráttal

A tesztelt flavonoidok és konjugátumaik hatását az endogén szubsztráttal szemben is megvizsgáltuk (***11. ábra***). A reakció során 5 µM xantint inkubáltunk 0,0012 U/mL XO enzim, valamint emelkedő koncentrációjú inhibitorok (0-20 µM) jelenlétében termomixerben (700 rpm, 37 °C). Pozitív kontrollként APU-t alkalmaztunk. A kísérletet 0,05 M nátrium-foszfát pufferben (pH 7,5) végeztük, 500 µL-es mintatérfogattal. A reakciót az enzim hozzáadásával indítottuk, majd 4, 8 és 12 perces inkubációkat követően 30 µL 6 M-os perklórsav hozzáadásával állítottuk le. Ezekhez vortexelés után 97 µL 1 M-os kálium-hidroxid oldatot adtunk. A $KClO_4$ kicsapódásának elősegítésére a mintákat 4 °C-ra hűtöttük, majd az 5 perces centrifugálást követően (4°C, 14.000 g) a felülúszók xantin és húgysav tartalmának meghatározása HPLC-UV módszerrel történt (lásd a IV.6. pontban).

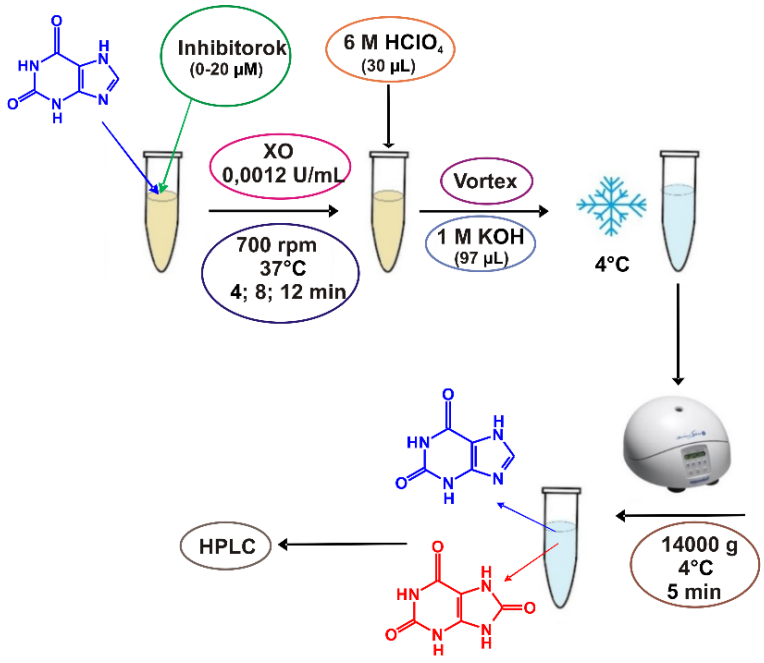

11. ábra: A XO esszé sematikus bemutatása xantin szubsztrát esetében.

IV.4.3. Xantin-oxidáz esszé hipoxantin szubsztráttal

Mivel a 6-MP két lépésben alakul át inaktív 6-thiohúgysavvá, viszont a xantin → húgysav átalakulás egylépéses folyamat, a Q és egyes Q konjugátumok hatását a hipoxantin → xantin → húgysav átalakulásra vonatkozóan is megvizsgáltuk. A hipoxantint (5 µM) 0,012 U/mL XO enzim jelenlétében inkubáltuk emelkedő koncentrációjú (0,0; 0,1; 0,5; 1,0 és 3,0 µM) Q, Q3'S, APU és oxipurinol jelenlétében. A reakciót 4 perces inkubációt követően állítottuk le. Az egyéb kísérleti paraméterek megegyeznek a IV.4.2. pontban leírtakkal. Mivel az *in vitro* reakció során az inkubátumokban a xantin és a húgysav képződés is detektálható volt, az értékelés során a képződő xantin és húgysav együttes mennyiségét vettük alapul.

IV.5. Citokróm P450 esszék

A CHR és a Q, valamint konjugátumaik CYP enzimekre kifejtett hatásainak vizsgálatára *in vitro* enzim esszéket alkalmaztunk, melynek során CypExpress™ humán enzim kiteket használtunk. Minden CYP esszé esetében az FDA (U.S. Food and Drug Administration) által javasolt szubsztrátokat (CYP2C9: diclofenac, CYP2C19: *S*-mephenytoin, CYP2D6: dextromethorphan, CYP3A4: testosteron) és pozitív kontrollokat (CYP2C9: sulfaphenazol, CYP2C19: ticlopidin, CYP2D6: quinidin, CYP3A4:

ketoconazol) alkalmaztuk. Minden kísérlet során oldószer kontrollokat is használtunk (a DMSO mennyisége egyik esetben sem haladta meg a 0,6 v/v%-ot).

IV.5.1. CYP2C9 esszé

Az *in vitro* esszék során az inkubátumok 5 μM diclofenac (szubsztrát) és 6 mg/mL CypExpress™ 2C9 reagenst tartalmaztak az inhibitorok emelkedő koncentrációinak (0-30 μM) jelenlétében. A CYP2C9-katalizált reakciót 0,05 M kálium-foszfát pufferben (pH 7,5; minták végtérfogata: 200 μL) az enzim hozzáadásával indítottuk, majd a mintákat 120 percig inkubáltuk termomixerben (700 rpm, 30 °C). Ezt követően a reakció leállítása 100 μL hideg metanollal történt, majd a mintákat vortexeltük és szobahőmérsékleten 10 percig centrifugáltuk (14.000 g). A felülúszóból a szubsztrát (diclofenac) és a termék (4'-hydroxydiclofenac) meghatározása HPLC-UV módszerrel történt (lásd a IV.6. pontban).

IV.5.2. CYP2C19 esszé

A kísérlet során a minták 5 μM *S*-mephenytoint (szubsztrát), 15 mg/mL CypExpress™ 2C19 reagenst, 200 μM $NADP^+$-t és 500 μM G6P-ot tartalmaztak az inhibitorok növekvő koncentrációinak (0-30 μM) jelenlétében. Az inkubációt 0,05 M kálium-foszfát pufferben (pH 7,5) az enzim hozzáadásával indítottuk (minták végtérfogata: 200 μL), majd a mintákat 120 percig inkubáltuk termomixerben (600 rpm, 30 °C). Az enzimkatalizált reakciót 100 μL hideg metanol hozzáadásával állítottuk le, majd alapos vortexelést követően a mintákat szobahőmérsékleten 10 percig centrifugáltuk (14.000 g). A felülúszó *S*-mephenytoin és 4-hydroxymephenytoin tartalmát HPLC-UV módszerrel határoztuk meg (lásd a IV.6. pontban).

IV.5.3. CYP2D6 esszé

A CYP2D6-katalizált reakció során 5 μM dextromethorphant (szubsztrát) inkubáltunk 10 mg/mL CypExpress™ 2D6 reagens, 200 μM $NADP^+$, 500 μM G6P és emelkedő inhibitor koncentrációk (0-30 μM) jelenlétében, 0,05 M kálium-foszfát pufferben (pH 7,5; minták végtérfogata: 200 μL). Az inkubációt termomixerben (600 rpm, 30 °C, 20 min) végeztük, az enzim hozzáadásával indítottuk és 100 μL hideg metanollal állítottuk le. Ezt követően a mintákat alaposan vortexeltük, majd 10 percig szobahőmérsékleten centrifugáltuk (14.000 g). A felülúszóban a dextromethorphan és dextrorphan mennyiségi meghatározása HPLC-UV módszerrel történt (lásd a IV.6. pontban).

IV.5.4. CYP3A4 esszé

Az esszék során (***12. ábra***) a minták 5 µM testosteront (szubsztrát), 15 mg/mL CypExpress™ 3A4 reagenst, 200 µM $NADP^+$-t és 500 µM G6P-ot tartalmaztak, emelkedő flavonoid koncentrációk (0-30 µM) jelenlétében. A reakciót az enzim hozzáadásával, 0,05 M kálium-foszfát pufferben (pH 7,5; minták végtérfogata: 200 µL) indítottuk, majd a mintákat 180 percig inkubáltuk termomixerben (600 rpm, 30 °C), végül 100 µL hideg metanollal állítottuk le. Ezt követően a mintákat vortexeltük és centrifugáltuk (10 min, 14.000 g, 25 °C), majd a felülúszóban a szubsztrát és a termék kvantifikálása HPLC-UV módszerrel történt (lásd a IV.6. pontban).

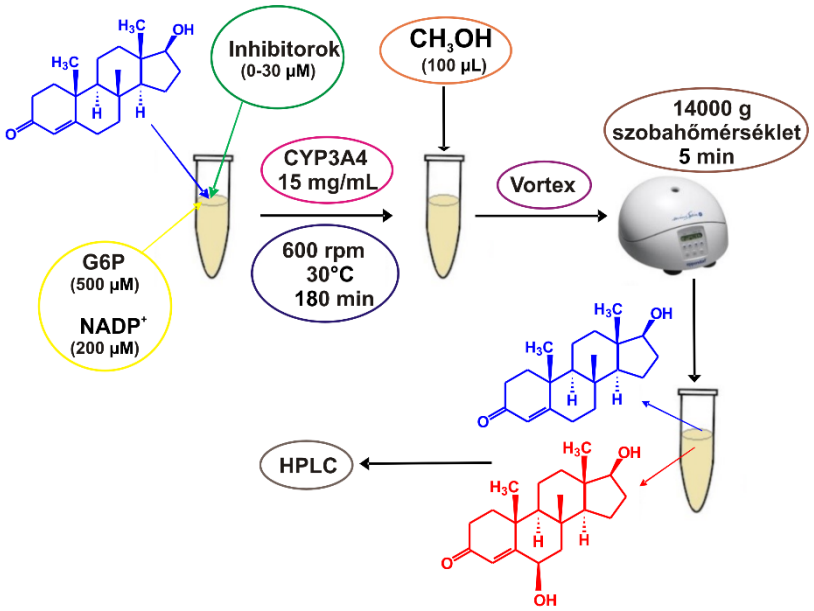

12. ábra: A CYP3A4 esszé sematikus bemutatása.

IV.6. HPLC analízis

A HPLC analízisekhez az alábbi rendszert alkalmaztuk: pumpa (Waters 510), injektor (Rheodyne 7125), UV detektor (Waters 486) és fluoreszcens detektor (Jasco FP-920, Reanal). Az analízisek során minden esetben 20 µL mintát injektáltunk. A kromatográfiás adatok rögzítése és kiértékelése a Millenium Chromatographic Managers szoftver (Waters) segítségével történt.

A szűrlet warfarin tartalmának mennyiségi meghatározása a következő módszer alapján történt: az elválasztást egy Phenomenex Security Guard™ C18 (4,0 × 3,0 mm) előtétoszlophoz kapcsolt Nova-Pak C18 (150 × 3,9 mm, 4 µm) analitikai oszlop

felhasználásával végeztük. A mobilfázis metanolt, acetonitrilt és 20 mM nátrium-foszfát puffert (pH 7,0) tartalmazott (25:5:70 v/v%). Az izokratikus elúciót 1,0 mL/min áramlási sebesség mellett, szobahőmérsékleten végeztük, a warfarint 310 nm excitációs és 390 nm emissziós hullámhosszokon detektáltuk.

A naproxen kvantifikálása az alábbi módszert felhasználva történt: az izokratikus elúció során az eluens acetonitrilt és nátrium-acetát puffert (6,9 mM, pH 4,0) tartalmazott (50:50 v/v%). Az elúciót egy Phenomenex Security Guard™ C18 (4,0 × 3,0 mm) előtétoszlop és egy Gemini C18 (150 × 4,6 mm, 3 μm) analitikai oszlop segítségével végeztük, szobahőmérsékleten, 1,0 mL/min áramlási sebességgel. A naproxen detektálása 230 nm-en történt.

A xantin, hipoxantin és húgysav mennyiségi meghatározása során a következő módszert alkalmaztuk: az elválasztást Phenomenex Security Guard™ C18 (4,0 × 3,0 mm) előtétoszlophoz kapcsolt Phenomenex C18 (250 × 4,6 mm, 5 μm) analitikai oszlop felhasználásával végeztük. Az izokratikus elúció során 0,01 M-os nátrium-foszfát puffert (pH 4,55) és metanolt tartalmazó (98:2 v/v%) mobil fázist használtunk. Az elválasztás szobahőmérsékleten, 1,1 mL/min áramlási sebességgel történt. A hipoxantint, xantint és húgysavat 275 nm-en detektáltuk.

A 6-MP és a 6-thiohúgysav kvantifikálása során az eluens metanolt, acetonitrilt és 0,02 M foszforsavat tartalmazott (4:5:91 v/v%). Az izokratikus elúciót egy Phenomenex Security Guard™ C18 (4,0 × 3,0 mm) előtétoszlophoz kapcsolt Phenomenex Gemini NX-C18 (150 × 4,6 mm, 3 μm) analitikai oszlop segítségével végeztük. Az elválasztás 0,8 mL/min áramlási sebesség alkalmazásával, szobahőmérsékleten történt, a 6-MP és 6-thiohúgysav detektálását 334 nm-en végeztük.

A diclofenac és a 4'-hydroxydiclofenac mennyiségi meghatározása során az izokratikus elúció egy Phenomenex Security Guard™ C8 (4,0 × 3,0 mm) előtétoszlophoz kapcsolt Eclipse C8 (150 × 4,6 mm, 5 μm) analitikai oszlop alkalmazásával történt. A mobil fázis acetonitrilt és 6 mM-os ortofoszforsav oldatot tartalmazott (52:48 v/v%). Az elválasztás 1,0 mL/min áramlási sebességgel, szobahőmérsékleten történt, a diclofenacot és a 4'-hydroxydiclofenacot 275 nm-en detektáltuk.

Az *S*-mephenytoin és a 4-hydroxymephenytoin kvantifikálása a következők szerint történt: az izokratikus elúció során használt mobilfázis acetonitrilt, metanolt és nátrium-foszfát puffert (10 mM, pH 4,55) tartalmazott (20:15:65 v/v%). Az elválasztást egy Phenomenex Security Guard™ C8 (4,0 × 3,0 mm) előtétoszlophoz kapcsolt Phenomenex C8 (100 × 4,6 mm, 2,6 μm) analitikai oszlop segítségével végeztük. Az elúció

szobahőmérsékleten, 1,0 mL/min áramlási sebességgel történt. Az *S*-mephenytoint és a 4-hydroxymephenytoint 275 nm-en detektáltuk. A Q és konjugált metabolitjai esetén koelúció miatt az eluens összetételét módosítani kellett, ezért ebben az esetben a mobil fázis 17:10:73 v/v% arányban tartalmazott acetonitrilt, metanolt és nátrium-foszfát puffert (10 mM, pH 4,55). A HPLC-módszer további paraméterei nem változtak.

A dextromethorphan és a dextrorphan mennyiségi meghatározása során az elválasztást egy Phenomenex Security Guard™ C8 (4,0 × 3,0 mm) előtétoszlophoz kapcsolt Teknokroma Mediterranea Sea8 C8 (150 × 4,6 mm, 5 μm) analitikai oszlop felhasználásával végeztük. A mobilfázis nátrium-acetát puffert (6,9 mM, pH 4,0) és acetonitrilt tartalmazott (69:31 v/v%). Az izokratikus elúciót szobahőmérsékleten, 1,0 mL/min áramlási sebesség alkalmazása mellett végeztük, a dextromethorphant és a dextrorphant 280 nm-en detektáltuk. Mivel a C7G koeluálódott a metabolittal, a C7G-ot tartalmazó minták analízise egy módosított eluenssel ment végbe, mely nátrium-acetát puffert (6,9 mM, pH 4,0) és metanolt tartalmazott (72:28 v/v%). A módszer további paramétereit nem módosítottuk.

A testosteron és a 6β-hydroxytestosteron mennyiségi meghatározása az alábbiak szerint történt: az izokratikus elúció során a mobil fázis metanolt, vizet és ecetsavat tartalmazott (59:40:1 v/v%). Az elválasztást egy Phenomenex Security Guard™ C18 (4,0 × 3,0 mm) előtétoszloppal és egy Kinetex EVO C18 (150 × 4,6 mm, 5 μm) analitikai oszloppal, szobahőmérsékleten, 1,2 mL/min áramlási sebességgel végeztük. A testosteront és a 6β-hydroxytestosteront 240 nm-en detektáltuk. A Q és konjugátumai esetében koelúciót tapasztaltunk, ezért az eluens módosítása volt szükséges: metanol, víz és ecetsav (53:46:1 v/v%). A HPLC-módszer egyéb paramétereit nem változtattuk.

IV.7. Statisztikai értékelés és IC_{50} értékek meghatározása

Az ábrákon és a táblázatokban feltüntetett eredmények a minimum három független kísérletből kapott adatok átlagát és a hozzájuk tartozó standard hibát (SEM) demonstrálják. A statisztikai értékelés one-way ANOVA (és Tukey's post-hoc) teszttel történt, IBM SPSS Statistics (IBM) szoftver (Armonk, New York, Amerikai Egyesült Államok) felhasználásával ($^*p < 0,05$ és $^{**}p < 0,01$). Az IC_{50} értékeket logaritmikus ábrázolást követően szigmoid illesztéssel határoztuk meg, a GraphPad Prism 8 (San Diego, Kalifornia, Amerikai Egyesült Államok) szoftver segítségével.

V. Eredmények

V.1. Chrysin és konjugátumainak kölcsönhatásai szérum albuminnal

A CHR, C7S és C7G albumin komplexeinek stabilitását fluoreszcencia kioltás alapú módszerrel teszteltük. A CHR és konjugátumai koncentrációfüggő módon, szignifikánsan csökkentették a HSA fluoreszcencia emissziós jelét 340 nm-en (***13./A ábra***; λ_{ex} = 295 nm). A CHR-hez képest a glükuronid konjugátum gyengébb, míg a szulfát metabolit erősebb kioltó hatást mutatott. A Stern-Volmer egyenlet grafikus ábrázolása során az adatok jó illeszkedést mutattak az 1:1 sztöchiometriájú modellel (***13./B ábra***). Vizsgálataink során a flavonoid-albumin komplexek Stern-Volmer kioltási állandóit (K_{SV}) a Stern-Volmer egyenlet grafikus ábrázolásával, míg a kötési állandókat (K) a Hyperquad2006 szoftver segítségével határoztuk meg. A K_{SV} és a K értékek alapján a C7S képezte a legstabilabb komplexet albuminnal, melyet a CHR-albumin és C7G-albumin komplexek követtek (***1. táblázat***). C7S-HSA komplex esetében kb. 3-szor nagyobb, míg a C7G-HSA esetén közel 3-szor kisebb kötési állandó értéket tapasztaltunk a CHR-HSA komplexhez viszonyítva.

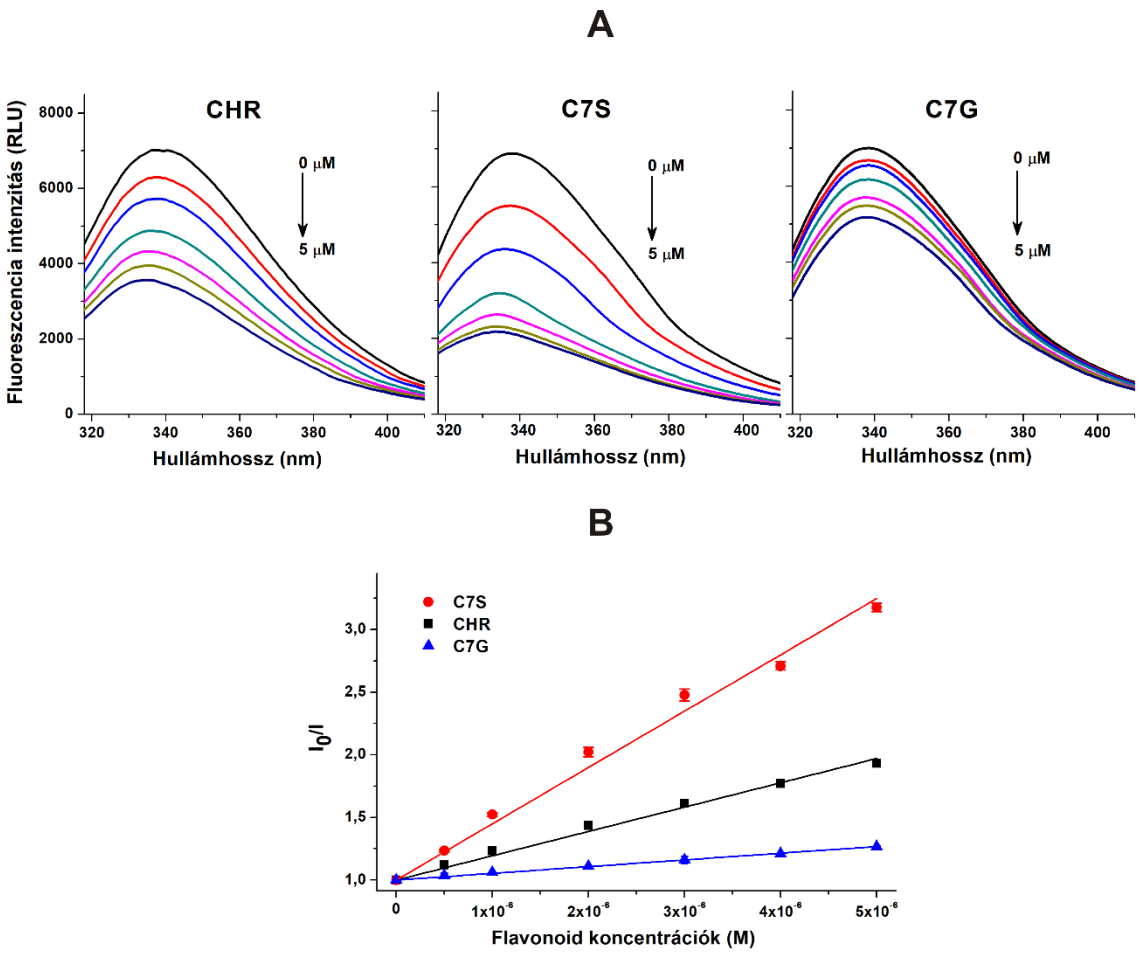

13. ábra: (A) A HSA (2 μM) fluoreszcencia emissziós spektruma (λ_{ex} = 295 nm) emelkedő koncentrációjú (0,0; 0,5; 1,0; 2,0; 3,0; 4,0 és 5,0 μM) CHR, C7S és C7G jelenlétében PBS-ben (pH 7,4). ***(B)*** A flavonoid-HSA komplexek Stern-Volmer függvényei (λ_{ex} = 295 nm, λ_{em} = 340 nm; CHR: chrysin, C7S: chrysin-7-szulfát, C7G: chrysin-7-glükuronid).

Komplex	**logK_{SV}**	**log$K$**
CHR-HSA	5,25 ± 0,02	5,41 ± 0,01
C7S-HSA	5,61 ± 0,03	5,88 ± 0,02
C7G-HSA	4,71 ± 0,03	4,89 ± 0,00

1. táblázat: A flavonoid-HSA komplexek Stern-Volmer kioltási állandó (K_{SV}; mértékegység: L/mol) és kötési állandó (K; mértékegység: L/mol) értékeinek tízes alapú logaritmusai (CHR: chrysin, C7S: chrysin-7-szulfát, C7G: chrysin-7-glükuronid, HSA: humán szérum albumin).

A következő ultraszűréses kísérletekben megvizsgáltuk a CHR és konjugátumainak leszorítóképességét warfarinnal és naproxennel szemben. A kísérlet során 30 kDa cut-off értékű filtercsöveket használtunk, melyeken az albumin és az albumin-kötött molekulák méretükből adódóan nem képesek átjutni. A C7G nem, a CHR pedig csak magasabb koncentrációban (20 µM) növelte szignifikánsan a warfarin mennyiségét a szűrletben, míg a C7S már az alacsonyabb alkalmazott koncentrációban (10 µM) is jelentős növekedést okozott (***14./A ábra***). Érdekes módon a CHR és konjugált metabolitjai a Site II marker naproxen mennyiségét is megemelték a szűrletben: a CHR és szulfát konjugátuma már kisebb koncentrációban (10 µM) is, míg a C7G csak magasabb mennyiségben (20 µM) okozott szignifikáns hatást (***14./B ábra***).

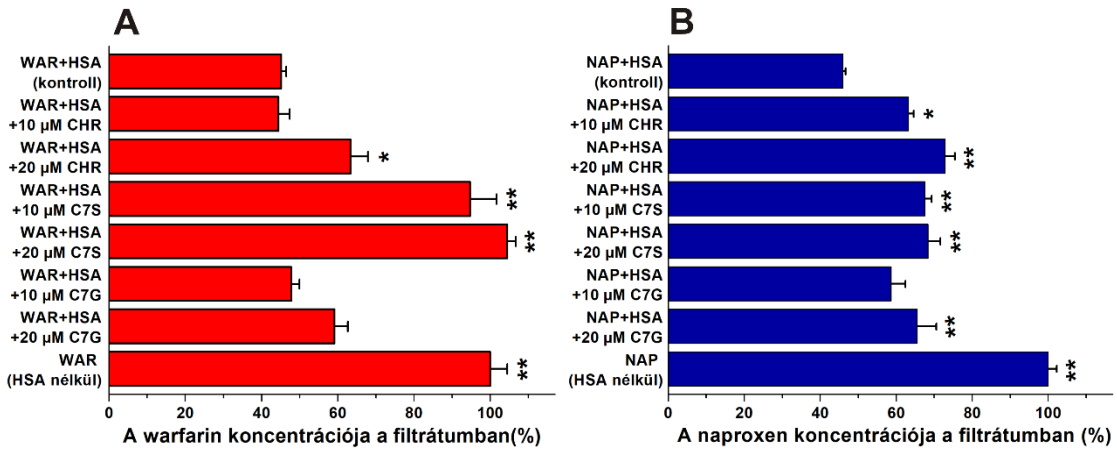

14. ábra: A warfarin ***(A)*** és a naproxen ***(B)*** koncentrációi a filtrátumban CHR, C7S és C7G jelenlétében. Az ultraszűrés előtt a minták 1,0 µM warfarint és 5,0 µM HSA-t vagy 1,0 µM naproxent és 1,7 µM HSA-t tartalmaztak 0, 10 vagy 20 µM flavonoid koncentrációk jelenlétében (*$p < 0,05$; **$p < 0,01$; CHR: chrysin, C7S: chrysin-7-szulfát, C7G: chrysin-7-glükuronid, HSA: humán szérum albumin, WAR: warfarin, NAP: naproxen).

Az ultraszűréses eredményekre alapozva a flavonoidok leszorítóképességét warfarinnal szemben további, fluoreszcencia spektroszkópiai módszerekkel is teszteltük. Kísérleteink első felében a flavonoidok emelkedő koncentrációit (0-10 µM) adtuk a warfarin (1 µM) és a HSA (3,5 µM) standard mennyiségéhez, majd a warfarin-albumin komplex fluoreszcencia emissziós intenzitását 379 nm-en (az albuminkötött warfarin emissziós maximuma) vizsgáltuk. Mivel a warfarin-albumin komplex fluoreszcencia

emissziós intenzitása jóval magasabb, mint a szabad warfariné, a site marker albuminról történő leszorítása jelentős fluoreszcencia csökkenést okoz. Mindhárom vizsgált flavonoid szignifikánsan csökkentette a warfarin-HSA komplex emissziós intenzitását: a C7S okozta a legnagyobb csökkenést, ezt követte a CHR és a C7G (***15./A ábra***). A glükuronid konjugátum statisztikailag ugyan szignifikáns, de gyenge leszorító hatást mutatott (***15./A ábra***).

A CHR és konjugátumainak hatását a warfarin albuminkötődésére fluoreszcencia anizotrópia módszerrel is teszteltük. Ennek során a warfarin anizotrópia értékeit egy warfarint (1 µM) és HSA-t (2 µM) tartalmazó oldatban vizsgáltuk, emelkedő flavonoid koncentrációk jelenlétében (0-5 µM). A fluoreszcencia anizotrópia a molekulák rotációs szabadságáról ad információt. Vizsgálataink során a C7G nem, míg a CHR és a C7S a warfarin fluoreszcencia anizotrópia értékeinek jelentős csökkenését okozta (***15./B ábra***).

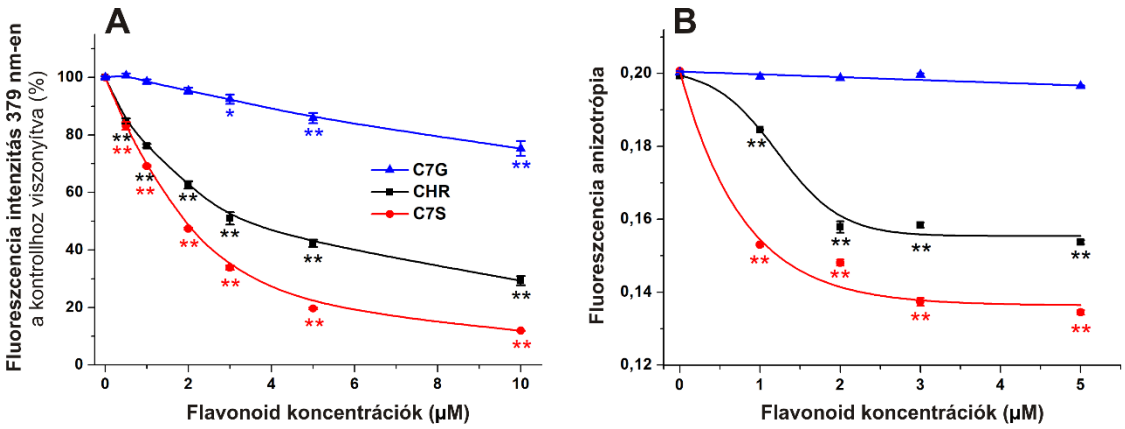

15. ábra: (A) A warfarin-HSA komplex (1,0 µM warfarin és 3,5 µM HSA) fluoreszcencia emissziós intenzitásának koncentrációfüggő csökkenése emelkedő flavonoid koncentrációk (0,0; 0,5; 1,0; 2,0; 3,0; 5,0 és 10,0 µM) jelenlétében. ***(B)*** A warfarin-HSA komplex (1,0 µM warfarin és 2,0 µM HSA) fluoreszcencia anizotrópia értékei CHR, C7S és C7G emelkedő koncentrációinak (0,0; 1,0; 2,0; 3,0 és 5,0 µM) jelenlétében (λ_{ex} = 317 nm, λ_{em} = 379 nm; *p < 0,05; **p < 0,01; CHR: chrysin, C7S: chrysin-7-szulfát, C7G: chrysin-7-glükuronid).

V.2. A chrysin és quercetin konjugátumok kölcsönhatásai CYP enzimekkel

V.2.1. A chrysin konjugátumok kölcsönhatásai CYP2C9, CYP2C19, CYP3A4 és CYP2D6 enzimekkel

A CHR és konjugált metabolitjainak hatását a különböző CYP (2C9, 2C19, 2D6 és 3A4) enzimekre a ***16. ábra*** mutatja be. Annak ellenére, hogy a C7G még a szubsztráthoz viszonyított 6-szoros koncentrációban (30 μM) sem gátolta a CYP2C9-katalizált 4'-hydroxydiclofenac képződést, a CHR és a C7S potens gátló hatást mutattak (***16./A ábra***): a CHR csak 2,5-szer (IC_{50} = 3,2 μM), míg a C7S mindössze 2-szer (IC_{50} = 2,7 μM) gyengébben gátolta a CYP2C9 enzimet, mint a pozitív kontroll (sulfaphenazol; IC_{50} = 1,3 μM). A szulfát konjugátum tehát még az anyavegyületnél is erősebb gátlószernek bizonyult (***16./A ábra***).

A 4-hydroxymephenytoin CYP2C19-katalizált képződését a C7G és a C7S statisztikailag ugyan szignifikánsan, de gyengén gátolták (***16./B ábra***). Ezzel szemben az anyavegyület (IC_{50} = 4,6 μM) a pozitív kontroll ticlopidinhez (IC_{50} = 4,4 μM) hasonlóan, erős gátló hatást fejtett ki az enzimre (***16./B ábra***).

A CHR és konjugátumai az alkalmazott kísérleti körülmények között nem befolyásolták a CYP2D6-katalizált dextrorphan képződést (***16./C ábra***), a testosteron CYP3A4 általi hidroxilációját pedig nem (C7G) vagy csak kisebb mértékben (CHR, C7S) gátolták az alkalmazott körülmények között (***16./D ábra***).

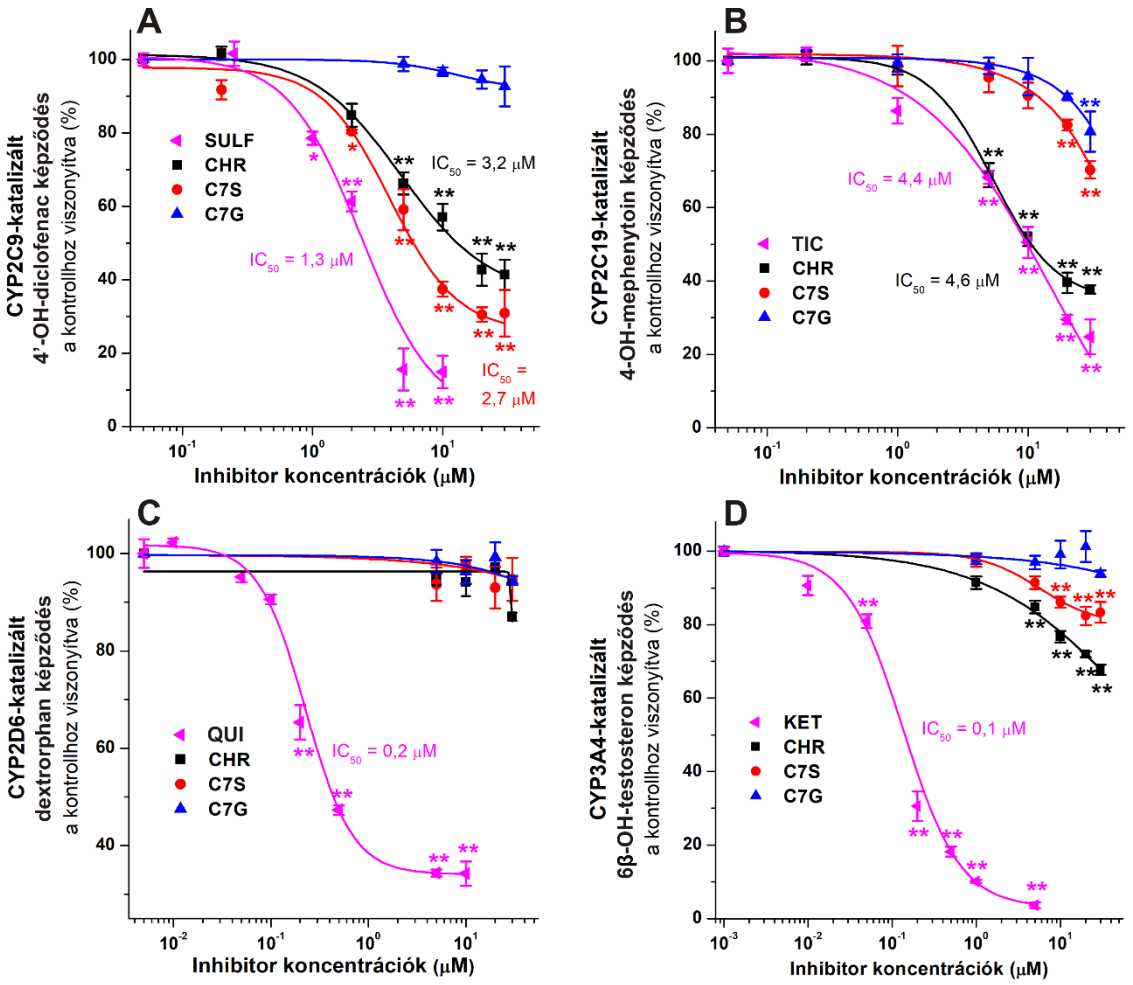

16. ábra: A CHR, C7S, C7G és a pozitív kontrollok hatása a CYP enzimekre: ***(A)*** A CYP2C9-katalizált 4'-hydroxydiclofenac képződés, emelkedő inhibitor koncentrációk jelenlétében (0-30 µM), 120 perces inkubációt követően. ***(B)*** A CYP2C19-katalizált 4-hydroxymephenytoin képződés, emelkedő inhibitor koncentrációk jelenlétében (0-30 µM), 120 perces inkubációt követően. ***(C)*** A CYP2D6-katalizált dextrorphan képződés, emelkedő inhibitor koncentrációk jelenlétében (0-30 µM), 20 perces inkubációt követően. ***(D)*** A CYP3A4-katalizált 6β-hydroxytestosteron képződés, emelkedő inhibitor koncentrációk jelenlétében (0-30 µM), 180 perces inkubációt követően (*p < 0,05; **p < 0,01; CHR: chrysin, C7S: chrysin-7-szulfát, C7G: chrysin-7-glükuronid, 4'-OH-diclofenac: 4'-hydroxydiclofenac, 4-OH-mephenytoin: 4-hydroxymephenytoin, 6β-OH-testosteron: 6β-hydroxytestosteron, SULF: sulfaphenazol, TIC: ticlopidin, QUI: quinidin, KET: ketoconazol).

V.2.2. A quercetin konjugátumok kölcsönhatásai CYP2C19, CYP3A4 és CYP2D6 enzimekkel

A Q és konjugátumainak hatását a CYP2C19-katalizált 4-hydroxymephenytoin, a CYP2D6-katalizált dextrorphan és a CYP3A4-katalizált 6β-hydroxytestosteron képződésre nézve is megvizsgáltuk (***17. ábra***). Az összes tesztelt flavonoid koncentrációfüggő módon, már 5-20 μM-os koncentrációkban szignifikánsan gátolta a CYP2C19 és CYP3A4 enzimeket (***17./A és 17./B ábrák***). A Q konjugátumok hasonló mértékű gátlást okoztak, mint az anyavegyület, de a pozitív kontrollokhoz (ticlopidin, ketoconazol) képest csak gyenge gátlószernek bizonyultak. Az alkalmazott kísérleti körülmények között, a tesztelt flavonoidok a szubsztrátokhoz viszonyított 6-szoros koncentrációban (30 μM) a metabolit képződés 25-35 %-os (CYP2C19 esszé) valamint 30-45%-os (CYP3A4 esszé) csökkenését okozták (***17./A és B ábrák***). Azonban a Q és konjugátumai nem befolyásolták szignifikáns módon a CYP2D6 enzimet (***17./C ábra***).

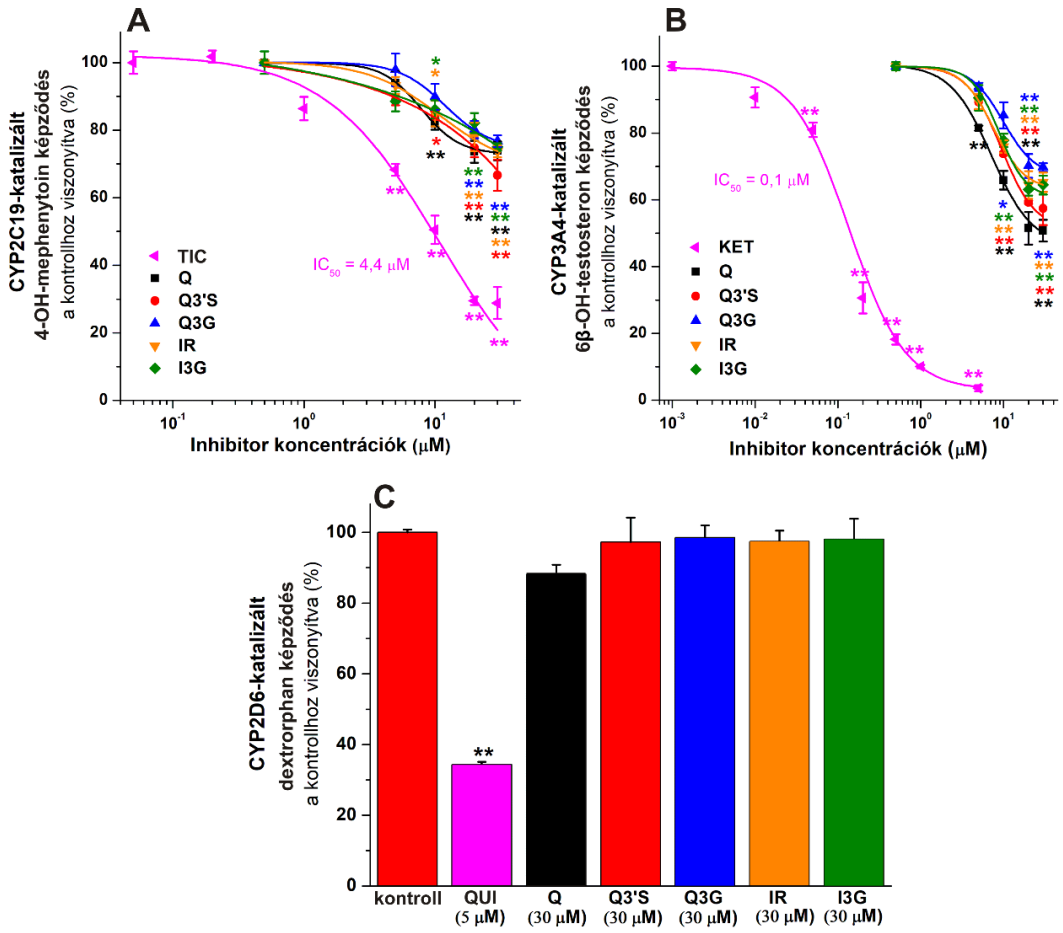

17. ábra: A Q, a Q konjugátumok és a pozitív kontrollok hatásai a CYP enzimeken: ***(A)*** A CYP2C19-katalizált 4-hydroxymephenytoin képződés, emelkedő inhibitor koncentrációk jelenlétében (0-30 μM), 120 perces inkubációt követően. ***(B)*** A CYP3A4-katalizált 6β-hydroxytestosteron képződés, emelkedő inhibitor koncentrációk jelenlétében (0-30 μM), 180 perces inkubációt követően. ***(C)*** A CYP2D6-katalizált dextrorphan képződés, 30 μM inhibitor koncentrációk jelenlétében, 20 perces inkubációt követően (*p < 0,05; **p < 0,01; Q: quercetin, Q3'S: quercetin-3'-szulfát, Q3G: quercetin-3-glükuronid, IR: isorhamnetin, I3G: isorhamnetin-3-glükuronid, 4-OH-mephenytoin: 4-hydroxymephenytoin, 6β-OH-testosteron: 6β-hydroxytestosteron, TIC: ticlopidin, KET: ketoconazol, QUI: quinidin).

V.3. Chrysin és quercetin konjugátumok kölcsönhatásai xantin-oxidáz enzimmel

V.3.1. Chrysin és konjugátumainak kölcsönhatásai xantin-oxidáz enzimmel

Mivel az oxipurinol a terápiásan alkalmazott APU farmakológiailag aktív metabolitja, az anyavegyület és a metabolit hatásait is teszteltük a XO enzimen. Meglepő módon, eredményeink azt mutatták, hogy az oxipurinol szignifikánsan gyengébb inhibitora volt a 6-MP és a xantin oxidációjának is, mint az APU (***18. ábra***). Tekintettel arra, hogy a metabolit lényegesen gyengébben gátolt mindkét *in vitro* esszében, kísérleteink további fázisaiban minden esetben az APU-t használtuk pozitív kontrollként.

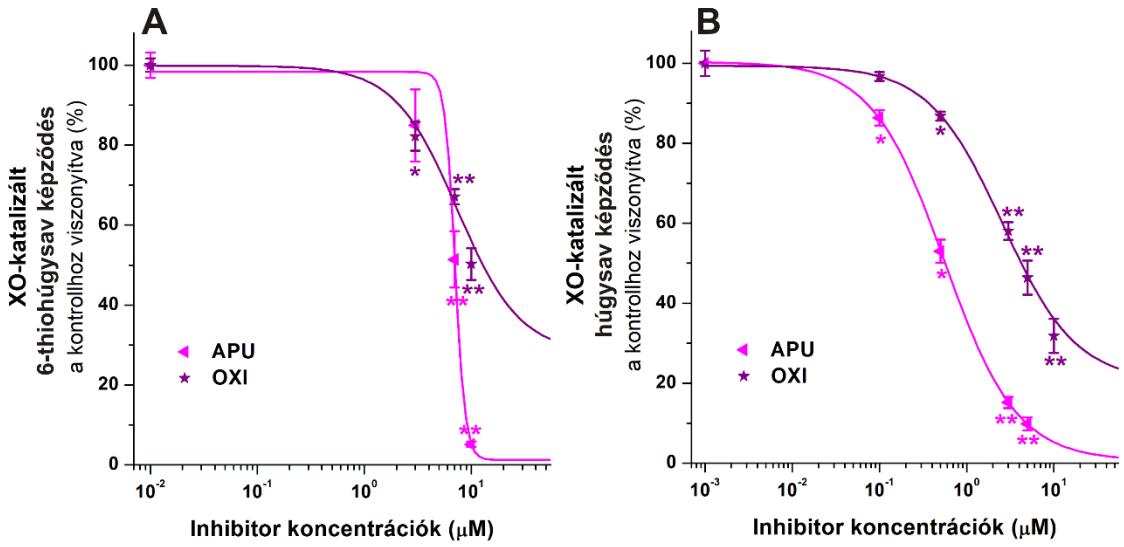

18. ábra: Az APU és az oxipurinol koncentrációfüggő gátló hatásai a 6-thiohúgysav ***(A)*** és a húgysav ***(B)*** képződésre. Az ábrák a XO-katalizált 6-thiohúgysav ***(A)*** és húgysav ***(B)*** kontrollhoz viszonyított százalékos képződését illusztrálják, emelkedő inhibitor koncentrációk jelenlétében (0-10 μM), 40 (6-MP) illetve 8 perces (xantin) inkubációt követően, logaritmikus skálán (* $p < 0,05$; ** $p < 0,01$; APU: allopurinol, OXI: oxipurinol).

Mivel a szakirodalomban a különböző tesztanyagok XO enzim gátló hatását jellemzően xantin szubsztráttal vizsgálják, kísérleteink során a 6-MP oxidációját a xantin oxidációval hasonlítottuk össze. A CHR és konjugátumainak koncentrációfüggő gátló hatását a 6-MP és a xantin oxidációra vonatkozóan a ***19. ábra*** demonstrálja. Annak

ellenére, hogy a C7S és a C7G is statisztikailag szignifikáns gátló hatást fejtettek ki a 6-MP és a xantin oxidációra, a CHR-hez képest mindkét esetben lényegesen gyengébb gátlószernek bizonyultak. A CHR a xantin oxidációt gyengébben (2-szer), míg a 6-thiohúgysav képződését lényegesen (9-szer) erősebben gátolta, mint a pozitív kontroll, APU (***19. ábra***; ***2. táblázat***). Míg az APU a xantin oxidációjára kb. 5-ször erősebb gátló hatást fejtett ki a 6-MP oxidációhoz képest, addig a CHR körülbelül 3-szor potensebb gátlószere volt a 6-MP oxidációnak a xantin oxidációhoz viszonyítva (***2. táblázat***).

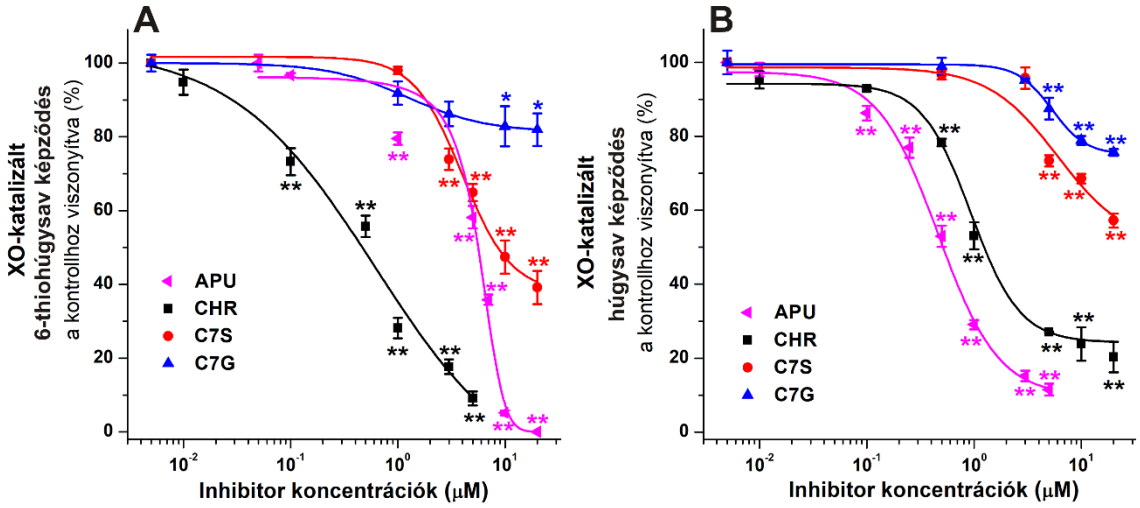

19. ábra: A CHR, a C7S, a C7G és az APU koncentrációfüggő gátló hatása a XO-katalizált 6-MP ***(A)*** és xantin ***(B)*** oxidációra (5-5 μM szubsztrát). Az ábrák a XO-katalizált 6-thiohúgysav ***(A)*** és húgysav ***(B)*** kontrollhoz viszonyított százalékos képződését illusztrálják, emelkedő inhibitor koncentrációk jelenlétében (0-20 μM), 40 (6-MP) illetve 8 perces (xantin) inkubációt követően, logaritmikus skálán (* $p < 0,05$; ** $p < 0,01$; APU: allopurinol, CHR: chrysin, C7S: chrysin-7-szulfát, C7G: chrysin-7-glükuronid).

	6-MP oxidáció		Xantin oxidáció		IC_{50}(6-MP)/ IC_{50}(xantin)
	IC_{50} (μM)	**α**	**IC_{50} (μM)**	**α**	
APU	1,97	1,00	0,38	1,00	5,18
CHR	0,22	0,11	0,70	1,84	0,31
C7S	2,23	1,13	> 20,0	-	-
C7G	> 20,0	-	> 20,0	-	-

2. táblázat: A CHR, C7S, C7G és az APU gátló hatásai a XO-katalizált 6-MP és xantin oxidációra. α = az inhibitor IC_{50} értéke osztva a pozitív kontroll IC_{50} értékével (APU: allopurinol, CHR: chrysin, C7S: chrysin-7-szulfát, C7G: chrysin-7-glükuronid).

V.3.2. Quercetin és konjugátumainak kölcsönhatásai xantin-oxidáz enzimmel

A Q és konjugátumainak hatását a 6-MP oxidációra először az idő függvényében vizsgáltuk (***20. ábra***). A Q3G és az I3G még magas koncentrációban (20 μM, a szubsztrát koncentráció négyszerese) sem gátolták az enzim működését, míg az anyavegyület, valamint a szulfát (Q3'S) és a metil (IR, TAM) konjugátumok még a pozitív kontrollként alkalmazott APU-nál is erősebb gátló hatást mutattak (***20. ábra***). Míg 3 μM APU csak a metabolit képződés enyhe gátlását okozta, addig a Q, Q3'S, IR és TAM közel teljes gátlást eredményeztek ugyanilyen koncentrációban. Emellett a Q3'S és a TAM már 0,25 μM-os koncentrációban is számottevően gátolták a 6-thiohúgysav képződést (***20. ábra***).

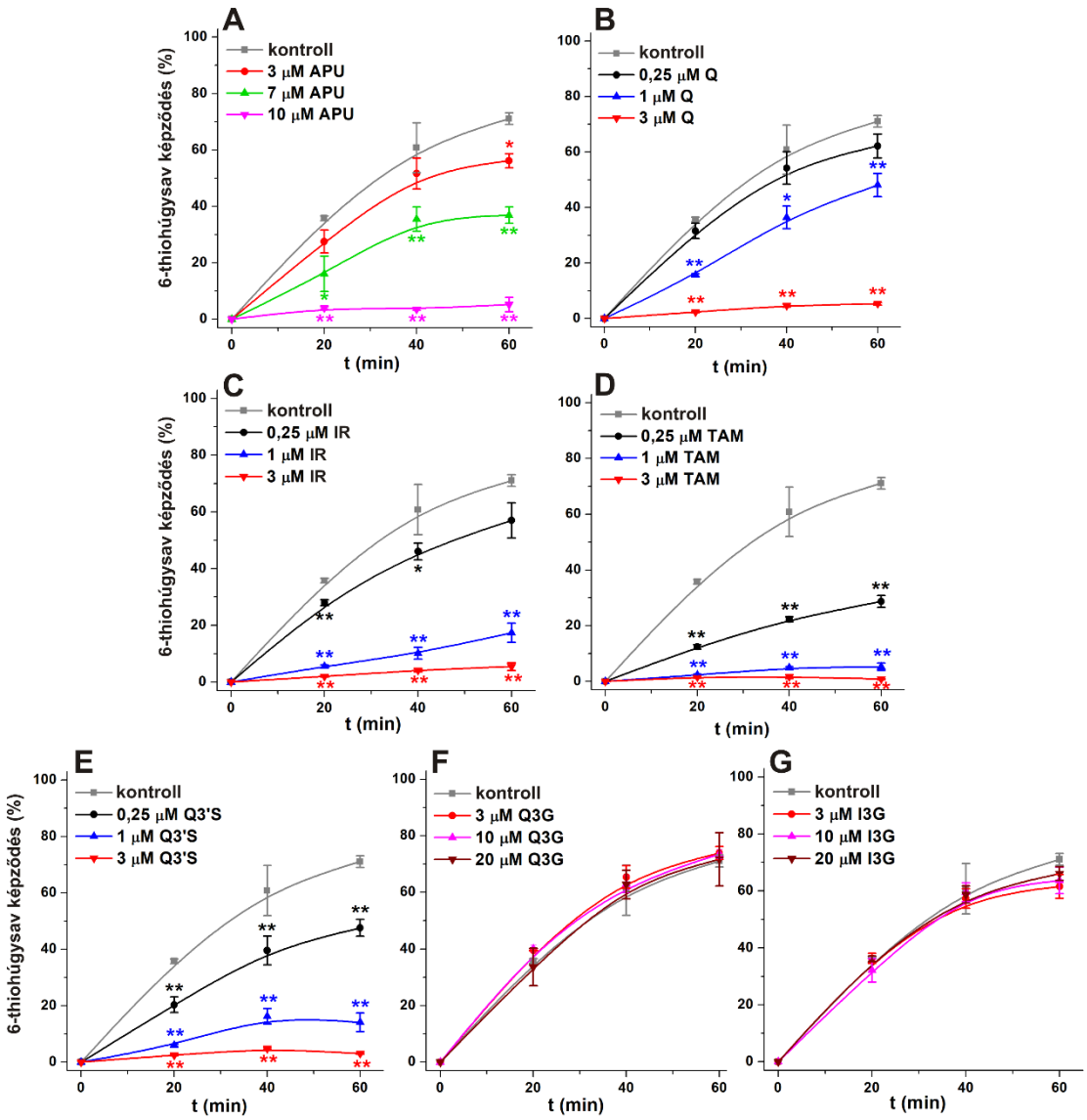

20. ábra: A Q, a Q konjugátumok és az APU (0-20 μM) hatása a XO-katalizált 6-MP oxidációra az idő függvényében. Az ábra a 6-MP 6-thiohúgysavvá történő százalékos átalakulását ábrázolja APU ***(A)***, Q ***(B)***, IR ***(C)***, TAM ***(D)***, Q3'S ***(E)***, Q3G ***(F)*** és I3G ***(G)*** jelenlétében (*p < 0,05; **p < 0,01; APU: allopurinol, Q: quercetin, IR: isorhamnetin, TAM: tamarixetin, Q3'S: quercetin-3'-szulfát, Q3G: quercetin-3-glükuronid, I3G: isorhamnetin-3-glükuronid).

A Q, a Q konjugátumok, valamint az APU koncentrációfüggő gátló hatásait a 6-MP és a xantin oxidációra a ***21. ábra*** mutatja be. A glükuronid konjugátumok (Q3G, I3G) még magas koncentrációban (20 μM) sem befolyásolták az enzim működését egyik szubsztrát esetében sem. Ezzel szemben a Q, Q3'S, IR és TAM még az APU-hoz képest is lényegesen erősebb gátló hatást fejtettek ki a XO-katalizált 6-thiohúgysav képződésre

(***21./A ábra***). Ugyanezek a flavonoidok a xantin oxidációját szintén erősen gátolták, azonban itt az APU-hoz hasonló hatást mutattak (***21./B ábra***).

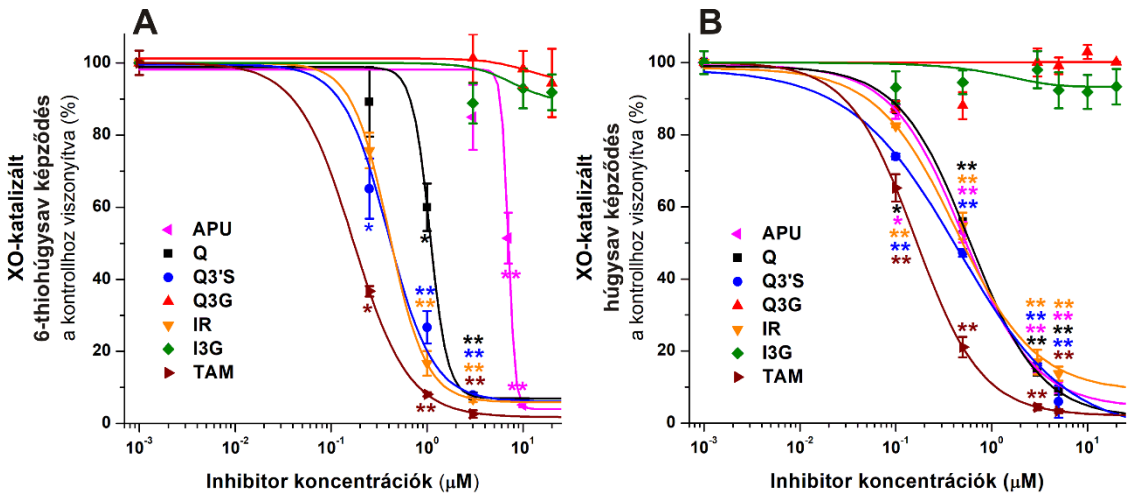

21. ábra: A Q, a Q konjugátumok és az APU koncentrációfüggő gátló hatása a XO-katalizált 6-MP ***(A)*** és xantin ***(B)*** oxidációra (5-5 μM szubsztrát). Az ábrák a XO-katalizált 6-thiohúgysav ***(A)*** és húgysav ***(B)*** kontrollhoz viszonyított százalékos képződését illusztrálják, emelkedő inhibitor koncentrációk jelenlétében (0-20 μM), 40 (6-MP) illetve 8 perces (xantin) inkubációt követően, logaritmikus skálán (* $p < 0,05$; ** $p < 0,01$; APU: allopurinol, Q: quercetin, Q3'S: quercetin-3'-szulfát, Q3G: quercetin-3-glükuronid, IR: isorhamnetin, I3G: isorhamnetin-3-glükuronid, TAM: tamarixetin).

A számolt IC_{50} értékek (***3. táblázat***) alapján már a Q is erősebb gátlószere volt a 6-MP oxidációnak a pozitív kontrollnál, míg az IR és a Q3'S kb. 3-4-szer, a TAM pedig közel 10-szer potensebben gátolta a 6-thiohúgysav képződést, mint az APU. Ráadásul, e konjugátumok még az anyavegyület Q-nél is 2-7-szer erősebb gátlószernek bizonyultak. Ezzel szemben a xantin szubsztrát esetében a Q, a Q3'S, az IR, a TAM és az APU IC_{50} értékei hasonlóak voltak (0,20-0,80 μM). Fontos emellett hangsúlyozni, hogy míg a Q és a Q konjugátumok a xantin és a 6-MP oxidációját is hasonló mértékben gátolták, addig az APU a xantin oxidációjára kb. 5-ször erősebb gátló hatást fejtett ki a 6-MP oxidációhoz képest (***3. táblázat***).

	6-MP oxidáció		Xantin oxidáció		IC_{50}(6-MP)/ IC_{50}(xantin)
	IC_{50} (μM)	α	IC_{50} (μM)	α	
APU	1,97	1,00	0,38	1,00	5,18
Q	1,40	0,71	0,80	2,11	1,75
Q3'S	0,50	0,25	0,40	1,1	1,25
IR	0,60	0,30	0,70	1,84	0,86
TAM	0,20	0,10	0,20	0,53	1,00
Q3G	> 20,0	-	> 20,0	-	-
I3G	> 20,0	-	> 20,0	-	-

3. táblázat: A Q, a Q konjugátumok és az APU gátló hatásai a XO-katalizált 6-MP és xantin oxidációra. α = az inhibitor IC_{50} értéke osztva a pozitív kontroll IC_{50} értékével (APU: allopurinol, Q: quercetin, Q3'S: quercetin-3'-szulfát, IR: isorhamnetin, TAM: tamarixetin, Q3G: quercetin-3-glükuronid, I3G: isorhamnetin-3-glükuronid).

A Q és konjugátumai esetében a gátlás áttörhetőségét is megvizsgáltuk (***22. ábra***). A kísérlet során a XO enzimet 3 μM Q, Q3'S, IR és TAM jelenlétében előinkubáltuk (15 perc), ezután a mintákhoz a 6-MP növekvő koncentrációit (5, 20 és 50 μM) adtuk, majd 40 perces inkubációt követően vizsgáltuk a 6-thiohúgysav képződését. Noha 5 μM 6-MP esetén a Q és szulfát/metil konjugátumai már alacsony koncentrációban (3 μM) is a termékképződés közel teljes gátlását okozták (***21./A ábra***), a szubsztrát magasabb koncentrációi a 6-thiohúgysav képződésének szignifikáns emelkedését eredményezték (***22./A ábra***).

A xantin esszé esetében a gátlás áttörhetőségének vizsgálatára a XO-t 10 μM Q, Q3'S, IR és TAM jelenlétében előinkubáltuk (15 perc), ezt követően mintákhoz a xantin növekvő koncentrációit (5, 50 és 100 μM) adva 8 perces inkubációt követően a képződött metabolit mennyiségét határoztuk meg. Az 5 μM-os szubsztrát koncentráció mellett a flavonoidok 10 μM koncentrációban alkalmazva majdnem teljesen gátolták a húgysav képződését (***21./B ábra***), de a xantin magasabb koncentrációi mellett a termékképződés szignifikáns növekedését tapasztaltuk (***22./B ábra***).

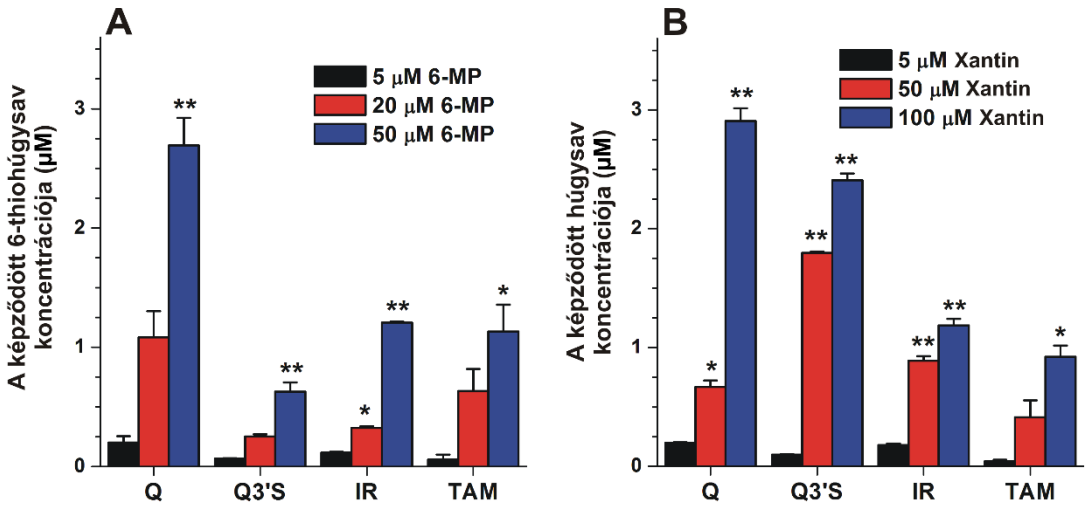

22. ábra: A reakció során képződött 6-thiohúgysav (3 μM flavonoid koncentráció mellett) ***(A)*** és húgysav (10 μM flavonoid koncentráció mellett) ***(B)*** koncentrációi Q, Q3'S, IR és TAM jelenlétében, a szubsztrátok emelkedő koncentrációi mellett (* $p < 0,05$; ** $p < 0,01$; Q: quercetin, Q3'S: quercetin-3'-szulfát, IR: isorhamnetin, TAM: tamarixetin, 6-MP: 6-mercaptopurin).

Fontos kiemelni, hogy míg a 6-MP két oxidációs lépesben alakul át 6-thiohúgysavvá (***6. ábra***), addig a xantin húgysavvá történő átalakulása egylépéses folyamat (***5. ábra***). Ezért olyan kísérleteket is végeztünk, melynek során a Q, Q3'S, APU és oxipurinol hatásait hipoxantin szubsztráttal szemben teszteltük (***23. ábra***). A reakció ebben az esetben szintén két lépésben zajlik, mivel a hipoxantinból előbb xantin, majd a xantinból húgysav képződik (***5. ábra***). A hipoxantin esszé során a xantin és a húgysav is jelentős koncentrációkban megjelentek a mintákban, ezért mindkét termék mennyiségének figyelembevételével értékeltük az eredményeket. Hasonlóan az előzőekhez, az oxipurinol ($IC_{50} > 3,0$ μM) a hipoxantin oxidációját gyengébben gátolta, mint az APU ($IC_{50} = 0,66$ μM), míg a Q ($IC_{50} = 0,24$ μM) és a Q3'S ($IC_{50} = 0,21$ μM) potensebb gátlószereknek bizonyultak az APU-hoz viszonyítva (***23. ábra***).

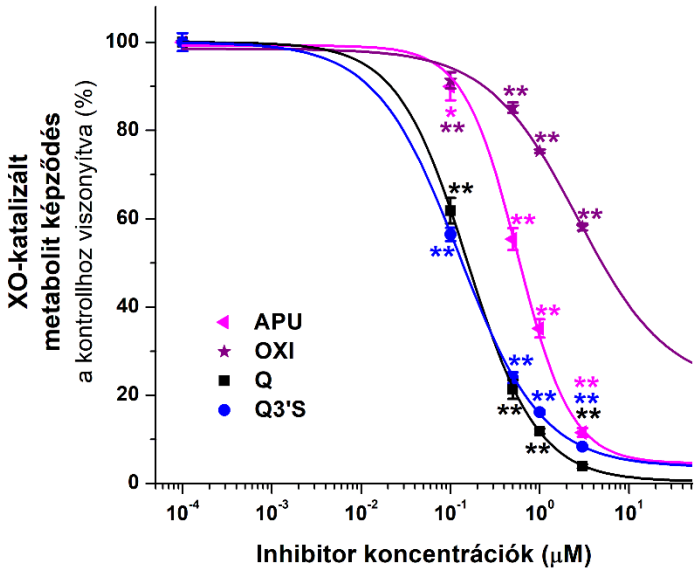

23. ábra: Az APU, oxipurinol, Q és Q3'S gátló hatásai a XO-katalizált hipoxantin (5 μM) oxidációra. Az ábra a xantin és a húgysav képződés kontrollhoz viszonyított százalékos értékeit illusztrálja emelkedő inhibitor koncentrációk (0-3 μM) jelenlétében, 4 perces inkubációt követően, logaritmikus skálán (*$p < 0,05$; **$p < 0,01$; APU: allopurinol, OXI: oxipurinol, Q: quercetin, Q3'S: quercetin-3'-szulfát).

VI. Megbeszélés, következtetések

VI.1. Chrysin és konjugátumainak kölcsönhatásai humán szérum albuminnal

A belső szűrő effektus korrekcióját (***1. egyenlet***) követően a CHR, a C7S és a C7G szignifikánsan csökkentették a HSA fluoreszcencia emissziós jelét 340 nm-en (***13./A ábra***), ami flavonoid-albumin komplexek kialakulására utal. A HSA által emittált fény (λ_{ex} = 295 nm, λ_{em} = 340 nm) legnagyobb részben a fehérje Site I régiójában található triptofán (TRP214) aminosavnak tulajdonítható (Il'ichev és mtsai., 2002; Fanali és mtsai., 2012). Ezért, figyelembe véve a CHR és konjugátumainak jelentős kioltó hatását, feltételezhetjük, hogy a vizsgált flavonoidok kötőhelye a TRP214 közelében, tehát a Site I régióban vagy attól nem nagy távolságra található. Továbbá, a Stern-Volmer egyenlet grafikus ábrázolásával kapott adatok jó illeszkedése, valamint a Hyperquad szoftver felhasználásával számolt eredményeink alapján 1:1 sztöchiometriájú komplexek képződnek. A vizsgálatainkban meghatározott flavonoid-albumin komplexek K_{SV} és K értékei jól korrelálnak egymással (***1. táblázat***), emellett a CHR-HSA komplex kapcsán számolt kötési állandó a korábbi tanulmányokkal is jó egyezést mutat (Xiao és mtsai., 2010; Tu és mtsai., 2015). Mindemellett eredményeink azt mutatták, hogy hasonlóan a Q-hez (Dangles és mtsai., 2001; Janisch és mtsai., 2004; Poór és mtsai., 2017; Poór és mtsai., 2018a), a CHR szulfát metabolitja is magasabb affinitással kötődik HSA-hoz, mint az anyavegyület.

Mivel a korábbi vizsgálatok alapján a CHR albuminhoz történő kötődésében a Site I vagy a Site II régió lehet érintett (Xiao és mtsai., 2010; Tu és mtsai., 2015), a CHR és konjugátumainak leszorítóképességét a Site I marker warfarinnal és a Site II marker naproxennel szemben is megvizsgáltuk. Tekintve, hogy a HSA egy makromolekula (kb. 66,5 kDa), mérete miatt az albumin és az albuminkötött molekulák nem képesek átjutni a 30 kDa cut-off értékű filtereken. Ezért ultraszűréses kísérleteinkben a site marker koncentrációjának szignifikáns emelkedése a szűrletben, az albuminról történő leszorításra utal. A C7S mindkét alkalmazott koncentrációban a warfarin mennyiségének jelentős emelkedését okozta a filtrátumban, lényegesen magasabb leszorítást okozva, mint a CHR vagy a C7G (***14./A ábra***). Érdekes módon a CHR és konjugátumai a naproxen albuminkötődését is befolyásolták, bár leszorító hatásuk lényegesen elmaradt a C7S warfarinnal szemben mutatott leszorítóképességével szemben (***14. ábra***). Tehát eredményeink alapján feltételezhetjük, hogy a C7S nagy affinitású kötőhelye a HSA Site

I régiójában (IIA aldomén) található. Azt, hogy a CHR, C7S és C7G kötőhelye a Site I, molekulamodellezés is alátámasztja: a CHR és a C7S kötési pozíciói hasonlóak, de a C7S szulfát csoportja sóhidat képez a Site I régió egy lizin és egy arginin aminosavával, melynek eredményeként a szulfát konjugátum stabilabb komplexet alakít ki HSA-nal; míg a C7G alacsonyabb affinitású kötődését eltérő kötési pozíciója magyarázhatja (Mohos és mtsai., 2018a). A CHR és konjugátumainak naproxennel szembeni leszorító hatása pedig feltételezhetően alloszterikus kölcsönhatással magyarázható.

A CHR és metabolitjainak hatását a warfarin albuminkötődésére steady-state fluoreszcencia spektroszkópia és fluoreszcencia anizotrópia módszerekkel is megvizsgáltuk. Mivel az albuminkötött warfarin fluoreszcens emissziós intenzitása megközelítőleg 20-szor nagyobb a szabad warfarinéhoz viszonyítva (Poór és mtsai., 2017; Poór és mtsai., 2018b), a CHR, C7S és C7G jelenlétében tapasztalt koncentrációfüggő csökkenés a warfarin fluoreszcens jelében (***15./A ábra***), a warfarin albuminról történő leszorítására utal. Eredményeink alapján a flavonoidok egymáshoz viszonyított, warfarinnal szembeni leszorítóképessége jól korrelál azok kötési affinitásával (C7S > CHR > C7G). A warfarin kismolekula révén nagy rotációs szabadsággal és ebből adódóan relatíve kis fluoreszcencia anizotrópia értékkel rendelkezik. Ugyanakkor, a warfarin-HSA kölcsönhatás során a warfarin rotációs szabadsága nagymértékben lecsökken (mivel a fluorofór egy nagyméretű makromolekulához kapcsolódik), ezzel együtt pedig anizotrópia értéke jelentősen megnő. Ezért, egy kisméretű fluorofór albuminról történő leszorítása a molekula fluoreszcencia anizotrópiájának csökkenését okozza (Zhang és mtsai., 2012; Poór és mtsai., 2018b). Fluoreszcencia anizotrópiai méréseink alapján szintén a C7S rendelkezik a legnagyobb leszorítóképességgel, míg ezt a CHR követi (***15./B ábra***). Mindezek alapján lehetséges, hogy a C7S képes leszorítani egyes Site I kötőhelyhez kapcsolódó gyógyszereket albuminról.

VI.2. A chrysin és quercetin konjugátumok kölcsönhatásai CYP enzimekkel

Vizsgálataink során a CHR erős gátló hatást fejtett ki a CYP2C9 enzimre, ami összhangban van korábbi *in vitro* vizsgálatok eredményeivel (Kimura és mtsai., 2010; Shimada és mtsai., 2010). E tanulmányokban a CHR az alkalmazott szubsztrátokkal (diclofenac, flurbiprofen) összemérhető koncentrációkban is szignifikáns gátló hatást

mutatott. Ráadásul a szulfát konjugátum még az anyavegyület CHR-nél is erősebben gátolta a CYP2C9 enzimet (***16./A ábra***).

Kísérleteinkben a CHR a CYP2C19-katalizált 4-hydroxymephenytoin képződésre is erős gátlást fejtett ki (IC_{50} = 4,6 μM). Emellett egy korábbi vizsgálatban a CHR-t (23,6 μg/mg) is tartalmazó propolisz kivonat szintén gátolta az enzimet (Ryu és mtsai., 2016). Vizsgálatainkban azonban a C7S és a C7G a CYP2C19 gyenge gátlószereinek bizonyultak (***16/B. ábra***).

Hasonlóan egy korábbi (szintén dextromethorphan szubsztráttal végzett) vizsgálathoz (Bojić és mtsai., 2019), jelen munkánkban a CHR és metabolitjai nem gátolták a CYP2D6 enzimet (***16./C ábra***).

Annak ellenére, hogy korábbi *in vitro* tanulmányokban a CHR a CYP3A4-katalizált testosteron (IC_{50} = 0,9 és 7,4 μM) (Tsujimoto és mtsai., 2009; Kimura és mtsai., 2010), midazolam (IC_{50} = 3,8 μM) (Shimada és mtsai., 2010) és quinin (IC_{50} = 70-86 μM) (Ho és Saville, 2001) hidroxilációt is gátolta, vizsgálatainkban a CHR a CYP3A4 gyenge gátlószerének bizonyult (***16./D ábra***). Továbbá a C7G nem, a C7S pedig csak alig gátolta az enzimet (***16./D ábra***).

Az interneten számos CHR-tartalmú étrend-kiegészítő kapható, melyek extrém magas mennyiségben (gyakran 500 mg/kiszerelési egység) tartalmaznak CHR-t aglikon formájában (Mohos és mtsai., 2018a). Habár 400 mg CHR egyszeri *per os* bevételét követően a C7S mindössze 400-800 nmol/L-es plazmakoncentrációkat ér el egészséges önkéntesekben (Walle és mtsai., 2001), feltételezhető, hogy magasabb CHR dózisok esetében μmol/L-es plazmakoncentrációk is kialakulhatnak, hasonlóan a Q-hez (Conquer és mtsai., 1998; Kelly, 2011; Del Rio és mtsai., 2013). A CHR kinetikai kölcsönhatásaival kapcsolatban ugyan nem találtunk humán tanulmányt a szakirodalomban, de állatkísérletekben a CHR CYP enzimekkel valamint különböző transzporterekkel (pl. BCRP) kölcsönhatásba lépve több gyógyszer (pl. coffein, nitrofurantoin, paracetamol) farmakokinetikai paramétereit is befolyásolta (Wang és Morris, 2007; Kawase és mtsai., 2009; Noh és mtsai., 2016; Pingili és mtsai., 2019). Eredményeinkben a CHR a CYP2C9 és a CYP2C19 enzimet is erősen gátolta, sőt a C7S még az anyavegyületnél is potensebb gátlószere volt a CYP2C9-nek. Ezért feltételezhető, hogy magas CHR bevitel befolyásolhatja egyes gyógyszerek CYP2C9- és/vagy CYP2C19-mediált biotranszformációját.

HEK293 sejtekben a Q gátolta a CYP1A1 és a CYP1B1 enzimeket, míg a CYP3A4 és a CYP2D6 enzimekre nem fejtett ki releváns gátló hatást (Sharma és mtsai., 2017).

Továbbá egy korábbi vizsgálatban a Q, valamint szulfát (Q3'S) és metil (IR és TAM) származékai a CYP2C9 enzim gyenge gátlószereinek bizonyultak (Poór és mtsai., 2017).

Jelen munkánkban a Q és konjugátumai csak kisebb mértékben csökkentették az *S*-mephenytoin hidroxilációját (***17./A ábra***). A korábbi vizsgálatokban a Q a CYP2C19-katalizált *S*-mephenytoin hidroxiláció erős (Rastogi és Jana, 2014), míg más kísérletekben gyenge (He és mtsai., 2006; Cao és mtsai., 2017) gátlószerének bizonyult.

Eredményeinkkel összhangban (***17./C ábra***), a Q csak mérsékelt vagy jelentéktelen gátló hatásokat mutatott a CYP2D6-katalizált bufuralol hidroxilációra (He és mtsai., 2006; Rastogi és Jana, 2014) és dextromethorphan *O*-demetilációra (Cao és mtsai., 2017).

A Q gátló hatását a CYP3A4-katalizált midazolam (Rastogi és Jana, 2014) és testosteron (Kimura és mtsai., 2010) hidroxilációra is leírták. Vizsgálatainkban azonban a Q és metabolitjai esetében statisztikailag szignifikáns, de viszonylag gyenge gátló hatásokat tapasztaltunk (***17./B ábra***). Emellett az IR kapcsán ellentmondásos eredményeket találtunk a szakirodalomban. Ugyanis humán CYP enzimmel végzett kísérletek során az IR gátolta a testosteron CYP3A4-katalizált hidroxilációját (Kimura és mtsai., 2010), de a 7-benzyloxy-4-trifluoromethylcoumarin *O*-demetilációját nem befolyásolta sem a rekombináns, sem a humán májmikroszómák esetében (Östlund és mtsai., 2017). Ezzel szemben, sertés májmikroszomális frakcióban az IR gátolta a 7-benzyloxy-4-trifluoromethylcoumarin *O*-demetilációját (Ekstrand és mtsai., 2015).

Eredményeink alapján tehát a Q konjugátumok statisztikailag ugyan szignifikáns, de gyenge gátlószerei a CYP2C19 és CYP3A4 enzimeknek, továbbá nem befolyásolják a CYP2D6 működését (***17. ábra***). Így nem tűnik valószínűnek, hogy a Q jelentősen befolyásolja a gyógyszerek CYP2C19-, 3A4- és/vagy 2D6-mediált biotranszformációját. Azonban az összes tesztelt metabolit a Q-hez hasonló, szignifikáns gátlószere volt a CYP2C19 és CYP3A4 enzimeknek, így elképzelhetőek enyhébb farmakokinetikai kölcsönhatások nagyon magas Q bevitelt követően. Ezt a feltételezést egy korábbi tanulmány is alátámasztja, mely szerint egészséges önkéntesekben napi kétszer 500 mg Q *per os* bevétele szignifikánsan csökkentette az együttesen szedett diclofenac CYP2C9-katalizált eliminációját (Bedada és Neerati, 2018a), holott egy másik *in vitro* vizsgálatban a Q és egyes konjugátumai (Q3'S, IR, TAM) csak gyenge gátlószerei voltak a CYP2C9-mediált diclofenac hidroxilációnak (Poór és mtsai., 2017). Továbbá, azt is fontos kiemelni, hogy *in vivo* tanulmányokban a Q több gyógyszer CYP3A4-katalizált biotranszformációját is befolyásolta (Choi és Han, 2004; Choi és Li, 2005; Shin és mtsai., 2006; Umathe és mtsai., 2008; Babu és mtsai., 2013; Duan és mtsai., 2012; Nguyen és

mtsai., 2015). Ezek alapján az ilyen jellegű kinetikai interakciók kialakulása nem zárható ki, különösen extrém magas Q bevitelt követően.

VI.3. Chrysin és quercetin konjugátumok kölcsönhatásai xantin-oxidáz enzimmel

Korábbi *in vitro* tanulmányok alapján a CHR és a Q a xantin oxidáció potens gátlószerei (Cos és mtsai., 1998; Lin és mtsai., 2002; Van Hoorn és mtsai., 2002; Lin és mtsai., 2015a, b). Azonban a CHR és a Q, valamint konjugált metabolitjaik hatásait a XO-katalizált 6-MP oxidációra eddig még nem vizsgálták. A különböző *in vitro* vizsgálatokban leírt IC_{50} és α értékek a xantin oxidáció gátlása kapcsán nagy varianciát mutatnak a CHR és a Q esetében: egyes tanulmányokban erősebben (Van Hoorn és mtsai., 2002; Lin és mtsai., 2015a, b), míg más vizsgálatokban gyengébben (Iio és mtsai., 1985; Cos és mtsai., 1998; Lin és mtsai., 2002) gátolták az enzimet a pozitív kontroll APU-hoz viszonyítva. Emellett egy Q-nel kapcsolatos újabb vizsgálat kitűnő egyezést mutat eredményeinkkel, mely szerint a flavonoid és az APU hasonlóan erős gátlószerei a xantin oxidációnak (Zhang és mtsai., 2018). Egy másik tanulmányban egyes Q konjugátumok (Q-3-szulfát, Q3G, Q-7-glükuronid, Q-3'-glükuronid, Q-4'-glükuronid) hatásait is megvizsgálták a XO-katalizált xantin oxidációra: a Q3G és a Q-7-glükuronid gyenge gátlószereknek bizonyultak (Day és mtsai., 2000), ami összhangban van eredményeinkkel. Ezzel szemben a Q-3'-glükuronid és a Q-4'-glükuronid a XO-katalizált húgysav képződésre a Q-hez hasonló, erős gátló hatást fejtettek ki (Day és mtsai., 2000), viszont e konjugátumok nem képződnek releváns mennyiségben a humán szervezetben (Mullen és mtsai., 2006). Emellett a szulfát csoport pozíciója is fontos lehet a gátlás kapcsán: a Q-3-szulfát ugyanis a xantin oxidációját csak nagyon magas koncentrációban gátolta (Day és mtsai., 2000), míg vizsgálatunkban a Q3'S már alacsony koncentrációban is potens inhibitornak bizonyult (***3. táblázat***). Ezzel szemben a CHR szulfát szubsztitúciója (7-es pozícióban) lényegesen csökkentette a XO-ra kifejtett gátló hatást (***2. táblázat***). A CHR metabolitok XO-ra kifejtett hatása kapcsán nem találtunk adatot a szakirodalomban, de hasonlóan a Q glükuronid konjugátumaihoz (Q3G, I3G), a C7G is csak gyenge gátlószere volt az enzimnek, míg a C7S a 6-MP oxidáció tekintetében bizonyult potens inhibitornak (***2. és 3. táblázat***).

Az enzim esszék során (6-MP, xantin, hipoxantin) APU-t használtunk pozitív kontrollként, mert előzetes vizsgálatainkban az oxipurinol a xantin és a 6-MP oxidációját is gyengébben gátolta, mint az APU (***18. ábra***). Ezt a megfigyelést korábbi *in vitro*

vizsgálatok is alátámasztják (Elion, 1966). Az APU ugyanis nemcsak kompetitív gátlószere, de szubsztrátja is a XO enzimnek, így a kölcsönhatás során oxipurinollá alakul (Galbusera és mtsai., 2006). A XO-t az APU és a képződő metabolit egyaránt gátolja, de az APU hatása *in vitro* erősebb, mivel oxidációja során az enzim katalitikus centrumában elhelyezkedő molibdén atom redukálódik, az oxipurinol pedig csak a redukált molibdén atommal alakít ki nagy affinitású kölcsönhatást (Spector, 1977). Ezért az APU-ból a XO által képzett oxipurinol jóval erősebb inhibitora a XO-nak, mint az enzimhez „kívülről" hozzáadott oxipurinol (Spector, 1977). Ezt azért is fontos kiemelni, mert az APU gátló hatását főként az oxipurinolnak tulajdonítják. Az APU gyógyszerként való alkalmazása is előnyösebb, mint az oxipurinol adagolása, annak ellenére, hogy utóbbi ún. „pszeudo-irreverzibilis" gátlószere (nagyon lassan disszociál le a XO-ról) az enzimnek. Az oxipurinol eliminációs felezési ideje hosszabb (reabszorbeálódik a vesetubulusokban), valamint plazmakoncentrációja is magasabb az APU-hoz viszonyítva, mivel az APU viszonylag gyorsan oxidálódik a szervezetben XO vagy aldehid-oxidáz enzimek által (Spector, 1977; Day és mtsai., 2007).

A vizsgált Q metabolitok közül a szulfát (Q3'S) és a metil (IR és TAM) konjugátumok fejtettek ki erős gátló hatást a XO enzimre (mindkét szubsztrát esetében) (***21. ábra***), míg a C7S valamivel gyengébb, de potens inhibitora volt a 6-MP oxidációnak (***19./A ábra***). Mivel a xantin és a 6-MP esszé során is 5-5 µM szubsztrát koncentrációt alkalmaztunk, a tesztvegyületek IC_{50} értékei összehasonlíthatók. Ez alapján a CHR, a Q, a Q3'S, az IR és a TAM hasonló vagy még erősebb inhibitorai voltak a xantin oxidációjának, mint az APU; míg a C7S az APU-hoz képest jóval gyengébb gátlást mutatott (***2. és 3. táblázat***). Ugyanakkor a pozitív kontrollhoz képest a C7S hasonló, míg a CHR, Q, Q3'S, IR és TAM kb. 1,5-10-szer erősebb gátló hatást fejtettek ki a 6-MP oxidációra (***2. és 3. táblázat***). Azonban figyelembe kell vennünk azt a tényt is, hogy az APU a 6-MP oxidációt jóval gyengébben gátolta a xantin oxidációhoz képest. Ezzel szemben a CHR, Q, Q3'S, IR és TAM IC_{50} értékei a két szubsztrát esetében hasonlóak voltak. Érdekes módon a C7S volt az egyetlen vizsgált metabolit, ami a xantin oxidációt csak gyengén, míg a 6-MP oxidációt erősen gátolta (***19. ábra***). Tehát pont fordítva „viselkedett", mint az APU.

A xantin és a 6-MP magasabb koncentrációival sikerült inhibitorok jelenlétében is jelentősen emelni a 6-thiohúgysav és a húgysav képződését (***22. ábra***), ami a gátlás áttörhetőségét, tehát a reverzibilis gátlást igazolja. A kompetitív kötődést molekula modellezéses vizsgálatok is megerősítették (Mohos és mtsai., 2019).

Korábban felmerült, hogy a flavonoidok a XO-ra kifejtett erős *in vitro* gátló hatásuk révén alkalmasak lehetnek hiperurikémia kezelésében (Nagao és mtsai., 1999). A potens *in vitro* hatás ellenére, a gátlással kapcsolatos állatkísérletes eredmények ellentmondásosak. Például hiperurikémiás egerekben a szérum urát szinteket 100 mg/kg Q szignifikánsan csökkentette (Zhu és mtsai., 2004), míg egy másik tanulmányban az egészséges és hiperurikémiás egereknek orálisan beadott 400 mg/kg Q nem befolyásolta (Huang és mtsai., 2011). Egy korábbi vizsgálatban a *per os* adagolt Q jóval nagyobb hatást gyakorolt a húgysav szintekre az *intraperitoneális* alkalmazáshoz képest (Zhu és mtsai., 2004), ami a preszisztémás elimináció során képződő konjugátumok fontosságát jelzi. Emellett humán vizsgálatokban a Q még 1000 és 2000 mg-os napi dózisai sem befolyásolták a szérum húgysav szinteket (Abbey és mtsai., 2011; Boots és mtsai., 2011) és csak minimális csökkentést figyeltek meg négy hetes Q-kezelést (500 mg/nap) követően is (Shi és mtsai., 2016). Tehát a flavonoidok klinikai felhasználása e területen egyelőre nem tűnik megalapozottnak.

Eredményeink alapján a CHR, Q, Q3'S, IR és TAM hasonló erősséggel gátolták a húgysav képződést, mint az APU. De fontos megjegyezni, hogy egészséges önkéntesekben 400 mg CHR egyszeri *per os* bevételét követően a C7S csúcs plazmakoncentrációja kb. 400-800 nmol/L (Walle és mtsai., 2001). Emellett a Q 12 héten keresztül, napi 1000 mg-os orális adagolását követően az össz-Q (Q és konjugátumai) csúcs plazmakoncentrációja több µmol/L-es értéket ér el (Heinz és mtsai., 2010). Ezzel szemben, az APU egyszeri 200 mg-os *per os* bevételét követően az APU és az oxipurinol együttes csúcs plazmakoncentrációja kb. 35-40 µmol/L (Turnheim és mtsai., 1999), de nagyobb dózisok esetében ez ennél is magasabb lehet. Tehát a flavonoidok és egyes metabolitjaik *in vitro* gátló hatása az APU-éhoz hasonló, míg mennyiségük a keringésben (és feltehetőleg a szövetekben is) jóval alacsonyabb. E megfontolások megmagyarázhatják a flavonoidok húgysavszintre gyakorolt gyenge *in vivo* hatását. Emellett érdemes azt is megfontolni, hogy megfelelő formulálással a flavonoidok felszívódása és/vagy rossz orális biohasznosulása jelentősen javítható, pl. ilyen esetekben az 500 mg-os egyszeri Q bevitel akár 5-10 µmol/L-es plazmakoncentrációkat is eredményezhet össz-Q-re vonatkozóan (Kaushik és mtsai. 2012).

Az APU és a 6-MP (vagy azathioprin) konvencionális dózisainak egyidejű alkalmazása súlyos toxikus következményeket vonhat maga után (pl. mieloszupresszió), mivel az APU gátolja a 6-MP XO-katalizált eliminációját (McLeod, 1988). A dózis csökkentésével és a terápia folyamatos nyomon követésével megfontolható e két

gyógyszer együttes használata, de csak fokozott elővigyázatosság mellett (Leong és mtsai., 2008). Igaz, hogy az APU és az oxipurinol jóval magasabb koncentrációt ér el a keringésben (és valószínűleg egyes szövetekben is) mint a CHR, a Q, valamint konjugált metabolitjaik, azonban egyes Q metabolitok (Q3'S, IR és TAM) jóval erősebben gátolják a 6-MP oxidációját, mint az APU (***2. és 3. táblázat***). Korábbi humán vizsgálatok alapján a Q3'S (Mullen és mtsai., 2006) és az I3G (Cialdella-Kam és mtsai., 2013) lehetnek a Q keringésben megjelenő domináns metabolitjai. Vizsgálatainkban a TAM a XO enzim erős gátlószere volt, viszont e konjugátum a humán szervezetben csak kisebb mennyiségben képződik, mivel a COMT enzim a katechol szerkezeti egység 3'-*O*-metilációját preferálja (De Santi és mtsai., 2002). Ezzel szemben az I3G keringésben megjelenő magas mennyisége (Day és mtsai., 2001; Mullen és mtsai., 2006; Cialdella-Kam és mtsai., 2013), az IR szignifikáns intracelluláris képződésére utal, mely potens gátlószere volt az enzimnek. Mindezek alapján feltételezhető, hogy az extrém magas Q bevitel (étrend-kiegészítőkkel akár több gramm naponta) 6-MP-nal (vagy azathioprinnel) együttesen alkalmazva akár súlyos következményekkel is járhat.

VII. Összefoglalás

Eredményeink alapján nemcsak az anyavegyületek, de egyes konjugált metabolitjaik is képesek kölcsönhatásba lépni különböző farmakokinetikai szempontból fontos fehérjével. Sőt, némely konjugátum hatása még az anyavegyületét is meghaladja. Tekintve, hogy az *in vitro* megközelítés számos kinetikai aspektus figyelembevételét korlátozza, eredményeink relevanciájának igazolásához további, *in vivo* kísérletek elvégzése is szükséges. Az *in vitro* módszertan korlátai közé tartozik, hogy a vegyületek hatását izolált fehérjéken vizsgáljuk, arról azonban nem áll rendelkezésre kísérletes adat, hogy az anyavegyületből és a metabolitokból mekkora koncentrációk jelenhetnek meg az intracelluláris térben. Utóbbi kapcsán érdekes lehet a flavonoidok celluláris felvételének és biotranszformációjának sebessége, de az efflux transzporterek érintettsége is nagyon fontos. Emellett az sem mindig világos, hogy a metabolizmus főként az enterocitákban vagy a hepatocitákban megy végbe, ugyanis különböző flavonoidok kapcsán mindkét esetre olvasható példa a szakirodalomban. Továbbá a felszívódás mértéke és az eliminációs utak (pl. szulfát konjugáció) esetleges telítődése is lényeges aspektusok. Mindezek mellett az *in vitro* kísérletek fontosak és előnyösek, mert *in vitro* rendszerekben könnyebben megállapítható, hogy az anyavegyület és/vagy egyes metabolitjai képesek-e kölcsönhatásba lépni egy fehérjével. Valamint az *in vitro* vizsgálatok elengedhetetlenek ahhoz, hogy megállapítsuk az *in vivo* tanulmányok elvégzésének indokoltságát. A fentebb részletezett limitációkat is figyelembe véve, eredményeink felhívják a figyelmet arra, hogy a magas CHR- és/vagy Q-tartalmú étrend-kiegészítők gyógyszerekkel történő együttes alkalmazása fokozott körültekintést igényel, különösen a szűk terápiás szélességű hatóanyagok esetében.

VIII. Új megállapítások

1. Nemcsak a CHR, de konjugátumai is képesek stabil komplexeket kialakítani HSA-nal, meghatároztuk e komplexek kötési állandóit. A CHR és konjugátumai valószínűleg a Site I régióhoz kapcsolódnak a HSA-on.

2. A C7S az anyavegyületnél magasabb affinitással kötődik HSA-hoz és a Site I marker warfarinnal szemben is jóval erősebb leszorítóképességet mutatott.

3. A C7G nem, vagy csak kismértékben gátolta a tesztelt CYP enzimeket, a C7S azonban a CYP2C9 erős gátlószerének bizonyult.

4. Az összes tesztelt Q konjugátum (Q3'S, IR, Q3G és I3G) az anyavegyülettel hasonló mértékű, de viszonylag gyenge gátló hatást fejt ki a CYP2C19 és a CYP3A4 enzimekre.

5. A Q3G, I3G és C7G nem, vagy csak gyengén gátolják a XO enzimet. Ezzel szemben, egyes Q konjugátumok (Q3'S, IR, TAM) még az anyavegyületnél is erősebb gátló hatást mutattak.

6. A xantin és 6-MP oxidációt a CHR, Q, Q3'S, IR és TAM hasonló erősséggel gátolják, míg az APU a xantin oxidáció, a C7S pedig a 6-MP oxidáció potensebb inhibitorai.

IX. Irodalomjegyzék

Abbey, E.L.; Rankin, J.W. Effect of quercetin supplementation on repeated-sprint performance, xanthine oxidase activity, and inflammation. *Int. J. Sport Nutr. Exerc. Metab.* **2011**, *21*, 91–96.

Äbelö, A.; Andersson, T.B.; Antonsson, M.; Naudot, A.K.; Skånberg, I.; Weidolf, L. Stereoselective metabolism of omeprazole by human cytochrome P450 enzymes. *Drug Metab. Dispos.* **2000**, *28*, 966–969.

Adkins, W.K.; Taylor A.E. Role of xanthine oxidase and neutriphils in ischemia-reperfusion injury in rabbit lung. *J. Appl. Physiol.* **1990**, *69*, 2012–2018.

Aherne, S.A.; O'Brien, N.M. Dietary flavonols: chemistry, food content, and metabolism. *Nutrition* **2002**, *18*, 75–81.

Akhlaghi, M.; Foshati, S. Bioavailability and metabolism of flavonoids: a review. *Int. J. Nutr. Sci.* **2017**, *2*, 180–184.

Ali, F.; Rahul; Naz, F.; Jyoti, S.; Siddique, Y.H. Health functionality of apigenin: a review. *Int. J. Food Prop.* **2017**, *20*, 1197–1238.

Alvarez, A.I.; Real, R.; Pérez, M.; Mendoza, G.; Prieto, J.G.; Merino, G. Modulation of the activity of ABC transporters (P-glycoprotein, MRP2, BCRP) by flavonoids and drug response. *J. Pharm. Sci.* **2010**, *99*, 598–617.

An, G.; Gallegos, J.; Morris, M.E. The bioflavonoid kaempferol is an ABCG2 substrate and inhibits ABCG2-mediated quercetin efflux. *Drug Metab. Dispos.* **2011**, *39*, 426–432.

Andres, S.; Pevny, S.; Ziegenhagen, R.; Bakhiya, N.; Schäfer, B.; Hirsh-Ernst, K.I.; Lampen, A. Safety aspects of the use of quercetin as a dietary supplement. *Mol. Nutr. Food Res.* **2018**, *62*, 1700447.

Anton, A.H. Increasing activity of sulfonamides with displacing agents: a review. *Ann. N. Y. Acad. Sci.* **1973**, *226*, 273–292.

Arts, I.C.W.; Sesink, A.L.A.; Faassen-Peters, M.; Hollman, P.C.H. The type of sugar moiety is a major determinant of the small intestinal uptake and subsequent biliary excretion of dietary quercetin glycosides. *Br. J. Nutr.* **2004,** *91*, 841–847.

Ascenzi, P.; Fasano, M. Allostery in a monomeric protein: the case of human serum albumin. *Biophys. Chem.* **2010**, *148*, 16–22.

Aura, A.M. Microbial metabolism of dietary phenolic compounds in the colon. *Phytochem. Rev.* **2008**, *3*, 407–429.

Babu, P.R.; Babu, K.N.; Peter, P.L.H.; Rajesh, K.; Babu, P.J. Influence of quercetin on the pharmacokinetics of ranolazine in rats and in vitro models. *Drug Dev. Ind. Pharm.* **2013**, *39*, 873–879.

Backman, J.T.; Olkkola, K.T.; Ojala, M.; Laaksovirta, H.; Neuvonen, P.J. Concentrations and effects of oral midazolam are greatly reduced in patients treated with carbamazepine or phenytoin. *Epilepsia* **1996**, *37*, 253–257.

Barkas, F.; Elisaf, M.; Liberopoulos, E.; Kalaitzidis, R.; Liamis, G. Uric acid and incident chronic kidney disease in dyslipidemic individuals. *Curr. Med. Res. Opin.* **2018**, *34*, 1193–1199.

Bedada, S.K.; Neerati, P. Evaluation of the effect of quercetin treatment on CYP2C9 enzyme activity of diclofenac in healthy human volunteers. *Phytother. Res.* **2018a**, *32*, 305–311.

Bedada, S.K.; Neerati, P. The effect of quercetin on the pharmacokinetics of chlorzoxazone, a CYP2E1 substrate, in healthy subjects. *Eur. J. Clin. Pharmacol.* **2018b**, *74*, 91–97.

Beecher, G.R. Overview of dietary flavonoids: nomenclature, occurrence and intake. *J. Nutr.* **2003**, *133*, 3248S–3254S.

Berry, C.E.; Hare, J.M. Xanthine oxidoreductase and cardiovascular disease: molecular mechanisms and pathophysiological implications. *J. Physiol.* **2004**, *555*, 589–606.

Bibi, Z. Role of cytochrome P450 in drug interactions. *Nutr. Metab.* **2008**, *5*, 27.

Bojić, M.; Kondža, M.; Rimac, H.; Benković, G.; Maleš, Z. The effect of flavonoid aglycones on the CYP1A2, CYP2A6, CYP2C8 and CYP2D6 enzymes activity. *Molecules* **2019**, *24*, 3174.

Boots, A.W.; Haenen, G.R.M.M.; Bast, A. Health effects of quercetin: from antioxidant to nutraceutical. *Eur. J. Pharmacol.* **2008**, *585*, 325–337.

Boots, A.W.; Drent, M.; De Boer, V.C.; Bast, A.; Haenen, G.R. Quercetin reduces markers of oxidative stress and inflammation in sarcoidosis. *Clin. Nutr.* **2011**, *30*, 506–512.

Borrelli, F.; Izzo, A.A. Herb–drug interactions with St John's wort (Hypericum perforatum): an update on clinical observations. *AAPS J.* **2009**, *11*, 710–727.

Braganhol, E.; Zamin, L.; Canedo, A.D.; Horn, F.; Tamajusuku, A.S.K.; Wink, M.R.; Salbego, C.; Battastini, A.M.O. Antiproliferative effect of quercetin in the human U138MG glioma cell line. *Anti-Cancer Drugs* **2006**, *17*, 663–671.

Brand, W.; Schutte, M.E.; Williamson, G.; Van Zanden, J.J.; Cnubben, N.H.P.; Groten, J.P.; Van Bladeren, P.J.; Rietjens, I.M.C.M. Flavonoid-mediated inhibition of intestinal ABC transporters may affect the oral bioavailability of drugs, food-borne toxic compounds and bioactive ingredients. *Biomed. Pharmacother.* **2006**, *60*, 508–519.

Butterweck, V.; Jürgenliemk, G.; Nahrstedt, A.; Winterhoff, H. Flavonoids from *Hypericum perforatum* show antidepressant activity in the forced swimming test. *Planta Med.* **2000**, *66*, 3–6.

Cao, J.; Zhang, Y.; Chen, W.; Zhao, X. The relationship between fasting plasma concentrations of selected flavonoids and their ordinary dietary intake. *Br. J. Nutr.* **2010**, *103*, 249.

Cao, L.; Kwara, A.; Greenblatt, D.J. Metabolic interactions between acetaminophen (paracetamol) and two flavonoids, luteolin and quercetin, through in-vitro inhibition studies. *J. Pharm. Pharmacol.* **2017**, *69*, 1762–1772.

Cao, Y.; Chen, Z.-J.; Jiang, H.-D.; Chen, J.-Z. Computational studies of the regioselectivities of COMT-catalyzed meta-/para-*O* methylations of luteolin and quercetin. *J. Phys. Chem. B* **2014**, *118*, 470−481.

Carter, D.C.; Ho, J.X. Structure of serum albumin. *Adv. Protein Chem.* **1994**, *45*, 153–203.

Cermak, R.; Landgraf, S.; Wolffram, S., Quercetin glucosides inhibit glucose uptake into brush-bordermembrane vesicles of porcine jejunum. *Br. J. Nutr.* **2004**, *91*, 849–855.

Challa, V.R.; Babu, P.R.; Challa, S.R.; Johnson, B.; Maheswari, C. Pharmacokinetic interaction study between quercetin and valsartan in rats and in vitro models. *Drug Dev. Ind. Pharm.* **2013**, *39*, 865–872.

Chambers, D.E.; Parks, D.A.; Patterson, G.; Roy, R.; McCord, J.M.; Yoshida, S.; Parmely, L.F.; Downey, J.M. Xanthine oxidase as a source of free radical damage in myocardiol ischemia. *J. Mol. Cell Cardiol.* **1985**, *17*, 145–152.

Chang, T.K.H.; Chen, J.; Yeung, E.Y.H. Effect of ginkgo biloba extract on procarcinogen-bioactivating human CYP1 enzymes: identification of isorhamnetin, kaempferol, and quercetin as potent inhibitors of CYP1B1. *Toxicol. Appl. Pharmacol.* **2006**, *213*, 18–26.

Chen, G.L.; Fan, M.X.; Wu, J.L.; Li, N.; Guo, M.Q. Antioxidant and anti-inflammatory properties of flavonoids from lotus plumule. *Food Chem.* **2019**, *277*, 706–712.

Chen, X.W.; Sneed, K.B.; Pan, S.Y.; Cao, C.; Kanwar, J.R.; Chew, H.; Zhou, S.-F. Herb–drug interactions and mechanistic and clinical considerations. *Curr. Drug Metabol.* **2012**, *13*, 640–651.

Cho, H.; Yun, C.W.; Park, W.K.; Kong, J.Y.; Kim, K.S.; Park, Y.; Lee, S.; Kim, B.K. Modulation of the activity of pro-inflammatory enzymes, COX-2 and iNOS, by chrysin derivatives. *Pharmacol. Res.* **2004**, *49*, 37–43.

Choi, H.K.; Mount, D.B.; Reginato, A.M. Pathogenesis of gout. *Ann. Intern. Med.* **2005**, *143*, 499–516.

Choi, J.-S.; Han, H.-K. The effect of quercetin on the pharmacokinetics of verapamil and its major metabolite, norverapamil, in rabbits. *J. Pharm. Pharmacol.* **2004**, *56*, 537–1542.

Choi, J.-S.; Li, X. Enhanced diltiazem bioavailability after oral administration of diltiazem with quercetin to rabbits. *Int. J. Pharm.* **2005**, *297*, 1–8.

Christensen, H.; Baker, M.; Tucker, G.T.; Rostami-Hodjegan, A. Prediction of plasma protein binding displacement and its implications for quantitative assessment of metabolic drug–drug interactions from in vitro data. *J. Pharm. Sci.* **2006**, *95*, 2778–2787.

Cialdella-Kam, L.; Nieman, D.C.; Sha, W.; Meaney, M.P.; Knab, A.M.; Shanely, R.A. Dose-response to 3 months of quercetin-containing supplements on metabolite and quercetin conjugate profile in adults. *Br. J. Nutr.* **2013**, *109*, 1923–1933.

Conquer, J.A.; Maiani, G.; Azzini, E.; Raguzzini, A.; Holub, B.J. Supplementation with quercetin markedly increases plasma quercetin concentration without effect on selected risk factors for heart disease in healthy subjects. *J. Nutr.* **1998**, *128*, 593–597.

Cook, N.C.; Samman, S. Flavonoids-Chemistry, metabolism, cardioprotective effects, and dietary sources. *J. Nutr. Biochem.* **1996**, *7*, 66–76.

Cos, P.; Ying, L.; Calomme, M.; Hu, J.P.; Cimanga, K.; Van Poel, B.; Pieters, L.; Vlietinck, A.J.; Vanden Berghe, D. Structure−activity relationship and classification of flavonoids as inhibitors of xanthine oxidase and superoxide scavengers. *J. Nat. Prod.* **1998**, *61*, 71–76.

Cropp, J.S.; Bussey, H.I. A review of enzyme induction of warfarin metabolism with recommendations for patient management. *Pharmacotherapy* **1997**, *17*, 917–928.

Curry, S.; Mandelkow, H.; Brick, P.; Franks, N. Crystal structure of human serum albumin complexed with fatty acid reveals an asymmetric distribution of binding sites. *Nat. Struct. Biol.* **1998**, *5*, 827–835.

Curry, S. Lessons from the crystallographic analysis of small molecule binding to human serum albumin. *Drug Metab. Pharmacokinet.* **2009,** *24*, 342–357.

Daly, A.K.; Brockmöller, J.; Broly, F.; Eichelbaum, M.; Evans, W.E.; Gonzalez, F.J.; Huang, J.D.; Idle, J.R.; Ingelman-Sundberg, M.; Ishizaki, T.; Jacqz-Aigrain, E.; Meyer, U.A.; Nebert, D.W.; Steen, V.M.; Wolf, C.R.; Zanger, U.M. Nomenclature for human CYP2D6 alleles. *Pharmacogenetics* **1996**, *6*, 193–201.

Dangles, O.; Dufour, C.; Manach, C.; Morand, C.; Remesy, C. Binding of flavonoids to plasma proteins. *Methods Enzymol.* **2001**, *335*, 319–333.

Danielson, P.B. The Cytochrome P450 Superfamily: biochemistry, evolution and drug metabolism in humans. *Curr. Drug Metab.* **2002**, *3*, 561–597.

Dawson, J.; Walters, M. Uric acid and xanthine oxidase: future therapeutic targets in the prevention of cardiovascular disease? *Br. J. Clin. Pharmacol.* **2006**, *62*, 633−644.

Day, A.J.; Bao, Y.; Morgan, M.R.; Williamson, G. Conjugation position of quercetin glucuronides and effect on biological activity. *Free Radic. Biol. Med.* **2000**, *29*, 1234–1243.

Day, A.J.; Mellon, F.; Barron, D.; Sarrazin, G.; Morgan, M.R.; Williamson, G. Human metabolism of dietary flavonoids: identification of plasma metabolites of quercetin. *Free Radic. Res.* **2001**, *35*, 941–952.

Day, A.J.; Gee, J.M.; Dupont, M.S.; Johnson, I.T.; Williamson, G. Absorption of quercetin-3-glucoside and quercetin-4‘-glucoside in the rat small intestine: the role of lactase phlorizin hydrolase and the sodium-dependent glucose transporter. *Biochem. Pharmacol.* **2003**, *65*, 1199–1206.

Day, R.O.; Birkett, D.J.; Hicks, M.; Miners, J.O.; Graham, G.G.; Brooks, P.M. New Uses for Allopurinol. *Drugs* **1994**, *48*, 339–344.

Day, R.O.; Graham, G.G.; Hicks, M.; McLachlan, A.J.; Stocker, S.L.; Williams, K.M. Clinical Pharmacokinetics and Pharmacodynamics of Allopurinol and Oxypurinol. *Clin. Pharmacokinet.* **2007**, *46*, 623–644.

De Montellano, P.R.O. Hydrocarbon hydroxylation by cytochrome P450 enzymes. *Chem. Rev.* **2010**, *110*, 932–948.

De Santi, C.; Pietrabissa, A.; Mosca, F.; Pacifici, G.M. Methylation of quercetin and fisetin, flavonoids widely distributed in edible vegetables, fruits and wine, by human liver. *Int. J. Clin. Pharmacol. Ther.* **2002**, *40*, 207–212.

Del Rio, D.; Rodriguez-Mateos, A.; Spencer, J.P.E.; Tognolini, M.; Borges, G.; Crozier, A. Dietary (poly)phenolics in human health: Structures, bioavailability, and evidence of protective effects against chronic diseases. *Antioxid. Redox Signal.* **2013**, *18*, 1818–1892.

Della Corte, E.; Gozzetti, G.; Novello, F.; Stirpe, F. Properties of the xanthine oxidase from human liver. *Biochim. Biophys. Acta-Enzymology* **1969**, *191*, 164–166.

Depeint, F.; Gee, J.M.; Williamson, G.; Johnson, I.T. Evidence for consistent patterns between flavonoid structures and cellular activities. *Proc. Nutr. Soc.* **2002**, *61*, 97–103.

Devi, K.P.; Malar, D.S.; Nabavi, S.F.; Sureda, A.; Xiao, J.; Nabavi, S.M.; Daglia, M. Kaempferol and inflammation: from chemistry to medicine. *Pharmacol. Res.* **2015**, *99*, 1–10.

Di Carlo, G.; Mascolo, N.; lzzo, A.A. Flavonoids: old and new aspects of a class of natural therapeutic drugs. *Life Sci.* **1999**, *65*, 337–353.

Dong, D.; Quan, E.; Yuan, X.; Xie, Q.; Li, Z.; Wu, B. Sodium oleate-based nanoemulsion enhances oral absorption of chrysin through inhibition of UGT mediated metabolism. *Mol. Pharm.* **2017**, *14*, 2864–2874.

Dong, H.; Xu, Y.; Zhang, X.; Tian, S. Visceral adiposity index is strongly associated with hyperuricemia independently of metabolic health and obesity phenotypes. *Sci. Rep.* **2017**, *7*, 8822.

Dresser, G.K.; Spence, J.D.; Bailey, D.G. Pharmacokinetic-pharmacodynamic consequences and clinical relevance of cytochrome P450 3A4 inhibition. *Clin. Pharmacokinet.* **2000**, *38*, 41–57.

Duan, K.-M.; Wang, S.-Y.; Ouyang, W.; Mao, Y.-M.; Yang, L.-J. Effect of quercetin on CYP3A activity in chinese healthy participants. *J. Clin. Pharmacol.* **2012**, *52*, 940–946.

Dubinsky, M.C.; Lamothe, S.; Yang, H.Y.; Targan, S.R.; Sinnett, D.; Théorêt, Y.; Seidman, E.G. Pharmacogenomics and metabolite measurement for 6-mercaptopurine therapy in inflammatory bowel disease. *Gastroenterology* **2000**, *118*, 705–713.

Dufour, C.; Dangles, O. Flavonoid–serum albumin complexation: determination of binding constants and binding sites by fluorescence spectroscopy. *Biochim. Biophys. Acta* **2005**, *1721*, 164–173.

Egert, S.; Wolffram, S.; Bosy-Westphal, A.; Boesch-Saadatmandi, C.; Wagner, A.E.; Frank, J.; Rimbach, G.; Mueller, M.J. Daily quercetin supplementation dose-dependently increases plasma quercetin concentrations in healthy humans. *J. Nutr.* **2008**, *138*, 1615–1621.

Eichelbaum, M.; Gross, A.S. The genetic polymorphism of debrisoquine/sparteine metabolism-clinical aspects. *Pharmacol. Ther.* **1990**, *46*, 377–394.

Ekstrand, B.; Rasmussen, M.K.; Woll, F.; Zlabek, V.; Zamaratskaia, G. In vitro gender-dependent inhibition of porcine cytochrome P450 activity by selected flavonoids and phenolic acids. *BioMed Res. Int.* **2015**, *2015*, 387918.

Elion, G.B. Enzymatic and metabolic studies with allopurinol. *Ann. Rheum. Dis.* **1966**, *25*, 608–614.

Elkader, A.; Sproule, B. Buprenorphine. *Clin. Pharmacokinet.* **2005**, *44*, 661–680.

Enroth, C.; Eger, B.T.; Okamoto, K.; Nishino, T.; Nishino, T.; Pai, E.F. Crystal structures of bovine milk xanthine dehydrogenase and xanthine oxidase: structure-based mechanism of conversion. *Proc. Natl. Acad. Sci. U S A* **2000**, *97*, 10723– 10728.

Fanali, G.; Trezza, V.; Marino, M.; Fasano, M.; Ascenzi, P. Human serum albumin: from bench to bedside. *Mol. Aspects Med.* **2012**, *33*, 209–290.

Feierman, D.E.; Lasker, J.M. Metabolism of fentanyl, a synthetic opioid analgesic, by human liver microsomes. Role of CYP3A4. *Drug Metab. Dispos.* **1996,** *24*, 932–939.

Filho, C.B.; Jesse, C.R.; Donato, F.; Fabbro, L.D.; de Gomes, M.G.; Goes, A.T.R.; Souza, L.C.; Boeira, S.P. Chrysin promotes attenuation of depressive-like behavior and hippocampal dysfunction resulting from olfactory bulbectomy in mice. *Chem. Biol. Interact.* **2016**, *260*, 154–162.

Galbusera, C.; Orth, P.; Fedida, D.; Spector, T. Superoxide radical production by allopurinol and xanthine oxidase. *Biochem. Pharmacol.* **2006**, *71*, 1747–1752.

Gao, F.; Wei, D.; Bian, T.; Xie, P.; Zou, J.; Mu, H.; Zhang, B.; Zhou, X. Genistein attenuated allergic airway inflammation by modulating the transcription factors T-bet, GATA-3 and STAT-6 in a murine model of asthma. *Pharmacology* **2012**, *89*, 229–236.

Ge, S.; Gao, S.; Yin, T.; Hu, M. Determination of pharmacokinetics of chrysin and its conjugates in wild-type FVB and BCRP1 knockout mice using a validated LC-MS/MS method. *J. Agric. Food Chem.* **2015**, *63*, 2902–2910.

Gee, J.M.; DuPont, S.M.; Day, A.J.; Plumb, G.W.; Williamson, G.; Johnson, I.T. Intestinal transport of quercetin glycosides in rats involves both deglycoslylation and interaction with the hexose transport pathway. *J. Nutr.* **2000**, *130*, 2765–2771.

George, C.; Minter, D.A. Hyperuricemia. In: *StatPearls [Internet]*. *Treasure Island (FL): StatPearls Publishing,* **2020**, www.ncbi.nlm.nih.gov/books/NBK459218/

Ghahramani, P.; Ellis, S.W.; Lennard, M.S.; Ramsay, L.E.; Tucker, G.T. Cytochromes P450 mediating the N-demethylation of amitriptyline. *Br. J. Clin. Pharmacol.* **1997**, *43*, 137–144.

Ghorbani, A. Mechanisms of antidiabetic effects of flavonoid rutin. *Biomed. Pharmacother.* **2017**, *96*, 305–312.

Ghuman, J.; Zunszain, P.; Petitpas, I.; Bhattacharya, A.A.; Otagiri, M.; Curry, S. Structural basis of the drug-binding specificity of human serum albumin. *J. Mol. Biol.* **2005**, *353*, 38–52.

Gillum, J.G; Israel, D.S; Polk, R.E. Pharmacokinetic drug interactions with antimicrobial agents. *Clin. Pharmacokinet.* **1993**, *25*, 450–482.

Gonzalez, F.J. Role of cytochromes P450 in chemical toxicity and oxidative stress: studies with CYP2E1. *Mutat. Res.* **2005**, *569*, 101–110.

Grandison, M.K.; Boudinot, F.D. Age-related changes in protein binding of drugs: implications for therapy. *Clin. Pharmacokinet.* **2000**, *38*, 271–290.

Granfors, M.T.; Backman, J.T.; Laitila, J.; Neuvonen, P.J. Tizanidine is mainly metabolized by cytochrome P450 1A2 in vitro. *Br. J. Clin. Pharmacol.* **2004**, *57*, 349–353.

Greenblatt, D.J.; Von Moltke, L.L.; Harmatz, J.S.; Ciraulo, D.A.; Shader, R.I. Alprazolam pharmacokinetics, metabolism, and plasma levels: clinical implications. *J. Clin. Psychiatry* **1993**, *54*, 4–14.

Grub, S.; Bryson, H.; Goggin, T.; Lüdin, E.; Jorga, K. The saquinavir (soft gelatin capsule) with ketoconazole, erythromycin and rifampicin: comparison of the effect in healthy volunteers and in HIV-infected patients. *Eur. J. Clin. Pharmacol.* **2001**, *57*, 115–121.

Guengerich, F.P. Common and uncommon cytochrome P450 reactions related to metabolism and chemical toxicity. *Chem. Res. Toxicol.* **2001**, *14*, 611–650.

Guengerich, F.P. Mechanisms of cytochrome P450-catalyzed oxidations. *ACS Catal.* **2018**, *8*, 10964−10976.

Guerciolini, R.; Szumlanski, C.; Weinshilboum, R.M. Human liver xanthine oxidase: Nature and extent of individual variation. *Clin. Pharmacol. Ther.* **1991**, *50*, 663–672.

Gupta, D.; Lis, C.G. Pretreatment serum albumin as a predictor of cancer survival: a systematic review of the epidemiological literature. *Nutr. J.* **2010**, *9*, 69–85.

Hamelin, B.A.; Bouayad, A.; Méthot, J.; Jobin, J.; Desgagnés, P.; Poirier, P.; Allaire, J.; Dumesnil, J.; Turgeon, J. Significant interaction between the nonprescription antihistamine diph enhydramine and the CYP2D6 substrate metoprolol in healthy men with high or low CYP2D6 activity. *Clin. Pharmacol. Ther.* **2000**, *67*, 466–477.

Harris, M.D.; Siegel, L.B.; Alloway, J.A. Gout and hyperuricemia. *Am. Fam. Physician.* **1999**, *59*, 925–934.

Harrison, R. Physiological roles of xanthine oxidoreductase. *Drug Metab. Rev.* **2004**, *36*, 363–375.

He, L.; He, F.; Bi, H.; Li, J.; Zeng, S.; Luo, H.-B.; Huang, M. Isoform-selective inhibition of chrysin towards human cytochrome P450 1A2. Kinetics analysis, molecular docking, and molecular dynamics simulations. *Bioorganic Med. Chem. Lett.* **2010**, *20*, 6008–6012.

He, N.; Xie, H.-G.; Collins, X.; Edeki, T.; Yan, Z. Effects of individual ginsenosides, ginkgolides and flavonoids on CYP2C19 and CYP2D6 activity in human liver microsomes. *Clin. Exp. Pharmacol. Physiol.* **2006**, *33*, 813–815.

Heimm, K.E.; Tagliaferro, A.R.; Bobilya, D.J. Flavonoid antioxidants: chemistry, metabolism and structure-activity relationships. *J. Nutr. Biochem.* **2002**, *13*, 572–584.

Heinz, S.A.; Henson, D.A.; Nieman, D.C.; Austin, M.D. A 12-week supplementation with quercetin does not affect natural killer cell activity, granulocyte oxidative burst activity or granulocyte phagocytosis in female human subjects. *Br. J. Nutr.* **2010**, *104*, 849–857.

Hendset, M.; Hermann, M.; Lunde, H.; Refsum, H.; Molden, E. Impact of the CYP2D6 genotype on steady-state serum concentrations of aripiprazole and dehydroaripiprazole. *Eur. J. Clin. Pharmacol.* **2007**, *63*, 1147–1151.

Herman, R.J.; Nakamura, K.; Wilkinson, G.R.; Wood, A.J. Induction of propranolol metabolism by rifampicin. *Br. J. Clin. Pharmacol.* **1983**, *16*, 565–569.

Hiemke, C.; Härtter, S. Pharmacokinetics of selective serotonin reuptake inhibitors. *Pharmacol. Ther.* **2000**, *85*, 11–28.

Hille, R.; Nishino, T. Flavoprotein structure and mechanism. Part IV: xanthine oxidase and xanthine dehydrogenase. *FASEB J.* **1995**, *9*, 995–1003.

Ho, P.C.; Saville, D.J.; Wanwimolruk, S. Inhibition of human CYP3A4 activity by grapefruit flavonoids, furanocoumarins and related compounds. *J. Pharm. Pharm. Sci.* **2001**, *4*, 217–27.

Hollman, P.C.; De Vries, J.H.; Van Leeuwen, S.D.; Mengelers, M.J.; Katan, M.B. Absorption of dietary quercetin glycosides and quercetin in healthy ileostomy volunteers. *Am. J. Clin. Nutr.* **1995**, *62*, 1276–1282.

Hollman, P.C.H.; Hertog, M.G.L.; Katan, M.B. Analysis and health effects of flavonoids. *Food Chem.* **1996**, *57*, 43–46.

Hollman, P.C.H.; Katan, M.B. Dietary flavonoids: intake, health effects and bioavailability. *Food Chem. Toxicol.* **1999**, *37*, 937–942.

Hollman, P.C.H.; Arts, I.C.W. Flavonols, flavones and flavanols – nature, occurrence and dietary burden. *J. Sci. Food Agric.* **2000**, *80*, 1081–1093.

Honoré, B.; Brodersen, R. Albumin binding of anti-inflammatory drugs utility of a site-oriented versus a stoichiometric analysis. *Mol. Pharmacol.* **1984**, *25*, 137–150.

Huang, H.-C.; Wang, H.-R.; Hsieh, L.-M. Antiproliferative effect of baicalein, a flavonoid from a chinese herb, on vascular smooth muscle cell. *Eur. J. Pharmacol.* **1994**, *251*, 91–93.

Huang, J.; Wang, S.; Zhu, M.; Chen, J.; Zhu, X.; Chen, J.; Zhu, X. Effects of genistein, apigenin, quercetin, rutin and astilbin on serum uric acid levels and xanthine oxidase activities in normal and hyperuricemic mice. *Food Chem. Toxicol.* **2011**, *49*, 1943–1947.

Huang, W.H.; Lee, A.R.; Yang, C.H. Antioxidative and anti-inflammatory activities of polyhydroxyflavonoids of Scutellaria baicalensis GEORGI. *Biosci. Biotechnol. Biochem.* **2006**, *70*, 2371–2380.

Iio, M.; Moriyama, A.; Matsumoto, Y.; Takaki, N.; Fukumoto, M. Inhibition of xanthine oxidase by flavonoids. *Agr. Biol. Chem.* **1985**, *49*, 2173–2176.

Il'ichev, I.V.; Perry, J.L.; Simon, J.D. Interaction of ochratoxin A with human serum albumin. A common binding site of ochratoxin A and warfarin in subdomain IIA. *J. Phys. Chem. B* **2002**, *106*, 460–465.

Inami, Y.; Waguri, S.; Sakamoto, A.; Kouno, T.; Nakada, K.; Hino, O.; Watanabe, S.; Ando, J.; Iwadate, M.; Yamamoto, M.; Lee, M.-S.; Tanaka, K.; Komatsu, M. Persistent activation of Nrf2 through p62 in hepatocellular carcinoma cells. *J. Cell. Biol.* **2011**, *193*, 275–284.

Inoue-Choi, M.; Yuan, J.M.; Yang, C.S.; Van Den Berg, D.J.; Lee, M.J.; Gao, Y.T.; Yu, M.C. Genetic association between the COMT genotype and urinary levels of tea polyphenols and their metabolites among daily green tea drinkers. *Int. J. Mol. Epidemiol. Genet.* **2010**, *1*, 114–23.

Ishii, T.; Itoh, K.; Takahashi, S.; Sato, H.; Yanagawa, T.; Katoh, Y.; Bannai, S.; Yamamoto, M. Transcription factor Nrf2 coordinately regulates a group of oxidative stress-inducible genes in macrophages. *J. Biol. Chem.* **2000**, *275*, 16023–16029.

Itoh, K.; Tong, K.I.; Yamamoto, M. Molecular mechanism activating nrf2–keap1 pathway in regulation of adaptive response to electrophiles. *Free Radic. Biol. Med.* **2004**, *36*, 1208–1213.

Itoh, T.; Saura, Y.; Tsuda, Y.; Yamada, H. Stereoselectivity and enantiomer–enantiomer interactions in the binding of ibuprofen to human serum albumin. *Chirality* **1997**, *9*, 643–649.

Janisch, K.M.; Williamson, G.; Needs, P.; Plumb, G.W. Properties of quercetin conjugates: modulation of LDL oxidation and binding to human serum albumin. *Free Radic. Res.* **2004**, *38*, 877–884.

Jurva, U.; Wikström, H.V.; Weidol, L.; Bruins, A.P. Comparison between electrochemistry/mass spectrometryand cytochrome P450 catalyzed oxidation reactions. *Rapid Commun. Mass Spectrom.* **2003**, *17*, 800–810.

Jusko, W.J.; Gretch, M. Plasma and tissue protein binding of drugs in pharmacokinetics. *Drug Metab. Rev.* **1976**, *5*, 43–140.

Kalogeropoulos, N.; Yanni, A.E.; Koutrotsios, G.; Aloupi, M. Bioactive microconstituents and antioxidant properties of wild edible mushrooms from the island of Lesvos, Greece. *Food Chem. Toxicol.* **2013**, *55*, 378–385.

Kaminsky, L.S.; Zhang, Z.-Y. Human P450 metabolism of warfarin. *Pharmacol. Ther.* **1997**, *73*, 67–74.

Kang, D.H.; Ha, S.K. Uric Acid Puzzle: Dual role as antioxidantand pro-oxidant. *Electrolyte Blood Press.* **2014**, *12*, 1–6.

Kao, J.C.; Zhou, C.; Sherman, M.; Laughton, C.A.; Chen, S. Molecular basis of the inhibition of human aromatase (estrogen synthetase) by flavone and isoflavone phytoestrogens: a site-directed mutagenesis study. *Environ. Health Perspect.* **1998**, *106*, 85–92.

Kaushik, D.; O'Fallon, K.; Clarkson, P.M.; Dunne, C.P.; Conca, K.R.; Michniak-Kohn, B. Comparison of quercetin pharmacokinetics following oral supplementation in humans. *J. Food Sci.* **2012**, *77*, H231–H238.

Kawase, A.; Matsumoto, Y.; Hadano, M.; Ishii, Y.; Iwaki, M. Differential effects of chrysin on nitrofurantoin pharmacokinetics mediated by intestinal breast cancer resistance protein in rats and mice. *J. Pharm. Pharm. Sci.* **2009**, *12*, 150–163.

Kelly, G.S. Quercetin. *Altern. Med. Rev.* **2011**, *16*, 172–194.

Kimata, M.; Shichijo, M.; Miura, T.; Serizawa, I.; Inagaki, N.; Nagai, H. Effects of luteolin, quercetin and baicalein on immunoglobulin E-mediated mediator release from human cultured mast cells. *Clin. Exp. Allergy* **2000**, *30*, 501–508.

Kimura, S.; Warabi, E.; Yanagawa, T.; Ma, D.; Itoh, K.; Ishii, Y.; Kawachi, Y.; Ishii, T. Essential role of Nrf2 in keratinocyte protection from UVA by quercetin. *Biochem. Biophys. Res. Commun.* **2009**, *387*, 109–114.

Kimura, Y.; Ito, H.; Ohnishi, R.; Hatano, T. Inhibitory effects of polyphenols on human cytochrome P450 3A4 and 2C9 activity. *Food Chem. Toxicol.* **2010**, *48*, 429–435.

Kivistö, K.T.; Lamberg, T.S.; Kantola, T.; Neuvonen, P.J. Plasma buspirone concentrations are greatly increased by erythromycin and itraconazole. *Clin. Pharmacol. Ther.* **1997**, *62*, 348–354.

Knekt, P.; Kumpulainen, J.; Järvinen, R.; Rissanen, H.; Heliövaara, M.; Reunanen, A.; Hakulinen, T.; Aromaa, A. Flavonoid intake and risk of chronic diseases. *Am. J. Clin. Nutr.* **2002**, *76*, 560–568.

Koch-Weser, J.; Sellers, E.M. Binding of drugs to serum albumin. *N. Engl. J. Med.* **1976**, *294*, 311–316.

Korobkova, E.A. Effect of natural polyphenols on CYP metabolism: implications for diseases. *Chem. Res. Toxicol.* **2015**, *28*, 1359–1390.

Kragh-Hansen, U. Evidence for a large and flexible region of human serum albumin possessing high affinity binding sites for salicylate, warfarin, and other ligands. *Mol. Pharmacol.* **1988**, *34*, 60–171.

Kragh-Hansen, U.; Chuang, V.T.G.; Otagiri, M. Practical aspects of the ligand-binding and enzymatic properties of human serum albumin. *Biol. Pharm. Bull.* **2002**, *25*, 695–704.

Kudo, M.; Sasaki, T.; Ishikawa, M.; Hirasawa, N.; Hiratsuka, M. Kinetics of 6-thioxanthine metabolism by allelic variants of xanthine oxidase. *Drug Metab. Pharmacokinet.* **2010**, *25*, 361–366.

Kumar, S.; Pandey, A.K. Chemistry and biological activities of flavonoids: an overview. *Sci. World J.* **2013**, *162750*.

Kupiec, T.; Raj, V. Fatal seizures due to potential herb-drug interactions with ginkgo biloba. *J. Anal. Toxicol.* **2005**, *29*, 755–758.

Larsson, T.; Wedborg, M.; Turner, D. Correction of inner-filter effect in fluorescence excitation-emission matrix spectrometry using Raman scatter. *Anal. Chim. Acta* **2007**, *583*, 357–363.

Laursen, T.; Jensen, K.; Møller, B.L. Conformational changes of the NADPH-dependent cytochrome P450 reductase in the course of electron transfer to cytochromes P450. *Biochim. Biophys. Acta* **2011**, *1814*, 132–138.

Lee, E.J.; Ji, G.E.; Sung M.K. Quercetin and kaempferol suppress immunoglobulin E-mediated allergic inflammation in RBL-2H3 and Caco-2 cells. *Inflamm. Res.* **2010**, *59*, 847–854.

Lee, J.; Mitchell, A.E. Pharmacokinetics of quercetin absorption from apples and onions in healthy humans. *J. Agric. Food Chem.* **2012**, *60*, 3874−3881.

Leemann, T.; Transon, C.; Dayer, P. Cytochrome P450TB (CYP2C): a major monooxygenase catalyzing diclofenac 4′-hydroxylation in human liver. *Life Sci.* **1993**, *52*, 29–34.

Leong, R.W.L.; Gearry, R.B.; Sparrow, M.P. Thiopurine hepatotoxicity ininflammatory bowel disease: the role for adding allopurinol. *Expert Opin. Drug Saf.* **2008**, *7*, 607–616.

Li, D.; Peng, C.; Xie, X.; Mao, Y.; Li, M.; Cao, Z.; Fan, D. Antidiabetic effect of flavonoids from *Malus toringoides* (Rehd.) Hughes leaves in diabetic mice and rats. *J. Ethnopharmacol.* **2014**, *153*, 561–567.

Li, W.; Sun, H.; Zhang, X.; Wang, H.; Wu, B. Efflux transport of chrysin and apigenin sulfates in HEK293 cells overexpressing SULT1A3: the role of multidrug resistance-associated protein 4 (MRP4/ABCC4). *Biochem. Pharmacol.* **2015**, *98*, 203–214.

Li, X.; Jiang, Q.; Wang, T.; Liu, J.; Chen, D. Comparison of the antioxidant effects of quercitrin and isoquercitrin: understanding the role of the 6 ″-OH group. *Molecules* **2016**, *21*, 1246.

Li, X.; Wang, H.; Gao, Y.; Li, L.; Tang, C.; Wen, G.; Zhou, Y.; Zhou, M.; Mao, L.; Fan, Y. Protective effects of quercetin on mitochondrial biogenesis in experimental traumatic brain injury via the Nrf2 signaling pathway. *PLoS One.* **2016**, *11*, 1–13.

Li, Y.; Lu, J.; Paxton, J.W. The role of ABC and SLC transporters in the pharmacokinetics of dietary and herbal phytochemicals and their interactions with xenobiotics. *Curr. Drug Metab.* **2012**, *13*, 624–639.

Lin, C.-M.; Chen, C.-S.; Chen, C.-T.; Liang, Y.-C.; Lin, J.-K. Molecular modeling of flavonoids that inhibits xanthine oxidase. *Biochem. Biophys. Res. Commun.* **2002**, *294*, 167–172.

Lin, J.H.; Lu, A.Y.H. Inhibition and induction of cytochrome P450 and the clinical implications. *Clin. Pharmacokinet.* **1998**, *35*, 361–390.

Lin, S.; Zhang, G.; Liao, Y.; Pan, J. Inhibition of chrysin on xanthine oxidase activity and its inhibition mechanism. *Int. J. Biol. Macromol.* **2015a**, *81*, 274–282.

Lin, S.; Zhang, G.; Liao, Y.; Pan, J.; Gong, D. Dietary flavonoids as xanthine oxidase inhibitors: structure–affinity and structure–activity relationships. *J. Agric. Food Chem.* **2015b**, *63*, 7784–7794.

Linas, L.S.; Whittenburg, D.; Repine, J.E. Role of xanthine oxidase is ischemia/reperfusion. *Am. J. Physiol.* **1990**, *258*, G711–G716.

Litwack, G. Nucleic acids and molecular genetics. In: Litwack, G. (ed) *Human Biochemistry*, **2018**, Academic Press, London, UK, pp. 257-317. ISBN 978-0-12-3838643.

Lobo, E.D.; Bergstrom, R.F.; Reddy, S.; Quinlan, T.; Chappell, J.; Hong, Q.; Ring, B.; Knadler, M.P. In vitro and in vivo evaluations of cytochrome P450 1A2 interactions with duloxetine. *Clin. Pharmacokinet.* **2008**, *47*, 191–202.

Lynch, T.; Price, A. The effect of cytochrome P450 metabolism on drug response, interactions, and adverse effects. *Am. Fam. Physician* **2007**, *76*, 391–396.

Manach, C.; Donovan, J.L. Pharmacokinetics and metabolism of dietary flavonoids in humans. *Free Radic. Res.* **2004**, *38*, 771–785.

Manach, C.; Scalbert, A.; Morand, C.; Rémésy, C.; Jiménez, L. Polyphenols: food sources and bioavailability. *Am. J. Clin. Nutr.* **2004**, *79*, 727–747.

Mandery, K.; Glaeser, H.; Bujok, K.; Schmidt, I.; Fromm, M.F. Organic anion transporting polypeptides and organic cation transporter 1 contribute to the cellular uptake of the flavonoid quercetin. *Naunyn Schmiedebergs Arch. Pharmacol.* **2014**, *387*, 883–891.

Martin, K.R.; Appel, C.L. Polyphenols as dietary supplements: a double-edged sword. *Nutr. Diet. Suppl.* **2010**, *2*, 1–12.

Masuda, S.; Maeda-Yamamoto, M.; Usui, S.; Fujisawa, T. 'Benifuuki'Green tea containing *O*-methylated catechin reduces symptoms of japanese cedar pollinosis: a randomized, double-blind, placebo-controlled trial. *Allergol. Int.* **2014**, *632*, 11–217.

McCord, J.M. Oxygen-derived free radicals in postischemic tissue injury. *N. Engl. J. Med.* **1985**, *312*, 159–163.

McDonnell, A.M.; Dang, C.H. Basic review of the cytochrome P450 system. *J. Adv. Pract. Oncol.* **2013**, *4*, 263–268.

McKay, D.L.; Blumberg, J.B. A Review of the bioactivity and potential health benefits of chamomile tea (*Matricariarecutita L.*). *Phytother. Res.* **2006**, *20*, 519–530.

McLeod, H.L. Clinically relevant drug-drug interactions in oncology. *Br. J. Clin. Pharmacol.* **1998**, *45*, 539–544.

Meech, R.; Mackenzie, P.I. Structure and function of uridine diphosphate glucuronosyltransferases. *Clin. Exp. Pharmacol. Physiol.* **1997**, *24*, 907–915.

Meunier, B.; De Visser, S.P.; Shaik, S. Mechanism of oxidation reactions catalyzed by cytochrome P450 enzymes. *Chem. Rev.* **2004**, *104*, 3947–3980.

Meyer, M.C.; Guttman, D.E. The binding of drugs by plasma proteins. *J. Pharm. Sci.* **1968**, *57*, 895–918.

Miron, A.; Aprotosoaie, A.C.; Trifan, A.; Xiao, J. Flavonoids as modulators of metabolic enzymes and drug transporters. *Ann. N.Y. Acad. Sci.* **2017**, *1398*, 152–167.

Mohos, V.; Fliszár-Nyúl, E.; Schilli, G.; Hetényi, C.; Lemli, B.; Kunsági-Máté, S.; Bognár, B.; Poór, M. Interaction of chrysin and its main conjugated metabolites chrysin-7-sulfate and chrysin7-glucuronide with serum albumin. *Int. J. Mol. Sci.* **2018a**, *19*, 4073.

Mohos, V.; Bencsik, T.; Boda, G.; Fliszár-Nyúl, E.; Lemli, B.; Kunsági-Máté, S.; Poór, M. Interactions of casticin, ipriflavone, and resveratrol with serum albumin and their inhibitory effects on CYP2C9 and CYP3A4 enzymes. *Biomed. Pharmacother.* **2018b**, *107*, 777–784.

Mohos, V.; Pánovics, A.; Fliszár-Nyúl, E.; Schilli, G.; Hetényi, C.; Mladenka, P.; Needs, P.W.; Kroon, P.A.; Pethő, G.; Poór, M. Inhibitory effects of quercetin and its human and microbial metabolites on xanthine oxidase enzyme. *Int. J. Mol. Sci.* **2019**, *20*, 2681.

Montero, M.T.; Pouplana, R.; Valls, O.; García, S. On the binding of cinmetacin and indomethacin to human serum albumin. *J. Pharm. Pharmacol.* **1986**, *38*, 925–927.

Moon, Y.J.; Wang, X.; Morris, M.E. Dietary flavonoids: effects on xenobiotic and carcinogen metabolism. *Toxicol. Vitro* **2006**, *20*, 187–210.

Morris, M.E.; Zhang, S. Flavonoid–drug interactions: Effects of flavonoids on ABC transporters. *Life Sci.* **2006**, *78*, 2116–2130.

Mullen, W.; Edwards, C.A.; Crozier, A. Absorption, excretion and metabolite profiling of methyl, glucuronyl-, glucosyl- and sulpho-conjugates of quercetin in human plasma and urine after ingestion of onions. *Br. J. Nutr.* **2006**, *96*, 107–116.

Murota, K.; Terao, J. Antioxidative flavonoid quercetin: implication of its intestinal absorption and metabolism. *Arch. Biochem. Biophys.* **2003**, *417*, 12–17.

Murrell, G.A.C.; Rapeport, W.G. Clinical pharmacokinetics of allopurinol. *Clin. Pharmacokinet.* **1986**, *11*, 343–353.

Nabavi, S.F.; Braidy, N.; Habtemariam, S.; Orhan, I.E.; Daglia, M.; Manayi, A.; Gortzi, O.; Nabavi, S.M. Neuroprotective effects of chrysin: From chemistry to medicine. *Neurochem. Int.* **2015**, *90*, 224–231.

Nagao, A.; Seki, M.; Kobayashi, H. Inhibition of xanthine oxidase by flavonoids. *Biosci. Biotechnol. Biochem.* **1999**, *63*, 1787–1790.

Ndanusa, B.U.; Mustapha, A.; Abdu-Aguye, I. The effect of single dose of rifampicin on the pharmacokinetics of oral nifedipine. *J. Pharm. Biomed. Anal.* **1997**, *15*, 1571–1575.

Neal, G.E. Genetic implications in the metabolism and toxicity of mycotoxins. *Toxicol. Lett.* **1995**, *82–83*, 861–867.

Nebert, D.W.; Russell, D.W. Clinical importance of the cytochromes P450. *Lancet* **2002**, *360*, 1155–62.

Needs, P.W.; Kroon, P.A. Convenient synthesis of metabolically important glucuronides and sulfates. *Tetrahedron* **2006**, *62*, 6862–6868.

Neuvonen, P.J.; Niemi, M.; Backman, J.T. Drug interactions with lipid-lowering drugs: mechanisms and clinical relevance. *Clin. Pharmacol. Ther.* **2006**, *80*, 565–581.

Nguyen, M.A.; Staubach, P.; Wolffram, S.; Langguth, P. The influence of single-dose and short-term administration of quercetin on the pharmacokinetics of midazolam in humans. *J. Pharm. Sci.* **2015**, *104*, 3199–3207.

Niemi, M.; Backman, J.T.; Fromm, M.F.; Neuvonen, P.J.; Kivistö, K.T. Pharmacokinetic interactions with rifampicin. *Clin. Pharmacokinet.* **2003**, *42*, 819–850.

Noh, K.; Oh, D.G.; Nepal, M.R.; Jeong, K.S.; Choi, Y.; Kang, M.J.; Kang, W.; Jeong, H.G.; Jeong, T.C. Pharmakokinetic interaction of chrysin with caffeine in rats. *Biomol. Ther.* **2016**, *24*, 446–452.

Novak, R.F.; Woodcroft, K.J. The alcohol-inducible form of cytochrome P450 (CYP2E1): role in toxicology and regulation of expression. *Arch. Pharm. Res.* **2000**, *23*, 267–282.

Ohnhaus, E.E.; Brockmeyer, N.; Dylewicz, P.; Habicht, H. The effect of antipyrine and rifampin on the metabolism of diazepam. *Clin. Pharmacol. Ther.* **1987**, *42*, 148–156.

Otagiri, M.A molecular functional study on the interactions of drugs with plasma proteins. *Drug Metab. Pharmacokinet.* **2005**, *20*, 309–323.

Otake, Y.; Hsieh, F.; Walle, T, Glucuronidation versus oxidation of the flavonoid galangin by human liver microsomes and hepatocytes. *Drug Metab. Dispos.* **2002**, *30*, 576–581.

Otton, S.V.; Crewe, H.K.; Lennard, M.S.; Tucker, G.T.; Woods, H.F. Use of quinidine inhibition to define the role of the sparteine/debrisoquine cytochrome P450 in metoprolol oxidation by human liver microsomes. *J. Pharmacol. Exp. Ther.* **1988**, *247*, 242–247.

Östlund, J.; Zlabek, V.; Zamaratskaia, G. In vitro inhibition of human CYP2E1 and CYP3A by quercetin and myricetin in hepatic microsomes is not gender dependent. *Toxicology* **2017**, *381*, 10–18.

Pacher, P.; Nivorozhkin, A.; Szabo, C. Therapeutic effects of xanthine oxidase inhibitors: renaissance half a century after the discovery of allopurinol. *Pharmacol. Rev.* **2006**, *58*, 87−114.

Pal, S.; Saha, C. A review on structure–affinity relationship of dietary flavonoids with serum albumins. *J. Biomol. Struct. Dyn.* **2014**, *32*, 1132–1147.

Panche, A.N.; Diwan, A.D.; Chandra, S.R. Flavonoids: an overview. *J. Nutr. Sci.* **2016**, *5*, 1–15.

Patten, C.J.; Thomas, P.E.; Guy, R.L.; Lee, M.; Gonzalez, F.J; Guengerich, F.P.; Yang, C.S. Cytochrome P450 enzymes involved in acetaminophen activation by rat and human liver microsomes and their kinetics. *Chem. Res. Toxicol.* **1993**, *6*, 511–518.

Pearce, R.E.; Leeder, J.S.; Kearns, G.L. Biotransformation of fluticasone: in vitro characterization. *Drug Metab. Dispos.* **2006**, *34*, 1035–1040.

Pereira, O.R.; Silva, A.M.S.; Domingues, M.R.M.; Cardoso, S.M. Identification of phenolic constituents of cytisus multiflorus. *Food Chem.* **2012**, *131*, 652–659.

Pietta, P.G. Flavonoids as antioxidants. *J. Nat. Prod.* **2000**, *63*, 1035–1042.

Pingili, R.B.; Pawar, A.K.; Challa, S.R. Systemic exposure of paracetamol (acetaminophen) was enhanced by quercetin and chrysin co-administration in Wistar rats and in vitro model: risk of liver toxicity. *Drug Dev. Ind. Pharm.* **2015**, *41*, 1793–1800.

Pingili, R.B.; Pawar, A.K.; Challa, S.R. Effect of chrysin on the formation of N-acetyl-p-benzoquinoneimine, a toxic metabolite of paracetamol in rats and isolated rat hepatocytes. *Chem. Biol. Interact.* **2019**, *302*, 123–134.

Pirmohamed, M. Drug-grapefruit juice interactions. *BMJ* **2013**, *346*, f1–f1.

Poór, M.; Boda, G.; Needs, P.W.; Kroon, P.A.; Lemli, B.; Bencsik, T. Interaction of quercetin and its metabolites with warfarin: displacement of warfarin from serum albumin and inhibition of CYP2C9 enzyme. *Biomed. Pharmacother.* **2017**, *88*, 574–581.

Poór, M.; Boda, G.; Kunsági-Máté, S.; Needs, P.W.; Kroon, P.A.; Lemli, B. Fluorescence spectroscopic evaluation of the interactions of quercetin, isorhamnetin, and quercetin-3′-sulfate with different albumins. *J. Lumin.* **2018a**, *194*, 156–163.

Poór, M.; Boda, G.; Mohos, V.; Kuzma, M.; Bálint, M.; Hetényi, C.; Bencsik, T. Pharmacokinetic interaction of diosmetin and silibinin with other drugs: inhibition of CYP2C9-mediated biotransformation and displacement from serum albumin. *Biomed. Pharmacother.* **2018b**, *102*, 912–921.

Preissner, S.C.; Hoffmann, M.F.; Preissner, R.; Dunkel, M.; Gewiess, A.; Preissner, S. Polymorphic cytochrome P450 enzymes (CYPs) and their role in personalized therapy. *PLoS ONE* **2013**, *8*, e82562.

Pritsos, C.A. Cellular distribution, metabolism and regulation of the xanthine oxidoreductase enzyme system. *Chem. Biol. Interact.* **2000**, *129*, 195–208.

Pushpavalli, G.; Kalaiarasi, P.; Veeramani, C.; Pugalendi, K.V. Effect of chrysin on hepatoprotective and antioxidant status in d-galactosamine-induced hepatitis in rats. *Eur. J. Pharmacol.* **2010**, *631*, 36–41.

Rastogi, H.; Jana, S. Evaluation of Inhibitory Effects of caffeic acid and quercetin on human liver cytochrome P450 activities. *Phytother. Res.* **2014**, *28*, 1873–1878.

Raucy, J.L.; Lasker, J.M.; Lieber, C.S.; Black, M. Acetaminophen activation by human liver cytochromes P450IIE1 and P450IA2. *Arch. Biochem. Biophys.* **1989**, *271*, 270–283.

Ravishankar, D.; Salamah, M.; Attina, A.; Pothi, R.; Vallance, T.M.; Javed, M.; Williams, H.F.; Alzahrani, E.M.S.; Kabova, E.; Vaiyapuri, R.; Shankland, K.; Gibbins, J.; Strohfeldt, K.; Greco, F.; Osborn, H.M.I.; Vaiyapuri, S. Ruthenium-conjugated chrysin analogues modulate platelet activity, thrombus formation and haemostasis with enhanced efficacy. *Sci. Rep.* **2017**, *7*, 5738.

Rechner, A.R.; Kuhnle, G.; Bremner, P.; Hubbard, G.P.; Moore, K.P.; Rice-Evans, C.A. the metabolic fate of dietary polyphenols in humans. *Free Rad. Biol. Med.* **2002**, *33*, 220–235.

Rice-Evans, C.; Spencer, J.P.E.; Schroeter, H.; Rechner, A.R. Bioavailability of flavonoids and potential bioactive forms in vivo. *Drug Metab. Pers. Ther.* **2000**, *17*, 291–310.

Rice-Evans, C. Flavonoid antioxidants. *Curr. Med. Chem.* **2001**, *8*, 797–807.

Ritchie, R.F.; Palomaki, G.E.; Neveux, L.M.; Navolotskaia, O.; Ledu, T.B.; Craig, W.Y. Reference distributions for the negative acute-phase serum proteins, albumin, transferrin and transthyretin: a practical, simple and clinically relevant approach in a large cohort. *J. Clin. Lab. Anal.* **1999**, *13*, 273–279.

Riva, R.; Albani, F.; Contin, M.; Baruzzi, A. Pharmacokinetic interactions between antiepileptic drugs: clinical considerations. *Clin. Pharmacokinet.* **1996**, *31*, 470–493.

Rogerio, A.P.; Dora, C.L.; Andrade, E.L.; Chaves, J.S.; Silva, L.F.; Lemos-Senna, E.; Calixto, J.B. Anti-inflammatory effect of quercetin-loaded microemulsion in the airways allergic inflammatory model in mice. *Pharmacol. Res.* **2010**, *61*, 288–297.

Rundles, RW. The development of allopurinol. *Arch. Intern. Med.* **1982**, *145*, 89–94.

Russo, E.; Scicchitano, F.; Whalley, B.J.; Mazzitello, C.; Ciriaco, M.; Esposito, S.; Patanè, M.; Upton, R.; Pugliese, M.; Chimirri, S.; Mammì, M.; Palleria, C.; De Sarro, G. *Hypericum perforatum*: pharmacokinetic, mechanism of action, tolerability, and clinical drug–drug interactions. *Phytother. Res.* **2014**, *28*, 643–655.

Ryu, C.S.; Oh. S.J.; Oh, J.M.; Lee, J.Y.; Lee, S.Y.; Chae, J.; Kwon, K.; Kim, S.K. Inhibition of cytochrome P450 by propolis in human liver microsomes. *Toxicol. Res.* **2016**, *32*, 207–213.

Saha, N. Clinical pharmacokinetics and drug interactions. In: Vohora, D; Singh, G. (eds) *Pharmaceutical Medicine and Translational Clinical Research*, **2018**, Academic Press, Boston, USA, pp. 81–106. ISBN 9780128021033.

Sakela, M.; Lapatto, R.; Raivio, K.O. xanthine oxidoreductase gene expression and enzyme activity in developing human tissues. *Biol. Neonate.* **1998**, *74*, 274–280.

Samanta, A.; Das, G.; Das, S.K. Roles of flavonoids in plants. *Int. J. Pharm. Sci. Tech.* **2011**, *6*, 12–35.

Sanoski, C.A.; Bauman, J.L. Clinical observations with the amiodarone/warfarin interaction: dosing relationships with long-term therapy. *Chest* **2002**, *121*, 19–23.

Sarawek, S.; Feistel, B.; Pischel, I.; Butterweck, V. Flavonoids of *Cynara scolymus* possess potent xanthin oxidase inhibitory activity in vitro but are devoid of hypouricemic effects in rats after oral application. *Planta Med.* **2008**, *74*, 221–227.

Sarmah, S.; Das, S.; Roy, A.S. Protective actions of bioactive flavonoids chrysin and luteolin on the glyoxal induced formation of advanced glycation end products and aggregation of human serum albumin: In vitro and molecular docking analysis. *Int. J. Biol. Macromol.* **2020**, *165*, 2275–2285.

Sarnesto, A.; Linder, N.; Raivio, K.O. Organ distribution and molecular forms of human xanthine dehydrogenase/xanthine oxidase protein. *Lab. Invest.* **1996**, *74*, 48–56.

Satyanarayana, K.; Sravanthi, K.; Shaker, I.A.; Ponnulakshmi, R.; Selvaraj, J. Role of chrysin on expression of insulin signaling molecules. *J. Ayurveda Integr. Med.* **2015**, *6*, 248–258.

Sbarouni, E.; Georgiadou, P.; Voudris, V. Ischemia modified albumin changes – review and clinical implications. *Clin. Chem. Lab. Med.* **2011**, *49*, 177–184.

Scambia, G.; De Vincenzo, R.; Ranelletti, P.O.; Benedetti Panici, P.; Ferrandina, G.; D'Agostino, G.; Fattorossi, A.; Bombardelli, E.; Mancuso, S. Antiproliferative effect of silybin on gynaecological malignancies: synergism with cisplatin and doxorubicin. *Eur. J. Cancer* **1996**, *32*, 877–882.

Scandlyn, M.J.; Stuart, E.C.; Rosengren, R.J. Sex-specific differences in CYP450 isoforms in humans. *Expert Opin. Drug Metab. Toxicol.* **2008**, *4*, 413–424.

Schlesinger, N. Dietary factors and hyperuricaemia. *Curr. Pharm. Des.* **2005**, *11*, 4133–4138.

Schmider, J.; Brockmöller, J.; Arold, G.; Bauer, S.; Roots, I. Simultaneous assessment of CYP3A4 and CYP1A2 activity in vivo with alprazolam and caffeine. *Pharmacogenetics* **1999**, *9*, 725–734.

Sengupta, B.; Sengupta, P.K. The interaction of quercetin with human serum albumin: a fluorescence spectroscopic study. *Biochem. Biophys. Res. Commun.* **2002**, *299*, 400–403.

Serra, A.; Macia, A.; Romero, M.P.; Reguant, J.; Ortega, N.; Motilva, M.J. Metabolic pathways of the colonic metabolism of flavonoids (flavonols, flavones and flavanones) and phenolic acids. *Food Chem.* **2012**, *130*, 383–393.

Sesink, A.L.A.; Arts, I.C.W.; De Boer, V.C.J.; Breedveld, P.; Schellens, J.H.M.; Hollman, P.C.H.; Russel, F.G.M. Breast cancer resistance protein (BCRP1/ABCG2) limits net intestinal uptake of quercetin in rats by facilitating apical efflux of glucuronides. *Mol. Pharmacol.* **2005**, *67*, 1999–2006.

Setoguchi, N.; Takamura, N.; Fujita, K.; Ogata, K.; Tokunaga, J.; Nishio, T.; Chosa, E.; Arimori, K.; Kawai, K.; Yamamoto, R. A diclofenac suppository-nabumetone combination therapy for arthritic pain relief and a monitoring method for the diclofenac binding capacity of HSA site II in rheumatoid arthritis. *Biopharm. Drug Dispos.* **2013**, *34*, 125–136.

Seyoum, A.; Asres, K.; El-Fiky, F.K. Structure–radical scavenging activity relationships of flavonoids. *Phytochemistry* **2006**, *67*, 2058–2070.

Sharma, R.; Gatchie, L.; Williams, I.S.; Jain, S.K.; Vishwakarma, R.A.; Chaudhuri, B.; Bharate, S.B. *Glycyrrhiza glabra* extract and quercetin reverses cisplatin resistance in triple-negative MDA-MB-468 breast cancer cells via inhibition of cytochrome P450 1B1 enzyme. *Bioorg. Med. Chem. Lett.* **2017**, *27*, 5400–5403.

Shi, Y.; Williamson, G. Quercetin lowers plasma uric acid in pre-hyperuricaemic males: a randomised, double-blinded, placebo-controlled, cross-over trial. *Br. J. Nutr.* **2016**, *115*, 800–806.

Shimada, T.; Tanaka, K.; Takenaka, S.; Murayama, N.; Martin, M.V.; Foroozesh, M.K.; Yamazaki, H.; Guengerich, F.P.; Komori, M. Structure−function relationships of inhibition of human cytochromes P450 1A1, 1A2, 1B1, 2C9, and 3A4 by 33 flavonoid derivatives. *Chem. Res. Toxicol.* **2010**, *23*, 1921–1935.

Shin, S.-C.; Choi, J.-S.; Lib, X. Enhanced bioavailability of tamoxifen after oral administration of tamoxifen with quercetin in rats. *Int. J. Pharm.* **2006**, *313*, 144–149.

Shipley, M. Hyperuricaemia and gout. *J.R. Coll Physicians Edinb.* **2011**, *41*, 229–33.
Siddoway, L.A. Amiodarone: guidelines for use and monitoring. *Am. Fam. Physician* **2003**, *68*, 2189–2196.

Siess, M.H.; Le Bon, A.M.; Canivenc-Lavier, M.C.; Amiot, M.J.; Sabatier, S.; Aubert, S.Y.; Suschetet, M. Flavonoids of honey and propolis: characterization and effects on hepatic drug-metabolizing enzymes and benzo [a]pyrene-DNA binding in rats. *J. Agric. Food Chem.* **1996**, *44*, 2297–2301.

Sim, S.C.; Ingelman-Sundberg, M. The human cytochrome P450 (CYP) allele nomenclature website: a peer-reviewed database of CYP variants and their associated effects. *Hum. Genomics* **2010**, *4*, 278–281.

Simard, J.R.; Zunszain, P.A.; Ha, C.E.; Yang, J.S.; Bhagavan, N.V.; Petitpas, I.; Curry, S.; Hamilton, J.A. Locating high-affinity fatty acid-binding sites on albumin by X-ray crystallography and NMR spectroscopy. *Proc. Natl. Acad. Sci. U.S.A.* **2005**, *102*, 17958–17963.

Slaughter, R.L.; Edwards, D.J. Recent advances: the cytochrome P450 enzymes. *Ann. Pharmacother.* **1995**, *29*, 619–24.

Smith, D.A.; Di, L.; Kerns, E.H. The effect of plasma protein binding on in vivo efficacy: misconceptions in drug discovery. *Nat. Rev. Drug Discov.* **2010**, *9*, 929–939.

Spector, T. Inhibition of urate production by allopurinol. *Biochem. Pharmacol.* **1977**, *26*, 355–358.

Srinivasan, S.; Pari, L. Antihyperlipidemic effect of diosmin: a citrus flavonoid on lipid metabolism in experimental diabetic rats. *J. Funct. Foods* **2013**, *5*, 484–492.

Stirpe, F.; Della Corte, E. The regulation of rat liver xanthine oxidase – conversion in vitro of the enzyme activity from dehydrogenase (type D) to oxidase (type O). *J. Biol. Chem.* **1969**, *244*, 3855–3863.

Syvalahti, E.; Pihlajamaki, K.; Iisalo, E. Effect of tuberculostatic agents on the response of serum growth hormone and immunoreactive insulin to intravenous tolbutamide, and on the halflife of tolbutamide. *Int. J. Clin. Pharmacol. Biopharm.* **1976**, *13*, 83–89.

Tahir, M.; Sultana, S. Chrysin modulates ethanol metabolism in wistar rats: a promising role against organ toxicities. *Alcohol Alcohol.* **2011**, *46*, 383–392.

Takamura, N.; Maruyama, T.; Chosa, E.; Kawai, K.; Tsutsumi, Y.; Uryu, Y.; Yamasaki, K.; Deguchi, T.; Otagiri, M. Bucolome, a potent binding inhibitor for furosemide, alters the pharmacokinetics and diuretic effect of furosemide: potential for use of bucolome to restore diuretic response in nephrotic syndrome. *Drug Metab. Dispos.* **2005**, *33*, 596–602.

Takemura, H.; Itoh, T.; Yamamoto, K.; Sakakibara, H.; Shimoi, K. Selective Inhibition of Methoxyflavonoids on Human CYP1B1 Activity. *Bioorgan. Med. Chem.* **2010**, *18*, 6310–6315.

Tan, H.; Chen, L.; Ma, L.; Liu, S.; Zhou, H.; Zhang, Y.; Guo, T.; Liu, W.; Dai, H.; Yu, Y. Fluorescence spectroscopic investigation of competitive interactions between quercetin and aflatoxin B1 for binding to human serum albumin. *Toxins* **2019**, *11*, 214.

Tanigawa, S.; Fujii, M.; Hou, D.-X. Action of Nrf2 and Keap1 in ARE-mediated NQO1 expression by quercetin. *Free Radic. Biol. Med.* **2007**, *42*, 1690–1703.

Tapas, A.R.; Sakarkar, D.M.; Kakde, R.B. Flavonoids as nutraceuticals: a review. *Trop. J. Pharm. Res.* **2008**, *7*, 1089–1099.

Terada, L.S.; Willinghan, I.R.; Rosandich, M.E.; Leff, J.A.; Kindt, G.W.; Repine, J.E. Generation of superoxide anion by brain endothelial cell xanthine oxidase. *J. Cell Physiol.* **1991**, *148*, 191–196.

Thilakarathna, S.H.; Rupasinghe, H.P.V. Flavonoid bioavailability and attempts for bioavailability enhancement. *Nutrients* **2013,** *5*, 3367–87.

Toh, J.Y.; Tan, V.M.H.; Lim, P.C.Y.; Lim, S.T.; Chong, M.F.F. Flavonoids from fruit and vegetables: a focus on cardiovascular risk factors. *Curr. Atheroscler. Rep.* **2013**, *15*, 368.

Trafalis, D.T.; Panteli, E.S.; Grivas, A.; Tsigris, C.; Karamanakos, P.N. CYP2E1 and risk of chemically mediated cancers. *Expert Opin. Drug Metab. Toxicol.* **2010**, *6*, 307–319.

Tsao, D.; Liu, S.; Dokholyan, N.V. Regioselectivity of catechol *O*-methyltransferase confers enhancement of catalytic activity. *Chem. Phys. Lett.* **2011**, *506*, 135–138.

Tsujimoto, M.; Horie, M.; Honda, H.; Takara, K.; Nishiguchi, K. The structure-activity correlation on the inhibitory effects of flavonoids on cytochrome P450 3A activity. *Biol. Pharm. Bull.* **2009**, *32*, 671–676.

Tu, B.; Chen, Z.-F.; Liu, Z.-J.; Li, R.-R.; Ouyang, Y.; Hu, Y.-J. Study of the structure-activity relationship of flavonoids based on their interaction with human serum albumin. *RSC Adv.* **2015**, *5*, 73290–73300.

Turnheim, K.; Krivanek, P.; Oberbauer, R. Pharmacokinetics and pharmacodynamics of allopurinol in elderly and young subjects. *Br. J. Clin. Pharmacol.* **1999**, *48*, 501–509.

Umathe, S.N.; Dixit, P.V.; Kumar, V.; Bansod, K.U.; Wanjari, M.M. Quercetin pretreatment increases the bioavailability of pioglitazone in rats: involvement of CYP3A inhibition. *Biochem. Pharmacol.* **2008**, *75*, 1670–1676.

Unnikrishnan, M.K.; Veerapur, V.; Nayak, Y.; Mudgal, P.P.; Mathew, G. Antidiabetic, antihyperlipidemic and antioxidant effects of the flavonoids. In: Watson, R.R.; Preedy, V.R.; Zibadi, S. (eds) *Polyphenols in Human Health and Disease,* Chapter 13, **2014**, Academic Press, San Diego, CA, USA, pp. 143–161.

Usuda, N.; Reddy, M.K.; Hashimoto, T.; Rao, M.S.; Reddy, J.K. Tissue specificity and species differences in the distribution of urate oxidase in peroxisomes. *Lab. Invest.* **1988**, *58*, 100–111.

Vallner, J.J. Binding of drugs by albumin and plasma protein. *J. Pharm. Sci.* **1977**, *66*, 447–465.

Van Hoorn, D.E.C.; Nijveldt, R.J.; Van Leeuwen, P.A.M.; Hofman, Z.; M'Rabet, L.; De Bont, D.B.A.; Van Norren, K. Accurate prediction of xanthine oxidase inhibition based on the structure of flavonoids. *Eur. J. Pharmacol.* **2002**, *451*, 111–118.

Vida, R.G.; Fittler, A.; Somogyi-Végh, A.; Poór, M. Dietary quercetin supplements: assessment of online product informations and quantitation of quercetin in the products by high-performance liquid chromatography. *Phytother. Res.* **2019**, *33*, 1912–1920.

Viskupičová, J.; Ondrejovič, M.; Sturdík, E. Bioavailability and metabolism of flavonoids. *J. Food Nutr. Res.* **2008**, *47*, 151–162.

Vukics, V.; Guttman, A. Structural characterization of flavonoid glycosides by multi-stage mass spectrometry. *Mass Spectrom. Rev.* **2010**, *29*, 1–16.

Wach, A.; Pyrzyńska, K.; Biesaga, M. Quercetin content in some food and herbal samples. *Food Chem.* **2007**, *100*, 699–704.

Wajner, M.; Harkness, R.A. Distribution of xanthine dehydrogenase and oxidase activities in human and rabbit tissues. *Biochem. Biophys. Acta* **1989**, *991*, 79–84.

Walle, T.; Otake, Y.; Brubaker, J.A.; Walle, U.K.; Halushka, P.V. Disposition and metabolism of the flavonoid chrysin in normal volunteers. *Br. J. Clin. Pharmacol.* **2001**, *51*, 143–146.

Walle, T. Methylation of dietary flavones greatly improves their hepatic metabolic stability and intestinal absorption. *Mol. Pharm.* **2007**, *4*, 826–832.

Walle, U.K.; Galijatovic, A.; Walle, T. Transport of the flavonoid chrysin and its conjugated metabolites by the human intestinal cell line Caco-2. *Biochem. Pharmacol.* **1999**, *58*, 431–438.

Wang, L.S.; Zhu, B.; Abd El-Aty, A.M.; Zhou, G.; Li, Z.; Wu, J.; Chen, G.L.; Liu, J.; Tang, Z.R.; An, W.; Li, Q.; Wang, D.; Zhou, H.H. The influence of St John's wort on CYP2C19 activity with respect to genotype. *J. Clin. Pharmacol.* **2004**, *44*, 577–581.

Wang, T.-Y.; Li, Q.; Bi, K.-S. Bioactive flavonoids in medicinal plants: structure, activity and biological fate. *Asian J. Pharm. Si.* **2018**, *13*, 12–23.

Wang, X.; Morris, M.E. Effects of the flavonoid chrysin on nitrofurantoin pharmacokinetics in rats: potential involvement of ABCG2. *Drug Metab. Dispos.* **2007**, *35*, 268–274.

Wang, X.D.; Li, J.L.; Lu, Y.; Chen, X.; Huang, M.; Chowbay, B.; Zhou, S.-F. Rapid and simultaneous determination of nifedipine and dehydronifedipine in human plasma by liquid chromatography–tandem mass spectrometry: application to a clinical herb–drug interaction study. *J. Chromatogr. B* **2007**, *852*, 534–544.

Waud, W.R.; Rajagopalan, K.V. The mechanism of conversion of rat liver xanthine dehydrogenase from an NAD+-dependent form (type D) to an O2-dependent form (type O). *Arch. Biochem. Biophys.* **1976**, *172*, 365–379.

Wilkinson, G.R. Drug metabolism and variability among patients in drug response. *N. Engl. J. Med.* **2005**, *352*, 2211–2221.

Wink, M. Biochemistry, physiology and ecological functions of secondary metabolites. In: Wink, M. (ed) *Biochemistry of Plant Secondary Metabolism (second edition),* **2010**, New York: Wiley–Blackwell Publishing, USA, pp. 1–17. ISBN 9781405183970.

Wong, C.C.; Botting, N.P.; Orfila, C.; Al-Maharik, N.; Williamson, G. Flavonoid conjugates interact with organic anion transporters (OATs) and attenuate cytotoxicity of adefovir mediated by organic anion transporter 1 (OAT1/SLC22A6). *Biochem. Pharmacol.* **2011**, *81*, 942–949.

Wu, L.-X.; Guo, C.-X.; Qu, Q.; Yu, J.; Chen, W.-Q.; Wang, G.; Fan, L.; Li, Q.; Zhang W.; Zhou, H.-H. Effects of natural products on the function of human organic anion transporting polypeptide 1B1. *Xenobiotica* **2011**, *42*, 339–348.

Wynalda, M.A.; Hutzler, J.M.; Koets, M.D.; Podoll, T.; Wienkers, L.C. In vitro metabolism of clindamycin in human liver and intestinal microsomes. *Drug Metab. Dispos.* **2003**, *31*, 878–887.

Xiao, J.; Cao, H.; Wang, Y.; Yamamoto, K.; Wei, X. Structure-affinity relationship of flavones on binding to serum albumins: Effect of hydroxyl groups on ring A. *Mol. Nutr. Food Res.* **2010**, *54*, 253–260.

Xiao, J.; Zhao, Y.; Wang, H.; Yuan, Y.; Yang, F.; Zhang, C.; Yamamoto, K. Noncovalent interaction of dietary polyphenols with common human plasma proteins. *J. Agric. Food Chem.* **2011**, *59*, 10747–10754.

Xiao, J.; Zhai, H.; Yao, Y.; Wang, C.; Jiang, W.; Zhang, C.; Simard, A.R.; Zhang, R.; Hao, J. Chrysin attenuates experimental autoimmune neuritis by suppressing immuno-inflammatory responses. *Neuroscience* **2014**, *262*, 156–164.

Yamasaki, K.; Maruyama, T.; Kragh-Hansen, U.; Otagiri, M. Characterization of site I on human serum albumin: concept about the structure of a drug binding site. *Biochim. Biophys. Acta* **1996**, *1295*, 147–157.

Yamasaki, K.; Chuang, V.T.G.; Maruyama, T.; Otagiri, M. Albumin–drug interaction and its clinical implication. *Biochim. Biophys. Acta Gen. Subj.* **2013**, *1830*, 5435–5443.

Yan, R.; Cao, Y.; Chen, C.; Dai, H.; Yu, S.; Wei, J.; Li, H.; Yang, B. Antioxidant flavonoids from the seed of Oroxylum indicum. *Fitoterapia* **2011**, *82*, 841–848.

Yao, L.H.; Jiang, Y.M.; Shi, J.; Tomás-Barberán, F.A.; Datta, N.; Singanusong, R.; Chen, S.S. Flavonoids in food and their health benefits. *Plant Foods Hum. Nutr.* **2004**, *59*, 113–122.

Yasumori, T.; Chen, L.S.; Li, Q.H.; Ueda, M.; Tsuzuki, T.; Goldstein, J.A.; Kato, R.; Yamazoe, Y. Human CYP2C-mediated stereoselective phenytoin hydroxylation in Japanese: difference in chiral preference of CYP2C9 and CYP2C19. *Biochem. Pharmacol.* **1999**, *57*, 1297–1303.

Zand, R.S.R.; Jenkins, D.J.A.; Diamandis, E.P. Flavonoids andsteroid hormone-dependent cancers. *J. Chromatogr. B* **2002**, *777*, 219–232.

Zanger, U.M.; Turpeinen, M.; Klein, K.; Schwab, M. Functional pharmacogenetics/genomics of human cytochromes P450 involved in drug biotransformation. *Anal. Bioanal. Chem.* **2008**, *392*, 1093–1108.

Zanger, U.M.; Schwab, M. Cytochrome P450 enzymes in drug metabolism: Regulation of gene expression, enzyme activities, and impact of genetic variation. *Pharmacol. Ther.* **2013**, *138*, 103–141.

Zhang, C.; Wang, R.; Zhang, G.; Gong, D. Mechanistic insights into the inhibition of quercetin on xanthine oxidase. *Int. J. Biol. Macromol.* **2018**, *112*, 405–412.

Zhang, G.; Wang, L.; Pan, J. Probing the binding of the flavonoid diosmetin to human serum albumin by multispectroscopic techniques. *J. Agric. Food Chem.* **2012**, *60*, 2721–2729.

Zhang, Y.; Liao, P.; Li, W.; Hu, D.; Chen, L.; Guan, S. Baicalin attenuates cardiac dysfunction and myocardial remodeling in a chronic pressure-overload mice model. *Cell. Physiol. Biochem.* **2017**, *41*, 849–864.

Zhou, S.; Chan, E.; Pan, S.Q.; Huang, M.; Lee, E.J. Pharmacokinetic interactions of drugs with St John's wort. *J. Psychopharmacol.* **2004**, *18*, 262–276.

Zhu, J.X.; Wang, Y.; Kong, L.D.; Yang, C.; Zhang, X. Effects of *Biota orientalis* extract and its flavonoid constituents, quercetin and rutin on serum uric acid levels in oxonate-induced mice and xanthine dehydrogenase and xanthine oxidase activities in mouse liver. *J. Ethnopharmacol.* **2004**, *93*, 133–140.

Zhu, S.; Xu, T.; Luo, Y.; Zhang, Y.; Xuan, H.; Ma, Y.; Pan, D.; Zhu, H. Luteolin enhances sarcoplasmic reticulum Ca2+-ATPase activity through p38 MAPK signaling thus improving rat cardiac function after ischemia/reperfusion. *Cell. Physiol. Biochem.* **2017**, *41*, 999–1010.

Zsila, F. Subdomain IB is the third major drug binding region of human serum albumin: toward the three-sites model. *Mol. Pharm.* **2013**, *10*, 1668–1682.

X. Saját közlemények listája:

X.1. Az értekezés alapjául szolgáló folyóiratcikkek:

Violetta Mohos, Eszter Fliszár-Nyúl, Gabriella Schilli, Csaba Hetényi, Beáta Lemli, Sándor Kunsági-Máté, Balázs Bognár, Miklós Poór, Interaction of chrysin and its main conjugated metabolites chrysin-7-sulfate and chrysin-7-glucuronide with serum albumin. *Int. J. Mol. Sci.* 19 (**2018**) 4073. [**IF: 4,183; Q1**]

Violetta Mohos, Attila Pánovics, Eszter Fliszár-Nyúl, Gabriella Schilli, Csaba Hetényi, Přemysl Mladěnka, Paul W. Needs, Paul A. Kroon, Gábor Pethő, Miklós Poór, Inhibitory effects of quercetin as well as its human and microbial metabolites on xanthine oxidase enzyme. *Int. J. Mol. Sci.* 20 (**2019**) 2681. [**IF: 4,556; Q1**]

Violetta Mohos, Eszter Fliszár-Nyúl, Miklós Poór, Inhibition of xanthine oxidase-catalyzed xanthine and 6-mercaptopurine oxidation by flavonoid aglycones and some of their conjugates. *Int. J. Mol. Sci.* 21 (**2020**) 3256. [***IF: 4,556; Q1**]

Violetta Mohos, Eszter Fliszár-Nyúl, Orsolya Ungvári, Éva Bakos, Katalin Kuffa, Tímea Bencsik, Balázs Zoltán Zsidó, Csaba Hetényi, Ágnes Telbisz, Csilla Özvegy-Laczka, Miklós Poór, Effects of chrysin and its major conjugated metabolites chrysin-7-sulfate and chrysin-7-glucuronide on cytochrome P450 enzymes, and on OATP, P-gp, BCRP and MRP2 transporters. *Drug Metab. Dispos.* 48 (**2020**) 1064–1073. [***IF: 3,231; D1/Q1**]

Violetta Mohos, Eszter Fliszár-Nyúl, Orsolya Ungvári, Katalin Kuffa, Paul W. Needs, Paul A. Kroon, Ágnes Telbisz, Csilla Özvegy-Laczka, Miklós Poór, Inhibitory effects of quercetin and its main methyl, sulfate, and glucuronic acid conjugates on cytochrome P450 enzymes, and on OATP, BCRP and MRP2 transporters. *Nutrients* 12 (**2020**) 2306. [***IF: 4,546; D1/Q1**]

A dolgozat alapjául szolgáló folyóiratcikkek összesített impakt faktora: 21,072

Kumulatív impakt faktor: 55,433

Független hivatkozások (mtmt.hu): 39

X.2. Az értekezés alapjául szolgáló kongresszusi előadások és poszter prezentációk:

Violetta Mohos, Attila Pánovics, Miklós Poór, The inhibitory effect of quercetin and chrysin metabolites on xanthine oxidase enzyme by the biotransformation of 6-mercaptopurine and xanthine. ***4th International Cholnoky Symposium*** (Pécs, Magyarország, 2018.05.10-11.) [**előadás**]

Violetta Mohos, Attila Pánovics, Eszter Fliszár-Nyúl, Monika Moravcova, Přemysl Mladěnka, Paul W. Needs, Paul A. Kroon, Miklós Poór, Interaction of human and microbial metabolites of quercetin with serum albumin and biotransformation enzymes. ***5th International Cholnoky Symposium*** (Pécs, Magyarország, 2019.04.25.) [**előadás**]

Miklós Poór, Eszter Fliszár-Nyúl, **Violetta Mohos**, Zelma Faisal, Beáta Lemli, Pharmacological/toxicological importance of albumin-ligand interactions. ***5th International Cholnoky Symposium*** (Pécs, Magyarország, 2019.04.25.) [**előadás**]

Violetta Mohos, Attila Pánovics, Eszter Fliszár-Nyúl, Monika Moravcova, Přemysl Mladěnka, Paul W. Needs, Paul A. Kroon, Miklós Poór, Interactions of human and microbial metabolites of quercetin with serum albumin and biotransformation enzymes. ***4th Symposium on Weak Molecular Interactions*** (Matsue, Japán, 2019.05.17-19.) [**előadás**]

Miklós Poór, Eszter Fliszár-Nyúl, **Violetta Mohos**, Zelma Faisal, Beáta Lemli, Csaba Hetényi, Sándor Kunsági-Máté, Pharmacological/toxicological importance and investigation of albumin-ligand interactions. ***4th Symposium on Weak Molecular Interactions*** (Matsue, Japán, 2019.05.17-19.) [**előadás**]

Miklós Poór, **Violetta Mohos**, Eszter Fliszár-Nyúl, Interactions of conjugated and colon metabolites of flavonoids with serum albumin and biotransformation enzymes. ***13th World Congress on Polyphenols Applications*** (Valletta, Málta, 2019.09.30-10.01.) [**előadás**]

Poór Miklós, **Mohos Violetta**, Fliszár-Nyúl Eszter, Interactions of flavonoid metabolites with serum albumin and biotransformation enzymes. ***XVI. Congressus Pharmaceuticus Hungaricus*** (2020.09.10-12.) [**előadás**]

Violetta Mohos, Beáta Lemli, Sándor Kunsági-Máté, Gabriella Boda, Balázs Bognár, Miklós Poór, Interaction of chrysin and its metabolites with human serum albumin. ***12th World Congress on Polyphenols Applications*** (Bonn, Németország, 2018.09.25-28.) [**poszter**]

Violetta Mohos, Eszter Fliszár-Nyúl, Tímea Bencsik, Balázs Bognár, Miklós Poór, Interactions of chrysin conjugates with cytrochrome P450 enzymes. ***13th World Congress on Polyphenols Applications*** (Valletta, Málta, 2019.09.30-10.01.) [**poszter**]

Mohos Violetta, Pánovics Attila, Fliszár-Nyúl Eszter, Poór Miklós, Quercetin és chrysin konjugált metabolitjaik kölcsönhatásai xantin-oxidáz enzimmel. ***TOX'2019 Tudományos Konferencia*** (Szeged, Magyarország, 2019.10.9-11.) [**poszter**]

X.3. Egyéb folyóiratcikkek:

Miklós Poór, Gabriella Boda, **Violetta Mohos**, Mónika Kuzma, Mónika Bálint, Csaba Hetényi, Tímea Bencsik, Pharmacokinetic interaction of diosmetin and silibinin with other drugs: Inhibition of CYP2C9-mediated biotransformation and displacement from serum albumin. *Biomed. Pharmacother.* 102 (**2018**) 912–921. [**IF: 3,743; Q1**]

Violetta Mohos, Tímea Bencsik, Gabriella Boda, Eszter Fliszár-Nyúl, Beáta Lemli, Sándor Kunsági-Máté, Miklós Poór, Interactions of casticin, ipriflavone, and resveratrol with serum albumin and their inhibitory effects on CYP2C9 and CYP3A4 enzymes. *Biomed. Pharmacother.* 107 (**2018**) 777–784. [**IF: 3,743; Q1**]

Nikolett Szentes, Valéria Tékus, **Violetta Mohos**, Éva Borbély, Zsuzsanna Helyes, Exploratory and locomotor activity, learning and memory functions in somatostatin receptor subtype 4 gene-deficient mice in relation to aging and sex. *GEROSCIENCE* 41, (**2019**) 631–641. [**Q1**]

Eszter Fliszár-Nyúl, **Violetta Mohos**, Tímea Bencsik, Beáta Lemli, Sándor Kunsági-Máté, Miklós Poór, Interactions of 7,8-Dihydroxyflavone with serum albumin as well as with CYP2C9, CYP2C19, CYP3A4, and xanthine oxidase biotransformation enzymes. *Biomolecules* 9 (**2019**) 655. [**IF: 4,082; Q1**]

Balázs Zoltán Zsidó, Mária Balog, Nikolett Erős, Miklós Poór, **Violetta Mohos**, Eszter Fliszár-Nyúl, Csaba Hetényi, Masaki Nagane, Kálmán Hideg, Tamás Kálai, Balázs Bognár, Synthesis of spin-labelled bergamottin: a potent CYP3A4 inhibitor with antiproliferative activity. *Int. J. Mol. Sci.* 21 (**2020**) 508. [***IF: 4,556; Q1**]

Violetta Mohos, Eszter Fliszár-Nyúl, Beáta Lemli, Balázs Zoltán Zsidó, Csaba Hetényi, Přemysl Mladěnka, Pavel Horký, Milan Pour, Miklós Poór, Testing the pharmacokinetic interactions of 24 colonic flavonoid metabolites with human serum albumin and cytochrome P450 enzymes. *Biomolecules* 10 (**2020**) 409. [***IF: 4,082; Q1**]

Eszter Fliszár-Nyúl, **Violetta Mohos**, Rita Csepregi, Přemysl Mladěnka, Miklós Poór, Inhibitory effects of polyphenols and their colonic metabolites on CYP2D6 enzyme using two different substrates. *Biomed. Pharmacother.* 131 (**2020**) 110732. [***IF: 4,545; Q1**]

Zelma Faisal, **Violetta Mohos**, Eszter Fliszár-Nyúl, Kateřina Valentová, Kristýna Káňová, Beáta Lemli, Sándor Kunsági-Máté, Miklós Poór, Interaction of silymarin components and their sulfate metabolites with human serum albumin and cytochrome P450 (2C9, 2C19, 2D6, and 3A4) enzymes. *Biomed. Pharmacother.* 138 (**2021**) 111459. [***IF: 4,545; Q1**]

Eszter Fliszár-Nyúl, Zelma Faisal, **Violetta Mohos**, Diána Derdák, Beáta Lemli, Tamás Kálai, Cecília Sár, Balázs Zoltán Zsidó, Csaba Hetényi, Ádám I. Horváth, Zsuzsanna Helyes, Ruth Deme, Dóra Bogdán, Andrea Czompa, Péter Mátyus, Miklós Poór, Interaction of SZV 1287, a novel oxime analgesic drug candidate, and its metabolites with serum albumin. *J. Mol. Liq.* (**2021**) DOI: 10.1016/j.molliq.2021.115945 [***IF: 5,065; Q1**]

*2019-es évre számított impakt faktorok

X.4. Egyéb prezentációk:

Mohos Violetta, Bencsik Tímea, Boda Gabriella, Poór Miklós, Kaszticin, ipriflavon és rezveratrol kölcsönhatásainak vizsgálata szérum albuminnal, valamint CYP2C9 és CYP3A4 biotranszformációs enzimekkel. ***TOX'2018 Tudományos Konferencia*** (Lillafüred, Magyarország, 2018.10.17-19.) [**poszter**]

Mohos Violetta, Pánovics Attila, Fliszár-Nyúl Eszter, Monika Moravcova, Přemysl Mladěnka, Poór Miklós, A colon mikroflóra által képzett quercetin metabolitok kölcsönhatásainak vizsgálata szérum albuminnal, valamint xantin-oxidáz és CYP2C9 biotranszformációs enzimekkel. ***Farmakokinetika és Gyógyszermetabolizmus Szimpózium*** (Galyatető, Magyarország, 2019.04.10-12.) [**poszter**]

XI. Köszönetnyilvánítás

Nagy-nagy köszönettel tartozom témavezetőmnek, Dr. Poór Miklósnak, aki nélkül ez a munka nem születhetett volna meg. Köszönöm, hogy iránymutatásával és szakmai támogatásával mindig segítette munkámat, valamint azt, hogy szakmai kérdéseimre mindig készségesen válaszolt. Töretlen lelkesedése, kitartása és precizitása mindig példaértékű volt számomra. Továbbá, hálával tartozom a Gyógyszerhatástani Tanszék munkatársainak (Gábornak, Zelmának, Orsinak, Eszternek, Katának, Slávkának, Krisztinek és Ritának), akikkel mindig öröm volt együtt dolgozni. Emellett, köszönöm Dr. Hetényi Csabának, Dr. Zsidó Balázsnak, valamint Schilli Gabriellának, hogy szerkezeti vizsgálataikkal emelték munkám színvonalát, valamint hálás köszönettel tartozom Dr. Lemli Beátának is a Hyperquados mérések elvégzéséért. Köszönet illeti Dr. Fliszár-Nyúl Esztert, Fábián Katalint és Schveibert Istvánt a HPLC analízisekért. Továbbá, szeretném megköszönni TDK-hallgatóimnak, Pánovics Attilának, Gombor Boglárkának és Bognár Bendegúznak, hogy általuk az utánpótlás-nevelésbe is belekóstolhattam. Köszönettel tartozom Prof. Dr. Pethő Gábornak valamint Prof. Dr. Gregus Zoltánnak is, akik mindig érdeklődve figyelték szakmai előrehaladásomat, valamint köszönöm nekik azt, hogy személyiségükkel valamint előadásmódjukkal a gyógyszerhatástant és a toxikológiát már graduális hallgatóként is a kedvenc tantárgyaimmá tették. Végezetül leírhatatlan nagy hálával tartozom a családomnak, a páromnak és a barátaimnak, akik mindvégig támogattak és lelkesítettek, valamint végig kitartottak mellettem ezen a nehéz úton. Külön hálával tartozom apukámnak, aki már évekkel ezelőtt is tudta és mindig is hangoztatta, hogy képes vagyok helyt állni a kutatás világában.

International Journal of
Molecular Sciences

MDPI

Article

Interaction of Chrysin and Its Main Conjugated Metabolites Chrysin-7-Sulfate and Chrysin-7-Glucuronide with Serum Albumin

Violetta Mohos [1,2], Eszter Fliszár-Nyúl [1], Gabriella Schilli [3], Csaba Hetényi [3], Beáta Lemli [2,4], Sándor Kunsági-Máté [2,4], Balázs Bognár [5] and Miklós Poór [1,2,*]

1 Department of Pharmacology, University of Pécs, Faculty of Pharmacy, Szigeti út 12, H-7624 Pécs, Hungary; mohos.violetta@gytk.pte.hu (V.M.); eszter.nyul@aok.pte.hu (E.F.-N.)
2 János Szentágothai Research Center, University of Pécs, Ifjúság útja 20, H-7624 Pécs, Hungary; lemli.beata@gytk.pte.hu (B.L.); kunsagi-mate.sandor@gytk.pte.hu (S.K.-M.)
3 Department of Pharmacology and Pharmacotherapy, University of Pécs, Medical School, Szigeti út 12, H-7624 Pécs, Hungary; scgpecs@gmail.com (G.S.); csabahete@yahoo.com (C.H.)
4 Department of Pharmaceutical Chemistry, University of Pécs, Faculty of Pharmacy, Rókus utca 2, H-7624 Pécs, Hungary
5 Department of Organic and Pharmacological Chemistry, University of Pécs, Medical School, Honvéd utca 1, H-7624 Pécs, Hungary; bognar.balazs83@gmail.com
* Correspondence: poor.miklos@pte.hu; Tel.: +36-536-000 (ext. 34646)

Received: 12 November 2018; Accepted: 14 December 2018; Published: 17 December 2018

Abstract: Chrysin (5,7-dihydroxyflavone) is a flavonoid aglycone, which is found in nature and in several dietary supplements. During the biotransformation of chrysin, its conjugated metabolites chrysin-7-sulfate (C7S) and chrysin-7-glucuronide (C7G) are formed. Despite the fact that these conjugates appear in the circulation at much higher concentrations than chrysin, their interactions with serum albumin have not been reported. In this study, the complex formation of chrysin, C7S, and C7G with human (HSA) and bovine (BSA) serum albumins was investigated employing fluorescence spectroscopic, ultrafiltration, and modeling studies. Our major observations/conclusions are as follows: (1) Compared to chrysin, C7S binds with a threefold higher affinity to HSA, while C7G binds with a threefold lower affinity; (2) the albumin-binding of chrysin, C7S, and C7G did not show any large species differences regarding HSA and BSA; (3) tested flavonoids likely occupy Sudlow's Site I in HSA; (4) C7S causes significant displacement of Sudlow's Site I ligands, exerting an even stronger displacing ability than the parent compound chrysin. Considering the above-listed observations, the high intake of chrysin (e.g., through the consumption of dietary supplements with high chrysin contents) may interfere with the albumin-binding of several drugs, mainly due to the strong interaction of C7S with HSA.

Keywords: chrysin; chrysin-7-sulfate; chrysin-7-glucuronide; serum albumin; fluorescence spectroscopy; albumin–ligand complexes

1. Introduction

Flavonoids are polyphenolic compounds, which are widely distributed in the plant kingdom. Flavonoids can exert several beneficial effects in the body [1]; however, they can also interact with serum albumin [2,3], biotransformation enzymes [4], and transport proteins [5], leading to their ability to affect the pharmacokinetics of drugs [6]. Nowadays, many dietary supplements contain extremely high doses of flavonoids (ranging from several hundreds to thousands of milligrams), resulting in their unusually high appearance in the blood (and likely in tissues) [7].

After oral consumption/administration, flavonoids commonly undergo biotransformation; therefore, their naturally occurring structure may not have significant oral bioavailability [8]. Therefore, mainly the metabolites appear at high concentrations in the circulation.

Chrysin (5,7-dihydroxyflavone; Figure 1) is a flavonoid aglycone, which occurs in propolis, honey, flowers, mushrooms, and fruits [9–11]. Based on in vitro studies, chrysin inhibits the aromatase enzyme (which converts androstenedione to estrone and testosterone to estradiol) [12,13]; therefore, chrysin is widely used as a dietary supplement to maintain testosterone levels. Ciftci et al. [14] suggest that the oral consumption of chrysin (50 mg/kg per day) exerts positive reproductive effects and might be useful for the treatment of male infertility. As previous studies described, chrysin exerts a neuroprotective effect and alleviates neuro-inflammation and depression in mice [15,16]. In diabetic rats, orally administered chrysin normalized glucose and insulin levels [17]. Furthermore, chrysin showed anti-inflammatory [18,19] and antioxidant effects in rats [20]. Despite the absence of human clinical evidences, chrysin-containing dietary supplements are advertised to treat anxiety, inflammation, gout, erectile dysfunction, baldness, and even cancer (see Supplementary Material). The oral bioavailability of chrysin is low, due to its poor aqueous solubility and significant presystemic elimination in enterocytes and hepatocytes [7,21]. As a result of its biotransformation, conjugated metabolites are formed (Figure 1): The two dominant products are chrysin-7-sulfate (C7S) and chrysin-7-glucuronide (C7G) in humans and in mice [7,22]. After the oral administration of 20 mg/kg chrysin to mice, the C_{max} of chrysin was only 10 nmol/L, while 160 and 130 nmol/L peak plasma concentrations of C7S and C7G were quantified, respectively [22]. In another study, a 400 mg dose of chrysin was administered orally to healthy human volunteers, after which C7S reached approximately 30-fold higher $AUC_{0-\infty}$ values compared with chrysin (420–4220 $ng \cdot mL^{-1} \cdot h$ vs. 3–16 $ng \cdot mL^{-1} \cdot h$, respectively) [7]. Based on previous studies, chrysin is a potent inhibitor of some biotransformation enzymes (e.g., CYP3A4, CYP2C9, and xanthine oxidase) and is also able to affect drug transporters (e.g., P-glycoprotein) [5,23,24].

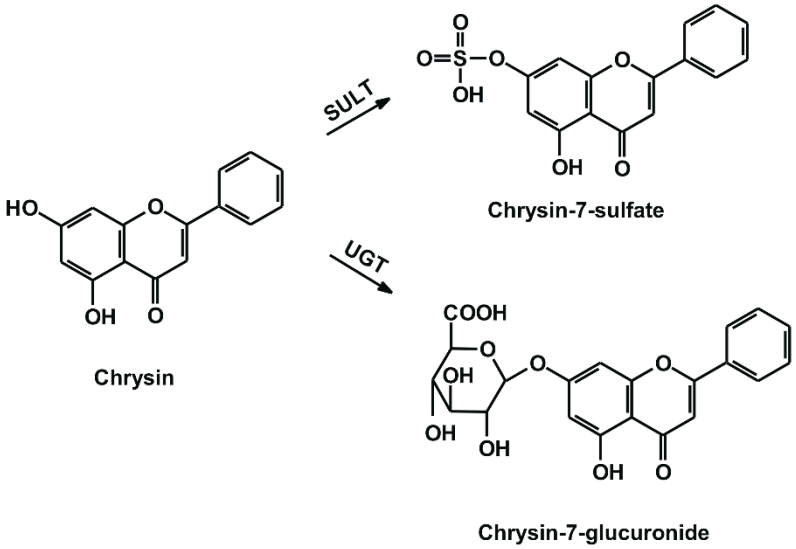

Figure 1. Chemical structures of chrysin, chrysin-7-sulfate, and chrysin-7-glucuronide (SULT: sulfotransferase; UGT: uridine 5′-diphospho-glucuronosyltransferase).

Human serum albumin (HSA) is the most abundant plasma protein [25,26]. Drugs and other xenobiotics commonly occupy one of the two major binding sites of HSA, namely Sudlow's Site I and Sudlow's Site II. Site I is an apolar cavity in Subdomain IIA [26]. It contains the only tryptophan residue of HSA (Trp-214), and specific ligands include warfarin and furosemide. Site II is located in Subdomain IIIA; e.g., naproxen and ibuprofen occupy this binding site with high affinity [26]. Displacement of a drug from HSA leads to the elevated free (not protein-bound) plasma concentration

of the drug, which can affect its tissue uptake and/or elimination [25]. Chrysin binds to HSA with high affinity (K is in the 10^5–10^6 L/mol range), occupying Site I or Site II as its high-affinity binding site on HSA [2,27,28]. However, based on our current knowledge, the interactions of C7S and C7G with serum albumin have not been reported, despite the fact that these are the dominant metabolites in the circulation.

In this study, the complex formation of chrysin, C7S, and C7G with HSA was investigated. Binding constants of formed flavonoid–albumin complexes were determined based on fluorescence quenching. Binding sites of chrysin, C7S, and C7G in HSA were examined using site markers of Sudlow's Site I (warfarin and ochratoxin A) and Sudlow's Site II (naproxen) by steady-state fluorescence spectroscopy, fluorescence anisotropy, ultrafiltration, and molecular modeling. This study demonstrates that both C7S and C7G form stable complexes with HSA. C7S binds with even greater affinity to HSA compared to chrysin, and it exerts stronger displacing ability vs. Sudlow's Site I ligands than the parent compound. Considering the above-listed observations, a high intake of chrysin may interfere with the albumin-binding of some drugs, mainly due to the strong interaction of C7S with HSA.

2. Results

2.1. Interaction of Chrysin, C7S, and C7G with Human and Bovine Serum Albumins

To investigate the binding affinity of chrysin, C7S, and C7G toward HSA and bovine serum albumin (BSA), fluorescence quenching experiments were performed. BSA is commonly applied as a model protein to examine albumin–ligand interactions (because it is cheaper and structurally similar to HSA) [29]. In a concentration-dependent fashion, chrysin and its metabolites induced a significant decrease in the fluorescence emission signal of HSA at 340 nm (Figure 2, top; λ_{ex} = 295 nm). C7G caused weaker, and C7S produced stronger, quenching effects on HSA than the parent compound. Stern–Volmer plots of flavonoid–HSA interactions show a good linearity (Figure 2, bottom). Chrysin and its metabolites induced very similar quenching effects on BSA compared to HSA (Figure 3). Stern–Volmer quenching constants (Ksv) and binding constants (K) were calculated based on the graphical application of the Stern–Volmer equation and evaluated by Hyperquad2006 software, respectively. Table 1 demonstrates the decimal logarithmic values of Ksv and K for flavonoid–albumin complexes. Both albumins formed the most stable complexes with C7S followed by chrysin and C7G. The stability of C7S–HSA and C7G–HSA complexes are approximately threefold higher and threefold lower vs. the chrysin–HSA complex, respectively. Affinities of the individual flavonoid–HSA and flavonoid–BSA complexes are similar; however, chrysin and C7G bind to HSA stronger than they do to BSA, while C7S forms a more stable complex with BSA (Table 1).

Table 1. Stability of flavonoid–albumin complexes. Decimal logarithmic values (±SEM) of Stern–Volmer quenching constants (Ksv, unit: L/mol) and binding constants (K, unit: L/mol).

Complex	logK_{SV}	log$K$
Chrysin–HSA	5.25 ± 0.02	5.41 ± 0.01
Chrysin-7-sulfate–HSA	5.61 ± 0.03	5.88 ± 0.02
Chrysin-7-glucuronide–HSA	4.71 ± 0.03	4.89 ± 0.00
Chrysin–BSA	5.03 ± 0.06	5.20 ± 0.00
Chrysin-7-sulfate–BSA	5.86 ± 0.04	6.20 ± 0.01
Chrysin-7-glucuronide–BSA	4.34 ± 0.03	4.63 ± 0.01

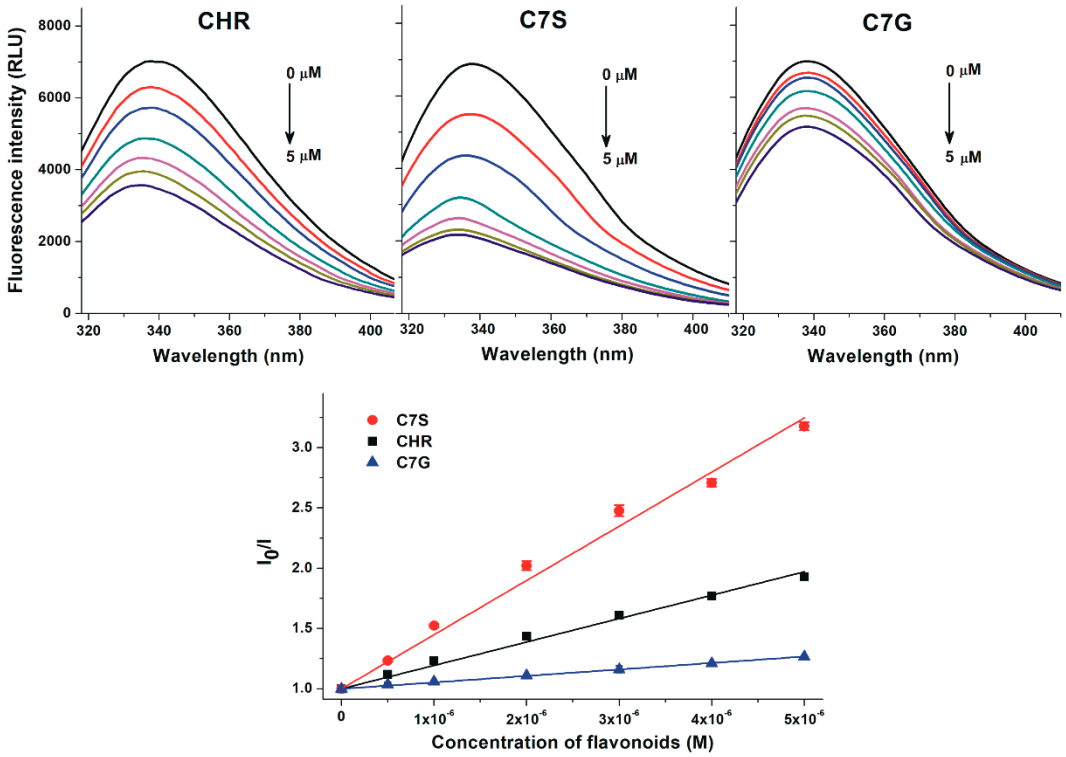

Figure 2. Top graphs: Fluorescence quenching effects of chrysin (CHR; left), chrysin-7-sulfate (C7S; middle), and chrysin-7-glucuronide (C7G; right) on HSA (2 μmol/L) in PBS (pH 7.4; λ_{ex} = 295 nm, λ_{em} = 340 nm). Bottom graph: Stern–Volmer plots of flavonoid–HSA complexes.

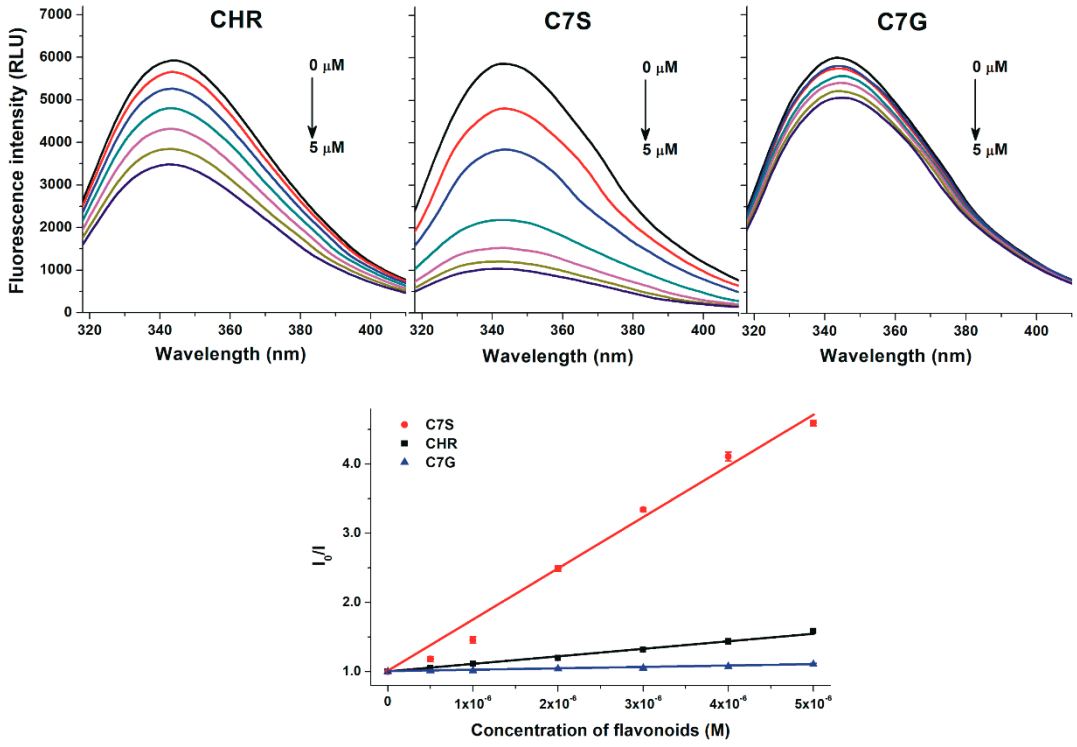

Figure 3. Top graphs: Fluorescence quenching effects of chrysin (CHR; left), chrysin-7-sulfate (C7S; middle), and chrysin-7-glucuronide (C7G; right) on BSA (2 μmol/L) in PBS (pH 7.4; λ_{ex} = 295 nm, λ_{em} = 340 nm). Bottom graph: Stern–Volmer plots of flavonoid–BSA complexes.

2.2. Effects of Flavonoids on Warfarin–HSA and Naproxen–HSA Interactions Based on Ultrafiltration Studies

In the following experiments, the displacing ability of chrysin, C7S, and C7G vs. the Site I ligand warfarin and the Site II ligand naproxen was evaluated based on ultrafiltration experiments. Interestingly, chrysin and its metabolites influenced the filtered fractions of both warfarin and naproxen. Under the applied conditions, C7G did not significantly change the concentration of filtered warfarin, while only the higher concentration of chrysin (20 μM) induced a statistically significant (albeit slight) increase of warfarin in the filtrate (Figure 4, left). However, even a 10 μM concentration of C7S caused a remarkable increase in warfarin in the filtrate. Furthermore, both concentrations of chrysin and C7S induced a statistically significant elevation of naproxen concentrations in the filtrate, while only a higher concentration of C7G produced a significant effect (Figure 4, right).

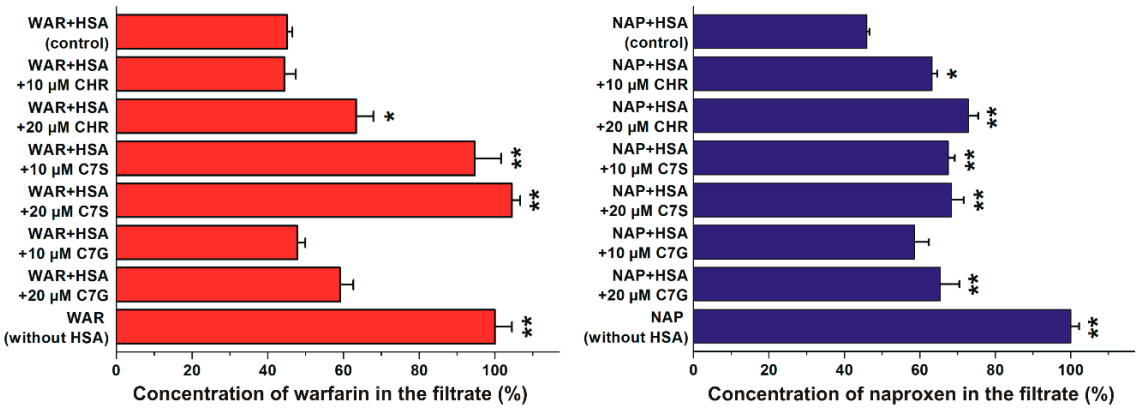

Figure 4. Concentrations of warfarin (left) and naproxen (right) in the filtrate. Left: Before ultrafiltration, samples contained 1 μmol/L warfarin (WAR) with 5 μmol/L HSA in the absence and presence of 10 or 20 μM flavonoid concentrations in PBS (pH 7.4). Right: Before ultrafiltration, samples contained 1 μmol/L naproxen (NAP) with 1.7 μmol/L HSA in the absence and presence of 10 or 20 μM flavonoid concentrations in PBS (pH 7.4). (* $p < 0.05$, * *$p < 0.01$; CHR: chrysin; C7S: chrysin-7-sulfate; C7G: chrysin-7 glucuronide).

2.3. Effects of Chrysin and Its Metabolites on the Albumin-Binding of Warfarin Based on Fluorescence Spectroscopic Studies

In order to test the displacement of the Sudlow's Site I ligand warfarin from HSA by flavonoids, increasing concentrations of chrysin and its metabolites were added to the warfarin–HSA complex. Displacement of warfarin from HSA results in a strong decrease in its fluorescence [30,31]. Our results demonstrate that each flavonoid significantly decreased the emission signal of warfarin at 379 nm (Figure 5, left): C7S induced the strongest decrease, followed by chrysin, while C7G showed only a slight (but statistically significant) effect.

In another model, fluorescence anisotropy was employed to test the effects of chrysin, C7S, and C7G on the albumin-binding of warfarin. Anisotropy gives information regarding the rotational freedom of a molecule. Our results demonstrate that C7G failed to affect the fluorescence anisotropy of warfarin, while chrysin and mainly C7S induced a strong decrease in anisotropy values (Figure 5, right).

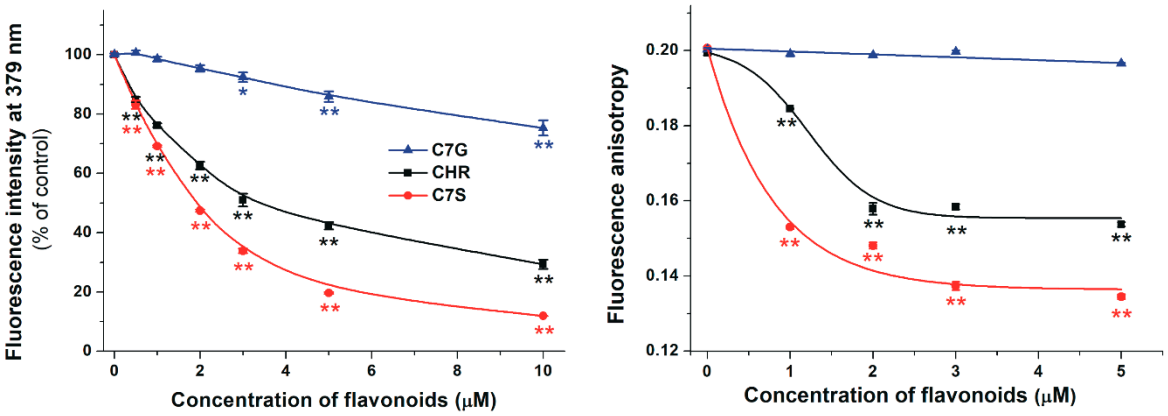

Figure 5. Left: A concentration-dependent decrease in the fluorescence emission intensity of the warfarin–HSA complex (1.0 and 3.5 μmol/L of warfarin and HSA, respectively) in the presence of increasing flavonoid concentrations (0.0, 0.5, 1.0, 2.0, 3.0, 5.0, and 10 μmol/L). Right: Fluorescence anisotropy values of the warfarin–HSA complex (1.0 and 2.0 μmol/L of warfarin and HSA, respectively) in the presence of increasing concentrations of chrysin, C7S, or C7G (0.0, 1.0, 2.0, 3.0, and 5.0 μmol/L). (λ_{ex} = 317 nm, λ_{em} = 379 nm; * $p < 0.05$, ** $p < 0.01$; CHR: chrysin; C7S: chrysin-7-sulfate; C7G: chrysin-7 glucuronide).

2.4. Effects of Chrysin and Its Metabolites on the Albumin-Binding of Ochratoxin A

The mycotoxin ochratoxin A binds to HSA with very high affinity, occupying Sudlow's Site I as a binding site [32,33]. Therefore, to confirm the involvement of Site I as the binding site of flavonoids tested, the displacement of ochratoxin A from HSA by chrysin, C7S, and C7G was examined by fluorescence anisotropy. Even high concentrations (2.5–30 μM vs. 1 μM ochratoxin A) of C7G and chrysin failed to affect the anisotropy of ochratoxin A; however, C7S induced a concentration-dependent decrease in anisotropy values (Figure 6).

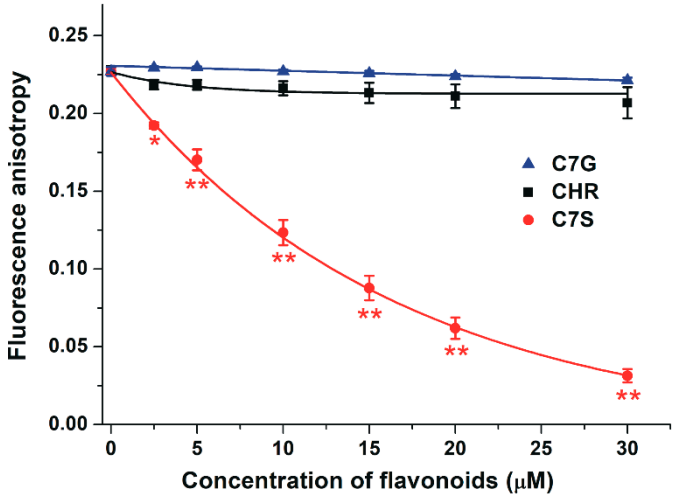

Figure 6. Fluorescence anisotropy of the ochratoxin A–HSA complex (1.0 and 1.5 μmol/L of ochratoxin A and HSA, respectively) in the presence of increasing concentrations of flavonoids (0.0, 2.5, 5.0, 10, 15, 20, and 30 μmol/L) in PBS (pH 7.4; λ_{ex} = 393 nm; λ_{em} = 446 nm; * $p < 0.05$, ** $p < 0.01$; CHR: chrysin; C7S: chrysin-7-sulfate; C7G: chrysin-7 glucuronide).

2.5. Modeling Studies

The binding positions of chrysin, C7S, and C7G in Sudlow's Site I were investigated employing focused docking calculations with Autodock 4. Ranking of binding positions was performed by the

binding energy calculated with the AutoDock 4 scoring function. Docking results show that the binding site of chrysin on HSA significantly overlaps with the binding site of the Sudlow's Site I ligand warfarin (Figure 7). The first rank positions of chrysin and C7S show large similarities (Figure 8, left). The chrysin–HSA interaction is stabilized by the salt bridge with K199 and by hydrogen bonds with R257 and Y150. C7S occupies Site I in a very similar position than chrysin, but the formed complex is further stabilized by salt bridges with K195 and R222. The binding position of C7G is different (Figure 7, left) compared to chrysin and C7S. The position of glucuronic acid moiety is fixed by hydrogen bonds with K195, Q196, and E292.

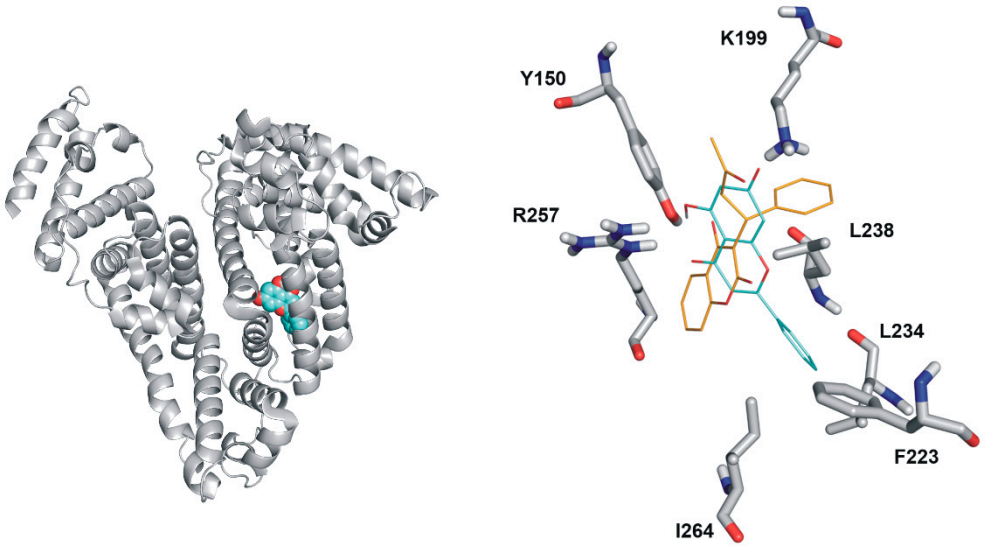

Figure 7. Left: Chrysin (cyan spheres) occupies Sudlow's Site I in HSA (represented with grey cartoon). Right: Rank1 binding positions of chrysin (cyan lines) and warfarin (orange lines; reference structure) in the HSA molecule.

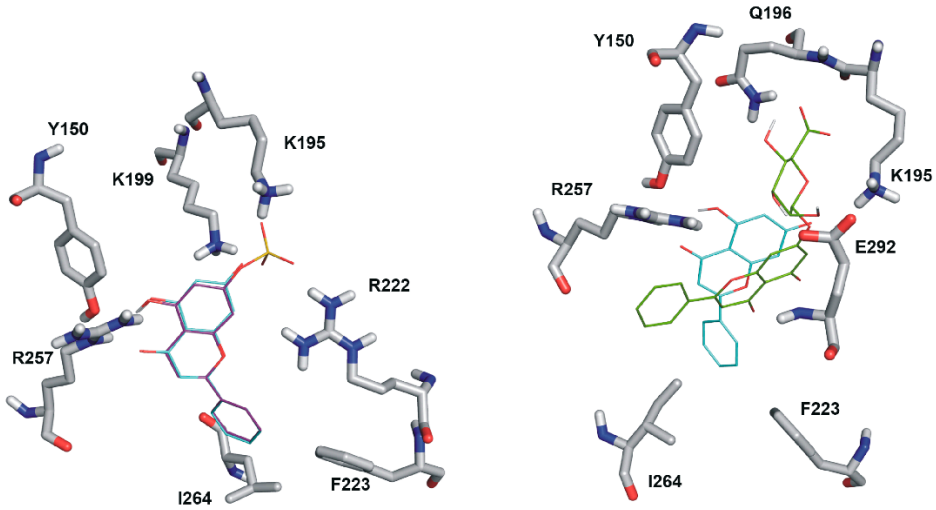

Figure 8. Left: Rank1 binding position of C7S (purple lines) vs. chrysin (cyan lines). Right: Rank1 binding position of C7G (green lines) compared to chrysin (cyan lines).

3. Discussion

Chrysin, C7S, and C7G induced the significant decrease in the fluorescence signal of HSA (Figure 2, top), suggesting the formation of flavonoid–HSA complexes. Since emission signals were corrected with absorbance values of flavonoids at the excitation and emission wavelengths used

(see in 4.2), we can exclude that the decrease in fluorescence resulting from the inner-filter effect. Using 295 nm as an excitation wavelength, the emitted light of HSA was exerted mainly by its only tryptophan moiety (Trp-214), which is located in Sudlow's Site I [26,32,33]. Because flavonoids caused the significant quenching of Trp-214 even at a relatively low concentration (0.5 μmol/L), it is reasonable to hypothesize that the binding site of flavonoids needs to be located close to the tryptophan residue (e.g., in Site I). Both the good linearity of Stern–Volmer plots (Figure 2, bottom) and the evaluation of data with the Hyperquad software suggest the 1:1 stoichiometry of complex formation. K_{SV} and K values showed good correlations (Table 1). Binding constant of the chrysin–HSA complex is in good agreement with the previously reported values [2,27,28]. Sometimes significant species differences in albumin-binding can be noticed [29,34]; however, the stability of the formed HSA and BSA complexes of chrysin (and chrysin conjugates) did not show large differences, as has also been described regarding the basic flavone structure by Xiao et al. [2]. Like previous investigations with quercetin and its sulfate metabolites [30,35–37], our results highlight that sulfate metabolites of flavonoids are able to bind to albumin with similar or even higher affinities than the aglycones. Considering these observations, it is reasonable to hypothesize that sulfate metabolites may also exert similar or higher effects on other proteins (e.g., biotransformation enzymes or transporters) than flavonoid aglycones, as has been reported regarding the interactions of quercetin-3′-sulfate with CYP2C9, CYP3A4, OAT1, or GLUT [30,38,39].

In order to test the binding sites of flavonoids in HSA as well as to investigate their displacing ability vs. drugs, site markers were applied. Since previous investigations suggest the possible involvement of Site I or Site II regarding chrysin–HSA interaction [2,28], the displacing effects of chrysin, C7S, and C7G were evaluated vs. warfarin (Site I) and naproxen (Site II) based on ultrafiltration studies. Because albumin is a large macromolecule (66.5 kDa), HSA and HSA-bound ligand molecules cannot pass through the filter unit with a 30 kDa molecular weight cut-off value. Therefore, albumin significantly decreases the concentrations of the site markers in the filtrate (Figure 4). In both cases (warfarin and naproxen), the same concentrations of the site markers (1 μmol/L both) were applied in the presence of HSA concentrations that induce an approximately 60% decrease in the site marker concentrations in the filtrate. Thus, the flavonoid-induced increase in filtered site marker concentrations suggests their displacement from HSA. C7G did not cause significant changes and chrysin induced slight (but statistically significant) interaction only at the higher concentration applied (20 μmol/L); however, C7S inflicted remarkable effects at both concentrations, resulting in practically the complete displacement of bound warfarin molecules from HSA (Figure 4, left). Chrysin, C7S, and C7G induced statistically significant (but only slight) displacement of the Site II marker naproxen (Figure 4, right). Based on these observations, it is reasonable to hypothesize that the high-affinity binding site of C7S is located in Site I (subdomain IIA), while the lower displacing ability of chrysin and C7G likely resulted from their lower affinity toward HSA. This hypothesis is also supported by the strong quenching effects of flavonoids on HSA, because the Trp-214 moiety is located in Subdomain IIA. Furthermore, chrysin and its conjugates may allosterically influence the albumin-binding of the Site II ligand naproxen as well.

To confirm our hypothesis that the examined flavonoids occupy Site I in HSA, further experiments were performed. Effects of chrysin, C7S, and C7G on the albumin-binding of warfarin were examined based on steady-state fluorescence spectroscopy and fluorescence anisotropy. The fluorescence emission intensity of HSA-bound warfarin is approximately 20-fold higher compared to free warfarin [30,31]. Therefore, the concentration-dependent reduction of the fluorescence signal of warfarin in the presence of flavonoids (Figure 5, left) suggests the displacement of warfarin from HSA. The displacing ability of flavonoids shows the same order than their binding affinity toward HSA: C7S > chrysin > C7G. In the following experiment, the effect of flavonoids on the fluorescence anisotropy of warfarin was examined. Warfarin, as a small molecule, has a large rotational freedom and consequently a relatively low anisotropy value. However, during its interaction with the HSA, its rotational freedom strongly decreases while its anisotropy value significantly increases. Therefore, the displacement

of a small fluorophore from the protein leads to the decrease in its fluorescence anisotropy [31,40]. Anisotropy measurements also suggest the strongest displacement of warfarin by C7S, while a weaker and only a slight impact was noticed regarding chrysin and C7G, respectively (Figure 5, right). Thus, spectroscopic measurements confirmed our results derived from ultrafiltration studies.

To further support these results, the interactions of chrysin, C7S, and C7G were investigated with ochratoxin A. Ochratoxin A occupies Site I in the albumin [32,33], during which it forms extremely stable non-covalent complexes with HSA (log$K$ = 7.4–7.6) [29,41]. In these experiments, only C7S was able to significantly decrease the fluorescence anisotropy of ochratoxin A (Figure 6), suggesting that the sulfate metabolite of chrysin can disrupt even this high-affinity interaction. Chrysin and C7G binds with lower affinity to HSA than C7S, which may explain why these flavonoids failed to displace ochratoxin A.

Finally, modeling studies were employed to explore the reason of the different binding affinities of chrysin, C7S, and C7G toward HSA. Our results suggest a similar binding position of chrysin and C7S (Figure 8). The sulfate group of C7S forms further two salt bridges with K195 and R222, which results in more stable complexes of C7S with HSA compared to chrysin. While the different binding position of C7G in Site I may explain its lower binding affinity compared to chrysin and C7S.

Several chrysin-containing dietary supplements are available on the Internet, which contain extremely high doses of chrysin (e.g., 500 mg or even higher dose/formulation unit) (see Supplementary Materials). The consumption of these supplements can result in the appearance of high total chrysin (chrysin and its metabolites) concentrations in the circulation, as has been reported regarding quercetin [42,43]. Since mainly the conjugated metabolites of chrysin appear at high concentrations in the circulation, C7S–HSA and C7G–HSA interactions may have high importance. C7S is the dominant metabolite of chrysin in the human circulation [7]. As it is demonstrated, compared with the parent compound, C7S binds with a higher affinity to HSA and exerts higher displacing ability vs. Sudlow's Site I ligands. Based on spectroscopic and ultrafiltration studies, C7S has a similar or even higher effect on the albumin-binding of warfarin than quercetin or quercetin-3′-sulfate [30]. Furthermore, the displacement of ochratoxin A by C7S in our experimental model also underlines that C7S is a powerful competitor of Site I ligands. Like chrysin or quercetin-3′-sulfate [23,30,38], C7S is likely able to interact with biotransformation enzymes and transporters that may exacerbate the pharmacokinetic interactions of chrysin. However, to confirm this hypothesis, further investigations are needed.

In summary, interactions of chrysin, C7S, and C7G with human and bovine serum albumins were examined. Binding constants show the formation of stable flavonoid–albumin complexes. C7S binds to HSA with a three-fold higher affinity compared with chrysin, while C7G binds with a threefold lower affinity. Based on site marker experiments and modeling studies, tested compounds occupy Sudlow's Site I in HSA; however, the binding position of C7G differs from chrysin or C7S. Interestingly, high concentrations of chrysin and its metabolites were also able to influence the albumin-binding of the Sudlow's Site II ligand naproxen. Considering our observations, the high intake of chrysin (e.g., through the consumption of dietary supplements with high chrysin content) may interfere with the albumin-binding of several drugs, mainly due to the strong interaction of C7S with HSA.

4. Materials and Methods

4.1. Reagents

Chrysin, racemic warfarin, naproxen, ochratoxin A, human serum albumin (HSA), and bovine serum albumin (BSA) were purchased from Sigma-Aldrich (Waltham, MA, USA). Chyrsin-7-sulfate (C7S) was synthetized based on a method described regarding the sulfation of baicalein [44]. Chrysin-7-glucuronide (C7G) was obtained from Carbosynth (Compton, Berkshire, UK). Chrysin and its metabolites were dissolved in dimethyl sulfoxide (DMSO; Reanal, Budapest, Hungary, spectroscopic grade), and stock solutions (2000 μM each) were stored and protected from light at −20 °C.

4.2. Spectroscopic Measurements

Fluorescence spectroscopic measurements were carried out employing a Hitachi F-4500 fluorimeter (Tokyo, Japan). Absorption spectra of flavonoids were recorded using a HALO DB-20 UV-Vis spectrophotometer (Dynamica, London, UK). Spectroscopic measurements were performed in phosphate-buffered saline (pH 7.4; PBS: 8.0 g/L NaCl, 0.2 g/L KCl, 1.81 g/L $Na_2HPO_4 \cdot 2H_2O$, and 0.24 g/L KH_2PO_4) at room temperature, in the presence of air.

The complex formation of flavonoids with albumin was tested with both HSA and BSA. Binding constants of flavonoid–albumin complexes were determined by fluorescence quenching, during which emission spectra of albumins (2 μmol/L) were recorded in the presence of increasing flavonoid concentrations (0.0, 0.5, 1.0, 2.0, 3.0, 4.0 and 5.0 μmol/L; λ_{exc} = 295 nm). Quenching studies were evaluated based on the graphical application of the Stern–Volmer equation [31,34]. To eliminate the potential inner filter effects of flavonoids, fluorescence intensities were corrected as described [31,34].

Binding constants (K) of flavonoid–albumin complexes were also evaluated by non-linear fitting employing the Hyperquad2006 program package (Protonic Software, Leeds, UK) as described elsewhere [34,37]. Binding constants and stoichiometry were quantified based on the model with the lowest standard deviation.

Displacement of warfarin (site marker of Sudlow's Site I) from HSA was examined based on the previously reported model [30,31]. Increasing concentrations of chrysin, C7S, and C7G (0.0, 0.5, 1.0, 2.0, 3.0, 5.0, and 10 μmol/L) were added to standard concentrations of warfarin and HSA (1.0 and 3.5 μmol/L, respectively). Thereafter, fluorescence emission spectra were recorded using 317 nm as excitation wavelength.

To confirm further the displacement of warfarin from HSA by chrysin, C7S, and C7G, fluorescence anisotropy measurements were also performed. Increasing concentrations of flavonoids (0.0, 1.0, 2.0, 5.0, and 10 μmol/L) were added to warfarin and HSA (1.0 and 2.0 μmol/L, respectively). Fluorescence anisotropy values were determined (λ_{ex} = 317 nm; λ_{em} = 379 nm) as described [31].

Our previously described fluorescence anisotropy-based model [45] was employed to examine the displacing ability of the test compounds vs. ochratoxin A (another ligand of Sudlow's Site I). Increasing concentrations of flavonoids (0.0, 2.5, 5.0, 10, 15, 20, and 30 μmol/L) were added to ochratoxin A and HSA (1.0 and 1.5 μmol/L, respectively), after which anisotropy values were determined at 393 and 446 nm excitation and emission wavelengths, respectively (wavelength maxima of albumin-bound ochratoxin A).

4.3. Ultrafiltration Experiments

Effects of chrysin, C7S, and C7G on the albumin-binding of Sudow's Site I (warfarin) and Site II (naproxen) markers were tested by ultrafiltration. In these experiments, Pall Microsep™ Advance Centrifugal Devices (Pall Corporation, Ann Arbor, MI, USA) (from VWR) with a 30 kDa molecular weight cut-off value were employed, as described elsewhere [46]. To examine the displacement of warfarin by flavonoids, samples contained warfarin and HSA (1.0 and 5.0 μmol/L, respectively) in the absence and presence of flavonoids (10 or 20 μmol/L). Furthermore, to test the displacing ability of chrysin and its metabolites vs. naproxen, flavonoids (10 or 20 μmol/L) were added to naproxen and HSA (1.0 and 1.7 μmol/L, respectively). Each sample was prepared in PBS (pH 7.4). Before ultrafiltration, filter units were washed once with 3 mL of water, and twice with 3 mL of PBS (to completely eliminate glycerol from the filters). Thereafter, samples (2.5 mL each) were driven through the filter units by centrifugation at 7500 g and 25 °C for 10 min (fixed angle rotor). Concentrations of warfarin and naproxen in the filtrate were quantified with HPLC (see details in Section 4.4).

4.4. HPLC Analyses

The HPLC system used to quantify warfarin and naproxen was equipped with a pump (model 510, Waters, Milford, MA, USA) and an injector (Rheodyne 7125, Rheodyne, Berkeley, CA, USA) with a 20 µL sample loop. Warfarin and naproxen were analyzed with a fluorescence detector (Jasco FP-920, Reanal) and an UV detector (Waters 486), respectively. Data were evaluated using Millennium Chromatography Manager (Waters).

Warfarin was analyzed based on the previously reported method without modifications [46]. Methanol (VWR), acetonitrile (VWR), and sodium phosphate buffer (20 mM, pH 7.0) (25:5:70 v/v%) were applied in the mobile phase with 1 mL/min flow rate during the isocratic elution. Samples were driven through a guard column (Phenomenex SecurityGuard^{TM} Catridge C18 4.0 × 3.0 mm) linked to an analytical column (Nova-Pak C18 150 × 3.9 mm, 4 µm). Separation and analysis were performed at room temperature, during which warfarin was detected by fluorescence employing 310 and 390 nm as excitation and emission wavelengths, respectively.

Naproxen was quantified based on the previously reported method without modifications [46]. Acetonitrile and sodium acetate buffer (6.9 mM, pH 4.0) (50:50 v/v%) were applied in the mobile phase with a 1 mL/min flow rate during the isocratic elution. Samples were driven through a guard column (Phenomenex SecurityGuardTM Catridge C18 4.0 × 3.0 mm) linked to an analytical column (Phenomenex Gemini C18 150 × 4.6 mm, 3 µm). Separation and analysis were performed at room temperature, during which naproxen was detected by absorbance at 230 nm.

4.5. Modeling Studies

Docking calculations were performed using the AutoDock 4.2 program package [47]. Ligand 3D structures were downloaded from pubchem [48], and the protonation and charge states of ligands were calculated at pH 7.4 by msketch [49]. Energy-minimization of molecules was performed by the semi-empirical quantum chemistry program package, MOPAC. The geometries were optimized at a 0.001 gradient norm and subjected to subsequent force calculations using PM7 parameterization. In all cases, the force constant matrices were positive definite. The apo structure of HSA (PDB code 1a06) was used as a target of docking. The Gasteiger–Marsilli partial charges [50] were added to both ligand and target atoms and a Kollman united atom representation was applied for groups with non-polar bonds. For BD, the grid box was centered on the center of Sudlow's Site I. A grid map with a box size of 90 × 90 × 90 points and 0.375 Å spacing was calculated by AutoGrid 4. During the focused docking calculations on Sudlow's Site I, the grid box of 90 × 90 × 90 was centered on 35.000 31.825 37.000. In all calculations, the number of docking runs was set to 10 numbers of energy evaluations and generations were 20 million. Ligand conformations that resulted from the docking runs were ordered by the corresponding calculated ΔG values and clustered using a tolerance of 1.75 Å distance between cluster members. Conformations with the lowest binding energy within a cluster were selected as representatives.

4.6. Statistics

Data demonstrate the means (±SEM) from at least three independent experiments. During statistical analyses, the one-way ANOVA test (IBS SPP Statistics Version 21) was applied, and the level of significance was set at $p < 0.05$ and $p < 0.01$.

Supplementary Materials: Supplementary materials can be found at http://www.mdpi.com/1422-0067/19/12/4073/s1.

Author Contributions: Conceptualization, M.P.; Formal analysis, V.M., E.F.-N., G.S., C.H., B.L., and S.K.-M.; Funding acquisition, C.H. and M.P.; Investigation, V.M., E.F.-N., G.S., C.H., B.L., S.K.-M., B.B., and M.P.; Methodology, V.M., E.F.-N., C.H., and M.P.; Resources, B.B.; Writing—original draft, V.M., C.H., and M.P. Spectroscopic studies and Stern–Volmer evaluations were performed by V.M. and M.P. V.M. and E.F-N. carried out ultrafiltration studies and the related HPLC analyses. B.L. and S.K-M. performed the Hyperquad evaluations

based on spectroscopic data. G.S. and C.H. carried out the modeling studies. B.B. synthetized chrysin-7-sulfate. All authors have read, edited, and approved the final version of the paper.

Funding: The project was founded by the European Union and co-financed by the European Social Fund (EFOP-3.6.1.-16-2016-00004). This work was supported by the Hungarian National Research, Development and Innovation Office (K123836: G.S. and C.H.; FK124331: B.B.).

Acknowledgments: The authors thank István Schweibert for his excellent assistance in the experimental work. The project was supported by the ÚNKP-18-3 and ÚNKP-18-4 New National Excellence Program of the Ministry of Human Capacities and by the University of Pécs in the frame of Pharmaceutical Talent Centre program. Financial support of the GINOP-2.3.2-15-2016-00049 grant is highly appreciated (S.K.). We acknowledge the grant of computer time from CSCS Swiss National Supercomputing Centre, and the Governmental Information Technology Development Agency, Hungary. We acknowledge that the results of this research have been achieved using the DECI resource Archer based in the UK at the National Supercomputing Service with support from the PRACE (Partnership for Advanced Computing in Europe) aisbl (Association internationale sans but lucratif). The University of Pécs is acknowledged for a support by the 17886-4/23018/FEKUTSTRAT excellence grant.

Conflicts of Interest: The authors declare no conflict of interest.

Abbreviations

BSA	bovine serum albumin
C7G	chrysin-7-glucuronide
C7S	chrysin-7-sulfate
CHR	chrysin
CYP	cytochrom P450 enzymes
GLUT	glucose transporter
HPLC	high-performance liquid chromatography
HSA	human serum albumin
OAT1	organic anion transporter 1
PBS	phosphate-buffered saline
SULT	sulfotransferase
UGT	uridine 5′-diphospho-glucuronosyltransferase

References

1. Havsteen, B.H. The biochemistry and medical significance of the flavonoids. *Pharmacol. Ther.* **2002**, *96*, 67–202. [CrossRef]
2. Xiao, J.; Cao, H.; Wang, Y.; Yamamoto, K.; Wei, X. Structure-affinity relationship of flavones on binding to serum albumins: Effect of hydroxyl groups on ring A. *Mol. Nutr. Food Res.* **2010**, *54*, 253–260. [CrossRef] [PubMed]
3. Liu, Q.; Chen, T.T.; Chao, H. Flavonoids inhibiting glycation of bovine serum albumin: Affinity-activity relationship. *Chem. Pap.* **2015**, *69*, 409–415. [CrossRef]
4. Korobkova, E.A. Effect of Natural Polyphenols on CYP Metabolism: Implications for Diseases. *Chem. Res. Toxicol.* **2015**, *28*, 1359–1390. [CrossRef]
5. Alvarez, A.I.; Real, R.; Pérez, M.; Mendoza, G.; Prieto, J.G.; Merino, G. Modulation of the activity of ABC transporters (P-glycoprotein, MRP2, BCRP) by flavonoids and drug response. *J. Pharm. Sci.* **2010**, *99*, 598–617. [CrossRef] [PubMed]
6. Cermak, R.; Wolffram, S. The potential of flavonoids to influence drug metabolism and pharmacokinetics by local gastrointestinal mechanisms. *Curr. Drug Metab.* **2006**, *7*, 729–744. [CrossRef] [PubMed]
7. Walle, T.; Otake, Y.; Brubaker, J.A.; Walle, U.K.; Halushka, P.V. Disposition and metabolism of the flavonoid chrysin in normal volunteers. *Br. J. Clin. Pharmacol.* **2001**, *51*, 143–146. [CrossRef] [PubMed]
8. Lambert, J.D.; Sang, S.; Lu, A.Y.H.; Yang, C.S. Metabolism of Dietary Polyphenols and Possible Interactions of Drugs. *Curr. Drug Metab.* **2007**, *8*, 499–507. [CrossRef]
9. Siess, M.H.; Le Bon, A.M.; Canivenc-Lavier, M.C.; Amiot, M.J.; Sabatier, S.; Aubert, S.Y.; Suschetet, M. Flavonoids of Honey and Propolis: Characterization and Effects on Hepatic Drug-Metabolizing Enzymes and Benzo [a]pyrene-DNA Binding in Rats. *J. Agric. Food Chem.* **1996**, *44*, 2297–2301. [CrossRef]
10. Anandhi, R.; Annadurai, T.; Anitha, T.S.; Muralidharan, A.R.; Najmunnisha, K.; Nachiappan, V.; Thomas, P.A.; Geraldine, P. Antihypercholesterolemic and antioxidative effects of an extract of the oyster mushroom,

Pleurotus ostreatus, and its major constituent, chrysin, in Triton WR-1339-induced hypercholesterolemic rats. *J. Physiol. Biochem.* **2013**, *69*, 313–323. [CrossRef]
11. Chen, F.; Li, H.L.; Tan, Y.F.; Li, Y.H.; Lai, W.Y.; Guan, W.W.; Zhang, J.Q.; Zhao, Y.S.; Qin, Z.M. Identification of known chemicals and their metabolites from Alpinia oxyphylla fruit extract in rat plasma using liquid chromatography/tandem mass spectrometry (LC–MS/MS) with selected reaction monitoring. *J. Pharm. Biomed. Anal.* **2014**, *97*, 166–177. [CrossRef] [PubMed]
12. Kao, J.C.; Zhou, C.; Sherman, M.; Laughton, C.A.; Chen, S. Molecular basis of the inhibition of human aromatase (estrogen synthetase) by flavone and isoflavone phytoestrogens: A site-directed mutagenesis study. *Environ. Health Perspect.* **1998**, *106*, 85–92. [CrossRef] [PubMed]
13. Moon, Y.J.; Wang, X.; Morris, M.E. Dietary flavonoids: Effects on xenobiotic and carcinogen metabolism. *Toxicol. Vitro* **2006**, *20*, 187–210. [CrossRef]
14. Ciftci, O.; Ozdemir, I.; Aydin, M.; Beytur, A. Beneficial effects of chrysin on the reproductive system of adult male rats. *Andrologia* **2012**, *44*, 181–186. [CrossRef] [PubMed]
15. Nabavi, S.F.; Braidy, N.; Habtemariam, S.; Orhan, I.E.; Daglia, M.; Manayi, A.; Gortzi, O.; Nabavi, S.M. Neuroprotective effects of chrysin: From chemistry to medicine. *Neurochem. Int.* **2015**, *90*, 224–231. [CrossRef] [PubMed]
16. Filho, C.B.; Jesse, C.R.; Donato, F.; Fabbro, L.D.; de Gomes, M.G.; Goes, A.T.R.; Souza, L.C.; Boeira, S.P. Chrysin promotes attenuation of depressive-like behavior and hippocampal dysfunction resulting from olfactory bulbectomy in mice. *Chem. Biol. Interact.* **2016**, *260*, 154–162. [CrossRef] [PubMed]
17. Satyanarayana, K.; Sravanthi, K.; Shaker, I.A.; Ponnulakshmi, R.; Selvaraj, J. Role of chrysin on expression of insulin signaling molecules. *J. Ayurveda Integr. Med.* **2015**, *6*, 248–258. [CrossRef]
18. Cho, H.; Yun, C.W.; Park, W.K.; Kong, J.Y.; Kim, K.S.; Park, Y.; Lee, S.; Kim, B.K. Modulation of the activity of pro-inflammatory enzymes, COX-2 and iNOS, by chrysin derivatives. *Pharmacol. Res.* **2004**, *49*, 37–43. [CrossRef]
19. Xiao, J.; Zhai, H.; Yao, Y.; Wang, C.; Jiang, W.; Zhang, C.; Simard, A.R.; Zhang, R.; Hao, J. Chrysin attenuates experimental autoimmune neuritis by suppressing immuno-inflammatory responses. *Neuroscience* **2014**, *262*, 156–164. [CrossRef]
20. Pushpavalli, G.; Kalaiarasi, P.; Veeramani, C.; Pugalendi, K.V. Effect of chrysin on hepatoprotective and antioxidant status in d-galactosamine-induced hepatitis in rats. *Eur. J. Pharmacol.* **2010**, *631*, 36–41. [CrossRef]
21. Galijatovic, A.; Otake, Y.; Walle, U.K.; Walle, T. Extensive metabolism of the flavonoid chrysin by human Caco-2 and Hep G2 cells. *Xenobiotica* **1999**, *29*, 1241–1256. [CrossRef] [PubMed]
22. Ge, S.; Gao, S.; Yin, T.; Hu, M. Determination of Pharmacokinetics of Chrysin and Its Conjugates in Wild-Type FVB and Bcrp1 Knockout Mice Using a Validated LC-MS/MS Method. *J. Agric. Food Chem.* **2015**, *63*, 2902–2910. [CrossRef] [PubMed]
23. Kimura, Y.; Ito, H.; Ohnishi, R.; Hatano, T. Inhibitory effects of polyphenols on human cytochrome P450 3A4 and 2C9 activity. *Food Chem. Toxicol.* **2010**, *48*, 429–435. [CrossRef] [PubMed]
24. Pingili, R.B.; Pawar, A.K.; Challa, S.R. Systemic exposure of Paracetamol (acetaminophen) was enhanced by quercetin and chrysin co-administration in Wistar rats and in vitro model: Risk of liver toxicity. *Drug Dev. Ind. Pharm.* **2015**, *41*, 1793–1800. [CrossRef] [PubMed]
25. Schmidt, S.; Gonzalez, D.; Derendorf, H. Significance of protein binding in pharmacokinetics and pharmacodynamics. *J. Pharm. Sci.* **2010**, *99*, 1107–1122. [CrossRef] [PubMed]
26. Fanali, G.; Di Masi, A.; Trezza, V.; Marino, M.; Fasano, M.; Ascenzi, P. Human serum albumin: From bench to bedside. *Mol. Asp. Med.* **2012**, *33*, 209–290. [CrossRef]
27. Zhang, G.; Chen, X.; Guo, J.; Wang, J. Spectroscopic investigation of the interaction between chrysin and bovine serum albumin. *J. Mol. Struct.* **2010**, *921*, 346–351. [CrossRef]
28. Tu, B.; Chen, Z.F.; Liu, Z.J.; Li, R.R.; Ouyang, Y.; Hu, Y.J. Study of the structure-activity relationship of flavonoids based on their interaction with human serum albumin. *RSC Adv.* **2015**, *5*, 73290–73300. [CrossRef]
29. Poór, M.; Li, Y.; Matisz, G.; Kiss, L.; Kunsági-Máté, S.; Kőszegi, T. Quantitation of species differences in albumin-ligand interactions for bovine, human and rat serum albumins, using fluorescence spectroscopy: A test case with some Sudlow's site I ligands. *J. Lumin.* **2014**, *145*, 767–773. [CrossRef]
30. Poór, M.; Boda, G.; Needs, P.W.; Kroon, P.A.; Lemli, B.; Bencsik, T. Interaction of quercetin and its metabolites with warfarin: Displacement of warfarin from human serum albumin and inhibition of CYP2C9. *Biomed. Pharmacother.* **2017**, *88*, 574–581. [CrossRef]

31. Poór, M.; Boda, G.; Mohos, V.; Kuzma, M.; Bálint, M.; Hetényi, C.; Bencsik, T. Pharmacokinetic interaction of diosmetin and silibinin with other drugs: Inhibiton of CYP2C9-mediated biotransformation and displacement from serul albumin. *Biomed. Pharmacother.* **2018**, *102*, 912–921. [CrossRef] [PubMed]
32. Il'ichev, I.V.; Perry, J.L.; Simon, J.D. Interaction of Ochratoxin A with Human Serum Albumin. A Common Binding Site of Ochratoxin A and Warfarin in Subdomain IIA. *J. Phys. Chem. B* **2002**, *106*, 460–465. [CrossRef]
33. Il'ichev, Y.V.; Perry, J.L.; Rüker, F.; Dockal, M.; Simon, J.D. Interaction of ochratoxin A with human serum albumin. Binding sites localized by competitive interactions with the native protein and its recombinant fragments. *Chem. Biol. Interact.* **2002**, *141*, 275–293. [CrossRef]
34. Faisal, Z.; Lemli, B.; Szerencsés, D.; Kunsági-Máté, S.; Bálint, M.; Hetényi, C.; Kuzma, M.; Mayer, M.; Poór, M. Interactions of zearalenone and its reduced metabolites α-zearalenol and β-zearalenol with serum albumins: Species differences, binding sites, and thermodynamics. *Mycotoxin Res.* **2018**, *34*, 269–278. [CrossRef] [PubMed]
35. Dangles, O.; Dufour, C.; Manach, C.; Morand, C.; Remesy, C. Binding of flavonoids to plasma proteins. *Methods Enzymol.* **2001**, *335*, 319–333. [CrossRef] [PubMed]
36. Janisch, K.M.; Williamson, G.; Needs, P.; Plumb, G.W. Properties of quercetin conjugates: Modulation of LDL oxidation and binding to human serum albumin. *Free Radic. Res.* **2004**, *38*, 877–884. [CrossRef] [PubMed]
37. Poór, M.; Boda, G.; Kunsági-Máté, S.; Needs, P.W.; Kroon, P.A.; Lemli, B. Fluorescence spectroscopic evaluation of the interactions of quercetin, isorhamnetin, and quercetin-3′-sulfate with different albumins. *J. Lumin.* **2018**, *194*, 156–163. [CrossRef]
38. Miron, A.; Aprotosoaie, A.C.; Trifan, A.; Xiao, J. Flavonoids as modulators of metabolic enzymes and drug transporters. *Ann. N. Y. Acad. Sci.* **2017**, *1398*, 152–167. [CrossRef] [PubMed]
39. Csepregi, R.; Temesfői, V.; Sali, N.; Poór, M.; Needs, P.W.; Kroon, P.A.; Kőszegi, T. A one-step extraction and luminescence assay for quantifying glucose and ATP levels in cultured HepG2 cells. *Int. J. Mol. Sci.* **2018**, *19*, 2670. [CrossRef] [PubMed]
40. Zhang, G.; Wang, L.; Pan, J. Probing the binding of the flavonoid diosmetin to human serum albumin by multispectroscopic techniques. *J. Agric. Food Chem.* **2012**, *60*, 2721–2729. [CrossRef] [PubMed]
41. Poór, M.; Kunsági-Máté, S.; Bencsik, T.; Petrik, J.; Vladimir-Knezevic, S.; Kőszegi, T. Flavonoid aglycones can compete with Ochratoxin A for human serum albumin: A new possible mode of action. *Int. J. Biol. Macromol.* **2012**, *51*, 279–283. [CrossRef] [PubMed]
42. Conquer, J.A.; Maiani, G.; Azzini, E.; Raguzzini, A.; Holub, B.J. Supplementation with quercetin markedly increases plasma quercetin concentration without effect on selected risk factors for heart disease in healthy subjects. *J. Nutr.* **1998**, *128*, 593–597. [CrossRef] [PubMed]
43. Heinz, S.A.; Henson, D.A.; Nieman, D.C.; Austin, M.D.; Jin, F. A 12-week supplementation with quercetin does not affect natural killer cell activity, granulocyte oxidative burst activity or granulocyte phagocytosis in female human subjects. *Br. J. Nutr.* **2010**, *104*, 849–857. [CrossRef] [PubMed]
44. Huang, W.H.; Lee, A.R.; Yang, C.H. Antioxidative and anti-inflammatory activities of polyhydroxyflavonoids of Scutellaria baicalensis GEORGI. *Biosci. Biotechnol. Biochem.* **2006**, *70*, 2371–2380. [CrossRef] [PubMed]
45. Poór, M.; Lemli, B.; Bálint, M.; Hetényi, C.; Sali, N.; Kőszegi, T.; Kunsági-Máté, S. Interaction of citrinin with human serum albumin. *Toxins* **2015**, *7*, 5155–5166. [CrossRef] [PubMed]
46. Mohos, V.; Bencsik, T.; Boda, G.; Fliszár-Nyúl, E.; Lemli, B.; Kunsági-Máté, S.; Poór, M. Interactions of casticin, ipriflavone, and resveratrol with serum albumin and their inhibitory effects on CYP2C9 and CYP3A4 enzymes. *Biomed. Pharmacother.* **2018**, *107*, 777–784. [CrossRef] [PubMed]
47. Morris, G.M.; Huey, R.; Lindstrom, W.; Sanner, M.F.; Belew, R.K.; Goodsell, D.S.; Olson, A.J. Autodock4 and AutoDockTools4: Automated docking with selective receptor flexiblity. *J. Comput. Chem.* **2009**, *16*, 2785–2791. [CrossRef]
48. Kim, S.; Thiessen, P.A.; Bolton, E.E.; Chen, J.; Fu, G.; Gindulyte, A.; Han, L.; He, J.; He, S.; Shoemaker, B.A.; et al. PubChem Substance and Compound databases. *Nucleic Acids Res.* **2016**, *44*, D1202–D1213. [CrossRef]

49. Csizmadia, F. Java Applets and Modules Supporting Chemical Database Handling from Web Browsers. *J. Chem. Inf. Comput. Sci.* **2000**, *40*, 323–324. [CrossRef]
50. Gasteiger, J.; Marsili, M. Iterative partial equalization of orbital electronegativity-a rapid access to atomic charges. *Tetrahedron* **1980**, *36*, 3219–3228. [CrossRef]

International Journal of
Molecular Sciences

MDPI

Article

Inhibitory Effects of Quercetin and Its Human and Microbial Metabolites on Xanthine Oxidase Enzyme

Violetta Mohos [1,2], Attila Pánovics [1], Eszter Fliszár-Nyúl [1,2], Gabriella Schilli [3], Csaba Hetényi [3], Přemysl Mladěnka [4], Paul W. Needs [5], Paul A. Kroon [5], Gábor Pethő [1,3] and Miklós Poór [1,2,*]

1 Department of Pharmacology, University of Pécs, Faculty of Pharmacy, Szigeti út 12, H-7624 Pécs, Hungary; mohos.violetta@gytk.pte.hu (V.M.); attilapanovics@gmail.com (A.P.); eszter.nyul@aok.pte.hu (E.F.-N.); gabor.petho@aok.pte.hu (G.P.)
2 János Szentágothai Research Center, University of Pécs, Ifjúság útja 20, H-7624 Pécs, Hungary
3 Department of Pharmacology and Pharmacotherapy, University of Pécs, Medical School, Szigeti út 12, H-7624 Pécs, Hungary; scgpecs@gmail.com (G.S.); csabahete@yahoo.com (C.H.)
4 Department of Pharmacology and Toxicology, Faculty of Pharmacy in Hradec Králové, Charles University, Heyrovského 1203, 500 05 Hradec Králové, Czech Republic; mladenkap@faf.cuni.cz
5 Quadram Institute Bioscience, Norwich Research Park, Norwich NR4 7UA, UK; paul.needs@quadram.ac.uk (P.W.N.); paul.kroon@quadram.ac.uk (P.A.K.)
* Correspondence: poor.miklos@pte.hu; Tel.: +36-536-000 (ext. 34646)

Received: 10 May 2019; Accepted: 29 May 2019; Published: 31 May 2019

Abstract: Quercetin is an abundant flavonoid in nature and is used in several dietary supplements. Although quercetin is extensively metabolized by human enzymes and the colonic microflora, we have only few data regarding the pharmacokinetic interactions of its metabolites. Therefore, we investigated the interaction of human and microbial metabolites of quercetin with the xanthine oxidase enzyme. Inhibitory effects of five conjugates and 23 microbial metabolites were examined with 6-mercaptopurine and xanthine substrates (both at 5 μM), employing allopurinol as a positive control. Quercetin-3′-sulfate, isorhamnetin, tamarixetin, and pyrogallol proved to be strong inhibitors of xanthine oxidase. Sulfate and methyl conjugates were similarly strong inhibitors of both 6-mercaptopurine and xanthine oxidations (IC_{50} = 0.2–0.7 μM); however, pyrogallol inhibited xanthine oxidation (IC_{50} = 1.8 μM) with higher potency vs. 6-MP oxidation (IC_{50} = 10.1 μM). Sulfate and methyl conjugates were approximately ten-fold stronger inhibitors (IC_{50} = 0.2–0.6 μM) of 6-mercaptopurine oxidation than allopurinol (IC_{50} = 7.0 μM), and induced more potent inhibition compared to quercetin (IC_{50} = 1.4 μM). These observations highlight that some quercetin metabolites can exert similar or even a stronger inhibitory effect on xanthine oxidase than the parent compound, which may lead to the development of quercetin–drug interactions (e.g., with 6-mercaptopurin or azathioprine).

Keywords: xanthine oxidase; quercetin metabolites; 6-mercaptopurine; xanthine; enzyme inhibition; pharmacokinetic interactions

1. Introduction

Quercetin (Q) is a flavonoid; it is found in many commonly consumed foods and beverages including apples, onions, tea, and red wine [1]. It is included in dietary supplements in high doses (from several hundreds to thousands of milligrams). These supplements are advertised and freely available through the Internet for several purported uses. The oral bioavailability of Q is low, due to its poor aqueous solubility and significant presystemic elimination [2,3]. As a result of the metabolism, Q is known to form methyl, sulfate, and glucuronic acid conjugates, such as 3′-O-methylquercetin (isorhamnetin, IR), 4′-O-methylquercetin (tamarixetin, TAM), quercetin-3′-sulfate

(Q3'S), quercetin-3-glucuronide (Q3G), and isorhamnetin-3-glucuronide (I3G) (Figure 1) [3–6]. Q3'S, Q3G, and I3G are the main circulating metabolites of Q with preserved flavonoid core in humans [7]. Even after high dietary intake of Q, total plasma Q (the parent compound and its metabolites) commonly only reaches nanomolar concentrations [3,6]. Micromolar total plasma Q concentrations were detected only after the administration of dietary supplements with exceedingly high Q content (e.g., 1000 mg/day) [8]. Furthermore, Q is biotransformed by the colonic microflora through degradation of the flavonoid ring(s) into smaller products. These can be classified in four major groups: hydroxybenzoic, hydroxyacetic, and hydroxycinnamic acids, and hydroxybenzenes [6,9–11].

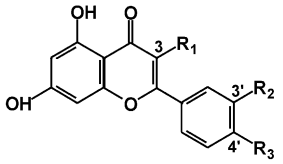

	R_1	R_2	R_3
Quercetin (Q)	-OH	-OH	-OH
Isorhamnetin (IR)	-OH	$-OCH_3$	-OH
Tamarixetin (TAM)	-OH	-OH	$-OCH_3$
Quercetin-3'-sulfate (Q3'S)	-OH	-sulfate	-OH
Quercetin-3-glucuronide (Q3G)	-glucuronate	-OH	-OH
Isorhamnetin-3-glucuronide (I3G)	-glucuronate	$-OCH_3$	-OH

Figure 1. Chemical structures of quercetin and its conjugated metabolites with preserved flavonoid structure.

Xanthine oxidase (XO) is a molybdenum-containing enzyme playing an important role in purine catabolism [12]. The antitumor drug 6-mercaptopurine (6-MP) is also biotransformed by XO, yielding pharmacologically inactive 6-thiouric acid (6-TU) [13]. Allopurinol (APU) is a well-known XO inhibitor used in the treatment of hyperuricemia or gout [12]. Besides the inhibition of uric acid formation, the inhibition of XO may also be beneficial by decreasing superoxide radicals under some pathological conditions [14,15]. However, the simultaneous administration of APU and 6-MP slows elimination of the latter compound, which may cause toxic effects, i.e., severe bone marrow depression [16].

Based on previous studies, Q is a strong competitive inhibitor of XO [17–19], while other authors suggest the involvement of noncompetitive mechanisms as well [20,21]. The effect of Q on the XO-catalyzed oxidation of xanthine has been described; however, the influence of Q on 6-MP oxidation has not been reported. Furthermore, as mentioned above, Q undergoes significant presystemic elimination; therefore, its metabolites reach higher concentrations in blood (and likely in tissues) than the parent compound, Q. Considering the fact that some Q metabolites produce similar or even stronger interaction with some proteins than Q itself [22,23], it is reasonable to hypothesize that some Q metabolites may influence the XO-catalyzed xanthine and/or 6-MP oxidation. Since the inhibition of 6-MP elimination may have serious adverse consequences, we aimed to investigate the interactions of Q as well as its human and microbial metabolites (including also other flavonoid microbial metabolites) with XO enzyme employing xanthine and 6-MP substrates as well as APU and oxipurinol (the active metabolite of APU) as positive controls.

2. Results

2.1. Inhibitory Effects of Q and Its Human Metabolites on XO-Catalyzed 6-MP Oxidation

First, the effects of Q and its conjugated metabolites on 6-MP oxidation were examined. Figure 2 demonstrates the time-dependence of 6-TU formation in the absence and presence of Q metabolites, where % conversion of 6-MP to 6-TU is expressed. Even relatively high concentrations (20 μM = four-fold excess vs. the substrate) of the glucuronide conjugates (Q3G and I3G) did not inhibit the formation of 6-TU. However, Q, as well as its methylated (IR and TAM) and sulfated (Q3'S) metabolites, proved to

be strong inhibitors, even stronger than the positive control APU (Figure 2). Q, Q3'S, IR, and TAM at 3 μM concentration almost completely inhibited 6-TU formation, while the same concentration of APU caused only a slight effect. Furthermore, Q showed only weak inhibitory action at 0.25 μM concentration, while at this concentrations Q3'S and TAM significantly decreased the metabolite formation throughout incubation.

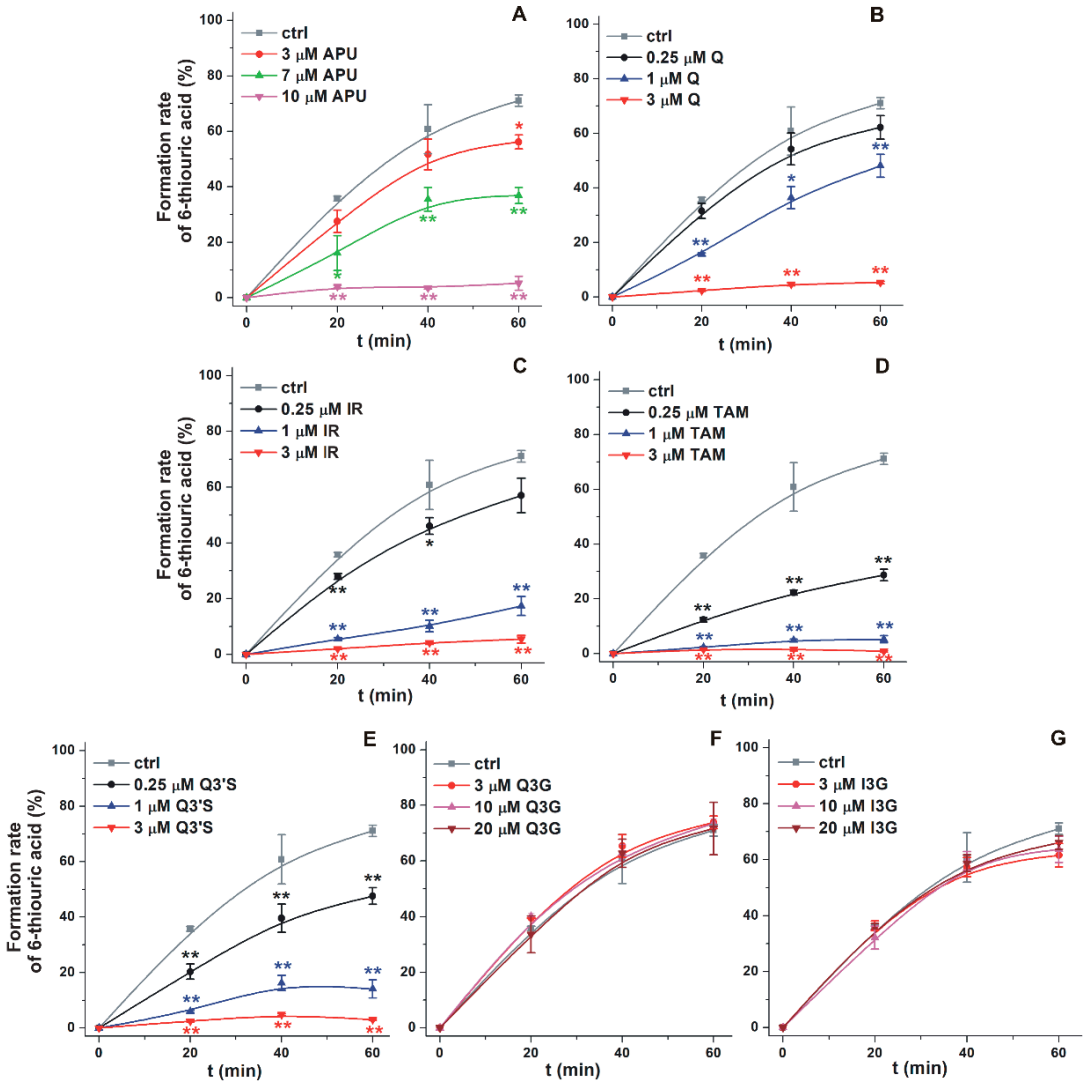

Figure 2. The time course of XO-catalyzed formation of 6-thiouric acid in the presence of increasing concentrations of APU, Q, and conjugated Q metabolites (see further details in the Materials and Methods). Graphs depict % conversion of 6-MP to 6-TU in the absence and presence of increasing concentrations of allopurinol (APU; **A**), quercetin (Q; **B**), isorhamnetin (IR; **C**), tamarixetin (TAM; **D**), quercetin-3'-sulfate (Q3'S; **E**), quercetin-3-glucuronide (Q3G; **F**), and isorhamnetin-3-glucuronide (I3G; **G**) (* $p < 0.05$; ** $p < 0.01$).

Figure 3 demonstrates the concentration-dependent inhibitory effect of APU, Q, and conjugated Q metabolites on the formation of 6-TU. These experiments also highlight the strong inhibitory effects of TAM, Q3'S, IR, and Q on 6-MP oxidation. Based on Figure 3, the IC_{50} values (i.e., the concentrations causing 50% decrease in metabolite formation) of Q and its metabolites were determined. Q (IC_{50} = 1.4 μM) was a five-fold stronger inhibitor than APU (IC_{50} = 7.0 μM), while the IC_{50} values of Q3'S, IR, and TAM were in the 0.2–0.5 μM range and showed approximately ten-fold stronger inhibition of XO-catalyzed 6-MP oxidation than the positive control APU (Table 1). Furthermore,

these conjugates were two- to seven-fold stronger inhibitors of 6-TU formation than the parent compound Q. The IC_{50} values of Q, Q3'S, IR, and TAM (0.2–1.4 μM) were much lower than the substrate concentration (5 μM). As the active metabolite of APU, the inhibitory effect of oxipurinol was also tested. Oxipurinol (IC_{50} = 10 μM) was a significant but weaker inhibitor of XO-catalyzed oxidation of 6-MP than APU (Figure 4, left).

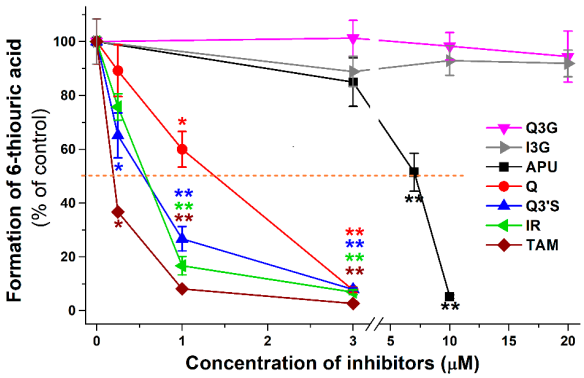

Figure 3. Inhibitory effects of Q and its conjugated metabolites on XO-catalyzed oxidation of 6-MP (5 μM) after 40 min incubation, in the presence of increasing concentrations of allopurinol (APU), quercetin (Q), isorhamnetin (IR), tamarixetin (TAM), quercetin-3'-sulfate (Q3'S), quercetin-3-glucuronide (Q3G), and isorhamnetin-3-glucuronide (I3G). The 50% inhibition of 6-thiouric acid formation (IC_{50}) is marked with dashed line (* $p < 0.05$; ** $p < 0.01$).

Table 1. Inhibition of XO-catalyzed 6-TU formation and uric acid formation by APU, Q, Q3'S, IR, TAM, Q3G, I3G, and PYR. IC_{50}: concentration of the compound which induces 50% inhibition of metabolite formation, $IC_{50(rel)}$ = IC_{50} of the inhibitor divided by the substrate concentration (5 μM 6-MP), α = IC_{50} of the inhibitor divided by IC_{50} of the positive control.

Test Compound	6-MP Oxidation			Xanthine Oxidation			IC_{50} (6-MP)/IC_{50} (Xanthine)
	IC_{50} (μM)	$IC_{50(rel)}$	α	IC_{50} (μM)	$IC_{50(rel)}$	α	
APU (positive ctrl)	7.00	1.40	1.00	0.60	0.12	1.00	11.67
Q	1.40	0.28	0.20	0.80	0.16	1.33	1.75
Q3'S	0.50	0.10	0.07	0.40	0.08	0.67	1.25
IR	0.60	0.12	0.09	0.70	0.14	1.17	0.86
TAM	0.20	0.04	0.03	0.20	0.04	0.33	1.00
Q3G	>20.0	>4.0	-	>20.0	>4.0	-	-
I3G	>20.0	>4.0	-	>20.0	>4.0	-	-
PYR	10.10	2.02	1.44	1.80	0.36	3.00	5.61

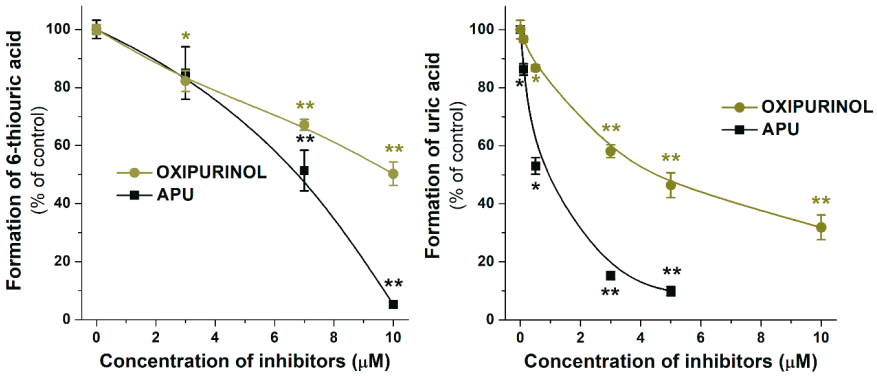

Figure 4. Inhibitory effects of oxipurinol and allopurinol (APU) on XO-catalyzed oxidation of 6-MP and xanthine after 40 and 8 min incubations, respectively. * $p < 0.05$; ** $p < 0.01$).

In another experiment, the reversibility of the inhibition was tested in the presence of 3 μM flavonoids (i.e., Q, Q3'S, IR, or TAM): XO was preincubated with the flavonoids for 15 min, after which, the substrate (6-MP) was added at increasing concentrations (5–50 μM) and the product formation was determined after a subsequent 40 min incubation. The flavonoids at 3 μM concentrations almost completely abolished the metabolite formation in the presence of 5 μM substrate (see in Figure 3); however, at higher concentrations of 6-MP, the metabolite formation increased markedly in a concentration-dependent fashion (Figure 5).

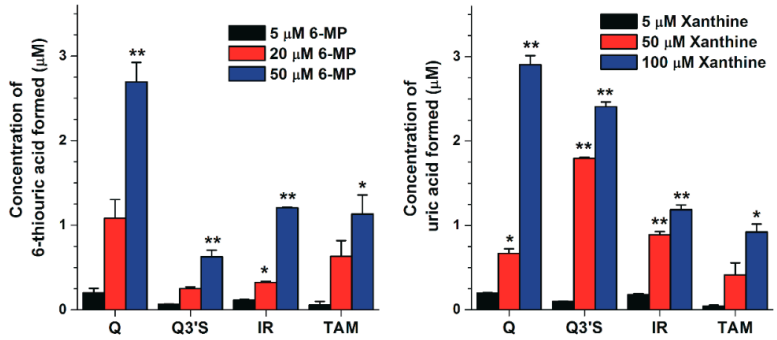

Figure 5. Concentrations of 6-thiouric acid (**left**) and uric acid (**right**) formed in the presence of 3 and 10 μM flavonoid concentrations, respectively (substrate concentrations are indicated in the figure; * $p < 0.05$, ** $p < 0.01$).

2.2. *Inhibitory Effects of Q and Its Human Metabolites on XO-Catalyzed Xanthine Oxidation*

The effects of Q and its conjugated metabolites on xanthine oxidation were also tested (Figure S1). Figure 6 demonstrates the concentration-dependent inhibitory effect of flavonoids on XO-catalyzed uric acid formation. Similar to the previous assay (see in Figure 3), glucuronide conjugates (Q3G and I3G) did not inhibit the XO activity even at four-fold concentration compared to the substrate. However, Q, as well as its methyl and sulfate conjugates, exerted a strong inhibitory effect on XO-catalyzed uric acid formation. Q, Q3'S, and IR inhibited xanthine oxidation to a similar extent as the positive control APU, whereas TAM was a stronger inhibitor compared to these compounds. As Table 1 demonstrates, IC_{50} values of APU, Q, Q3'S, IR, and TAM are in the same range (0.20–0.80 μM). These data highlight that Q as well as its methyl and sulfate conjugates are similarly strong inhibitors of XO-catalyzed xanthine oxidation than APU, producing a 50% decrease in metabolite formation at approximately 1/10th of the substrate concentration. The effect of oxipurinol was also tested; however, it induced significantly weaker effect (IC_{50} = 4.5 μM) on uric acid formation than APU (0.6 μM; Figure 4, right).

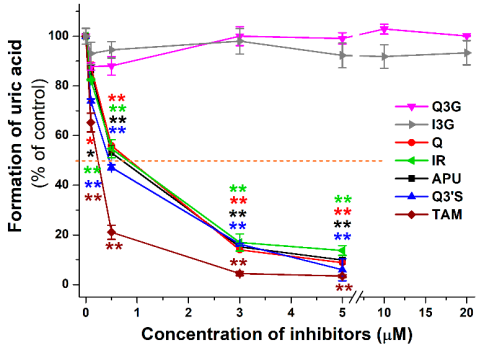

Figure 6. Inhibitory effects of Q and its conjugated metabolites on XO-catalyzed oxidation of xanthine (5 μM) after 8 min incubations, in the presence of increasing concentrations of allopurinol (APU), quercetin (Q), isorhamnetin (IR), tamarixetin (TAM), quercetin-3'-sulfate (Q3'S), quercetin-3-glucuronide (Q3G), and isorhamnetin-3-glucuronide (I3G). The 50% inhibition of uric acid formation (IC_{50}) is marked with dashed line (* $p < 0.05$, ** $p < 0.01$).

We examined the reversibility of the inhibition. XO was preincubated with 10 μM flavonoid (Q, Q3'S, IR, or TAM) for 15 min, after which the substrate (xanthine) was added at increasing concentrations (5–100 μM) and uric acid formation was determined after a subsequent 8 min incubation. These flavonoids at 10 μM concentrations almost completely abolished urate formation from 5 μM xanthine (see in Figure 6); however, xanthine strongly enhanced the metabolite formation in a concentration-dependent fashion (Figure 5).

2.3. Inhibitory Effects of Q, Q3'S, APU, and Oxipurinol on XO-Catalyzed Hypoxanthine Oxidation

Because xanthine is conventionally applied to examine XO activity, the effects of flavonoids on 6-MP oxidation were compared with xanthine oxidation. It is important to note that 6-MP forms 6-TU through two oxidation steps, while uric acid formation from xanthine is a one-step reaction. Therefore, we tested the effects of Q, Q3'S, APU, and oxipurinol on XO-catalyzed hypoxanthine oxidation, which is a two-step reaction (hypoxanthine → xanthine → uric acid), similar to the 6-MP oxidation (6-MP → 6-thipxanthine → 6-TU). During the hypoxanthine assay (see details in Section 4.4), as significant concentrations of both xanthine and uric acid appeared in incubates, the quantities of formed xanthine and uric acid were expressed as the sum of both. As Figure 7 demonstrates, oxipurinol induced weaker inhibition of hypoxanthine oxidation than APU, in accordance with xanthine and 6-MP oxidation (Figure 4). However, Q and Q3'S proved to be approximately three-fold stronger inhibitors of hypoxanthine oxidation than APU (Table 2). The IC_{50} values of APU, Q, and Q3'S for hypoxanthine oxidation were in the same range as for xanthine oxidation (Table 1).

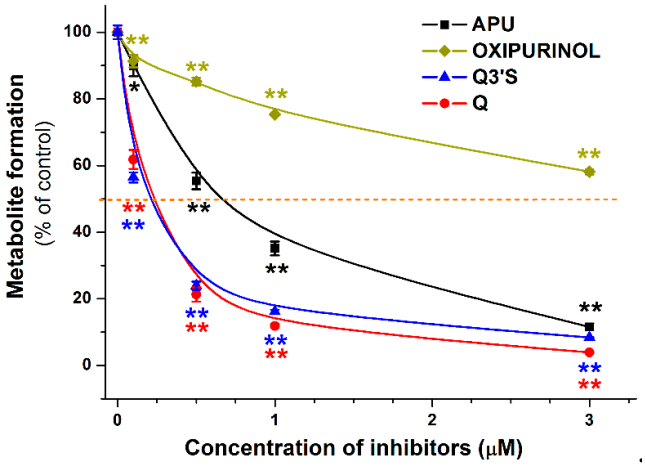

Figure 7. Inhibitory effects of quercetin (Q), quercetin-3'-sulfate (Q3'S), allopurinol (APU), and oxipurinol on XO-catalyzed oxidation of hypoxanthine (5 μM) after 4 min incubations. The 50% inhibition of metabolite (xanthine + uric acid) formation (IC_{50}) is marked with dashed line (* $p < 0.05$, ** $p < 0.01$).

Table 2. Inhibition of XO-catalyzed hypoxanthine oxidation by Q, Q3'S, APU, and oxipurinol. IC_{50}: concentration of the compound which induces 50% inhibition of metabolite formation, $IC_{50(rel)}$ = IC_{50} of the inhibitor divided by the substrate concentration (5 μM hypoxanthine), α = IC_{50} of the inhibitor divided by IC_{50} of the positive control (APU).

Test Compound	IC_{50} (μM)	$IC_{50(rel)}$	α
APU (positive ctrl)	0.66	0.13	1.00
Q	0.24	0.05	0.36
Q3'S	0.21	0.04	0.32
Oxipurinol	>3.00	>0.60	-

2.4. Inhibitory Effects of the Microbial Metabolites on XO-Catalyzed 6-MP and Xanthine Oxidation

Since several absorbable metabolites of flavonoids can be formed by the colonic microflora, these compounds can have systemic effects on XO. Hence, their effects on XO-catalyzed oxidation of 6-MP and xanthine were also evaluated. In the first screening, these metabolites were tested in a concentration of 20 μM with both 6-MP and xanthine as substrates (both at 5 μM). Most colonic metabolites (3H4MPAA, 24DHAP, HIPA, BA, 24DHBA, 2HPAA, 4HMPAA, 4HBA, 4HPAA, 324DHPPA, 34HPPA, 33HPPA, 3CA, 2H4MBA, 3PPA, and PYR) induced significant decreases of 6-TU formation, while only 2H4MBA and PYR inhibited of uric acid formation significantly (Figure 8). These results demonstrate that most of the colon metabolites are significantly stronger inhibitors of 6-MP than xanthine oxidation. PYR was the only colon metabolite which induced more than 50% inhibitory effect at 20 μM concentration (in both assays). Therefore, the concentration-dependent inhibitory effect of PYR on XO was further investigated. Figure 9 demonstrates the XO-catalyzed 6-TU and uric acid formation in the presence of increasing PYR concentrations. Contrary to other colonic metabolites, PYR proved to be a significantly stronger inhibitor of xanthine than 6-MP oxidation, showing an approximately five-fold lower IC_{50} value for uric acid vs. 6-TU formation (Table 1).

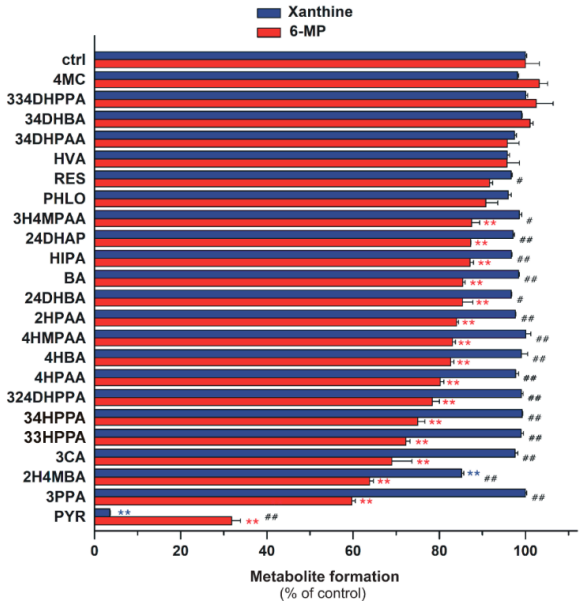

Figure 8. Effects of microbial flavonoid metabolites (each 20 μM) on XO-catalyzed xanthine (5 μM) and 6-MP (5 μM) oxidation. The hash signs indicate significant differences (# $p < 0.05$, ## $p < 0.01$) between xanthine and 6-MP oxidation. Whereas the asterisks mark significant decreases (* $p < 0.05$, ** $p < 0.01$) in xanthine or 6-MP oxidation, as compared to that of control.

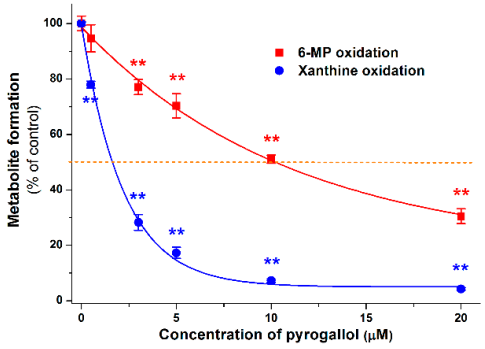

Figure 9. Inhibitory effect of PYR on 6-MP and xanthine oxidation. The 50% inhibition of metabolite formation (IC_{50}) is marked with dashed line (* $p < 0.05$; ** $p < 0.01$).

2.5. Modeling Studies

To test the docking methodology in the present study, the native ligand of XO was removed from the complex PDB structure 3eub, and the ligand-free protein was used for redocking of xanthine. The crystallographic conformation of xanthine (protonation state 1, see in Figure S2) was reproduced at a root mean squared deviation (RMDS) of 1.000 Å where all ten docked conformations found Rank 1 of the lowest ΔGb (Figure S3). Crystallographic structures are also available for ligands Q [24], 6-MP [25], xanthine [26], and oxipurinol [27] bound to XO (PDB IDs 3nyv, 3ns1, 3eub, 3bdj). The binding pockets of these ligands have the common amino acids surrounding the xanthine pocket Glu802, Ser876, Phe914, Phe1009, and Thr1010 (3eub numbering). Accordingly, the binding positions of the docked ligands Q, IR, Q3'S, 6-MP, xanthine, APU, oxipurinol, and PYR show common pharmacophore regions involving the (2,6)-oxo groups of xanthine (Figure 10). The common target residues were identified in our docking calculations of Q and Q3'S as well (Figure 11). Regarding Q3'S, the sulfate group was involved in a salt bridge with Lys771 which is outside the xanthine pocket and appears as an extra feature of the pharmacophore of this ligand.

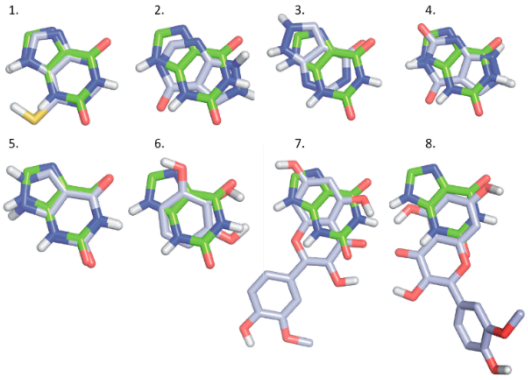

Figure 10. A series of docked ligands (light blue) shown together with the native ligand xanthine (green, used as reference): 6-MP (1; Rank 1); APU (2; Rank 1), APU (3; Rank 2); oxipurinol (4, Rank 1), oxipurinol (5, Rank 2), PYR (6; Rank 1), IR (7; Rank 1), and IR (8, Rank 2).

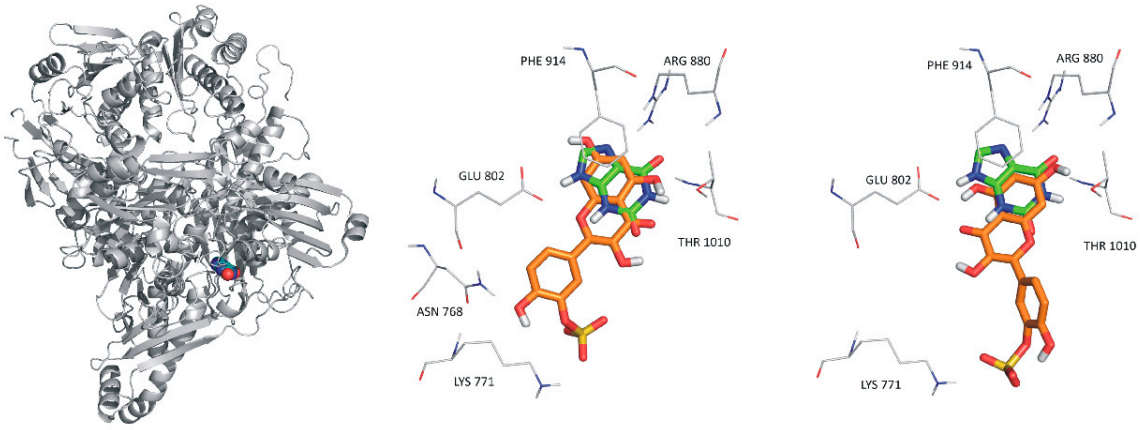

Figure 11. The reference ligand xanthine (spheres, left) occupying its binding site on XO (gray cartoon). In the rest of the panels (middle and right), xanthine is marked with green color. Rank 1 (orange, middle) and Rank 2 (orange, right) binding sites of quercetin-3'sulfate in the XO enzyme.

3. Discussion

Previous studies showed that Q can inhibit XO-catalyzed uric acid formation from xanthine [17,18,28,29]; however, the effects of Q and its metabolites on XO-catalyzed 6-MP oxidation have not been previously reported. Although Q proved to be a strong inhibitor of XO in several in vitro

studies, the IC_{50} and α values of Q show large variations. Some reports suggest the stronger [18] while other studies report the weaker [17,28] inhibition of XO-catalyzed uric acid formation by Q compared to APU. A recent study described similar inhibitory potency for Q and APU on xanthine oxidation [29], which is in good agreement with our results. In another study, the inhibitory effects of some sulfate (Q-3-sulfate) and glucuronide (Q3G, Q-7-glucuronide, Q-3′-glucuronide, and Q-4′-glucuronide) conjugates of Q on XO-catalyzed xanthine oxidation were tested [30]. They found that Q3G and Q-7-glucuronide were only weak inhibitors of XO-catalyzed xanthine oxidation, which is consistent with our negative results at low concentrations (0–20 μM) of Q3G. Interestingly, Q-3′-glucuronide and Q-4′-glucuronide were similarly strong inhibitors of xanthine oxidation as Q; however, these conjugates are poorly formed in humans [7,31]. Furthermore, the position of the sulfate group may be also highly relevant because Q-3-sulfate inhibited XO only at very high concentrations [30], while Q3′S proved to be a strong inhibitor in our investigation.

In each enzyme assay (6-MP, xanthine, and hypoxanthine oxidation), APU was applied as a positive control, because oxipurinol decreased the metabolite formation with lower potency (Figures 4 and 7). This observation is in agreement with the previously reported in vitro data [32]. APU itself is also a substrate of XO which can convert it to oxipurinol [14]; therefore, both the parent compound and the metabolite can inhibit the enzyme. Furthermore, during the oxidation of APU, oxipurinol is formed in the active site of XO, and binds strongly to the reduced state of molybdenum in XO [33]. Since the potent interaction of oxipurinol with XO occurs only when molybdenum is presented in its reduced state, and the molybdenum can be reduced by the substrates of XO (such as xanthine or APU), the oxipurinol formed by XO from APU is more effective compared to the simple addition of oxipurinol [33]. This also explains our initially surprising data, since oxipurinol is considered to be the major culprit of XO inhibition. Indeed, the antihyperuricemic effect of APU is attributed mainly to oxipurinol because of its "pseudoirreversible" (very slow dissociation from the enzyme) effect on XO as well as its much longer elimination half-life and peak plasma concentrations vs. APU (due to the rapid formation of oxipurinol by XO or aldehyde oxidase, and its active reabsorption in kidney tubules) [12,33].

Among the Q conjugates tested, methylated (IR, TAM) and sulfated (Q3′S) derivatives exerted strong inhibitory effect on XO enzyme (Table 1). Since both assays were performed with 5 μM substrate concentrations, the IC_{50} values of the tested compounds can be compared. Q, Q3′S, IR, and TAM were similar or more effective inhibitors of xanthine oxidation than APU. However, compared to APU, these metabolites proved to be approximately ten-fold stronger inhibitors of 6-MP oxidation (Table 1). Nevertheless, it is important to note that the observed difference resulted from the considerably weaker inhibition of 6-MP oxidation by APU, while IC_{50} values of Q, Q3′S, IR, and TAM were similar with both substrates.

Furthermore, 6-MP and xanthine at increasing concentrations could still be metabolized in the presence of the inhibitors, showing that the substrates competed with the flavonoid metabolites in both assays and suggesting that the interactions of flavonoids with the XO enzyme were reversible. This hypothesis is also supported by modeling studies because each tested ligand (APU, oxipurinol, Q, Q3′S, and IR) shares the same binding site with xanthine and 6-MP (see in Figures 10 and 11).

Most of the colonic metabolites exerted stronger effect on 6-MP oxidation than xanthine oxidation; only some less potent inhibitors (4MC, 334DHPPA, 34DHBA, 34DHPAA, HVA, and PHLO) showed similar effects in both assays (Figure 8). Interestingly, PYR was the only bacterial metabolite which strongly inhibited the XO-catalyzed 6-MP and xanthine oxidation. Furthermore, PYR was the sole metabolite which behaved similarly to APU, it exerted a significantly stronger inhibitory effect on xanthine than 6-MP oxidation (Figure 9 and Table 1).

It has been hypothesized that flavonoids may be useful in the treatment of hyperuricemia, based on their ability to inhibit the XO-catalyzed uric acid formation in vitro [21]. The results of animal studies are controversial. For example, Q (100 mg/kg) decreased the serum urate levels in hyperuricemic mice significantly [34], whereas in another study, even 400 mg/kg orally administered Q

failed to decrease the serum urate levels in either normal or hyperuricemic mice [35]. Interestingly, Zhu et al. [34] reported a considerably stronger effect on serum urate levels in mice after per os than intraperitoneal Q administration, suggesting the potential importance of presystemic metabolite formation. Human studies indicate that Q treatment does not influence the serum uric acid levels at 1000 or 2000 mg/day doses [36,37], and a minimal reduction in serum urate occurs even after a four-week treatment with Q (500 mg/day) [38]. We have found that Q, Q3'S, IR, and TAM have similar inhibitory effects on xanthine oxidation to APU. However, even after repeated daily oral administration of 1000 mg Q, the peak plasma concentrations of total Q are only in the low micromolar range [39], whereas the therapeutic peak plasma concentrations of APU and oxipurinol following a single 200 mg oral dose are ca. 35–40 μM [40]. Furthermore, the effect of Q and Q3'S on XO-catalyzed hypoxanthine oxidation showed that these flavonoids are only three-fold stronger inhibitors of hypoxanthine oxidation vs. APU (Table 2). Therefore, it is very unlikely that the approximately ten-fold lower total Q levels will produce similar therapeutic effects to APU and oxipurinol.

The simultaneous administration of conventional APU and 6-MP (or azathioprine, which is a prodrug of 6-MP) doses can result in toxic consequences, due to the decreased elimination of 6-MP by XO enzyme [16]. Nevertheless, the addition of low dose APU to decreased dose of thiopurine analogues (6-MP or azathioprine) can attenuate the incidence of thiopurine hepatotoxicity. The reason is that APU modulates not only the XO enzyme, but affects the formation of 6-methylmercaptopurine as well [16]. However, careful monitoring for adverse effects is strongly recommended [13]. It has to be again emphasized that APU and oxipurinol reach much higher concentrations in the human circulation (and likely in tissues) than Q and its conjugated metabolites; however, Q and its methyl and sulfate conjugates are approximately ten-fold stronger inhibitors of XO-catalyzed 6-MP oxidation compared to APU (Table 1). Mullen et al. [7] suggest that Q3'S is the dominant circulating metabolite of Q, while Cialdella-Kam et al. [41] describe I3G as the major conjugated metabolite. Q3'S has a three-fold stronger inhibitory effect on 6-MP oxidation than Q (Table 1). The potent interaction of Q3'S with XO may be explained by its interaction with Lys771 outside of the xanthine pocket (Figure 10). Since catechol-O-methyltransferase prefers the 3'-O-methylation of the catechol structure, TAM is only a minor metabolite of Q in humans [42]. However, high I3G levels in the circulation [7,31,41] suggest significant intracellular formation of IR, which is a strong inhibitor of XO-catalyzed 6-MP oxidation (Figure 3). Therefore, it is reasonable to hypothesize that the extremely high intake of Q (e.g., one or more grams daily intake through dietary supplements) may result in the dangerous pharmacokinetic interaction with 6-MP and/or azathioprine [43]. Because some websites suggest that Q exerts anti-inflammatory and antitumor effects, simultaneous administration of Q and thiopurine analogues may occur.

Among the tested microbial metabolites, only PYR strongly inhibited the XO-catalyzed oxidation of 6-MP and xanthine. Considering the fact that sulfate conjugates of PYR reached 10 μM or even higher plasma concentrations after the intake of mixed berry fruit puree [44], PYR-XO interaction may have biological relevance. Furthermore, PYR is apparently a metabolite of more dietary flavonoids and/or polyphenols. Currently, the direct data on plasma concentrations of PYR after high doses of food supplements containing flavonoids are missing; therefore, this hypothesis needs to be confirmed. Nevertheless, the PYR is able to significantly inhibit the XO enzyme; thus, PYR may interfere with uric acid formation and 6-MP oxidation.

4. Materials and Methods

4.1. Reagents

Quercetin, isorhamnetin, tamarixetin, and 3-coumaric acid were purchased from Extrasynthese. Quercetin-3'-sulfate, quercetin-3-glucuronide, and isorhamnetin-3-glucuronide were synthetized as described [45]. Xanthine oxidase (from bovine milk), allopurinol, 6-mercaptopurine, hypoxanthine, xanthine, uric acid, oxipurinol, 3-phenylpropionic acid,

3-(4-hydroxyphenyl)propionic acid, 3-(2,4-dihydroxyphenyl)propionic acid, 2-hydroxyphenylacetic acid, 4-hydroxyphenylacetic acid, 3,4-dihydroxyphenylacetic acid, 3-hydroxy-4-methoxyphenylacetic acid, 4-(hydroxymethyl)phenylacetic acid, benzoic acid, 4-hydroxybenzoic acid, 2,4-dihydroxybenzoic acid, 3,4-dihydroxybenzoic acid, hippuric acid, 2,4-dihydroxyacetophenon, 4-methylcatechol, resorcinol, pyrogallol, phloroglucinol, 4-methoxysalicylic acid, and homovanillic acid were obtained from Sigma-Aldrich (St. Louis, MO, US). 3-(3-hydroxyphenyl)propionic acid and 3-(3,4-dihydroxyphenyl)propionic acid were purchased from Toronto Research Chemicals. 6-thiouric acid was obtained from Carbosynth, 6-thioxanthine was purchased from 5A Pharmatech. Uric acid was dissolved in 0.01 M sodium hydroxide (2 mM), while Q and its metabolites, APU, 6-MP, 6-TX, 6-TU, and xanthine were dissolved in dimethyl sulfoxide (each 2 mM) and stored at –20 °C.

4.2. XO Assay with 6-MP Substrate

The substrate (6-MP; 5 μM) was incubated with 0.01 U/mL XO in the absence and presence of inhibitors (0–20 μM) in a thermomixer (700 rpm, 37 °C; Eppendorf), employing APU and oxipurinol as positive controls. The incubations were carried out in 0.05 M sodium phosphate buffer (pH 7.5; final volume of incubates: 500 μL). The reaction started with the addition of the enzyme, and was stopped with 30 μL of 6 M $HClO_4$ 20, 40, or 60 min later. Thereafter, the samples were vortexed and centrifuged at 14,000× *g* for 5 min at room temperature. A 300-μL aliquot of the supernatant was carefully removed, after which 36 μL of 1 M KOH was added to these aliquots. Samples were cooled to 4 °C to enhance the precipitation of the formed $KClO_4$, and centrifuged at 14,000× *g* for 5 min at 4 °C. The supernatants were carefully removed and the substrate together with metabolites were analyzed by HPLC (see details in Section 4.5). 6-MP is oxidized to 6-TX followed by 6-TU in the two-step reaction. However, only 6-MP and 6-TU were detectable, likely because 6-TX does not dissociate significantly from the enzyme before the second oxidation step. In the absence of XO enzyme, no metabolite formation was observed.

4.3. XO Assay with Xanthine Substrate

Xanthine (5 μM) was incubated with 0.0012 U/mL XO in the absence or presence of inhibitors (0–20 μM). Incubations were started with the addition of the enzyme (final volume of incubates: 500 μL), and stopped after 4, 8, and 12 min with 30 μL of 6 M $HClO_4$. Thereafter, the samples were vortexed, after which 97 μL of 1 M KOH was added, then samples were cooled to 4 °C and centrifuged. Other experimental conditions were the same as described in Section 4.2. Xanthine and uric acid were quantified by HPLC (see details in Section 4.5). In the absence of XO, no uric acid formation was detected.

4.4. XO Assay with Hypoxanthine Substrate

Hypoxanthine (5 μM) was incubated with 0.012 U/mL XO enzyme in the absence and presence of increasing concentrations of Q, Q3'S, APU or oxipurinol (0.1, 0.5, 1, and 3 μM). The experiments were started with the addition of the enzyme and stopped after 4 min with 30 μL of 6 M $HClO_4$. Other experimental conditions were the same as described in Section 4.3. XO-catalyzed oxidation of hypoxanthine results in the formation of xanthine and uric acid in two consecutive steps. During these incubations, both xanthine and uric acid appeared in incubates; therefore, for assaying hypoxanthine oxidation, it was necessary to sum the quantities of xanthine and uric acid formed.

4.5. HPLC Analyses

The HPLC system used to determine 6-MP, 6-TX, 6-TU, xanthine, hypoxanthine, and uric acid was equipped with a Rheodyne 7125 injector with a 20-μL sample loop, Waters 510 pump (Milford, MA, USA), and Waters 486 UV-detector. Data were evaluated by Millennium Chromatography Manager Software (Waters).

Quantification of xanthine, hypoxanthine, and uric acid was performed by the previously described method [46] with minor modifications. During the isocratic elution, the mobile phase contained 0.01 M potassium phosphate buffer (pH 4.55) and methanol (98:2 *v*/*v*%). Samples passed through a guard column (Phenomenex Security Guard™ Cartridge C18, 4.0 × 3.0 mm, Torrance, CA, USA) linked to an analytical column (Phenomenex C18, 250 × 4.6 mm, 5 µm) at a 1.1 mL/min flow rate at room temperature. Peak areas were determined at 275 nm. This method was suitable for the separation and quantification of xanthine and uric acid in the presence of most Q metabolites; however, 34DHPAA, 4HMPAA, and PYR co-eluted with xanthine, while 4HBA co-eluted with uric acid. Therefore, for the analysis of xanthine and uric acid in the presence of these metabolites, the mobile phase was modified to 0.01 M potassium phosphate buffer (pH 4.55) and methanol (99:1 *v*/*v*%); the other chromatographic parameters remained unchanged.

Quantitation of 6-MP, 6-TX, and 6-TU was performed by the previously described method [47] with minor modifications. During the isocratic elution, the samples passed through a guard column (Phenomenex Security Guard™ Cartridge C18, 4.0 × 3.0 mm) linked to an analytical column (Phenomenex Gemini®NX-C18, 150 × 4.6 mm, 3 µm), using methanol, acetonitrile, and 0.02 M phosphoric acid (4:5:91 *v*/*v*%) as mobile phase at a 0.8 mL/min flow rate at room temperature. Peak areas were determined at 334 nm.

4.6. Modeling Studies

Docking calculations were performed using the AutoDock 4.2 program package (Molecular Graphics Laboratory, Department of Molecular Biology, The Scripps Research Institute La Jolla, San Diego, CA, USA). Ligand structures of Q, IR, Q3'S, 6-MP, xanthine, APU, oxipurinol, and PYR were obtained from PubChem (National Center for Biotechnology Information, US National Library of Medicine, Bethesda, MD, USA) [48] as Spatial Data File, and hydrogenated using Avogadro [49]. Regarding the two protonation states of xanthine, the first one was set (Figure S2).

Energy-minimization of each ligand molecule was performed by the semiempirical quantum chemistry program package MOPAC (ver. 17.279L) (Stewart Computational Chemistry, Colorado Springs, CO, US) [50]. The geometries were optimized at a 0.001 gradient norm and subjected to subsequent force calculations using PM7 parameterization. In each calculation, the force constant matrices were positive definite. The structure of XO (PDB code 3eub) was used as a target of docking without the native ligand. Gasteiger-Marsilli partial charges [51] were added to the ligands as calculated by AutoDock 4.2 Tools [52].

During target preparation, the protein part was separated from the non-amino acid residues. For the protein part, a two-step energy minimization was performed. A steepest descent minimization was followed by a conjugate gradient run using convergence thresholds of 1000 and 10 kJ × mol × nm-1, respectively. Non-amino acid residues hydroxy(dioxo)molybdenum and phosphonic acid mono-(2-amino-5,6-dimercapto-4-oxo-3,7,8a,9,10,10a-hexahydro-4h-8-oxa-1,3,9,10-tetraaza-anthracen-7-ylmethyl)ester were prepared as the ligand molecules as described above. During MOPAC energy-minimization, their heavy atoms were position restrained. Finally, the target was reconstructed by merging the prepared protein parts with the non-amino acid residues.

A Kollman united atom representation was applied for target groups with non-polar bonds. Regarding focused docking, the grid box was centered on the center of xanthine in 3eub. A grid map was calculated by AutoGrid 4 [52] with a box size of 60 × 60 × 60 points and 0.375 Å spacing. In each calculation, the number of LGA docking runs was set to 10, numbers of energy evaluations and generations were 20 million. Ligand conformations resulted from the docking runs were ordered by the corresponding calculated binding free energy (ΔGb) values and clustered using a tolerance of 1.75 Å distance between cluster members. Conformations with the lowest ΔGb within a cluster were selected as cluster representatives and discussed in the text.

4.7. Statistical Analyses

Data represent mean ± SEM values derived from at least three independent experiments. Statistical analyses were performed employing one-way ANOVA and Student's *t*-test (IBM SPSS Statistics, Version 21, Armonk, NY, USA). The minimal level of significance was set to $p < 0.05$.

Supplementary Materials: Supplementary materials can be found at http://www.mdpi.com/1422-0067/20/11/2681/s1.

Author Contributions: M.P. and G.P. conceived the study. M.P., P.M., and C.H. wrote the paper. V.M. and A.P. performed the XO assays, E.F.-N. carried out HPLC analyses. Modeling studies were executed by G.S. and C.H. Sulfate and glucuronide metabolites of Q were synthetized by P.W.N. and P.A.K. Conceptualization, G.P. and M.P.; Formal analysis, V.M. and E.F.-N.; Funding acquisition, M.P.; Investigation, V.M., A.P., E.F.-N., G.S., C.H., P.W.N., P.A.K. and M.P.; Writing—original draft, V.M., P.M. and M.P.

Funding: The project was supported by the European Union, co-financed by the European Social Fund (EFOP-3.6.1.-16-2016-00004) and by the University of Pécs in the frame of Pharmaceutical Talent Center program.

Acknowledgments: The authors thank Monika Moravcová and István Schweibert for their excellent assistance in the experimental work. Supported by the ÚNKP-18-3 (V.M.) and ÚNKP-18-4 (M.P.) New National Excellence Program of the Ministry of Human Capacities.

Conflicts of Interest: The authors declare no conflict of interest.

Abbreviations

24DHAP	2,4-Dihydroxyacetophenon
24DHBA	2,4-Dihydroxybenzoic acid
2H4MBA	4-Methoxysalicylic acid
2HPAA	2-Hydroxyphenylacetic acid
324DHPPA	3-(2,4-Dihydroxyphenyl)propionic acid
334DHPPA	3-(3,4-Dihydroxyphenyl)propionic acid
33HPPA	3-(3-Hydroxyphenyl)propionic acid
34DHBA	3,4-Dihydroxybenzoic acid
34DHPAA	3,4-Dihydroxyphenylacetic acid
34HPPA	3-(4-Hydroxyphenyl)propionic acid
3CA	3-Coumaric acid
3H4MPAA	3-Hydroxy-4-methoxyphenylacetic acid
3PPA	3-Phenylpropionic acid
4HBA	4-Hydroxybenzoic acid
4HMPAA	4-(Hydroxymethyl)phenylacetic acid
4MC	4-Methylcatechol
6-MP	6-Mercaptopurine
6-TU	6-Thiouric acid
6-TX	6-Thioxanthine
APU	Allopurinol
BA	Benzoic acid
HIPA	Hippuric acid
HVA	Homovanillic acid
I3G	Isorhamnetin-3-glucuronide
IR	Isorhamnetin
PHLO	Phloroglucinol
PYR	Pyrogallol
Q	Quercetin
Q3G	Quercetin-3-glucuronide
Q3′S	Quercetin-3′-sulfate
RES	Resorcinol
TAM	Tamarixetin
XO	Xanthine oxidase

References

1. Formica, J.V.; Regelson, W. Review of the biology of Quercetin and related bioflavonoids. *Food Chem. Toxicol.* **1995**, *12*, 1061–1080. [CrossRef]
2. Hollman, P.C.; De Vries, J.H.; Van Leeuwen, S.D.; Mengellers, M.J.; Katan, M.B. Absorption of dietary quercetin glycosides and quercetin in healthy ileostomy volunteers. *Am. J. Clin. Nutr.* **1995**, *62*, 1276–1282. [CrossRef] [PubMed]
3. Kelly, G.S. Quercetin. *Altern. Med. Rev.* **2011**, *16*, 172–194. [PubMed]
4. Manach, C.; Texier, O.; Regerat, F.; Agullo, G.; Demigne, C.; Remesy, C. Dietary quercetin is recovered in rat plasma as conjugated derivatives of isorhamnetin and quercetin. *J. Nutr. Biochem.* **1996**, *7*, 375–380. [CrossRef]
5. Terao, J.; Murota, K.; Kawai, Y. Conjugated quercetin glucuronides as bioactive metabolites and precursors of aglycone in vivo. *Food Funct.* **2011**, *2*, 11–17. [CrossRef]
6. Del Rio, D.; Rodriguez-Mateos, A.; Spencer, J.P.E.; Tognolini, M.; Borges, G.; Crozier, A. Dietary (poly)phenolics in human health: Structures, bioavailability, and evidence of protective effects against chronic diseases. *Antioxid. Redox Signal.* **2013**, *18*, 1818–1892. [CrossRef] [PubMed]
7. Mullen, W.; Edwards, C.A.; Crozier, A. Absorption, excretion and metabolite profiling of methyl-, glucuronyl-, glucosyl- and sulpho-conjugates of quercetin in human plasma and urine after ingestion of onions. *Br. J. Nutr.* **2006**, *96*, 107–116. [CrossRef]
8. Conquer, J.A.; Maiani, G.; Azzini, E.; Raguzzini, A.; Holub, B.J. Supplementation with quercetin markedly increases plasma quercetin concentration without effect on selected risk factors for heart disease in healthy subjects. *J. Nutr.* **1998**, *128*, 593–597. [CrossRef]
9. Rechner, A.R.; Kuhnle, G.; Bremner, P.; Hubbard, G.P.; Moore, K.P.; Rice-Evans, C.A. The metabolic fate of dietary polyphenols in humans. *Free Rad. Biol. Med.* **2002**, *33*, 220–235. [CrossRef]
10. Aura, A.M. Microbial metabolism of dietary phenolic compounds in the colon. *Phytochem. Rev.* **2008**, *3*, 407–429. [CrossRef]
11. Serra, A.; Macia, A.; Romero, M.P.; Reguant, J.; Ortega, N.; Motilva, M.J. Metabolic pathways of the colonic metabolism of flavonoids (flavonols, flavones and flavanones) and phenolic acids. *Food Chem.* **2012**, *130*, 383–393. [CrossRef]
12. Day, R.O.; Graham, G.G.; Hicks, M.; McLachlan, A.J.; Stocker, S.L.; Williams, K.M. Clinical pharmacokinetics and pharmacodynamics of allopurinol and oxypurinol. *Clin. Pharmacokinet.* **2007**, *46*, 623–644. [CrossRef] [PubMed]
13. Leong, R.W.; Gearry, R.B.; Sparrow, M.P. Thiopurine hepatotoxicity in inflammatory bowel disease: The role for adding allopurinol. *Expert Opin. Drug Saf.* **2008**, *7*, 607–616. [CrossRef]
14. Galbusera, C.; Orth, P.; Fedida, D.; Spector, T. Superoxide radical production by allopurinol and xanthine oxidase. *Biochem. Pharmacol.* **2006**, *71*, 1747–1752. [CrossRef]
15. Berry, C.E.; Hare, J.M. Xanthine oxidoreductase and cardiovascular disease: Molecular mechanisms and pathophysiological implications. *J. Physiol.* **2004**, *555*, 589–606. [CrossRef]
16. McLeod, H.L. Clinically relevant drug-drug interactions in oncology. *Br. J. Clin. Pharmacol.* **1998**, *45*, 539–544. [CrossRef]
17. Lin, C.M.; Chen, C.S.; Chen, C.T.; Liang, Y.C.; Lin, J.K. Molecular modeling of flavonoids that inhibits xanthine oxidase. *Biochem. Biophys. Res. Commun.* **2002**, *294*, 162–172. [CrossRef]
18. Van Hoorn, D.E.C.; Nijveldt, R.J.; Van Leeuwen, P.A.M.; Hofman, Z.; M'Rabet, L.; De Bont, D.B.A.; Van Norren, K. Accurate prediction of xanthine oxidase inhibition based on the structure of flavonoids. *Eur. J. Pharmacol.* **2002**, *451*, 111–118. [CrossRef]
19. Mladenka, P.; Zatloukalová, L.; Filipský, T.; Hrdina, R. Cardiovascular effects of flavonoids are not caused only by direct antioxidant activity. *Free Radic. Biol. Med.* **2010**, *49*, 963–975. [CrossRef]
20. Iio, M.; Moriyama, A.; Matsumoto, Y.; Takaki, N.; Fukumoto, M. Inhibition of Xanthine Oxidase by Flavonoids. *Agric. Biol. Chem.* **1985**, *49*, 2173–2176. [CrossRef]
21. Nagao, A.; Seki, M.; Kobayashi, H. Inhibition of xanthine oxidase by flavonoids. *Biosci. Biotechnol. Biochem.* **1999**, *63*, 1787–1790. [CrossRef]
22. Miron, A.; Aprotosoaie, A.C.; Trifan, A.; Xiao, J. Flavonoids as modulators of metabolic enzymes and drug transporters. *Ann. N. Y. Acad. Sci.* **2017**, *1398*, 152–167. [CrossRef]

23. Poór, M.; Boda, G.; Needs, P.W.; Kroon, P.A.; Lemli, B.; Bencsik, T. Interaction of quercetin and its metabolites with warfarin: Displacement of warfarin from serum albumin and inhibition of CYP2C9 enzyme. *Biomed. Pharmacother.* **2017**, *88*, 574–581. [CrossRef]
24. Cao, H.; Pauff, J.M.; Hille, R. X-ray crystal structure of a xanthine oxidase complex with the flavonoid inhibitor quercetin. *J. Nat. Prod.* **2014**, *77*, 1693–1699. [CrossRef]
25. Cao, H.; Pauff, J.M.; Hille, R. Substrate orientation and catalytic specificity in the action of xanthine oxidase: The sequential hydroxylation of hypoxanthine to uric acid. *J. Biol. Chem.* **2010**, *285*, 28044–28053. [CrossRef]
26. Pauff, J.M.; Cao, H.; Hille, R. Substrate Orientation and Catalysis at the Molybdenum Site in Xanthine Oxidase: CRYSTAL STRUCTURES IN COMPLEX WITH XANTHINE AND LUMAZINE. *J. Biol. Chem.* **2009**, *284*, 8760–8770. [CrossRef]
27. Okamoto, K.; Eger, B.T.; Nishino, T.; Pai, E.F.; Nishino, T. Mechanism of inhibition of xanthine oxidoreductase by allopurinol: Crystal structure of reduced bovine milk xanthine oxidoreductase bound with oxipurinol. *Nucleosides Nucleotides Nucleic Acids* **2008**, *27*, 888–893. [CrossRef]
28. Cos, P.; Ying, L.; Calomne, M.; Hu, J.P.; Cimanga, K.; Van Poel, B.; Pieters, L.; Vlietinck, A.J.; Berghe, D.V. Structure-activity relationship and classification of flavonoids as inhibitors of xanthine oxidase and superoxide scavengers. *J. Nat. Prod.* **1998**, *61*, 71–76. [CrossRef]
29. Zhang, C.; Wang, R.; Zhang, G.; Gong, D. Mechanistic insights into the inhibition of quercetin on xanthine oxidase. *Int. J. Biol. Macromol.* **2018**, *112*, 405–412. [CrossRef]
30. Day, A.J.; Bao, Y.; Morgan, M.R.; Williamson, G. Conjugation position of quercetin glucuronides and effect on biological activity. *Free Radic. Biol. Med.* **2000**, *29*, 1234–1243. [CrossRef]
31. Day, A.J.; Mellon, F.; Barron, D.; Sarrazin, G.; Morgan, M.R.; Williamson, G. Human metabolism of dietary flavonoids: Identification of plasma metabolites of quercetin. *Free Radic. Res.* **2001**, *35*, 941–952. [CrossRef]
32. Elion, G.B. Enzymatic and metabolic studies with allopurinol. *Ann. Rheum. Dis.* **1966**, *25*, 608–614. [CrossRef] [PubMed]
33. Spector, T. Inhibition of urate production by allopurinol. *Biochem. Pharmacol.* **1977**, *26*, 355–358. [CrossRef]
34. Zhu, J.X.; Wang, Y.; Kong, L.D.; Yang, C.; Zhang, X. Effects of Biota orientalis extract and its flavonoid constituents, quercetin and rutin on serum uric acid levels in oxonate-induced mice and xanthine dehydrogenase and xanthine oxidase activities in mouse liver. *J. Ethnopharmacol.* **2004**, *93*, 133–140. [CrossRef] [PubMed]
35. Huang, J.; Wang, S.; Zhu, M.; Chen, J.; Zhu, X. Effects of Genistein, Apigenin, Quercetin, Rutin and Astilbin on serum uric acid levels and xanthine oxidase activities in normal and hyperuricemic mice. *Food Chem. Toxicol.* **2011**, *49*, 1943–1947. [CrossRef] [PubMed]
36. Abbey, E.L.; Rankin, J.W. Effect of quercetin supplementation on repeated-sprint performance, xanthine oxidase activity, and inflammation. *Int. J. Sport Nutr. Exerc. Metab.* **2011**, *21*, 91–96. [CrossRef]
37. Boots, A.W.; Drent, M.; De Boer, V.C.; Bast, A.; Haenen, G.R. Quercetin reduces markers of oxidative stress and inflammation in sarcoidosis. *Clin. Nutr.* **2011**, *30*, 506–512. [CrossRef] [PubMed]
38. Shi, Y.; Williamson, G. Quercetin lowers plasma uric acid in pre-hyperuricaemic males: A randomised, double-blinded, placebo-controlled, cross-over trial. *Br. J. Nutr.* **2016**, *115*, 800–806. [CrossRef] [PubMed]
39. Heinz, S.A.; Henson, D.A.; Nieman, D.C.; Austin, M.D. A 12-week supplementation with quercetin does not affect natural killer cell activity, granulocyte oxidative burst activity or granulocyte phagocytosis in female human subjects. *Br. J. Nutr.* **2010**, *104*, 849–857. [CrossRef] [PubMed]
40. Turnheim, K.; Krivanek, P.; Oberbauer, R. Pharmacokinetics and pharmacodynamics of allopurinol in elderly and young subjects. *Br. J. Clin. Pharmacol.* **1999**, *48*, 501–509. [CrossRef]
41. Cialdella-Kam, L.; Nieman, D.C.; Sha, W.; Meaney, M.P.; Knab, A.M.; Shanely, R.A. Dose-response to 3 months of quercetin-containing supplements on metabolite and quercetin conjugate profile in adults. *Br. J. Nutr.* **2013**, *109*, 1923–1933. [CrossRef] [PubMed]
42. De Santi, C.; Pietrabissa, A.; Mosca, F.; Pacifici, G.M. Methylation of quercetin and fisetin, flavonoids widely distributed in edible vegetables, fruits and wine, by human liver. *Int. J. Clin. Pharmacol. Ther.* **2002**, *40*, 207–212. [CrossRef] [PubMed]
43. Vida, R.G.; Fittler, A.; Somogyi-Végh, A.; Poór, M. Dietary quercetin supplements: Assessment of online product informations and quantitation of quercetin in the products by high performance liquid chromatography. *Phytother. Res.* **2019**. Accepted manuscript. [CrossRef]

44. Pimpão, R.C.; Ventura, M.R.; Ferreira, R.B.; Williamson, G.; Santos, C.N. Phenolic sulfates as new and highly abundant metabolites in human plasma after ingestion of a mixed berry fruit purée. *Br. J. Nutr.* **2015**, *113*, 454–463. [CrossRef]
45. Needs, P.W.; Kroon, P.A. Convenient synthesis of metabolically important glucuronides and sulfates. *Tetrahedron* **2006**, *62*, 6862–6868. [CrossRef]
46. Mei, D.A.; Gross, G.J.; Nithipatikom, K. Simultaneous determination of adenosine, inosine, hypoxanthine, xanthine, and uric acid in microdialysis samples using microbore column high-performance liquid chromatography with a diode array detector. *Anal. Biochem.* **1996**, *238*, 34–39. [CrossRef]
47. Hawwa, A.F.; Millership, J.S.; Collier, P.S.; McElnay, J.C. Development and validation of an HPLC method for the rapid and simultaneous determination of 6-mercaptopurine and four of its metabolites in plasma and red blood cells. *J. Pharm. Biomed. Anal.* **2009**, *49*, 401–409. [CrossRef]
48. Kim, S.; Thiessen, P.A.; Bolton, E.E.; Chen, J.; Fu, G.; Gindulyte, A.; Han, L.; He, J.; He, S.; Shoemaker, B.A.; Wang, J.; et al. PubChem Substance and Compound databases. *Nucleic Acids Res.* **2016**, *44*, D1202–D1213. [CrossRef]
49. Hanwell, M.D.; Curtis, D.E.; Lonie, D.C.; Vandermeersch, T.; Zurek, E.; Hutchison, G.R. Avogadro: An advanced semantic chemical editor, visualization, and analysis platform. *J. Cheminform.* **2012**, *4*, 17. [CrossRef]
50. Stewart, J.J.P. MOPAC: A semiempirical molecular orbital program. *Computer-Aided Mol. Des.* **1990**, *4*, 1–103. [CrossRef]
51. Gasteiger, J.; Marsili, M. Iterative partial equalization of orbital electronegativity—a rapid access to atomic charges. *Tetrahedron* **1980**, *36*, 3219–3228. [CrossRef]
52. Morris, G.M.; Huey, R.; Lindstrom, W.; Sanner, M.F.; Belew, R.K.; Goodsell, D.S.; Olson, A.J. AutoDock4 and AutoDockTools4: Automated docking with selective receptor flexibility. *J. Com. Chem.* **2009**, *16*, 2785–2791. [CrossRef] [PubMed]

International Journal of
Molecular Sciences

MDPI

Article

Inhibition of Xanthine Oxidase-Catalyzed Xanthine and 6-Mercaptopurine Oxidation by Flavonoid Aglycones and Some of Their Conjugates

Violetta Mohos [1,2], Eszter Fliszár-Nyúl [1,2] and Miklós Poór [1,2,*]

1 Department of Pharmacology, Faculty of Pharmacy, University of Pécs, Szigeti út 12, H-7624 Pécs, Hungary; mohos.violetta@gytk.pte.hu (V.M.); eszter.nyul@aok.pte.hu (E.F.-N.)
2 János Szentágothai Research Centre, University of Pécs, Ifjúság útja 20, H-7624 Pécs, Hungary
* Correspondence: poor.miklos@pte.hu; Tel.: +36-72-536-000 (ext. 35052)

Received: 23 March 2020; Accepted: 4 May 2020; Published: 5 May 2020

Abstract: Flavonoids are natural phenolic compounds, which are the active ingredients in several dietary supplements. It is well-known that some flavonoid aglycones are potent inhibitors of the xanthine oxidase (XO)-catalyzed uric acid formation in vitro. However, the effects of conjugated flavonoid metabolites are poorly characterized. Furthermore, the inhibition of XO-catalyzed 6-mercaptopurine oxidation is an important reaction in the pharmacokinetics of this antitumor drug. The inhibitory effects of some compounds on xanthine vs. 6-mercaptopurine oxidation showed large differences. Nevertheless, we have only limited information regarding the impact of flavonoids on 6-mercaptopurine oxidation. In this study, we examined the interactions of flavonoid aglycones and some of their conjugates with XO-catalyzed xanthine and 6-mercaptopurine oxidation in vitro. Diosmetin was the strongest inhibitor of uric acid formation, while apigenin showed the highest effect on 6-thiouric acid production. Kaempferol, fisetin, geraldol, luteolin, diosmetin, and chrysoeriol proved to be similarly strong inhibitors of xanthine and 6-mercaptopurine oxidation. While apigenin, chrysin, and chrysin-7-sulfate were more potent inhibitors of 6-mercaptopurine than xanthine oxidation. Many flavonoids showed similar or stronger (even 5- to 40-fold) inhibition of XO than the positive control allopurinol. Based on these observations, the extremely high intake of flavonoids may interfere with the elimination of 6-mercaptopurine.

Keywords: flavonoids; flavonoid conjugates; xanthine oxidase; xanthine; 6-mercaptopurine; biotransformation; food-drug interaction

1. Introduction

Flavonoids are plant-derived phenolic compounds found in numerous fruits, vegetables, and spices [1]. Several studies suggest the beneficial health effects of flavonoids (e.g., antioxidant, anti-inflammatory, and antiproliferative actions), therefore, many dietary supplements contain high doses of flavonoids (even more ten- or hundred-fold vs. the normal dietary intake) [2,3]. Typically, flavonoids have low oral bioavailability, due to their significant metabolism in enterocytes and hepatocytes [4]. The biotransformation of flavonoids by catechol-*O*-methyltransferase (COMT), sulfotransferase (SULT), and uridine diphosphate glucuronosyltransferase (UGT) results in the formation of methyl, sulfate, and glucuronide conjugates, respectively [5]. These derivatives commonly reach considerably higher concentrations in the systemic circulation than the parent compound [6,7]. Flavonoid chrysin (CHR) is extensively biotransformed by SULT and UGT, its dominant metabolites are chrysin-7-sulfate (C7S) and chrysin-7-glucuronide (C7G) in the human circulation [8]. COMT is also a frequently involved enzyme in flavonoid metabolism, the 3′-*O*-methylation of fisetin (FIS) results in geraldol (3′-*O*-methylfisetin, GER) [9,10], while diosmetin (4′-*O*-methylluteolin, DIO) and chrysoeriol (3′-*O*-methylluteolin, CHE) are formed from luteolin (LUT) by

COMT [11]. LUT is a rare substrate of COMT because its 4′-*O*-substitution is preferred (vs. the typical 3′-*O*-methylation) [12]. Furthermore, DIO is the dominant circulating metabolite of orally-administered diosmin, the latter is the active ingredient of several medications (e.g., Detralex® and Daflon®) and dietary supplements [13]. Methylated flavonoids are not only produced during the biotransformation in mammals, but also found in certain plants [14–16]. GER appears in *Trifolium subterraneum* [16,17], while CHE is a constituent of rooibos tea (*Aspalathus linearis*) and of *Digitalis purpurea* [14,15].

Xanthine oxidase (XO) is a non-microsomal molybdenum-containing enzyme involved in purine catabolism. XO oxidizes hypoxanthine to xanthine then to uric acid (Figure 1) [18]. Allopurinol is a potent inhibitor of XO, it is used as a medication to treat hyperuricemia or gout [18]. Allopurinol competitively inhibits XO and it is oxidized to oxipurinol, which in turn is a potent pseudo-irreversible inhibitor of XO [19]. Inhibition of XO results in the decreased formation of uric acid and also reduces the XO-mediated formation of superoxide anion radicals in some pathological conditions [20]. Furthermore, XO is also involved in the biotransformation of the antitumor drug 6-mercaptopurine (6MP) (Figure 1) [21]. Considering the fact that the simultaneous administration of allopurinol and 6MP slows down the elimination of the latter compound, the strong inhibition of XO-catalyzed 6MP oxidation can cause even serious myelosuppression [22].

The strong inhibition of XO by flavonoids has been reported in several in vitro studies [23–27]. Based on previous investigations, flavonoid aglycones apigenin (API), CHR, FIS, kaempferol (KAE), and LUT are potent inhibitors of the XO-catalyzed xanthine oxidation [23,26]. Besides their strong effects on XO, we selected these aglycones because they are contained in many dietary supplements widely marketed through the Internet. The extremely high intake of flavonoids (as a result of the consumption of dietary supplements) can lead to the high plasma concentrations of flavonoids and/or their metabolites [6,7,13]. Xanthine is the generally applied substrate in XO assays; however, the inhibitory effects of flavonoids on XO-catalyzed 6MP oxidation has been poorly studied. In our recent report, we demonstrated that quercetin as well as its sulfate and methyl conjugates are similarly potent inhibitors of xanthine and 6MP oxidation, while some inhibitors (e.g., 3-phenylpropionic acid, pyrogallol, and allopurinol) showed considerably stronger effects on xanthine or on 6MP oxidation [19].

The two main goals of this study were the following: (1) Comparison of the inhibitory potency of flavonoid conjugates vs. the parent compounds; (2) comparison of the effects of flavonoids on XO-catalyzed xanthine vs. 6MP oxidation. Therefore, the influence of the above-listed flavonoid aglycones and their metabolites (Figure 2) on the XO enzyme were tested employing in vitro enzyme assays (using allopurinol as positive control). After incubations, the substrates (xanthine and 6MP) and metabolites (uric acid and 6-thiouric acid) were quantified with high-performance liquid chromatography (HPLC).

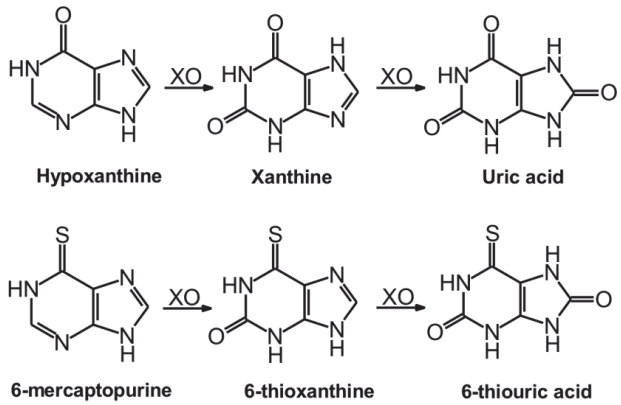

Figure 1. XO-catalyzed oxidation of hypoxanthine to uric acid (**top**) and 6-mercaptopurine to 6-thiouric acid (**bottom**).

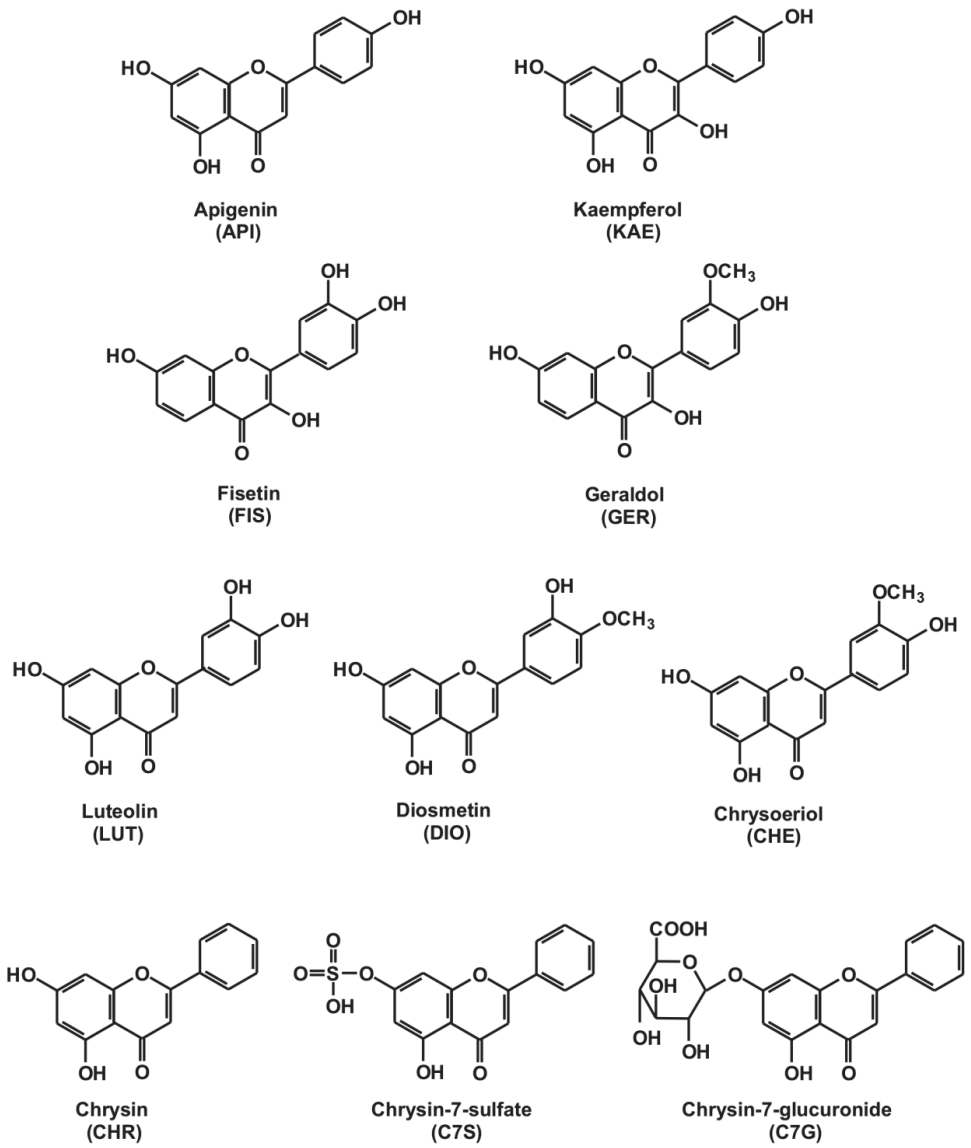

Figure 2. Chemical structures of apigenin (5,7,4′-trihydroxyflavone), kaempferol (3,5,7,4′-tetrahydroxyflavone), fisetin (3,7,3′,4′-tetrahydroxyflavone), geraldol (3′-*O*-methylfisetin), luteolin (5,7,3′,4′-tetrahydroxyflavone), diosmetin (4′-*O*-methylluteolin), chrysoeriol (3′-*O*-methylluteolin), chrysin (5,7-dihydroxyflavone), chrysin-7-sulfate, and chrysin-7-glucuronide.

2. Results

2.1. Inhibition of Xanthine and 6-Mercaptopurine Oxidation by Flavonoid Aglycones

First, the effects of flavonoid aglycones (API, CHR, FIS, KAE, and LUT) on the XO-catalyzed xanthine and 6MP oxidation were examined. Each flavonoid tested was able to inhibit both uric acid and 6-thiouric acid formation at nanomolar or low micromolar concentrations (Figure 3). Regarding xanthine oxidation, LUT was the strongest while CHR was the weakest inhibitor (Table 1); and each aglycone showed similar inhibitory potency to allopurinol. However, API and FIS were the strongest and weakest inhibitors of 6MP oxidation, respectively (Figure 3, right). In addition, each flavonoid aglycone was considerably stronger inhibitor of XO-catalyzed 6-thiouric acid formation compared to allopurinol (Table 1).

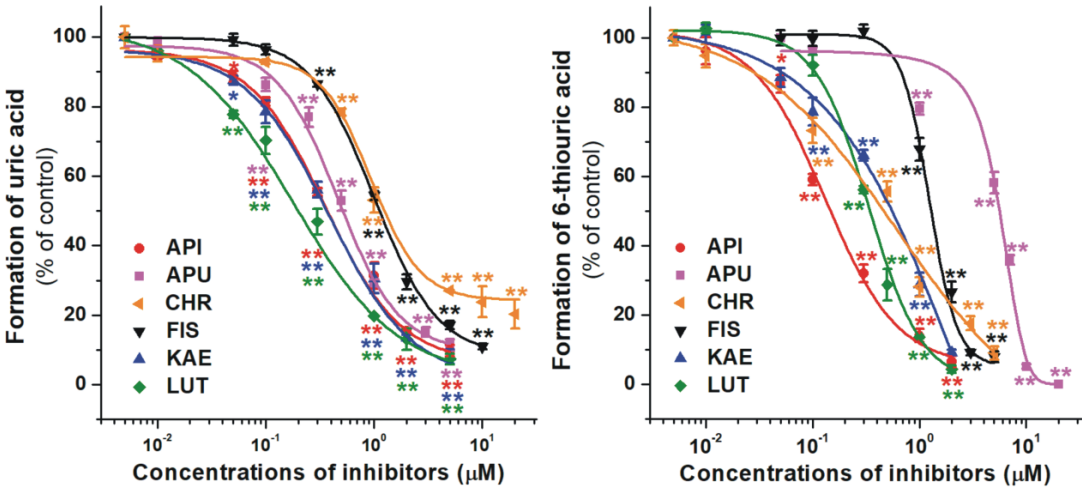

Figure 3. Concentration-dependent inhibitory effects of flavonoid aglycones and the positive control allopurinol (APU) on the XO enzyme. Inhibition of XO-catalyzed uric acid (**left**) and 6-thiouric acid (**right**) formation in the presence of increasing inhibitor concentrations (0–20 μM; substrate concentrations: 5 μM in both assays; API, apigenin; CHR, chrysin; FIS, fisetin; KAE, kaempferol; LUT, luteolin; * $p < 0.05$, ** $p < 0.01$).

Table 1. Inhibitory effects of flavonoids and their conjugated metabolites on XO-catalyzed xanthine and 6MP oxidation.

Test Compound	$IC_{50(xanthine)}$ (μM)	$IC_{50(6MP)}$ (μM)	$IC_{50\ (xanthine)}/IC_{50\ (6MP)}$
Allopurinol	0.38	1.97	0.19
Apigenin	0.27	0.09	3.00
Kaempferol	0.29	0.38	0.76
Fisetin	0.86	1.10	0.78
Geraldol	0.68	1.19	0.57
Luteolin	0.16	0.27	0.59
Diosmetin	0.04	0.05	0.80
Chrysoeriol	0.17	0.09	1.88
Chrysin	0.70	0.22	3.18
Chrysin-7-sulfate	>20.0	2.23	-
Chrysin-7-glucuronide	>20.0	>20.0	-

2.2. Inhibition of Xanthine and 6-Mercaptopurine Oxidation by Flavonoid Conjugates

The inhibitory effects of some flavonoid metabolites on XO enzyme were also investigated. Figure 4 demonstrates the formation of uric acid and 6-thiouric acid compared to the control, in the presence of increasing concentrations of FIS and its 3′-*O*-methyl derivative GER. Our results showed that GER induced similarly strong inhibition on both xanthine and 6MP oxidation to FIS (Table 1). Furthermore, FIS and GER were weaker inhibitors of uric acid formation than allopurinol, while they exerted significantly stronger effects on 6-thiouric acid production compared to the positive control (Figure 4, right).

The effects of LUT and its methylated metabolites DIO (4′-*O*-methylluteolin) and CHE (3′-*O*-methylluteolin) on XO were also tested. DIO and CHE were stronger and weaker inhibitors of uric acid formation than LUT, respectively (Figure 5, left). Furthermore, both metabolites showed stronger inhibitory effects on uric acid formation compared to allopurinol (Table 1). DIO and CHE proved to be more potent inhibitors of 6MP oxidation vs. the parent compound (Figure 5, right), showing considerably stronger effect than the positive control (Table 1).

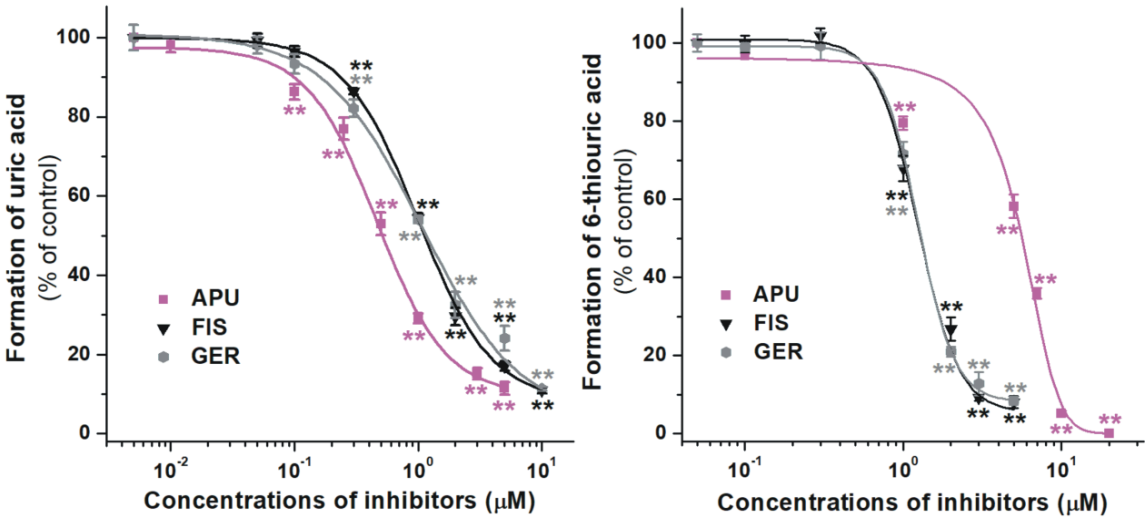

Figure 4. Concentration-dependent inhibitory effects of FIS, GER, and allopurinol (APU) on XO enzyme. Inhibition of XO-catalyzed uric acid (**left**) and 6-thiouric acid (**right**) formation in the presence of increasing inhibitor concentrations (0–20 μM; substrate concentrations: 5 μM in both assays; FIS, fisetin; GER, geraldol; ** $p < 0.01$).

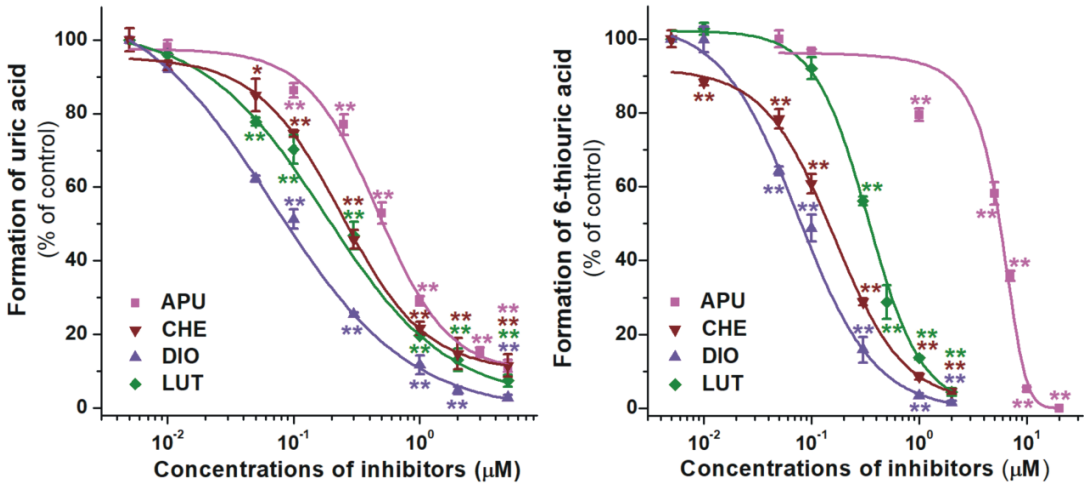

Figure 5. Concentration-dependent inhibitory effects of LUT, DIO, CHE, and allopurinol (APU) on XO enzyme. Inhibition of XO-catalyzed uric acid (**left**) and 6-thiouric acid (**right**) formation in the presence of increasing inhibitor concentrations (0–20 μM; substrate concentrations: 5 μM in both assays; CHE, chrysoeriol; DIO, diosmetin; LUT, luteolin; * $p < 0.05$, ** $p < 0.01$).

Finally, the effects of chrysin as well as its sulfate and glucuronide metabolites on XO were examined. Although, C7S and C7G exerted statistically significant inhibition on XO-catalyzed xanthine and 6MP oxidation, they proved to be considerably weaker inhibitors vs. the parent compound in both assays (Figure 6). C7G was a poor inhibitor of XO, while C7S did not induce a 50% decrease in the metabolite formation in the xanthine assay, even at four-fold concentration compared to the substrate. Furthermore, CHR showed weaker and considerably stronger inhibitory effects on xanthine and 6MP oxidation than allopurinol, respectively (Figure 6 and Table 1).

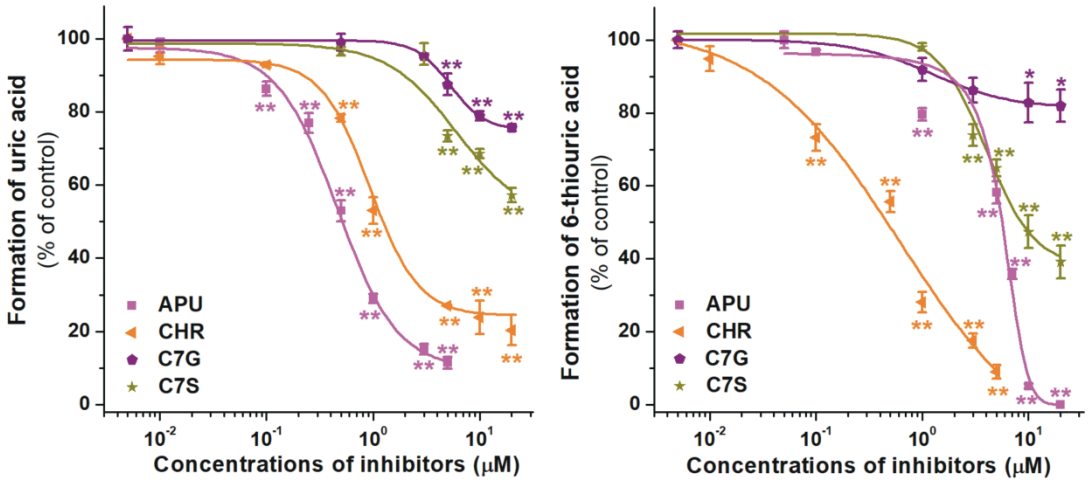

Figure 6. Concentration-dependent inhibitory effects of CHR, C7S, C7G, and allopurinol (APU) on XO enzyme. Inhibition of XO-catalyzed uric acid (**left**) and 6-thiouric acid (**right**) formation in the presence of increasing inhibitor concentrations (0–20 μM; substrate concentrations: 5 μM in both assays; C7G, chrysin-7-glucuronide; C7S, chrysin-7-sulfate; CHR, chrysin; * $p < 0.05$, ** $p < 0.01$).

3. Discussion

The strong in vitro inhibitory effects of API, CHR, FIS, KAE, and LUT on the XO-catalyzed xanthine oxidation have been widely investigated in earlier studies [23–27]. However, the effects of their conjugated metabolites on xanthine oxidation as well as the inhibitory action of these flavonoids on 6MP oxidation has not been or has been only poorly examined. Despite the fact that earlier studies characterized the strong inhibitory potential of flavonoids vs. xanthine oxidation, some studies suggest their similar [26,28], stronger [24,27], or even weaker [23,25,29] effects compared to allopurinol. Regarding the flavonoids examined in our study, their IC_{50} values showed large variances in previous investigations (API: 0.7 to 3.6 μM, CHR: 0.8 to 5.0 μM, FIS: 4.3 to 11.3 μM, KAE: 0.7 to 16.9 μM, LUT: 0.6 to 8.8 μM) [23–29]. Nevertheless, our results are consistent with previous reports, suggesting the nanomolar or low micromolar IC_{50} values regarding flavonoid aglycones tested in the current study (Table 1). Previously reported data are highly controversial regarding CHE: negligible [30], mild [31], and strong [32] inhibition of XO has been also described. In earlier studies, DIO proved to be a strong inhibitor of xanthine oxidation, however, both its weaker [25,33] and stronger [32] effects vs. allopurinol have been reported. Furthermore, we did not find any data regarding the impacts of GER, C7S, and C7G on XO. Similarly to C7G (Figure 6, right), the pharmacologically relevant glucuronide conjugates of quercetin were poor inhibitors of xanthine oxidation [19]. Interestingly, quercetin-3′-glucuronide and quercetin-4′-glucuronide exerted strong inhibitory effects on xanthine oxidation [34]; however, these conjugates are not typical in the human body. Methyl conjugates tested in this study (CHE, DIO, and GER) were similar or stronger inhibitors of the enzyme than the parent flavonoids (Table 1), which is in agreement with previous observations regarding LUT [32] and quercetin [19]. C7S showed significantly weaker effect than CHR (Table 1); while in another study, quercetin-3′-sulfate and quercetin were equally strong inhibitors of xanthine oxidation [19].

For the appropriate comparison, both xanthine and 6MP assays were performed with 5 μM substrate concentrations. It is important to note that, in the 6MP assay, the considerably stronger inhibitory effects of flavonoids vs. the positive control are resulted from the fact that allopurinol is a more than five-fold stronger inhibitor of xanthine than 6MP oxidation (Table 1). Under the applied conditions, C7G was the sole compound which showed only weak inhibition in both assays. Similar observations have been reported regarding quercetin-3-glucuronide and isorhamnetin-3-glucuronide [19,34]. Some of the flavonoids (CHE, DIO, FIS, GER, KAE, and LUT) showed same inhibitory effects on XO-catalyzed xanthine and 6MP oxidation. However, API, CHR, and C7S were more potent

inhibitors of 6-thiouric acid vs. uric acid formation (Table 1), similarly to several colonic flavonoid metabolites (e.g., 3-phenylpropionic acid, 4-methoxysalicylic acid, and 3-coumaric acid) [19]. DIO was highly the strongest inhibitor of xanthine oxidation, while the most potent effects on 6MP oxidation were produced by DIO, API, and CHE (the IC_{50} values of these flavonoids were lower than 100 nM).

We cannot directly extrapolate our in vitro data; however, based on the previously reported investigations, we may estimate the *in vivo* importance of flavonoid-XO interactions. Based on earlier studies, the *in vivo* effects of flavonoids on xanthine oxidation are controversial. The orally administered API (175–700 mg/kg) [35], LUT (16–100 mg/kg) and LUT-7-*O*-glucoside (50 and 100 mg/kg) [36] did not affect the serum uric acid levels in hyperuricaemic mice. However, in the latter study, LUT (50 mg/kg) induced a slight but significant decrease in uric acid levels after *i.p.* administration [36]. In another study, after *per os* treatment, API (50 and 100 mg/kg), KAE (50 and 100 mg/kg), and LUT (100 mg/kg) significantly decreased serum uric acid concentrations in hyperuricemic mice, and KAE also decreased uric acid levels in normal mice [37]. Only limited clinical data are available, however, the human studies with quercetin suggest its negligible antihyperuricemic effects [38–40]. Even the extremely high intake of flavonoids (more hundreds of milligrams to few grams) can lead to approximately ten-fold lower total peak plasma concentrations (flavonoids and their conjugated metabolites jointly) vs. allopurinol and oxipurinol together [13,41–43]. Because the inhibitory action of flavonoids on xanthine oxidation is similar to allopurinol (Table 1), it seems to be unlikely that the considerably lower levels of flavonoids can induce similar antihyperuricemic effects to allopurinol. However, some of the flavonoids tested (API, CHE, CHR, DIO, KAE, and LUT) exerted 5- to 40-fold stronger inhibitory effect on XO-catalyzed 6MP oxidation than allopurinol (Table 1), suggesting that even the significantly lower levels of flavonoids (vs. allopurinol/oxipurinol) may affect the elimination of 6MP. Because the simultaneous administration of the conventional therapeutic doses of 6MP and allopurinol can cause serious myelosuppression [22], the potential *in vivo* interaction of flavonoids with 6MP may have high pharmacological/toxicological importance.

Considering the above-listed observations, the possible extremely high intake of flavonoids (e.g., through the consumption of dietary supplements containing several hundreds of milligrams or even more grams of pure aglycones [3,44]) may interfere with the elimination of 6MP. Therefore, it is reasonable to perform *in vivo* studies in the near future to accept or reject this hypothesis.

4. Materials and Methods

4.1. Reagents

Xanthine oxidase (XO; from bovine milk), xanthine, uric acid, 6-mercaptopurine (6MP), allopurinol, apigenin (API), chrysin (CHR), diosmetin (DIO), fisetin (FIS), and kaempferol (KAE) were purchased from Sigma-Aldrich (St. Louis, MO, United States). Luteolin (LUT), geraldol (GER), and chrysoeriol (CHE) were obtained from Extrasynthese (Genay Cedex, France). Chrysin-7-glucuronide (C7G) and 6-thiouric acid were purchased from Carbosynth (Berkshire, UK). Chrysin-7-sulfate (C7S) was synthetized as described [44,45]. Stock solutions of flavonoids (each 2 mM) were prepared in dimethyl sulfoxide (DMSO) and stored at −20 °C.

4.2. XO Assays

To test the inhibitory effects of flavonoids and their metabolites on the XO-catalyzed oxidation of xanthine and 6MP, the previously reported methods were applied without modifications [19]. In both assays, allopurinol was applied as positive control. In each experiment, solvent controls (DMSO) were used. Metabolite formation (% of control) was plotted vs. the inhibitor concentrations in decimal logarithmic scale. IC_{50} values were evaluated by sigmoidal fitting, employing GraphPad Prism 8 software (San Diego, CA, USA).

4.3. HPLC Analyses

After the in vitro XO assays, xanthine and uric acid as well as 6MP and 6-thiouric acid were quantified by the HPLC-UV methods described in our previous report, without any modifications [19].

4.4. Statistics

Figures and table represent means and standard error of the mean (SEM) values (at least from three independent experiments). Statistical differences were analyzed ($p < 0.05$ and $p < 0.01$) employing one-way ANOVA, using Tukey's post-hoc test (IBM SPSS Statistics; Armonk, NY, USA).

Author Contributions: M.P. and V.M. conceived the study and wrote the paper. V.M. performed XO assays, E.F.-N. carried out HPLC analyses. Conceptualization, V.M. and M.P.; Formal analysis, V.M. and E.F.-N.; Funding acquisition, M.P.; Investigation, V.M., E.F.-N. and M.P.; Methodology, V.M., E.F.-N. and M.P.; Supervision, M.P.; Writing—original draft, V.M. and M.P. All authors have read and agreed to the published version of the manuscript.

Funding: The project has been supported by the European Union, co-financed by the European Social Fund (EFOP-3.6.1.-16-2016-00004).

Acknowledgments: The authors thank to Katalin Fábián and Boglárka Gombor for their excellent assistance in the experimental work, and to Balázs Bognár for providing chrysin-7-sulfate for the experiments.

Conflicts of Interest: The authors declare no conflict of interest.

Abbreviations

6MP	6-mercaptopurine
API	Apigenin
APU	Allopurinol
C7G	Chrysin-7-glucuronide
C7S	Chrysin-7-sulfate
CHE	Chrysoeriol
CHR	Chrysin
COMT	Catechol-*O*-methyltransferase
DIO	Diosmetin
DMSO	Dimethyl sulfoxide
FIS	Fisetin
GER	Geraldol
HPLC	High-performance liquid chromatography
KAE	Kaempferol
LUT	Luteolin
SEM	Standard error of the mean
SULT	Sulfotransferase
UGT	Uridine diphosphate glucuronosyltransferase
XO	Xanthine oxidase

References

1. Cook, N.C.; Samman, S. Flavonoids—Chemistry, metabolism, cardioprotective effects, and dietary sources. *J. Nutr. Biochem.* **1996**, *7*, 66–76. [CrossRef]
2. Nijveldt, R.J.; Van Nood, E.; Van Hoorn, D.E.C.; Boelens, P.G.; Van Norren, K.; Van Leeuwen, P.A.M. Flavonoids: A review of probable mechanisms of action and potential applications. *Am. J. Clin. Nutr.* **2001**, *74*, 418–425. [CrossRef]
3. Vida, R.G.; Fittler, A.; Somogyi-Végh, A.; Poór, M. Dietary quercetin supplements: Assessment of online product informations and quantitation of quercetin in the products by high-performance liquid chromatography. *Phytother. Res.* **2019**, *33*, 1912–1920. [CrossRef] [PubMed]
4. Manach, C.; Donovan, J.L. Pharmacokinetics and Metabolism of Dietary Flavonoids in Humans. *Free Radic. Res.* **2004**, *38*, 771–785. [CrossRef] [PubMed]

5. Chen, Z.; Zheng, S.; Li, L.; Jiang, H. Metabolism of Flavonoids in Human: A Comprehensive Review. *Curr. Drug Metab.* **2014**, *15*, 48–61. [CrossRef] [PubMed]
6. Wang, L.; Morris, M.E. Liquid chromatography–tandem mass spectroscopy assay for quercetin and conjugated quercetin metabolites in human plasma and urine. *J. Chromatogr.* **2005**, *821*, 194–201. [CrossRef] [PubMed]
7. Mullen, W.; Edwards, C.A.; Crozier, A. Absorption, Excretion and Metabolite Profiling of Methyl-, Glucuronyl-, Glucosyl- and Sulpho-Conjugates of Quercetin in Human Plasma and Urine After Ingestion of Onions. *Br. J. Nutr.* **2006**, *96*, 107–116. [CrossRef]
8. Walle, T.; Otake, Y.; Brubaker, J.A.; Walle, U.K.; Halushka, P.V. Disposition and metabolism of the flavonoid chrysin in normal volunteers. *Br. J. Clin. Pharmacol.* **2001**, *51*, 143–146. [CrossRef]
9. Khan, N.; Syed, D.N.; Ahmad, N.; Mukhtar, H. Fisetin: A Dietary Antioxidant for Health Promotion. *Antioxid. Redox Signal.* **2013**, *19*, 151–162. [CrossRef]
10. Touil, Y.S.; Auzeil, N.; Boulinguez, F.; Saighi, H.; Regazzetti, A.; Scherman, D.; Chabot, G.G. Fisetin disposition and metabolism in mice: Identification of geraldol as an active metabolite. *Biochem. Pharmacol.* **2011**, *82*, 1731–1739. [CrossRef]
11. Chen, Z.; Chen, M.; Pan, H.; Sun, S.; Li, L.; Zeng, S.; Jiang, H. Role of Catechol-O-Methyltransferase in the Disposition of Luteolin in Rats. *Drug Metab. Dispos.* **2011**, *39*, 667–674. [CrossRef] [PubMed]
12. Chen, Z.J.; Dai, Y.Q.; Kong, S.S.; Song, F.F.; Li, L.P.; Ye, J.F.; Wang, R.W.; Zeng, S.; Zhou, H.; Jiang, H.D. Luteolin is a rare substrate of human catechol-O-methyltransferase favoring a para-methylation. *Mol. Nutr. Food Res.* **2013**, *57*, 877–885. [CrossRef] [PubMed]
13. Campanero, M.A.; Escolar, M.; Perez, G.; Garcia-Quetglas, E.; Sadaba, B.; Azanza, J.R. Simultaneous determination of diosmin and diosmetin in human plasma by ion trap liquid chromatography–atmospheric pressure chemical ionization tandem mass spectrometry: Application to a clinical pharmacokinetic study. *J. Pharmac. Biomed. Anal.* **2010**, *51*, 875–881. [CrossRef] [PubMed]
14. Khan, A.U.; Gilani, A.H. Selective bronchodilatory effect of Rooibos tea (Aspalathus linearis) and its flavonoid, chrysoeriol. *Eur. J. Nutr.* **2006**, *45*, 463–469. [CrossRef] [PubMed]
15. Choi, D.Y.; Lee, J.Y.; Kim, M.R.; Woo, E.R.; Kim, Y.G.; Kang, K.W. Chrysoeriol potently inhibits the induction of nitric oxide synthase by blocking AP-1 activation. *J. Biomed. Sci.* **2005**, *12*, 949–959. [CrossRef]
16. Wong, E.; Francis, C.M. Flavonoids in genotypes of Trifolium subterraneum—I: The normal flavonoid pattern of the Geraldton variety. *Phytochemistry* **1968**, *7*, 2123–2129. [CrossRef]
17. Gupta, S.R.; Ravindranath, B.; Seshadri, T.R. Synthesis of some flavonoid glucosides of trifolium subterraneum. *Phytochemistry* **1971**, *10*, 877–882. [CrossRef]
18. Day, R.O.; Graham, G.G.; Hicks, M.; McLachlan, A.J.; Stocker, S.L.; Williams, K.M. Clinical Pharmacokinetics and Pharmacodynamics of Allopurinol and Oxypurinol. *Clin. Pharmacokinet.* **2007**, *46*, 623–644. [CrossRef]
19. Mohos, V.; Pánovics, A.; Fliszár-Nyúl, E.; Schilli, G.; Hetényi, C.; Mladěnka, P.; Needs, P.W.; Kroon, P.A.; Pethő, G.; Poór, M. Inhibitory Effects of Quercetin and Its Human and Microbial Metabolites on Xanthine Oxidase Enzyme. *Int. J. Mol. Sci.* **2019**, *20*, 2681. [CrossRef]
20. Galbusera, C.; Orth, P.; Fedida, D.; Spector, T. Superoxide radical production by allopurinol and xanthine oxidase. *Biochem. Pharmacol.* **2006**, *71*, 1747–1752. [CrossRef]
21. Leong, R.W.; Gearry, R.B.; Sparrow, M.P. Thiopurine hepatotoxicity in inflammatory bowel disease: The role for adding allopurinol. *Expert Opin. Drug Saf.* **2008**, *7*, 607–616. [CrossRef]
22. McLeod, H.L. Clinically relevant drug–drug interactions in oncology. *Br. J. Clin. Pharmacol.* **1998**, *45*, 539–544. [CrossRef] [PubMed]
23. Nagao, A.; Seki, M.; Kobayashi, H. Inhibition of Xanthine Oxidase by Flavonoids. *Biosci. Biotechnol. Biochem.* **1999**, *63*, 1787–1790. [CrossRef] [PubMed]
24. Lin, S.; Zhang, G.; Liao, Y.; Pan, J. Inhibition of chrysin on xanthine oxidase activity and its inhibition mechanism. *Int. J. Biol. Macromol.* **2015**, *81*, 274–282. [CrossRef] [PubMed]
25. Lin, S.; Zhang, G.; Liao, Y.; Pan, J.; Gong, D. Dietary Flavonoids as Xanthine Oxidase Inhibitors: Structure–Affinity and Structure–Activity Relationships. *J. Agric. Food Chem.* **2015**, *63*, 7784–7794. [CrossRef]
26. Cos, P.; Ying, L.; Calomme, M.; Hu, J.P.; Cimanga, K.; Van Poel, B.; Pieters, L.; Vlietinck, A.J.; Vanden Berghe, D. Structure–Activity Relationship and Classification of Flavonoids as Inhibitors of Xanthine Oxidase and Superoxide Scavengers. *J. Nat. Prod.* **1998**, *61*, 71–76. [CrossRef]

27. Van Hoorn, D.E.C.; Nijveldt, R.J.; Van Leeuwen, P.A.M.; Hofman, Z.; M'Rabet, L.; De Bont, D.B.A.; Van Norren, K. Accurate prediction of xanthine oxidase inhibition based on the structure of flavonoids. *Eur. J. Pharmacol.* **2002**, *451*, 111–118. [CrossRef]
28. Lin, C.M.; Chen, C.S.; Chen, C.T.; Liang, Y.C.; Lin, J.K. Molecular modeling of flavonoids that inhibits xanthine oxidase. *Biochem. Biophys. Res. Commun.* **2002**, *294*, 167–172. [CrossRef]
29. Iio, M.; Moriyama, A.; Matsumoto, Y.; Takaki, N.; Fukumoto, M. Inhibition of Xanthine Oxidase by Flavonoids. *Agric. Biol. Chem.* **1985**, *49*, 2173–2176. [CrossRef]
30. Cimanga, K.; De Bruyne, T.; Hu, J.P.; Cos, P.; Apers, S.; Pieters, L.; Tona, L.; Kambu, K.; Vanden Berghe, D.; Vlietinck, A.J. Constituents from Morinda morindoides Leaves as Inhibitors of Xanthine Oxidase and Scavengers of Superoxide Anions. *Pharm. Pharmacol. Commun.* **1999**, *5*, 419–424. [CrossRef]
31. Hayashi, T.; Sawa, K.; Kawasaki, M.; Arisawa, M.; Shimizu, M.; Morita, N. Inhibition of cow's milk xanthine oxidase by flavonoids. *J. Nat. Prod.* **1988**, *51*, 345–348. [CrossRef] [PubMed]
32. Nguyen, M.T.T.; Awale, S.; Tezuka, Y.; Ueda, J.; Tran, Q.L.; Kadota, S. Xanthine Oxidase Inhibitors from the Flowers of Chrysanthemum sinense. *Planta Med.* **2006**, *72*, 46–51. [CrossRef] [PubMed]
33. Qu, L.; Ruan, J.Y.; Jin, L.J.; Shi, W.Z.; Li, X.X.; Han, L.F.; Zhang, Y.; Wang, T. Xanthine oxidase inhibitory effects of the constituents of Chrysanthemum morifolium stems. *Phytochem. Lett.* **2017**, *19*, 39–45. [CrossRef]
34. Day, A.J.; Bao, Y.; Morgan, M.R.; Williamson, G. Conjugation position of quercetin glucuronides and effect on biological activity. *Free Radic. Biol. Med.* **2000**, *29*, 1234–1243. [CrossRef]
35. Huang, J.; Wang, S.; Zhu, M.; Chen, J.; Zhu, X.; Chen, J.; Zhu, X. Effects of Genistein, Apigenin, Quercetin, Rutin and Astilbin on serum uric acid levels and xanthine oxidase activities in normal and hyperuricemic mice. *Food Chem. Toxicol.* **2011**, *49*, 1943–1947. [CrossRef] [PubMed]
36. Sarawek, S.; Feistel, B.; Pischel, I.; Butterweck, V. Flavonoids of Cynara scolymus Possess Potent Xanthinoxidase Inhibitory Activity in vitro but are Devoid of Hypouricemic Effects in Rats after Oral Application. *Planta Med.* **2008**, *74*, 221–227. [CrossRef]
37. Mo, S.F.; Zhou, F.; Lv, Y.Z.; Hu, Q.H.; Zhang, D.M.; Kong, L.D. Hypouricemic Action of Selected Flavonoids in Mice: Structure–Activity Relationships. *Biol. Pharm. Bull.* **2007**, *30*, 1551–1556. [CrossRef]
38. Abbey, E.L.; Rankin, J.W. Effect of quercetin supplementation on repeated-sprint performance, xanthine oxidase activity, and inflammation. *Int. J. Sport Nutr. Exerc. Metab.* **2011**, *21*, 91–96. [CrossRef]
39. Boots, A.W.; Drent, M.; De Boer, V.C.; Bast, A.; Haenen, G.R. Quercetin reduces markers of oxidative stress and inflammation in sarcoidosis. *Clin. Nutr.* **2011**, *30*, 506–512. [CrossRef]
40. Shi, Y.; Williamson, G. Quercetin lowers plasma uric acid in pre-hyperuricaemic males: A randomised, double-blinded, placebo-controlled, cross-over trial. *Br. J. Nutr.* **2016**, *115*, 800–806. [CrossRef]
41. Cao, J.; Zhang, Y.; Chen, W.; Zhao, X. The relationship between fasting plasma concentrations of selected flavonoids and their ordinary dietary intake. *Br. J. Nutr.* **2010**, *103*, 249–255. [CrossRef] [PubMed]
42. Conquer, J.A.; Maiani, G.; Azzini, E.; Raguzzini, A.; Holub, B.J. Supplementation with Quercetin Markedly Increases Plasma Quercetin Concentration without Effect on Selected Risk Factors for Heart Disease in Healthy Subjects. *J. Nutr.* **1998**, *128*, 593–597. [CrossRef] [PubMed]
43. Turnheim, K.; Krivanek, P.; Oberbauer, R. Pharmacokinetics and pharmacodynamics of allopurinol in elderly and young subjects. *Br. J. Clin. Pharmacol.* **1999**, *48*, 501–509. [CrossRef] [PubMed]
44. Mohos, V.; Fliszár-Nyúl, E.; Schilli, G.; Hetényi, C.; Lemli, B.; Kunsági-Máté, S.; Bognár, B.; Poór, M. Interaction of Chrysin and Its Main Conjugated Metabolites Chrysin-7-Sulfate and Chrysin-7-Glucuronide with Serum Albumin. *Int. J. Mol. Sci.* **2018**, *19*, 4073. [CrossRef]
45. Huang, W.H.; Lee, A.R.; Yang, C.H. Antioxidative and anti-inflammatory activities of polyhydroxyflavonoids of Scutellaria baicalensis GEORGI. *Biosci. Biotechnol. Biochem.* **2006**, *70*, 2371–2380. [CrossRef]

1521-009X/48/10/1064–1073$35.00
Drug Metabolism and Disposition

https://doi.org/10.1124/dmd.120.000085
Drug Metab Dispos 48:1064–1073, October 2020

Special Section on Natural Products: Experimental Approaches to Elucidate Disposition Mechanisms and Predict Pharmacokinetic Drug Interactions

Effects of Chrysin and Its Major Conjugated Metabolites Chrysin-7-Sulfate and Chrysin-7-Glucuronide on Cytochrome P450 Enzymes and on OATP, P-gp, BCRP, and MRP2 Transporters

Violetta Mohos, Eszter Fliszár-Nyúl, Orsolya Ungvári, Éva Bakos, Katalin Kuffa, Tímea Bencsik, Balázs Zoltán Zsidó, Csaba Hetényi, Ágnes Telbisz, Csilla Özvegy-Laczka, and Miklós Poór

Department of Pharmacology, Faculty of Pharmacy (V.M., E.F.-N., M.P.), János Szentágothai Research Centre (V.M., E.F.-N., M.P.), Department of Pharmacognosy, Faculty of Pharmacy (T.B.), and Department of Pharmacology and Pharmacotherapy, Medical School (B.Z.Z., C.H.), University of Pécs, Pécs, Hungary; and Membrane Protein Research Group (O.U., É.B., C.Ö.-L.) and Biomembrane Research Group (K.K., Á.T.), Institute of Enzymology, Research Centre for Natural Sciences, Budapest, Hungary

Received April 17, 2020; accepted July 1, 2020

ABSTRACT

Chrysin is an abundant flavonoid in nature, and it is also contained by several dietary supplements. Chrysin is highly biotransformed in the body, during which conjugated metabolites chrysin-7-sulfate and chrysin-7-glucuronide are formed. These conjugates appear at considerably higher concentrations in the circulation than the parent compound. Based on previous studies, chrysin can interact with biotransformation enzymes and transporters; however, the interactions of its metabolites have been barely examined. In this in vitro study, the effects of chrysin, chrysin-7-sulfate, and chrysin-7-glucuronide on cytochrome P450 enzymes (2C9, 2C19, 3A4, and 2D6) as well as on organic anion-transporting polypeptides (OATPs; 1A2, 1B1, 1B3, and 2B1) and ATP binding cassette [P-glycoprotein, multidrug resistance–associated protein 2, and breast cancer resistance protein (BCRP)] transporters were investigated. Our observations revealed that chrysin conjugates are strong inhibitors of certain biotransformation enzymes (e.g., CYP2C9) and transporters (e.g., OATP1B1, OATP1B3, OATP2B1, and BCRP) examined. Therefore, the simultaneous administration of chrysin-containing dietary supplements with medications needs to be carefully considered due to the possible development of pharmacokinetic interactions.

SIGNIFICANCE STATEMENT

Chrysin-7-sulfate and chrysin-7-glucuronide are the major metabolites of flavonoid chrysin. In this study, we examined the effects of chrysin and its conjugates on cytochrome P450 enzymes and on organic anion-transporting polypeptides and ATP binding cassette transporters (P-glycoprotein, breast cancer resistance protein, and multidrug resistance–associated protein 2). Our results demonstrate that chrysin and/or its conjugates can significantly inhibit some of these proteins. Since chrysin is also contained by dietary supplements, high intake of chrysin may interrupt the transport and/or the biotransformation of drugs.

Introduction

Flavonoids are natural phenolic compounds in many edible plants, exerting some beneficial health effects (Kumar and Pandey, 2013). Flavonoids are rapidly biotransformed in the body; typically their metabolites reach high concentrations in the systemic circulation (and likely in some tissues) (Manach et al., 2005). As previous studies demonstrated, flavonoids can interfere with the pharmacokinetics of simultaneously administered drugs due to interaction with biotransformation enzymes and drug transporters (Miron et al., 2017; Vida et al., 2019). Chrysin (5,7-dihydroxyflavone; Fig. 1) is a flavone aglycone that appears in some plants, honey, and propolis (Siess et al., 1996). Despite the absence of clear human evidence, chrysin-containing dietary supplements are advertised to treat depression, anxiety, hypertension, and even cancer (Mohos et al., 2018a). Furthermore, chrysin is used to

This work was supported by the New National Excellence Program of the Ministry for Innovation and Technology [ÚNKP-18-4 to M.P. and ÚNKP-19-3-IV-PTE-164 to E.F.-N.]. The project was founded by the European Union and cofinanced by the European Social Fund [EFOP-3.6.1.-16-2016-00004 to M.P., V.M., and E.F.-N.] and by the National Research, Development, and Innovation Office [OTKA FK 128751 to C.Ö.-L.; K123836 to C.H. and B.Z.Z.].
https://doi.org/10.1124/dmd.120.000085.

ABBREVIATIONS: ABC, ATP binding cassette; BCRP, breast cancer resistance protein; C7G, chrysin-7-glucuronide; C7S, chrysin-7-sulfate; CDCF, 5(6)-carboxy-2′,7′-dichlorofluorescein; HPLC, high-performance liquid chromatography; LY, lucifer yellow; MRP2, multidrug resistance–associated protein 2; NMQ, *N*-methyl-quinidine; OATP, organic anion-transporting polypeptide; P-gp, P-glycoprotein; CYP, cytochrome P450; PDB, Protein Data Bank; RMSD, root mean squared deviation.

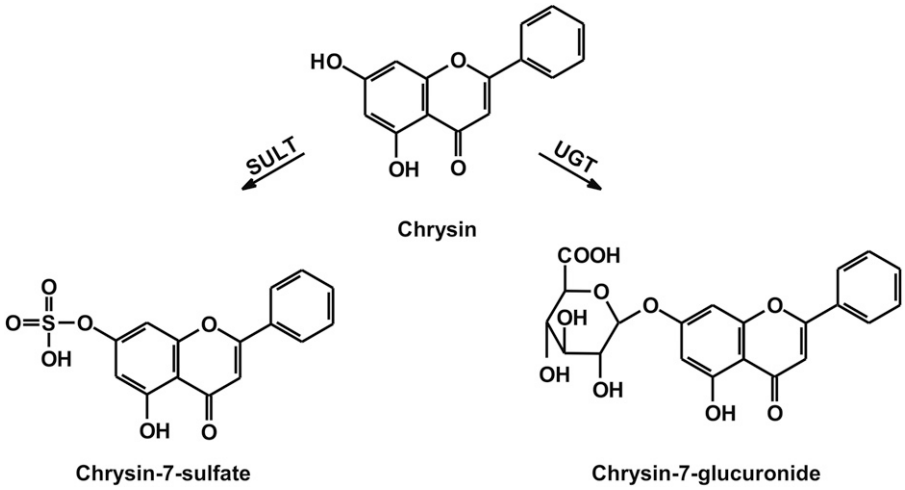

Fig. 1. Chemical structures of chrysin, chrysin-7-sulfate, and chrysin-7-glucuronide. SULT, sulfotransferase; UGT, uridine 5′-diphospho-glucuronosyltransferase.

maintain testosterone levels since it inhibits the aromatase enzyme (Kao et al., 1998). Many dietary supplements contain chrysin as their active ingredient. Some of the marketed tablets and capsules include 500 mg or even higher amounts of the aglycone, and the recommended daily dose can even be 1–2 g based on the description of the manufacturers (Mohos et al., 2018a).

Chrysin has low oral bioavailability because of its significant presystemic metabolism to chrysin-7-sulfate (C7S) and chrysin-7-glucuronide (C7G) in enterocytes and hepatocytes by sulfotransferase and uridine 5′-diphospho-glucuronosyltransferase enzymes, respectively (Galijatovic et al., 1999; Walle et al., 2001; Ge et al., 2015). Only limited data are available regarding the pharmacokinetics of chrysin in humans. Walle et al. (2001) reported that after the oral administration of a 400-mg single dose of chrysin to healthy human subjects, peak plasma concentration of the parent compound was only 16–63 nM, whereas C7S appeared approximately at 400–800 nM concentrations in the circulation. In rodent experiments, peak plasma concentrations of C7S and C7G were also considerably higher than that of chrysin (Ge et al., 2015; Noh et al., 2016; Dong et al., 2017). In mice, the 20 mg/kg oral dose of chrysin caused 10, 130, and 160 nM peak plasma concentrations of chrysin, C7S and C7G, respectively (Ge et al., 2015). After the oral administration of 30 and 100 mg/kg chrysin to rats, C_{max} values of C7G were approximately 750 nM (Dong et al., 2017) and 850 nM (Noh et al., 2016), respectively. In the latter study, micromolar concentrations of C7G also appeared in some rodents. Animal studies suggest the potential involvement of multidrug resistance–associated protein 2 (MRP2) and breast cancer resistance protein (BCRP) transporters in the disposition (e.g., biliary excretion) of chrysin and/or its conjugates (Walle et al., 2001; Ge et al., 2015), and the pharmacokinetic interactions of chrysin with some compounds due to the inhibition of cytochrome P450 (CYP) enzymes or BCRP were also reported (Wang and Morris, 2007; Kawase et al., 2009; Noh et al., 2016; Pingili et al., 2019).

The CYP enzyme superfamily plays an important role in the biotransformation of drugs and xenobiotics (McDonnell and Dang, 2013). Based on in vitro studies, chrysin is a potent inhibitor of some CYP enzymes, including CYP2C9 and 3A4 (Ho et al., 2001; Tsujimoto et al., 2009; Kimura et al., 2010; Noh et al., 2016). Since CYP-catalyzed oxidation is the major elimination route of several drugs, inhibitors of these enzymes can interfere with the pharmacokinetics of medications.

Organic anion-transporting polypeptides (OATPs) are membrane transporters that mediate the uptake of large organic anions and amphipatic molecules, including steroid and thyroid hormones, bile acids, and bilirubin. Among these polyspecific OATPs, OATP1B1 and OATP1B3 are exclusively expressed in hepatocytes (König et al., 2000) and are considered key determinants in the hepatic uptake of numerous drugs (Shitara et al., 2013; Durmus et al., 2016). The ubiquitously expressed OATP1A2 and OATP2B1 are also polyspecific transporters. They influence hepatic (OATP2B1), intestinal (OATP1A2 and OATP2B1), and central nervous system uptake (OATP1A2 and OATP2B1) of their substrates (Urquhart and Kim, 2009; Nakanishi and Tamai, 2012; Shitara et al., 2013). OATPs commonly play a key role in the absorption, tissue distribution, and elimination of drugs. Therefore, their inhibition may result in the altered pharmacokinetics of simultaneously administered medications.

Human ATP binding cassette (ABC) drug transporters, expressed in important tissue barriers, also play a significant role in the elimination and tissue distribution of drugs, toxic compounds, or metabolites. P-glycoprotein (P-gp)/ABCB1, BCRP/ABCG2, and MRP2/ABCC2 multidrug transporters form together an effective defense system in the canalicular surface of hepatocytes (Sarkadi et al., 2006; Szakács et al., 2008; Marquez and Van Bambeke, 2011; Wlcek and Stieger, 2014; Jetter and Kullak-Ublic, 2020). Previous publications revealed that flavonoids, including chrysin, are inhibitors of certain ABC transporters, and some flavonoids are also substrates of these transporters (Walle et al., 1999; Zhang et al., 2004; Morris and Zhang, 2006; Alvarez et al., 2010; Schumacher et al., 2010; Tran et al., 2011). Flavonoid conjugates can also be transported by ABC transporters, as was concluded in a few reports for BCRP and MRP2 (Walle et al., 1999; Ge et al., 2015; Li et al., 2015).

In this study, the interactions of chrysin and its major metabolites (C7S and C7G) were investigated with CYP (2C9, 2C19, 3A4, and 2D6) enzymes and with drug transporters (OATPs, P-gp, MRP2, and BCRP), employing in vitro assays. Our results demonstrate that both the aglycone and its conjugates are potent inhibitors of some CYP enzymes and drug transporters tested, which underlines the potential pharmacokinetic interactions of chrysin with drugs or endogenous substrates.

Materials and Methods

Reagents. Chrysin; testosterone; 6β-hydroxytestosterone; ketoconazole; sulfaphenazole; ticlopidine hydrochloride; quinidine; CypExpress 2C9, 2C19, 3A4 and 2D6 human kits; FBS; glutamine; penicillin; streptomycin; pyranine (trisodium 8-hydroxypyrene-1,3,6-trisulfonate); bromosulfophthalein; sulforhodamine 101; sodium orthovanadate; probenecid; verapamil; 5(6)-carboxy-2′,7′-dichlorofluorescein (CDCF); lucifer yellow (LY); and benzbromarone were purchased from Sigma-Aldrich (St. Louis, MO). C7G, diclofenac, 4′-hydroxydiclofenac, *S*-mephenytoin, 4-hydroxymephenytoin, dextromethorphan,

and dextrorphan were obtained from Carbosynth (Berkshire, UK). *N*-methylquinidine (NMQ) and Ko143 were purchased from Solvo Biotechnology (Budaörs, Hungary) and Tocris Bioscience (Bristol, UK), respectively. C7S was synthetized as previously described (Huang et al., 2006; Mohos et al., 2018a).

CYP Assays. Inhibition of CYP enzymes were tested in vitro, using CypExpress Cytochrome P450 human kits. The US Food and Drug Administration–recommended substrates (CYP2C9: diclofenac, CYP2C19: *S*-mephenytoin, CYP3A4: testosterone, CYP2D6: dextromethorphan) and positive controls (CYP2C9: sulfaphenazole, CYP2C19: ticlopidine, CYP3A4: ketoconazole, CYP2D6: quinidine) were applied. Chrysin, C7S, and C7G were dissolved in DMSO (that did not exceed 0.6% in samples); solvent controls were also applied.

Inhibitory effects of chrysin, C7S, and C7G on CYP2C9 (Mohos et al., 2020), CYP2C19 (Fliszár-Nyúl et al., 2019), and CYP3A4 (Mohos et al., 2018b) enzymes were investigated as has been reported, without modifications. Inhibition of CYP2D6 enzyme by chrysin and its conjugates was examined based on their effects on CYP2D6-catalyzed *O*-demethylation of dextromethorphan. Incubations were performed with 5 μM dextromethorphan and 10 mg/ml CypExpress 2D6 kit (containing glucose-6-phosphate dehydrogenase), $NADP^+$ (200 μM), and glucose-6-phosphate barium salt (500 μM) in the presence of chrysin, C7S, or C7G (0–30 μM) in 0.05 M potassium phosphate buffer (pH 7.5; final volume of incubates: 200 μl). Assays were started with the addition of the enzyme and stopped with 100 μl ice-cold methanol. Samples were incubated in a thermomixer (20 minutes, 600 rpm, 30°C). After centrifugation (10 minutes, 14,000*g*, room temperature), the concentrations of dextromethorphan and dextrorphan were directly analyzed from the supernatants with high-performance liquid chromatography (HPLC; see *HPLC Analyses*). To determine IC_{50} values, metabolite formation (% of control) was plotted as the function of the concentrations of inhibitors in a decimal logarithmic scale; then data were evaluated using GraphPad Prism 8 software (Graph Pad, La Jolla, CA).

HPLC Analyses. Substrates and products of CYP enzymes were separated and quantified employing the HPLC system built up by a Waters 510 pump (Milford, MA), a Rheodyne 7125 injector (Berkeley, CA) with a 20-μl sample loop, and a Waters 486 UV detector. Chromatograms were evaluated applying Waters Millennium Chromatography Manager.

To quantify substrates and products in CYP2C9, 2C19, and 3A4 assays, the previously described HPLC methods were applied without modifications (Mohos et al., 2018b; Fliszár-Nyúl et al., 2019). Regarding the CYP2D6 assay, dextromethorphan and dextrorphan were quantified employing a Phenomenex Security Guard (C8, 4.0 × 3.0 mm; Torrance, CA) guard cartridge linked to a Teknokroma Mediterranea Sea8 (C8, 150 × 4.6 mm, 5 μm; Barcelona, Spain) analytical column. The mobile phase contained 6.9 mM sodium acetate buffer (pH 4.0) and acetonitrile (69:31 v/v%). The isocratic elution was performed at 1.0 ml/min flow rate at room temperature; dextromethorphan and dextrorphan were detected at 280 nm. This HPLC method was suitable for the separation and quantification of the substrate and the product in the presence of chrysin and C7S; however, C7G coeluted with dextrorphan. Therefore, the analyses of incubates with C7G was carried out with a modified eluent, containing 6.9 mM sodium acetate buffer (pH 4.0) and acetonitrile (72:28 v/v%). Other chromatographic parameters remained unchanged.

Modeling Studies. Ligand structures of chrysin and C7S were built in Maestro (https://www.schrodinger.com/maestro) and energy-minimized with a quantum chemistry program package, MOPAC (Stewart, 1990), with a PM7 parametrization (Stewart, 2013) and a gradient norm set to 0.001. Force calculations were also performed using MOPAC; the force constant matrices were positive definite. Gasteiger-Marsilli partial charges were assigned in AutoDock Tools (Morris et al., 2009). Flexibility was allowed on the ligand at all active torsions. These prepared structures were used for docking.

Atomic coordinates of the target structures were obtained from the Protein Data Bank (PDB; retrieved November 18, 2019). For CYP2C9 only one apo structure (PDB code 1og2) was available and used as a target. The holo structure for CYP2C9 (PDB code: 1og5) was applied to extract the binding mode of *S*-warfarin for comparison as a reference. For CYP2C19, the only available structure was a cytochrome target (PDB code: 4gqs) in complex with (4-hydroxy-3,5-dimethylphenyl)(2-methyl-1-benzofuran-3-yl)methanone (CYP2C19 reference ligand). Atomic partial charges of heme were adopted as the ferric penta coordinate high spin charge model from reference (Shahrokh et al., 2012). The rest of the target molecules were equipped with polar hydrogen atoms and Gasteiger-Marsilli partial charges in AutoDock Tools.

Ligand structures were docked to the active site of the targets using AutoDock 4.2.6 (Morris et al., 2009). The number of grid points was set to 90 × 90 × 90 at a 0.375 Å grid spacing. Lamarckian genetic algorithm was used for global search, with the flexibility of all active torsions allowed on the ligand (Hetényi and van der Spoel, 2006). Ten docking runs were performed, and the resulted ligand conformations were ranked according to their calculated binding free energy values. Representative docked ligand conformations were used for subsequent evaluations and collection of the interacting target amino acid residues with a 3.500 Å cutoff distance calculated for heavy atoms. Root mean squared deviation (RMSD) values were calculated between the crystallographic and representative ligand conformations, if available.

OATP Overexpressing Cell Lines and OATP Interaction Tests. A431 cells overexpressing human OATPs, 1A2, 1B1, 1B3 or 2B1, or their mock transfected controls were generated as previously described (Patik et al., 2018; Bakos et al., 2020). Briefly, overexpression of OATP2B1 was achieved by transposase-mediated genetic insertion of the OATP2B1 cDNA (BC041095.1, HsCD00378878), followed by puromycin selection (1 μg/ml for 2 weeks). Regarding OATPs 1A2 (BC042452, HsCD00333163), 1B1 (Gene identifier: AB026257), and 1B3 (BC141525, HsCD00348132), overexpression was achieved by lentiviral transduction. To achieve maximal OATP expression, cells were further sorted based on Live/Dead Green uptake (Patik et al., 2018; Bakos et al., 2020). OATP expression was continuously monitored by functional measurements. Cells were used for maximum 10 passages until protein expression was stable. Cells were cultured in Dulbecco's modified Eagle's medium (Thermo Fischer Scientific, Waltham, MA) supplemented with 10% fetal bovine serum, 2 mM L-glutamine, 100 U/ml penicillin, and 100 μg/ml streptomycin, at 37°C with 5% CO_2.

The interaction between chrysin and its conjugates was investigated in an indirect assay (Patik et al., 2018) employing two recently described fluorescent dye substrates, pyranine and sulforhodamine 101 (Bakos et al., 2020; Székely et al., 2020) as an indicator of OATPs' function. Briefly, A431 cells overexpressing OATPs, 1A2, 1B1, 1B3, or 2B1 or their mock transfected controls (Patik et al., 2018) were seeded on 96-well plates in a density of 8×10^4 cells per well in 200 μl Dulbecco's modified Eagle's medium 1 day prior to the transport measurements. Next day, the medium was removed, and the cells were washed three times with 200 μl PBS (pH 7.4) and preincubated with 50 μl uptake buffer (125 mM NaCl, 4.8 mM KCl, 1.2 mM $CaCl_2$, 1.2 mM KH_2PO_4, 12 mM $MgSO_4$, 25 mM MES [2-(*N*-morpholino)ethanesulfonic acid and 5.6 mM glucose, pH 5.5] with or without increasing concentrations of bromosulfophthalein (as a reference inhibitor), chrysin, C7S, or C7G at 37°C. Each test compound was dissolved in DMSO (that did not exceed 0.5% in samples); solvent controls were also applied. The reaction was started by the addition of 50 μl uptake buffer containing pyranine in a final concentration of 10 μM (OATP1B1) or 20 μM (OATP1B3 and OATP2B1) or 0.5 μM sulforhodamine 101 (OATP1A2). Thereafter, cells were incubated at 37°C for 15 minutes (OATP1B1 and OATP2B1), 10 minutes (OATP1A2), or 30 minutes (OATP1B3). The reactions were stopped by removing the supernatants; then the cells were washed three times with ice-cold PBS. Fluorescence (in 200 μl PBS/well) was determined employing an Enspire plate reader (Perkin Elmer, Waltham, MA) with excitation/emission wavelengths of 403/517 nm (pyranine) or 586/605 nm (sulforhodamine 101). OATP-dependent transport was calculated by extracting fluorescence measured in mock transfected cells. Transport activity was calculated based on the fluorescence signal in the absence (100%) of chrysin or its conjugates. Experiments were repeated in three biologic replicates. IC_{50} values were calculated by Hill1 fit, using the Origin Pro8.6 software (GraphPad).

Transport Activity Measurements for ABC Transporters. Transport activity was measured in insect membrane vesicles, as has been previously reported (Sarkadi et al., 1992; Ozvegy et al., 2001, 2002; Bodo et al., 2003; Telbisz et al., 2007). Briefly, human P-gp, BCRP, and MRP2 were expressed in Sf9 insect cells by baculoviruses. At the third day of infection, cells were collected, and membrane vesicles were obtained by mechanical disruption and differential centrifugation. For BCRP, the cholesterol level of the vesicles was adjusted to the level of mammalian membranes to get full activity (Telbisz et al., 2007). Membrane vesicles were stored at −80°C, and total protein content of preparations was measured by Lowry method and used as a reference of the quantity. Appropriate amounts of membrane vesicles (50 μg protein/sample) were incubated with transporter-specific fluorescent substrates (BCRP: 10 μM LY, ABCB1: 5 μM NMQ, MRP2: 5 μM CDCF) at 37°C for 10 minutes without or

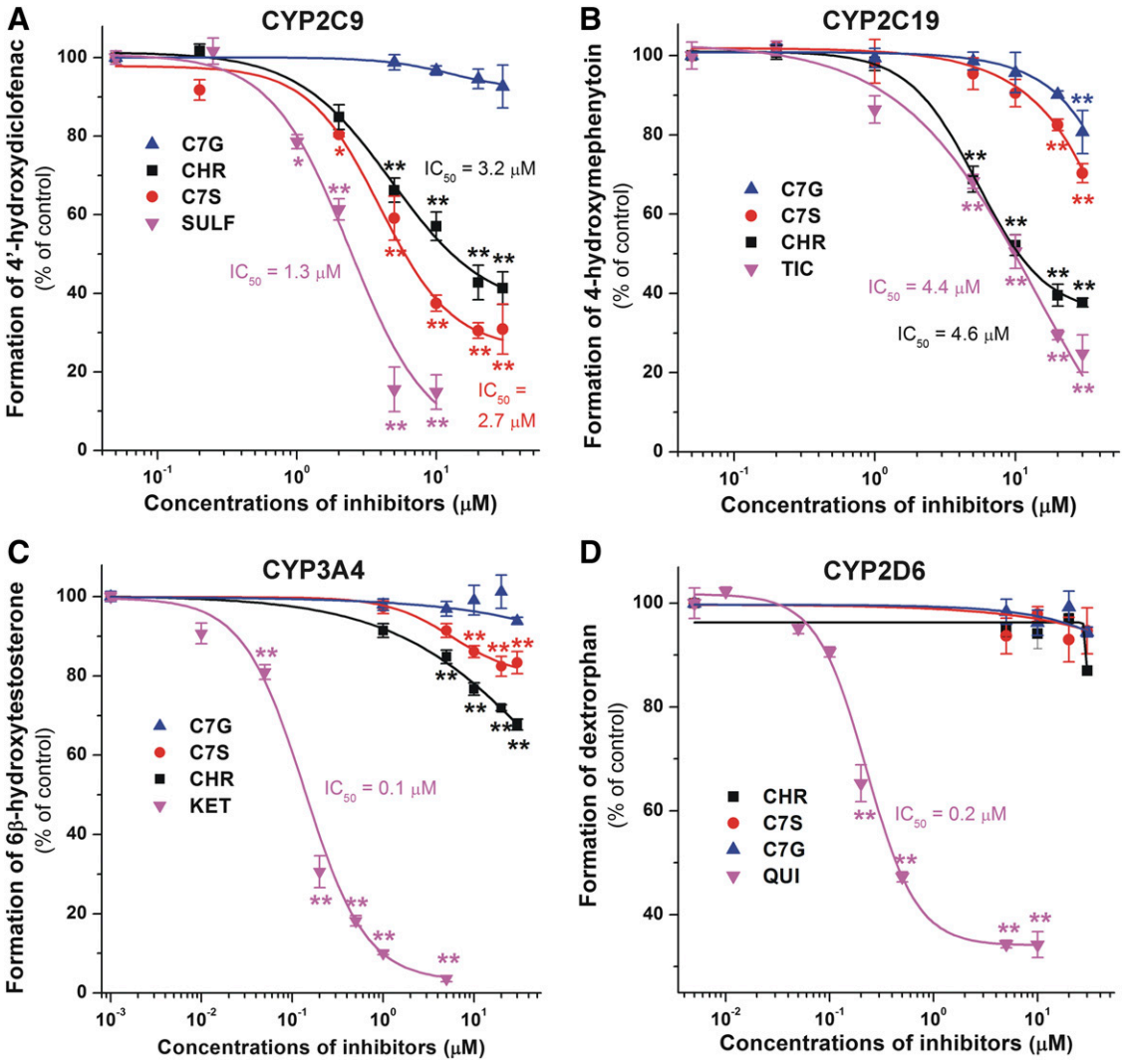

Fig. 2. Concentration-dependent inhibitory effects of chrysin, C7S, C7G, and positive controls on CYP enzymes. Inhibition of CYP2C9-catalyzed 4′-hydroxydiclofenac (A), CYP2C19-catalyzed 4-hydroxymephenytoin (B), CYP3A4-catalyzed 6β-hydroxytestosterone (C), and CYP2D6-catalyzed dextrorphan (D) formation in the presence of increasing inhibitor concentrations (0–30 μM; substrate concentrations: 5 μM in each assay). Mean ± S.E.M. values are derived from three independent experiments. CHR, chrysin; KET, ketoconazole; QUI, quinidine; SULF, sulfaphenazole; TIC, ticlopidine. *$P < 0.05$; **$P < 0.01$.

with 4 mM of Mg-ATP in 50 μl volume. Quality of membrane vesicles was confirmed applying known reference inhibitors (see details in the *Results* section). ATP-dependent uptake of fluorescent compounds was investigated in the presence of flavonoids (up to 50–200 μM). Each test compound was dissolved in DMSO. Although DMSO (2% final concentration in each sample) did not affect the assays used, the solvent controls were represented in the corresponding figures. After incubation, samples were rapidly filtered and washed on filter plate (MSFBN6B10; Millipore, Burlington, MA). Accumulated substrates in vesicles were solved back from the filter by 100 μl of 10% SDS and centrifuged into another plate. A 100 μl volume of fluorescence stabilizer additive was added to the samples (DMSO for LY, 0.1 M H_2SO_4 for NMQ, and 0.1 M NaOH for CDCF). Fluorescence of samples were measured by plate readers (Victor ×3 and Enspire; Perkin-Elmer) at appropriate wavelengths (filters in Victor ×3 reader were 405 and 535 nm for LY, 492 and 635 nm for CDCF, and in Enspire reader NMQ was measured at 360 and 430 nm excitation and emission wavelengths, respectively). ABC-related transport was calculated by subtracting passive uptake measured without Mg-ATP from values measured in the presence of Mg-ATP. The backgrounds with and without Mg-AMP were the same. Under the applied concentrations, we did not observe considerable quenching effects of flavonoids.

ATPase Activity Assays for ABC Transporter Interactions. ATPase activity was measured on Sf9 membrane vesicles containing human ABC transporters prepared as described in the section *Transport Activity Measurements for ABC Transporters*. Appropriate amounts of vesicles (BCRP: 10 μg/50 μl, P-gp: 20 μg/50 μl, MRP2: 30 μg/150 μl) were used in assays. Other parameters have been described previously (Sarkadi et al., 1992; Ozvegy et al., 2001, 2002; Bodo et al., 2003; Telbisz et al., 2007). Membrane vesicles were incubated with 3 mM of Mg-ATP for 25 (BCRP and P-gp) or 60 minutes (MRP2) at 37°C. Effects of flavonoids were investigated up to 50–200 μM. Chrysin, C7S, and C7G were dissolved in DMSO. Although DMSO (2% final concentration in each sample) did not affect the assays used, the solvent controls were represented in the corresponding figures. ABC transporter–related activity was determined as vanadate-sensitive ATPase activity. Liberated inorganic phosphate was measured by a colorimetric reaction, as previously described (Sarkadi et al., 1992). Absorbance of samples were measured after 25 minutes at 660 nm.

Statistics. The statistical significance ($P < 0.05$ and $P < 0.01$) was established based on one-way ANOVA test, using Tukey's post hoc test (IBM SPSS Statistics, Armonk, NY).

Results

Inhibition of CYP Enzymes by Chrysin, C7S, and C7G. The effects of chrysin, C7S, C7G, and the positive control sulfaphenazole on CYP2C9 are demonstrated in Fig. 2A. C7G did not inhibit the enzyme,

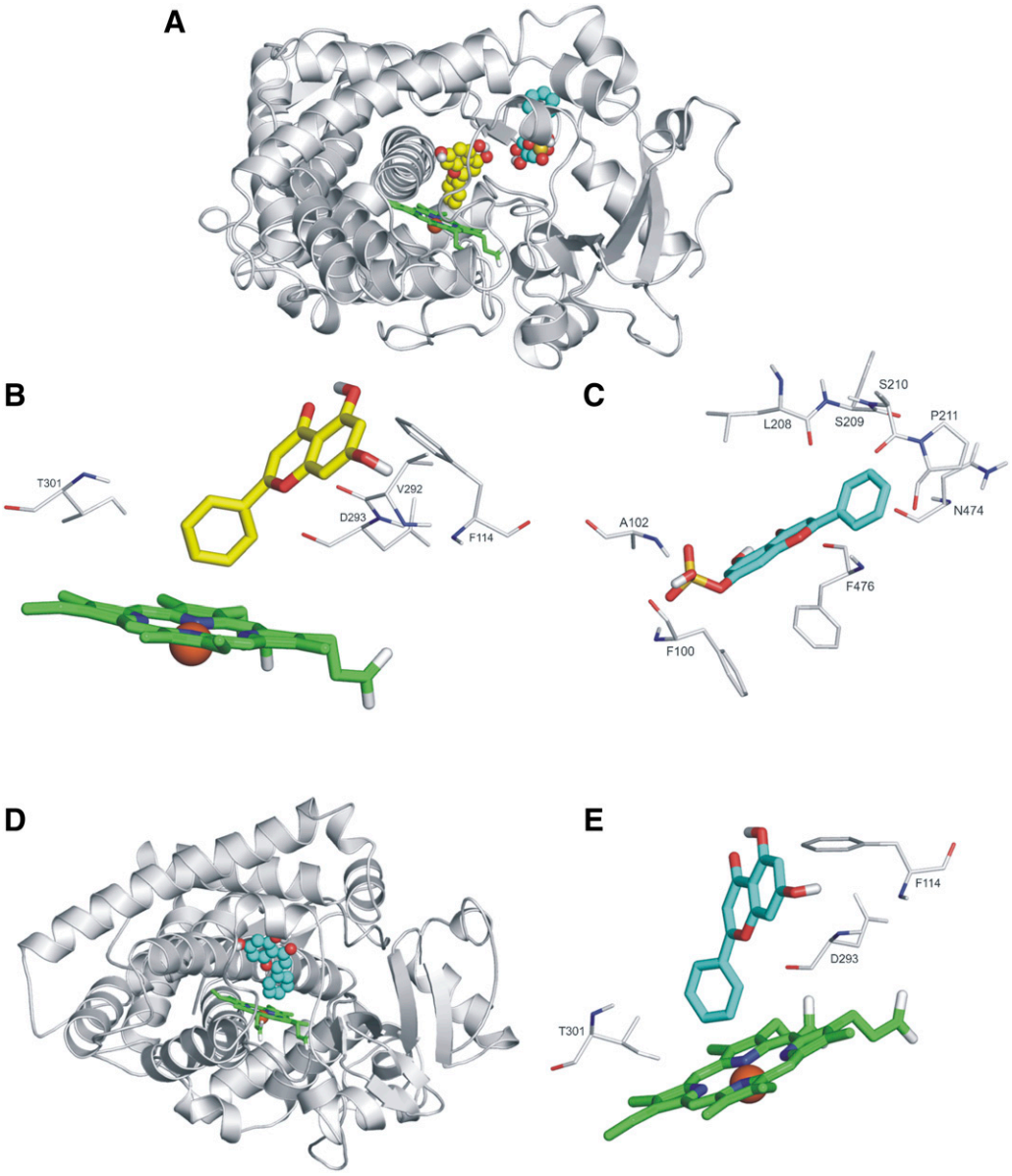

Fig. 3. (A) The binding modes of chrysin (space filling, yellow) and C7S (space filling, navy blue) as docked to the binding pocket of CYP2C9 enzyme (teal cartoon) above the heme ring (green sticks). (B) The close-up of binding mode of chrysin (yellow sticks) as docked to the binding pocket of CYP2C9 enzyme above the heme ring (Fe^{3+} ion in orange, heme as green sticks). (C) The close-up of binding mode of C7S (navy blue sticks) as docked to the binding pocket of CYP2C9 enzyme. (D) The binding mode of chrysin (space-filling, navy blue) as docked to the binding pocket of CYP2C19 enzyme (teal cartoon) above the heme ring (green sticks). (E) The close-up binding mode of chrysin (navy blue sticks) as docked to the binding pocket of CYP2C19 above the heme ring (Fe^{3+} ion in orange, heme as green sticks). In (B, C, and E) the interacting enzyme residues are labeled and shown as thin gray sticks.

even at 30 μM concentration. In contrast, chrysin (IC_{50} = 3.2 μM) and C7S (IC_{50} = 2.7 μM) proved to be strong inhibitors of CYP2C9, showing only 2.5- and 2-fold weaker effects versus sulfaphenazole (IC_{50} = 1.3 μM), respectively.

The impacts of flavonoids and the positive control ticlopidine on the CYP2C19 are demonstrated in Fig. 2B. C7S and C7G exerted statistically significant but only slight inhibitory effects on the enzyme. However, chrysin (IC_{50} = 4.6 μM) caused similarly potent inhibition on CYP2C19 to ticlopidine (IC_{50} = 4.4 μM).

The influence of chrysin and its conjugates on CYP3A4 is demonstrated in Fig. 2C. C7G did not affect the enzyme, whereas chrysin and C7S induced statistically significant but only slight inhibition of CYP3A4. Furthermore, under the applied conditions, chrysin and its metabolites did not inhibit CYP2D6 (Fig. 2D).

Modeling Studies. The ligand binding of *S*-warfarin (reference ligand for CYP2C9) was reproduced at an RMSD value of 1.240 Å in the top first rank (PDB structure: 1og5). Redocking of the reference ligand of CYP2C19 resulted in a somewhat increased RMSD value of 6.590 Å as top first rank still located at the experimental binding position. New ligands of the present study (chrysin and C7S) were also docked to the respective binding pockets of the enzymes located above the heme ring. Regarding the binding mode to CYP2C9, chrysin found a binding position that appears to be final (due to the close coordination of the benzene ring to the heme iron) with closest distances of 3.700 Å measured between benzene C atoms and heme Fe^{3+}, respectively (Fig. 3, A and B). This final position was probably acquired through a couple of prerequisite binding positions. Chrysin reached the final position in the top fifth rank. C7S remained at a prerequisite position of the previous

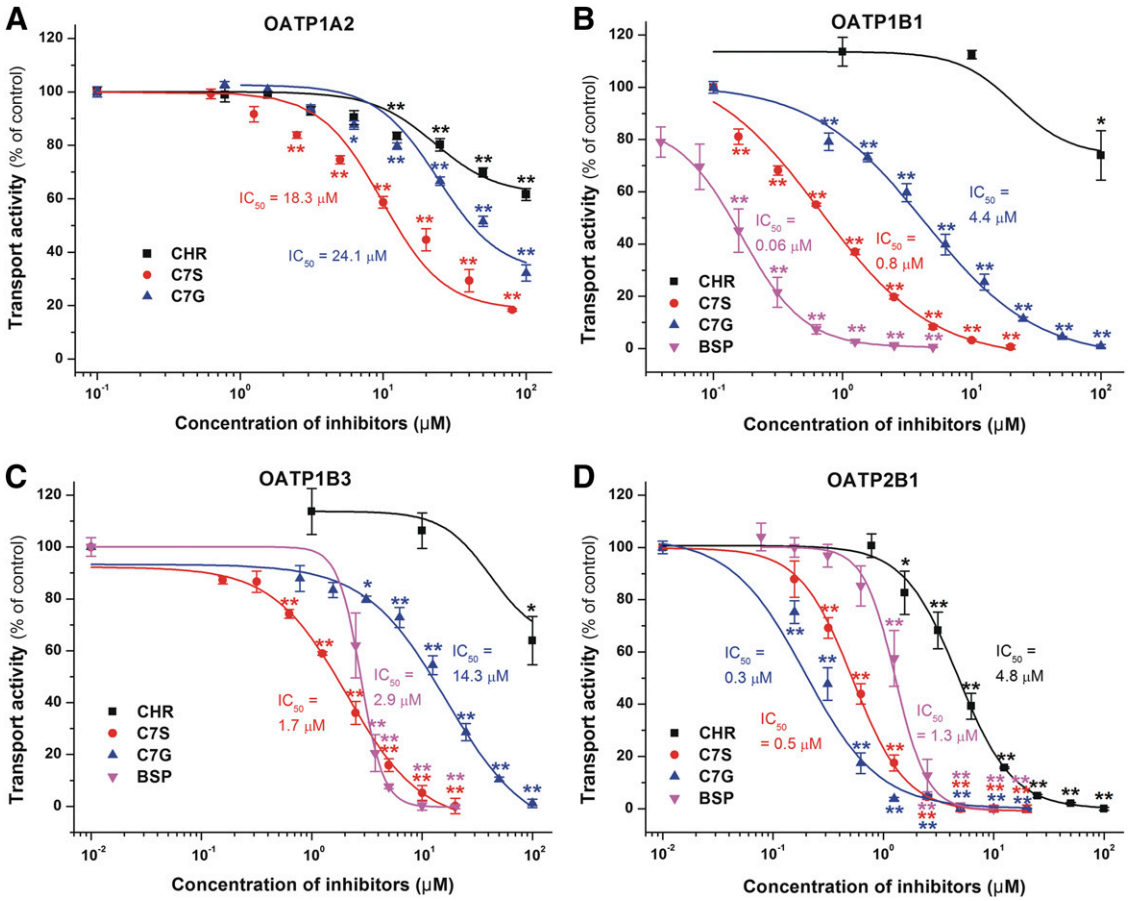

Fig. 4. Concentration-dependent inhibitory effects of bromosulfophthalein (BSP, positive control), chrysin (CHR), C7S, and C7G on OATPs. Uptake of pyranine in A431 cell overexpressing OATPs, 1B1, 1B3, or 2B1, and the uptake of sulforhodamine 101 (OATP1A2) was measured in the presence of increasing concentrations of chrysin, C7S, or C7G (0–100 μM). Effect of BSP on CYP1A2 has been reported previously (Bakos et al., 2020). OATP-dependent transport was determined by extracting the fluorescence measured in mock transfected cells. Fluorescence with the dyes alone was set as 100%. Dye concentrations and incubation times were the following: OATP1A2: 0.5 μM sulforhodamine 101, 10 minutes (A); OATP1B1: 10 μM pyranine, 15 minutes (B); OATP1B3: 20 μM pyranine, 30 minutes (C); and OATP2B1: 20 μM pyranine, 15 minutes (D). Mean ± S.E.M. values were obtained from three biologic replicates. $^{*}P < 0.05$; $^{**}P < 0.01$.

ligands (Fig. 3, A and C) without moving close to the heme iron. The calculated binding free energies suggest that C7S (−7.78 kcal/mol) binds with a higher binding affinity to CYP2C9 than chrysin (−6.11 kcal/mol), which is in agreement with our experimental observations. Regarding CYP2C19, the binding free energy of chrysin was −6.36 kcal/mol. Chrysin found its final binding position through one prerequisite step in top second rank position. The closest distance between the heme Fe^{3+} and benzene C atoms of chrysin was 3.600 Å (Fig. 3, D and E).

Inhibition of OATP Activity by Chrysin, C7S, and C7G. Fluorescent substrates pyranine and sulforhodamine 101 have recently been demonstrated as good indicators of substrate-inhibitor interactions of OATPs (Bakos et al., 2020; Székely et al., 2020). Uptake of these dyes was determined in A431 cells, engineered to overexpress one of the multispecific OATPs (1A2, 1B1, 1B3, or 2B1), and bromosulfophthalein was used as a reference inhibitor (Patik et al., 2018; Bakos et al., 2020). Figure 4A represents that chrysin is not a potent inhibitor of OATP1A2: only 40% inhibition was achieved in the presence of 100 μM chrysin concentration. In contrast, C7S and C7G showed stronger interactions with OATP1A2 (IC_{50} = 18.3 and 24.1 μM, respectively). Regarding OATP1B1 and OATP1B3, chrysin proved to be again a weak inhibitor ($IC_{50} > 100$ μM) (Fig. 4, B and C). However, C7S and C7G revealed more pronounced inhibition for both proteins than chrysin, C7S being a quite effective inhibitor of OATP1B1 (IC_{50} = 0.8 μM) and OATP1B3 (IC_{50} = 1.7 μM). C7G also showed relatively low IC_{50} values (OATP1B1: 4.4 μM; OATP1B3: 14.3 μM). In addition, among the four OATPs tested, OATP2B1 was the most sensitive to chrysin, C7S, and C7Gwith 4.8, 0.5, and 0.3 μM IC_{50} values, respectively (Fig. 4D).

Effects of Chrysin, C7S, and C7G on ABC Transporters. For the characterization of the transport activity of BCRP, ATP-dependent uptake of LY was measured. Ko143 was used as a reference inhibitor; it decreased ATP-dependent LY uptake by more than 95% at 5 μM concentration (data not shown). Chrysin and its sulfate conjugate strongly decreased LY uptake (Fig. 5A). IC_{50} values of chrysin and C7S were around 0.4–0.6 μM (and at 10 μM total inhibition was observed for both), whereas C7G caused much weaker inhibition (IC_{50} = 19.8 μM). The vanadate-sensitive ATPase activity in the presence of flavonoids was also tested. Each compound increased basal ATPase activity in a concentration-dependent fashion (Fig. 5B). Consistent with the IC_{50} values, chrysin and C7S showed a lower K_m (0.1 μM) and higher V_{max} (90 and 70 nmol Pi/min per milligram protein, respectively) values than C7G (K_m = 8.4 μM).

MRP2 typically has low substrate affinity and a low ATPase activity (Bodo et al., 2003); therefore, compounds were tested at higher concentrations. MRP2 transport activity was measured by ATP-dependent CDCF transport, which was sensitive to benzbromarone and partially to vanadate (data not shown). MRP2-mediated (ATP-dependent) uptake of CDCF was

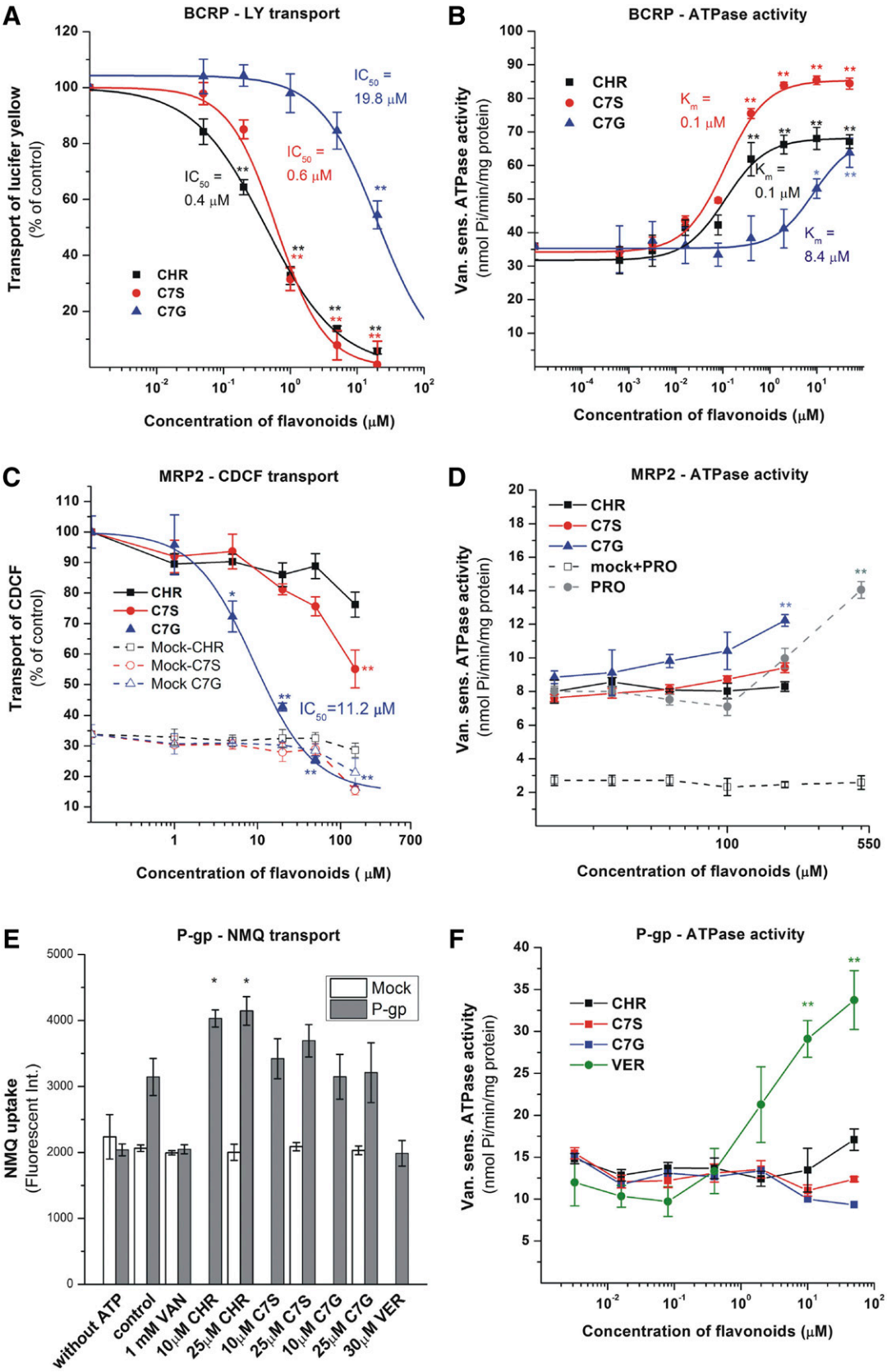

Fig. 5. Effects of chrysin (CHR) and its metabolites on ABC transporters. ABC transporter functions were measured in human ABC transporter (BCRP, MRP2, and P-gp) containing inverted insect cell membrane vesicles. Transport activities were characterized by vesicular uptake of specific fluorescent substrates (LY for BCRP, CDCF for MRP2, and NMQ for P-gp) where transport by the ABC transporter is defined as ATP-dependent uptake of the substrate into the vesicles. Vanadate (VAN)-sensitive ATPase activity of ABC transporters was measured by detecting inorganic, deliberated phosphate in a colorimetric reaction. (A) Effect of flavonoids on the transport of LY by BCRP. (B) Changes in the ATPase activity of BCRP in the presence of flavonoids. (C) Effects of flavonoids on the transport of CDCF by MRP2. Mock membrane data are also

considerably decreased by C7G (IC_{50} = 11.2 μM), whereas chrysin and C7S had no and minor effects, respectively (Fig. 5C). Since we observed a faint ATP-dependent CDCF transport in mock membranes, we also demonstrated the measurements with chrysin and its conjugates with mock membranes (Fig. 5C). Accordingly, only in the presence of C7G can an increased but faint (it did not exceed 6–7 nmol Pi/min per milligram protein) ATPase activity be observed (Fig. 5D). In these measurements, probenecid was also applied as a positive control (Bakos et al., 2000; Huisman et al., 2005).

Despite the fact that P-gp shares several substrates with BCRP, we found that P-gp–mediated NMQ uptake (which was completely inhibited by 1 mM vanadate or 30 μM verapamil) was not inhibited by chrysin, C7S, and C7G. However, chrysin significantly stimulated the transport (Fig. 5E). To confirm the P-gp–related phenomenon, NMQ uptake in mock membrane vesicles was also tested. In control vesicles, NMQ uptake was not influenced by the presence of flavonoids (Fig. 5E). In the ATPase assay, we did not find any significant effect of chrysin and its conjugates even at 50 μM concentrations (Fig. 5F); however, the positive control verapamil strongly increased the basal ATPase activity.

Discussion

Since high dose flavonoid-containing dietary supplements are widely advertised and marketed on the Internet for various purported uses (Vida et al., 2019), there is a high probability that some people apply these supplements together with their prescribed medicines. Because the pharmacokinetic interactions of dietary supplements are poorly characterized, in this study, the interactions of chrysin and its main conjugates with CYP enzymes, OATP uptake transporters, and ABC exporters were examined.

Chrysin showed potent inhibitory effects on CYP2C9 and 2C19. In other in vitro studies performed with diclofenac (IC_{50} = 6.5 μM) and flurbiprofen (IC_{50} = 0.8 μM) substrates, chrysin also strongly inhibited CYP2C9 at comparable concentrations with the substrates used (Kimura et al., 2010; Shimada et al., 2010). Furthermore, propolis extract (containing 23.6 μg/mg chrysin) significantly inhibited CYP2C19 (Ryu et al., 2016). Previous investigations with testosterone (IC_{50} = 0.9 and 7.4 μM) (Tsujimoto et al., 2009; Kimura et al., 2010), midazolam (IC_{50} = 3.8 μM) (Shimada et al., 2010), and quinine (IC_{50} = 70–86 μM) (Ho et al., 2001) substrates suggest the interaction of chrysin with CYP3A4. We found only a weak inhibitory effect of chrysin on CYP3A4. In a recent study, chrysin did not inhibit CYP2D6 (substrate: dextromethorphan) (Bojić et al., 2019), which is in agreement with our results. We did not find any data in the scientific literature regarding the inhibitory effects of C7S and C7G on CYP enzymes. In this study, C7G showed no or negligible inhibitory effects on CYP enzymes tested, whereas C7S proved to be even a stronger inhibitor of CYP2C9 than chrysin (but it had only weak effects on CYP2C19 and 3A4). Based on these observations, we may expect the slower elimination of CYP2C9 substrates as a result of the high consumption of chrysin.

We identified the key interacting residues involved in the binding of chrysin and C7S to CYP2C9 and/or 2C19. Chaichit et al. (2014) investigated the binding of chrysin to CYP2C9; they also identified F114, L208, and A297 as key interacting amino acids. A previous in silico study of flavonoid-CYP2C9 interactions (Sousa et al., 2013) suggests the importance of N474 and S209; we have the same findings regarding C7S (Fig. 3C). The binding free energies of naringenin (−5.98 kcal/mol) and quercetin (−6.77 kcal/mol) with CYP2C9 (Sousa et al., 2013) showed good correlation with our data. Furthermore, previous in silico studies with bavachin also suggest that the binding position of flavonoids is close to the heme iron in both CYP2C9 and 2C19 (Wang et al., 2018), as is demonstrated with chrysin in Figure 3, A and D. Investigation of corylifol A showed the importance of amino acid residues L208, A297, and T301 in the interaction with CYP2C9 enzyme, and the involvement of F100, F114, N204, L237, G296, L366, and F476 has been reported with CYP2C19 (Wang et al., 2018), showing good correlations with our observations.

The interaction between flavonoids and OATPs has been reviewed in several reports (Miron et al., 2017; Čvorović et al., 2018). Based on previous studies, chrysin seems to be a weak inhibitor of OATP1B1 (33% inhibition of estrone-3-sulfate uptake was observed by 100 μM chrysin) (Wang et al., 2005; Wu et al., 2012) and a potent inhibitor of OATP2B1 and OATP1A2 (Navrátilová et al., 2018). However, the interaction of chrysin metabolites with OATPs has not yet been investigated. We demonstrated here that chrysin is a potent inhibitor of OATP2B1 (IC_{50} = 4.8 μM), which is in agreement with the inhibition of OATP2B1-mediated estrone-3-sulfate uptake by chrysin (observed in MDCKII cells) (Navrátilová et al., 2018). Since OATP2B1 is expressed in enterocytes (Kobayashi et al., 2003), this transporter may be involved in the absorption of chrysin. The indirect transport assay applied in the current study does not distinguish competitive (substrate) and non-competitive inhibitors. Walle et al. (1999) reported a well measurable apical-to-basolateral transport of chrysin; however, Rastogi and Jana (2016) suggested passive diffusion as the main route of chrysin absorption. Therefore, further investigations are reasonable to make this issue clear. Based on our data, no significant interaction can be expected between chrysin and the other multispecific OATPs, 1A2, 1B1, and 1B3. In accordance with our observations, a weak or negligible inhibitory effect of chrysin on OATP1B1 was reported (Wang et al., 2005; Wu et al., 2012). On the other hand, the potent inhibition (IC_{50} = 0.15 μM) of OATP1A2-mediated estrone-3-sulfate uptake was noticed in HEK293 cells (Navrátilová et al., 2018). This discrepancy may be explained by the different test substrates used. In the current study, chrysin metabolites showed potent inhibitory effects on each OATP tested. C7G inhibited OATPs, 1A2, 1B1, and 1B3 in micromolar range and attenuated OATP2B1's function with a submicromolar IC_{50} value (0.33 μM). C7S proved to be the most potent inhibitor of OATPs, with IC_{50} values of 9.8 μM (OATP1A2), 0.76 μM (OATP1B1), 1.73 μM (OATP1B3), and 0.55 μM (OATP2B1). Since in vivo studies suggest that the peak plasma concentrations of C7S and/or C7G can be close to 1 μM (Walle et al., 2001; Noh et al., 2016; Dong et al., 2017), they may influence the pharmacokinetics of drug or endogenous substrates of these multispecific OATPs. OATP2B1 mediates the absorption of its substrates from the gut and (together with OATP1B1 and OATP1B3) the uptake of several compounds from the blood to hepatocytes (Kovacsics et al., 2017). OATP1A2 may have an important role in the transport of drugs through the blood-brain barrier. Considering these observations, the high intake of chrysin may interfere with the above-listed transport mechanisms. It is important to note that we used one probe substrate for each OATP, whereas inhibitors may have various effects depending on the substrates used (Izumi et al., 2013). Nevertheless, our data warrant further studies regarding the interactions of chrysin, C7S, and C7G with other OATP substrates. Importantly, OATPs are also responsible for the uptake of toxic compounds,

presented with dashed line. (D) Changes in the ATPase activity of MRP2 in the presence of flavonoids and probenecid (PRO, positive control). (E) Changes in the NMQ uptake into mock (white label) and P-gp (black label) containing vesicles in various conditions. (F) ATPase activity of P-gp in the presence of various concentrations of flavonoids and verapamil (VER, positive control). Mean ± S.E.M. values were obtained from three biologic replicates. $*P < 0.05$; $**P < 0.01$.

including α-amanitin (Letschert et al., 2006). Therefore, the potent inhibition of OATPs by C7S (the major circulating metabolite of chrysin) may be beneficial due to the decreased tissue uptake of these toxins.

ABC multidrug exporters are involved in the elimination of flavonoids as extruders at important tissue barriers. Previous studies suggest that P-gp, BCRP, and MRP2 interact with chrysin either directly or by transporting outwardly its metabolites (Walle et al., 1999; Zhang et al., 2004; Morris and Zhang, 2006; Alvarez et al., 2010; Schumacher et al., 2010; Tran et al., 2011). In cells expressing these ABC exporters, chrysin inhibited BCRP in all studies, but the results are controversial for P-gp (Zhang et al., 2004; Morris and Zhang, 2006; Alvarez et al., 2010; Tran et al., 2011), and the conjugates may be the substrates of BCRP and/or MRP2 exporters (Walle et al., 1999; Wang and Morris, 2007; An and Morris, 2011; Ge et al., 2015; Li et al., 2015). In the current study, inverted membranes were used, which gives the unique possibility to measure direct interactions of hydrophilic metabolites with ABC transporters. Our data show that chrysin and its metabolites are inhibitors of BCRP-mediated transport (Fig. 5A). ATPase activity measurements support the observation that chrysin and C7S have stronger inhibitory effects on BCRP compared with C7G (Fig. 5B). Since ATPase and transport activity are coupled processes and several transported flavonoids (e.g., flavopiridol, quercetin, and kaempferol) are known to increase ATPase activity of BCRP, chrysin and its conjugates may be transported by the protein. Nevertheless, these data give only circumstantial evidence; therefore, further experiments (measurement of direct transport) are reasonable to prove or reject this hypothesis. The transport activity of MRP2 was also inhibited by flavonoids tested. However, in this assay, C7G was a stronger inhibitor of MRP2 than chrysin and C7S (Fig. 5C). Flavonoids tested did not inhibit P-gp; however, chrysin significantly increased the transport of NMQ (Fig. 5E), which is in agreement with some of the previous studies (Tran et al., 2011; Reddy et al., 2016). Nevertheless, we cannot exclude the possibility that the latter cross-reaction is typical only for certain substrates (An and Morris, 2011; Tran et al., 2011) and resulted from special interactions between different binding sites or allosteric modifications.

Although chrysin has low oral bioavailability, its metabolites can reach high concentrations in body fluids (e.g., plasma, bile, and urine) (Walle et al., 2001; Noh et al., 2016; Dong et al., 2017). We have limited data regarding the pharmacokinetics and drug interactions of chrysin in humans; however, animal experiments showed that chrysin can influence the pharmacokinetics of different compounds (e.g., caffeine, nitrofurantoin, and paracetamol) due to its interactions with CYP enzymes and BCRP (Wang and Morris, 2007; Kawase et al., 2009; Noh et al., 2016; Pingili et al., 2019). There is only one human study where 400 mg single dose of chrysin was administered orally, after which the average C_{max} value of C7S was approximately 600 nM (Walle et al., 2001). However, the repeated administration of higher chrysin doses (even 1–2 g daily) can be estimated based on the recommended daily doses by manufacturers (Mohos et al., 2018a). Therefore, it is reasonable to hypothesize the low micromolar plasma concentrations of chrysin conjugates. In agreement with this hypothesis, the repeated administration of 1 g quercetin daily resulted in approximately 2 μM or even higher peak plasma concentration of quercetin conjugates (Conquer et al., 1998; Vida et al., 2019). Considering the above-listed data and our observations, the interactions of chrysin and/or it metabolites with CYP2C9, OATPs, and BCRP may have high pharmacological importance. Therefore, the simultaneous administration of high dose chrysin-containing dietary supplements and medications should be carefully considered, at least until clinical studies prove its safety. Since the Internet sale of dietary supplements is largely uncontrolled (Vida et al., 2019), health care professionals should be aware of the risk regarding drug-supplement interactions to prevent the corresponding health impairment. Nevertheless, to explore the in vivo pharmacological relevance of these interactions, animal studies need to be performed and/or human data should be analyzed and evaluated in the future.

Acknowledgments

The authors thank Katalin Fábián for her excellent assistance in the experimental work. The work of C.Ö.-L. and C.H. was supported by the János Bolyai Research Scholarship of the Hungarian Academy of Sciences. We acknowledge the grant of computer time from the Governmental Information Technology Development Agency (KIFÜ), Hungary.

Authorship Contributions

Participated in research design: Poór, Özvegy-Laczka, Telbisz, Bakos, Hetényi.

Conducted experiments: Mohos, Fliszár-Nyúl, Zsidó, Bencsik, Ungvári, Bakos, Kuffa.

Performed data analysis: Poór, Mohos, Fliszár-Nyúl, Bakos, Özvegy-Laczka, Telbisz.

Wrote or contributed to the writing of the manuscript: Mohos, Poór, Zsidó, Özvegy-Laczka, Telbisz.

References

Alvarez AI, Real R, Pérez M, Mendoza G, Prieto JG, and Merino G (2010) Modulation of the activity of ABC transporters (P-glycoprotein, MRP2, BCRP) by flavonoids and drug response. *J Pharm Sci* **99**:598–617 DOI: 10.1002/jps.21851.

An G and Morris ME (2011) The sulfated conjugate of biochanin A is a substrate of breast cancer resistant protein (ABCG2). *Biopharm Drug Dispos* **32**:446–457 DOI: 10.1002/bdd.772.

Bakos E, Evers R, Sinkó E, Váradi A, Borst P, and Sarkadi B (2000) Interactions of the human multidrug resistance proteins MRP1 and MRP2 with organic anions. *Mol Pharmacol* **57**: 760–768 DOI: 10.1124/mol.57.4.760.

Bakos É, Német O, Patik I, Kucsma N, Várady G, Szakács G, and Özvegy-Laczka C (2020) A novel fluorescence-based functional assay for human OATP1A2 and OATP1C1 identifies interaction between third-generation P-gp inhibitors and OATP1A2. *FEBS J* **287**:2468–2485 DOI: 10.1111/febs.15156.

Bodo A, Bakos E, Szeri F, Varadi A, and Sarkadi B (2003) Differential modulation of the human liver conjugate transporters MRP2 and MRP3 by bile acids and organic anions. *J Biol Chem* **278**: 23529–23537 DOI: 10.1074/jbc.M303515200.

Bojić M, Kondža M, Rimac H, Benković G, and Maleš Ž (2019) The effect of flavonoid aglycones on the CYP1A2, CYP2A6, CYP2C8 and CYP2D6 enzymes activity. *Molecules* **24**:3174 DOI: 10.3390/molecules24173174.

Chaichit S, Hongwiset D, and Jiranusornkul S (2014) Binding models of polyphenols to cytochrome P450 2C9: a molecular docking study, in Proceedings of the 3rd International Conference on Computation for Science and Technology; Advances in Computer Science Research **Vol 2**, pp 105–108 DOI: 10.2991/iccst-15.2015.20.

Conquer JA, Maiani G, Azzini E, Raguzzini A, and Holub BJ (1998) Supplementation with quercetin markedly increases plasma quercetin concentration without effect on selected risk factors for heart disease in healthy subjects. *J Nutr* **128**:593–597 DOI: 10.1093/jn/128.3.593.

Čvorović J, Ziberna L, Fornasaro S, Tramer F, and Passamonti S (2018) Bioavailability of flavonoids: the role of cell membrane transporters, in *Polyphenols: Mechanisms of Action in Human Health and Disease*, 2nd ed (Watson RR, Preedy VE, and Zibadi S 295–320, Academic Press, Amsterdam.

Dong D, Quan E, Yuan X, Xie Q, Li Z, and Wu B (2017) Sodium oleate-based nanoemulsion enhances oral absorption of chrysin through inhibition of UGT-mediated metabolism. *Mol Pharm* **14**:2864–2874 DOI: 10.1021/acs.molpharmaceut.6b00851.

Durmus S, van Hoppe S, and Schinkel AH (2016) The impact of organic anion-transporting polypeptides (OATPs) on disposition and toxicity of antitumor drugs: insights from knockout and humanized mice. *Drug Resist Updat* **27**:72–88 DOI: 10.1016/j.drup.2016.06.005.

Fliszár-Nyúl E, Mohos V, Bencsik T, Lemli B, Kunsági-Máté S, and Poór M (2019) Interactions of 7,8-dihydroxyflavone with serum albumin as well as with CYP2C9, CYP2C19, CYP3A4, and xanthine oxidase biotransformation enzymes. *Biomolecules* **9**:655 DOI: 10.3390/biom9110655.

Galijatovic A, Otake Y, Walle UK, and Walle T (1999) Extensive metabolism of the flavonoid chrysin by human Caco-2 and Hep G2 cells. *Xenobiotica* **29**:1241–1256 DOI: 10.1080/004982599237912.

Ge S, Gao S, Yin T, and Hu M (2015) Determination of pharmacokinetics of chrysin and its conjugates in wild-type FVB and Bcrp1 knockout mice using a validated LC-MS/MS method. *J Agric Food Chem* **63**:2902–2910 DOI: 10.1021/jf5056979.

Hetényi C and van der Spoel D (2006) Blind docking of drug-sized compounds to proteins with up to a thousand residues. *FEBS Lett* **580**:1447–1450 DOI: 10.1016/j.febslet.2006.01.074.

Ho PC, Saville DJ, and Wanwimolruk S (2001) Inhibition of human CYP3A4 activity by grapefruit flavonoids, furanocoumarins and related compounds. *J Pharm Pharm Sci* **4**:217–227.

Huang WH, Lee AR, and Yang CH (2006) Antioxidative and anti-inflammatory activities of polyhydroxyflavonoids of Scutellaria baicalensis GEORGI. *Biosci Biotechnol Biochem* **70**: 2371–2380 DOI: 10.1271/bbb.50698.

Huisman MT, Chhatta AA, van Tellingen O, Beijnen JH, and Schinkel AH (2005) MRP2 (ABCC2) transports taxanes and confers paclitaxel resistance and both processes are stimulated by probenecid. *Int J Cancer* **116**:824–829 DOI: 10.1002/ijc.21013.

Izumi S, Nozaki Y, Komori T, Maeda K, Takenaka O, Kusano K, Yoshimura T, Kusuhara H, and Sugiyama Y (2013) Substrate-dependent inhibition of organic anion transporting polypeptide 1B1: comparative analysis with prototypical probe substrates estradiol-17β-glucuronide,

estrone-3-sulfate, and sulfobromophthalein. *Drug Metab Dispos* **41**:1859–1866 DOI: 10.1124/dmd.113.052290.
Jetter A and Kullak-Ublic GA (2020) Drugs and hepatic transporters: a review. *Pharmacol Res* **154**:104234 DOI: 10.1016/j.phrs.2019.04.018.
Kao YC, Zhou C, Sherman M, Laughton CA, and Chen S (1998) Molecular basis of the inhibition of human aromatase (estrogen synthetase) by flavone and isoflavone phytoestrogens: a site-directed mutagenesis study. *Environ Health Perspect* **106**:85–92 DOI: 10.1289/ehp.9810685.
Kawase A, Matsumoto Y, Hadano M, Ishii Y, and Iwaki M (2009) Differential effects of chrysin on nitrofurantoin pharmacokinetics mediated by intestinal breast cancer resistance protein in rats and mice. *J Pharm Pharm Sci* **12**:150–163 DOI: 10.18433/j3v30r.
Kimura Y, Ito H, Ohnishi R, and Hatano T (2010) Inhibitory effects of polyphenols on human cytochrome P450 3A4 and 2C9 activity. *Food Chem Toxicol* **48**:429–435 DOI: 10.1016/j.fct.2009.10.041.
Kobayashi D, Nozawa T, Imai K, Nezu J, Tsuji A, and Tamai I (2003) Involvement of human organic anion transporting polypeptide OATP-B (SLC21A9) in pH-dependent transport across intestinal apical membrane. *J Pharmacol Exp Ther* **306**:703–708 DOI: 10.1124/jpet.103.051300.
König J, Cui Y, Nies AT, and Keppler D (2000) A novel human organic anion transporting polypeptide localized to the basolateral hepatocyte membrane. *Am J Physiol Gastrointest Liver Physiol* **278**:G156–G164 DOI: 10.1152/ajpgi.2000.278.1.G156.
Kovacsics D, Patik I, and Özvegy-Laczka C (2017) The role of organic anion transporting polypeptides in drug absorption, distribution, excretion and drug-drug interactions. *Expert Opin Drug Metab Toxicol* **13**:409–424 DOI: 10.1080/17425255.2017.1253679.
Kumar S and Pandey AK (2013) Chemistry and biological activities of flavonoids: an overview. *ScientificWorldJournal* **2013**:162750 DOI: 10.1155/2013/162750.
Letschert K, Faulstich H, Keller D, and Keppler D (2006) Molecular characterization and inhibition of amanitin uptake into human hepatocytes. *Toxicol Sci* **91**:140–149 DOI: 10.1093/toxsci/kfj141.
Li W, Sun H, Zhang X, Wang H, and Wu B (2015) Efflux transport of chrysin and apigenin sulfates in HEK293 cells overexpressing SULT1A3: the role of multidrug resistance-associated protein 4 (MRP4/ABCC4). *Biochem Pharmacol* **98**:203–214 DOI: 10.1016/j.bcp.2015.08.090.
Manach C, Williamson G, Morand C, Scalbert A, and Rémésy C (2005) Bioavailability and bioefficacy of polyphenols in humans. I. Review of 97 bioavailability studies. *Am J Clin Nutr* **81** (Suppl):230S–242S DOI: 10.1093/ajcn/81.1.230S.
Marquez B and Van Bambeke F (2011) ABC multidrug transporters: target for modulation of drug pharmacokinetics and drug-drug interactions. *Curr Drug Targets* **12**:600–620 DOI: 10.2174/138945011795378504.
McDonnell AM and Dang CH (2013) Basic review of the cytochrome p450 system. *J Adv Pract Oncol* **4**:263–268 DOI: 10.6004/jadpro.2013.4.4.7.
Miron A, Aprotosoaie AC, Trifan A, and Xiao J (2017) Flavonoids as modulators of metabolic enzymes and drug transporters. *Ann N Y Acad Sci* **1398**:152–167 DOI: 10.1111/nyas.13384.
Mohos V, Bencsik T, Boda G, Fliszár-Nyúl E, Lemli B, Kunsági-Máté S, and Poór M (2018b) Interactions of casticin, ipriflavone, and resveratrol with serum albumin and their inhibitory effects on CYP2C9 and CYP3A4 enzymes. *Biomed Pharmacother* **107**:777–784 DOI: 10.1016/j.biopha.2018.08.068.
Mohos V, Fliszár-Nyúl E, Lemli B, Zsidó BZ, Hetényi C, Mladěnka P, Horký P, Pour M, and Poór M (2020) Testing the pharmacokinetic interactions of 24 colonic flavonoid metabolites with human serum albumin and cytochrome P450 enzymes. *Biomolecules* **10**:E409 DOI: 10.3390/biom10030409.
Mohos V, Fliszár-Nyúl E, Schilli G, Hetényi C, Lemli B, Kunsági-Máté S, Bognár B, and Poór M (2018a) Interaction of chrysin and its main conjugated metabolites chrysin-7-sulfate and chrysin-7-glucuronide with serum albumin. *Int J Mol Sci* **19**:4073 DOI: 10.3390/ijms19124073.
Morris GM, Huey R, Lindstrom W, Sanner MF, Belew RK, Goodsell DS, and Olson AJ (2009) AutoDock4 and AutoDockTools4: automated docking with selective receptor flexibility. *J Comput Chem* **30**:2785–2791 DOI: 10.1002/jcc.21256.
Morris ME and Zhang S (2006) Flavonoid-drug interactions: effects of flavonoids on ABC transporters. *Life Sci* **78**:2116–2130 DOI: 10.1016/j.lfs.2005.12.003.
Nakanishi T and Tamai I (2012) Genetic polymorphisms of OATP transporters and their impact on intestinal absorption and hepatic disposition of drugs. *Drug Metab Pharmacokinet* **27**:106–121 DOI: 10.2133/dmpk.dmpk-11-rv-099.
Navrátilová L, Ramos Mandíková J, Pávek P, Mladěnka P, and Trejtnar F (2018) Honey flavonoids inhibit hOATP2B1 and hOATP1A2 transporters and hOATP-mediated rosuvastatin cell uptake in vitro. *Xenobiotica* **48**:745–755 DOI: 10.1080/00498254.2017.1358469.
Noh K, Oh G, Nepal MR, Jeong KS, Choi Y, Kang MJ, Kang W, Jeong HG, and Jeong TC (2016) Pharmacokinetic interaction of chrysin with caffeine in rats. *Biomol Ther (Seoul)* **24**:446–452 DOI: 10.4062/biomolther.2015.197.
Ozvegy C, Litman T, Szakács G, Nagy Z, Bates S, Váradi A, and Sarkadi B (2001) Functional characterization of the human multidrug transporter, ABCG2, expressed in insect cells. *Biochem Biophys Res Commun* **285**:111–117 10.1006/bbrc.2001.5130.
Ozvegy C, Váradi A, and Sarkadi B (2002) Characterization of drug transport, ATP hydrolysis, and nucleotide trapping by the human ABCG2 multidrug transporter. Modulation of substrate specificity by a point mutation. *J Biol Chem* **277**:47980–47990 DOI: 10.1074/jbc.M207857200.
Patik I, Székely V, Német O, Szepesi Á, Kucsma N, Várady G, Szakács G, Bakos É, and Özvegy-Laczka C (2018) Identification of novel cell-impermeant fluorescent substrates for testing the function and drug interaction of organic anion-transporting polypeptides, OATP1B1/1B3 and 2B1. *Sci Rep* **8**:2630 DOI: 10.1038/s41598-018-20815-1.
Pingili RB, Pawar AK, and Challa SR (2019) Effect of chrysin on the formation of N-acetyl-p-benzoquinoneimine, a toxic metabolite of paracetamol in rats and isolated rat hepatocytes. *Chem Biol Interact* **302**:123–134 DOI: 10.1016/j.cbi.2019.02.014.
Rastogi H and Jana S (2016) Evaluation of physicochemical properties and intestinal permeability of six dietary polyphenols in human intestinal colon adenocarcinoma caco-2 cells. *Eur J Drug Metab Pharmacokinet* **41**:33–43 DOI: 10.1007/s13318-014-0234-5.
Reddy DR, Khurana A, Bale S, Ravirala R, Reddy VSS, Mohankumar M, and Godugu C (2016) Natural flavonoids silymarin and quercetin improve the brain distribution of co-administered P-gp substrate drugs. *Springerplus* **5**:1618 DOI: 10.1186/s40064-016-3267-1.
Ryu CS, Oh SJ, Oh JM, Lee JY, Lee SY, Chae JW, Kwon KI, and Kim SK (2016) Inhibition of cytochrome P450 by propolis in human liver microsomes. *Toxicol Res* **32**:207–213 DOI: 10.5487/TR.2016.32.3.207.
Sarkadi B, Homolya L, Szakács G, and Váradi A (2006) Human multidrug resistance ABCB and ABCG transporters: participation in a chemoimmunity defense system. *Physiol Rev* **86**:1179–1236 DOI: 10.1152/physrev.00037.2005.
Sarkadi B, Price EM, Boucher RC, Germann UA, and Scarborough GA (1992) Expression of the human multidrug resistance cDNA in insect cells generates a high activity drug-stimulated membrane ATPase. *J Biol Chem* **267**:4854–4858.
Schumacher M, Hautzinger A, Rossmann A, Holzhauser S, Popovic D, Hertrampf A, Kuntz S, Boll M, and Wenzel U (2010) Chrysin blocks topotecan-induced apoptosis in Caco-2 cells in spite of inhibition of ABC-transporters. *Biochem Pharmacol* **80**:471–479 DOI: 10.1016/j.bcp.2010.04.038.
Shahrokh K, Orendt A, Yost GS, and Cheatham TE III (2012) Quantum mechanically derived AMBER-compatible heme parameters for various states of the cytochrome P450 catalytic cycle. *J Comput Chem* **33**:119–133 DOI: 10.1002/jcc.21922.
Shimada T, Tanaka K, Takenaka S, Murayama N, Martin MV, Foroozesh MK, Yamazaki H, Guengerich FP, and Komori M (2010) Structure-function relationships of inhibition of human cytochromes P450 1A1, 1A2, 1B1, 2C9, and 3A4 by 33 flavonoid derivatives. *Chem Res Toxicol* **23**:1921–1935 DOI: 10.1021/tx100286d.
Shitara Y, Maeda K, Ikejiri K, Yoshida K, Horie T, and Sugiyama Y (2013) Clinical significance of organic anion transporting polypeptides (OATPs) in drug disposition: their roles in hepatic clearance and intestinal absorption. *Biopharm Drug Dispos* **34**:45–78 DOI: 10.1002/bdd.1823.
Siess MH, Le Bon AM, Canivenc-Lavier MC, Amiot MJ, Sabatier S, Aubert SY, and Suschetet M (1996) Flavonoids of honey and propolis: characterization and effects on hepatic drug metabolizing enzymes and Benzo[a]pyrene-DNA binding in rats. *J Agric Food Chem* **44**:2297–2301 DOI: 10.1021/jf9504733.
Sousa MC, Braga RC, Cintra BAS, de Oliveira V, and Andrade CH (2013) In silico metabolism studies of dietary flavonoids by CYP1A2 and CYP2C9. *Food Res Int* **50**:102–110 DOI: 10.1016/j.foodres.2012.09.027.
Stewart JJ (1990) MOPAC: a semiempirical molecular orbital program. *J Comput Aided Mol Des* **4**:1–105 DOI: 10.1007/bf00128336.
Stewart JJP (2013) Optimization of parameters for semiempirical methods VI: more modifications to the NDDO approximations and re-optimization of parameters. *J Mol Model* **19**:1–32 DOI: 10.1007/s00894-012-1667-x.
Szakács G, Váradi A, Ozvegy-Laczka C, and Sarkadi B (2008) The role of ABC transporters in drug absorption, distribution, metabolism, excretion and toxicity (ADME-Tox). *Drug Discov Today* **13**:379–393 DOI: 10.1124/jpet.104.068536.
Székely Virág, Patik Izabel, Ungvári Orsolya, Telbisz Ágnes, Szakács Gergely, Bakos Éva, and Özvegy-Laczka Csilla (2020) Fluorescent probes for the dual investigation of MRP2 and OATP1B1 function and drug interactions. *Eur J Pharm Sci* **151**:105395, doi: 10.1016/j.ejps.2020.105395 32473861.
Telbisz A, Müller M, Ozvegy-Laczka C, Homolya L, Szente L, Váradi A, and Sarkadi B (2007) Membrane cholesterol selectively modulates the activity of the human ABCG2 multidrug transporter. *Biochim Biophys Acta* **1768**:2698–2713 DOI: 10.1016/j.bbamem.2007.06.026.
Tran VH, Marks D, Duke RK, Bebawy M, Duke CC, and Roufogalis BD (2011) Modulation of P-glycoprotein-mediated anticancer drug accumulation, cytotoxicity, and ATPase activity by flavonoid interactions. *Nutr Cancer* **63**:435–443 DOI: 10.1080/01635581.2011.535959.
Tsujimoto M, Horie M, Honda H, Takara K, and Nishiguchi K (2009) The structure-activity correlation on the inhibitory effects of flavonoids on cytochrome P450 3A activity. *Biol Pharm Bull* **32**:671–676 DOI: 10.1248/bpb.32.671.
Urquhart BL and Kim RB (2009) Blood-brain barrier transporters and response to CNS-active drugs. *Eur J Clin Pharmacol* **65**:1063–1070 DOI: 10.1007/s00228-009-0714-8.
Vida RG, Fittler A, Somogyi-Végh A, and Poór M (2019) Dietary quercetin supplements: assessment of online product informations and quantitation of quercetin in the products by high-performance liquid chromatography. *Phytother Res* **33**:1912–1920 DOI: 10.1002/ptr.6382.
Walle T, Otake Y, Brubaker JA, Walle UK, and Halushka PV (2001) Disposition and metabolism of the flavonoid chrysin in normal volunteers. *Br J Clin Pharmacol* **51**:143–146 DOI: 10.1111/j.1365-2125.2001.01317.x.
Walle UK, Galijatovic A, and Walle T (1999) Transport of the flavonoid chrysin and its conjugated metabolites by the human intestinal cell line Caco-2. *Biochem Pharmacol* **58**:431–438 DOI: 10.1016/s0006-2952(99)00133-1.
Wang L, Hai Y, Huang N, Gao X, Liu W, and He X (2018) Human cytochrome P450 enzyme inhibition profile of three flavonoids isolated from: Psoralea corylifolia: in silico predictions and experimental validation. *New J Chem* **42**:10922–10934 DOI: 10.1039/C7NJ00884H.
Wang X and Morris ME (2007) Effects of the flavonoid chrysin on nitrofurantoin pharmacokinetics in rats: potential involvement of ABCG2. *Drug Metab Dispos* **35**:268–274 DOI: 10.1124/dmd.106.011684.
Wang X, Wolkoff AW, and Morris ME (2005) Flavonoids as a novel class of human organic anion-transporting polypeptide OATP1B1 (OATP-C) modulators. *Drug Metab Dispos* **33**:1666–1672 DOI: 10.1124/dmd.105.005926.
Wlcek K and Stieger B (2014) ATP-binding cassette transporters in liver. *Biofactors* **40**:188–198 DOI: 10.1002/biof.1136.
Wu LX, Guo CX, Qu Q, Yu J, Chen WQ, Wang G, Fan L, Li Q, Zhang W, and Zhou HH (2012) Effects of natural products on the function of human organic anion transporting polypeptide 1B1. *Xenobiotica* **42**:339–348 DOI: 10.3109/00498254.2011.623796.
Zhang S, Yang X, and Morris ME (2004) Flavonoids are inhibitors of breast cancer resistance protein (ABCG2)-mediated transport. *Mol Pharmacol* **65**:1208–1216 DOI: 10.1124/mol.65.5.1208.

Address correspondence to: Dr. Miklós Poór, Department of Pharmacology, University of Pécs, Faculty of Pharmacy, Szigeti út 12, H-7624 Pécs, Hungary. E-mail: poor.miklos@pte.hu

nutrients

MDPI

Article

Inhibitory Effects of Quercetin and Its Main Methyl, Sulfate, and Glucuronic Acid Conjugates on Cytochrome P450 Enzymes, and on OATP, BCRP and MRP2 Transporters

Violetta Mohos [1,2], Eszter Fliszár-Nyúl [1,2], Orsolya Ungvári [3], Katalin Kuffa [4], Paul W. Needs [5], Paul A. Kroon [5], Ágnes Telbisz [4], Csilla Özvegy-Laczka [3] and Miklós Poór [1,2,*]

1 Department of Pharmacology, Faculty of Pharmacy, University of Pécs, Szigeti út 12, H-7624 Pécs, Hungary; mohos.violetta@gytk.pte.hu (V.M.); eszter.nyul@aok.pte.hu (E.F.-N.)
2 Lab-on-a-Chip Research Group, János Szentágothai Research Centre, University of Pécs, Ifjúság útja 20, H-7624 Pécs, Hungary
3 Membrane Protein Research Group, Institute of Enzymology, Research Centre for Natural Sciences, H-1117 Budapest, Hungary; ungvari.orsolya@ttk.mta.hu (O.U.); laczka.csilla@ttk.mta.hu (C.Ö.-L.)
4 Biomembrane Research Group, Institute of Enzymology, Research Centre for Natural Sciences, H-1117 Budapest, Hungary; kuffakatalin@gmail.com (K.K.); telbisz.agnes@ttk.mta.hu (Á.T.)
5 Quadram Institute Bioscience, Norwich Research Park, Norwich NR4 7UQ, UK; paul.needs@quadram.ac.uk (P.W.N.); paul.kroon@quadram.ac.uk (P.A.K.)
* Correspondence: poor.miklos@pte.hu; Tel.: +36-72-536-000 (ext. 35052)

Received: 9 July 2020; Accepted: 29 July 2020; Published: 31 July 2020

Abstract: Quercetin is a flavonoid, its glycosides and aglycone are found in significant amounts in several plants and dietary supplements. Because of the high presystemic biotransformation of quercetin, mainly its conjugates appear in circulation. As has been reported in previous studies, quercetin can interact with several proteins of pharmacokinetic importance. However, the interactions of its metabolites with biotransformation enzymes and drug transporters have barely been examined. In this study, the inhibitory effects of quercetin and its most relevant methyl, sulfate, and glucuronide metabolites were tested on cytochrome P450 (CYP) (2C19, 3A4, and 2D6) enzymes as well as on organic anion-transporting polypeptides (OATPs) (OATP1A2, OATP1B1, OATP1B3, and OATP2B1) and ATP (adenosine triphosphate) Binding Cassette (ABC) (BCRP and MRP2) transporters. Quercetin and its metabolites (quercetin-3′-sulfate, quercetin-3-glucuronide, isorhamnetin, and isorhamnetin-3-glucuronide) showed weak inhibitory effects on CYP2C19 and 3A4, while they did not affect CYP2D6 activity. Some of the flavonoids caused weak inhibition of OATP1A2 and MRP2. However, most of the compounds tested proved to be strong inhibitors of OATP1B1, OATP1B3, OATP2B1, and BCRP. Our data demonstrate that not only quercetin but some of its conjugates, can also interact with CYP enzymes and drug transporters. Therefore, high intake of quercetin may interfere with the pharmacokinetics of drugs.

Keywords: quercetin; quercetin conjugates; cytochrome P450 enzymes; OATP transporters; ABC transporters; pharmacokinetic interaction; food drug interaction

1. Introduction

Flavonoids are biologically active natural polyphenols. Quercetin (Q), including its glycosides, is one of the most abundant flavonoids in nature: it is contained in several fruits (e.g., apple, grapes, and berries), vegetables (e.g., onion and tomato), and medicinal plants (e.g., *Ginkgo Biloba* and *Hypericum perforatum*). Because of the cardioprotective and other suspected positive health

effects of Q [1], it is widely marketed through the Internet as the active ingredient of dietary supplements [2,3]. These supplements usually contain 200 to 1000 mg aglycone in one single tablet/capsule, and the recommended daily dose is between 250 and 4000 mg [3]. It means even a 100-fold higher intake of Q compared to its estimated average dietary intake (25–50 mg/day) [2,4]. Q has poor oral bioavailability, which shows large variation between individuals [1], partly because of its significant presystemic biotransformation in enterocytes and hepatocytes. As a result of its metabolism by catechol-*O*-methyltransferase (COMT), sulfotransferase (SULT) and uridine 5′-diphospho-glucuronosyltransferase (UGT), its methyl (3′-*O*-methylquercetin or isorhamnetin, IR), sulfate (quercetin-3′-sulfate, Q3′S) and glucuronic acid (quercetin-3-glucuronide, Q3G; isorhamnetin-3 -glucuronide, I3G) conjugates are produced (Figure 1) [1]. Human studies suggest that Q3′S, Q3G, and I3G are the dominant circulating metabolites of Q, and the total peak plasma concentration of Q conjugates can achieve 2 μM or even higher levels after the administration of 1000 mg Q daily for one month [5–8]. Furthermore, based on the study of Kaushik et al. [9], the peak plasma concentrations of total Q were as high as 5 to 10 μM in some human subjects, after the administration of a 500 mg single dose of Q contained by certain oral carrier systems.

Cytochrome P450 (CYP) enzymes have a major role in the metabolism of several endogenous compounds, drugs, and other xenobiotics. CYP3A4 is involved in the biotransformation of more than 50% of the orally administered drugs; furthermore, CYP2C19 and 2D6 are also relevant enzymes in drug metabolism [10]. As has been reported, Q can inhibit CYP enzymes, including CYP1A1, 1B1, 2C9, 2C19, 2D6, and 3A4 [11–13]. Furthermore, Q is an inducer of certain CYP enzymes [13]. Some Q metabolites can also interact with CYP. The inhibitory effects of Q3′S, IR, and tamarixetin (4′-*O*-methylquercetin) on CYP2C9 have been reported, while Q3G and I3G did not affect the enzyme [14]. In other studies, the inhibition of CYP1A1, 1A2, 1B1, 2C9, and 3A4 by IR have been also described [15–17]. Nevertheless, we did not find data regarding the effects of Q sulfates and glucuronides on CYP2C19, 2D6, and 3A4 enzymes.

Organic anion-transporting polypeptides (OATPs) are solute carrier membrane transporters. They have a major role in the absorption, tissue distribution, and elimination of endogenous molecules (e.g., steroids, bile acids, and bilirubin), drugs (e.g., statins), food components (e.g., Q and naringin), and toxins (e.g., alpha-amanitin and ochratoxin A) [18–22]. OATP1B1, OATP1B3, and OATP2B1 appear in hepatocytes [23]; furthermore, OATP1A2 and OATP2B1 are involved in the uptake of their substrates into enterocytes and/or the central nervous system [19,24–26]. The inhibition of OATPs 1A2, 1B1, and 2B1 by Q has been demonstrated in previous reports [27,28]. Furthermore, in vitro studies suggest that Q and IR are substrates of certain OATPs [29,30]. Some Q derivatives (e.g., isorhamnetin-3-glucoside and quercetin-3-*O*-alpha-L-arabinopyranosyl) also proved to be inhibitors of OATP1B1 or OATP2B1 [31,32]. However, the effects of the sulfate/glucuronic acid conjugates of Q and IR on the transport function of multispecific OATPs 1A2, 1B1, 1B3, and 2B1 has not yet been examined.

ATP (adenosine triphosphate) Binding Cassette (ABC) drug transporters, such as P-gp/MDR1, BCRP/ABCG2, and MRP2/ABCC2, are pharmacologically relevant, ATP-driven exporters, which are commonly involved in the urinary/biliary excretion of numerous compounds, including certain metabolites [33–37]. Furthermore, these efflux transporters also have high importance in drug exclusion at placental and blood–brain barriers. Their substrate specificity is partially overlapping; however, P-gp transports mostly hydrophobic compounds, MRP2 transports mainly organic anions and drug conjugates, while BCRP can handle various substrates (many hydrophobic compounds as well as some organic anions and conjugates are its substrates) [34]. As it has been reported earlier, flavonoids are able to inhibit the transport function of ABC transporters, which resulted in the development of strong and specific inhibitors for P-gp or BCRP [38–40]. Some flavonoids are transported substrates of BCRP such as flavopiridol or Q [41,42]. MRP2 can also transport some flavonoids, including Q and biochanin A [43–45]. In general, the interactions of flavonoids with ABC transporters have been examined in several studies; however, only limited information is available

about the sulfate/glucuronide metabolites, due to their poor accessibility and/or technical difficulties regarding their investigations.

In this in vitro study, we aimed to investigate the inhibitory effects of Q and its main conjugates (Q3'S, Q3G, IR, and I3G) on CYP (3A4, 2C19, and 2D6) enzymes as well as on OATP (OATP1A2, OATP1B1, OATP1B3, and OATP2B1) and ABC (BCRP and MRP2) transporters. Our results highlight that the Q metabolites examined can significantly inhibit certain enzymes/transporters tested; therefore, it is reasonable to hypothesize that the simultaneous administration of high dose Q-containing dietary supplements with drugs may result in the development of pharmacokinetic interactions.

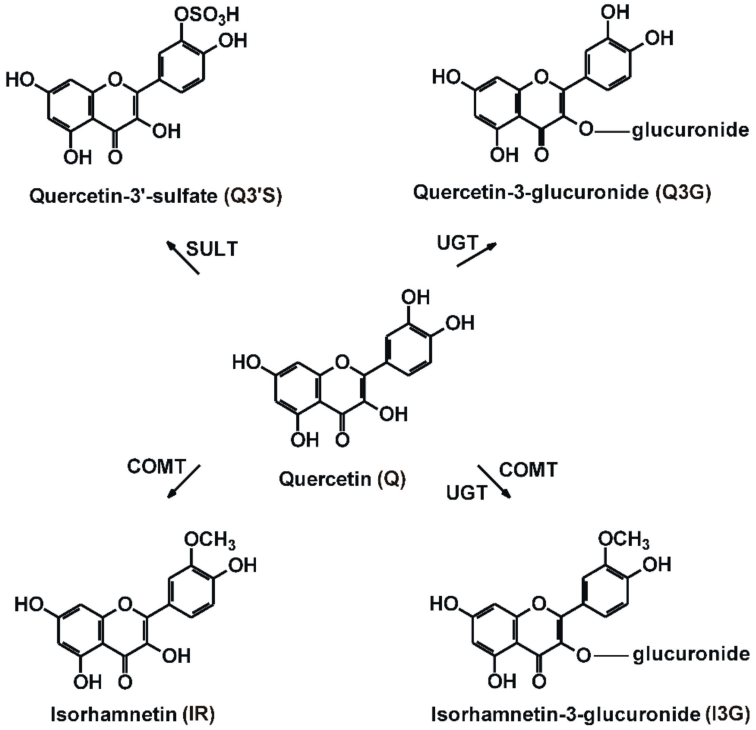

Figure 1. Chemical structures of quercetin (Q), quercetin-3'-sulfate (Q3'S), quercetin-3-glucuronide (Q3G), isorhamnetin (IR), and isorhamnetin-3-glucuronide (I3G). (COMT, catechol-*O*-methyltransferase; SULT, sulfotransferase; UGT, uridine 5'-diphospho-glucuronosyltransferase).

2. Materials and Methods

2.1. Reagents

CypExpress^{TM} 2C19, 2D6 and 3A4 human kits, quercetin (Q), ticlopidine hydrochloride, quinidine, testosterone, 6β-hydroxytestosterone, ketoconazole, fetal bovine serum (FBS), glutamine, penicillin, streptomycin, pyranine (trisodium 8-hydroxypyrene-1,3,6-trisulfonate), bromosulfophthalein, sulforhodamine 101, sodium orthovanadate, probenecid, 5(6)-carboxy-2',7'-dichlorofluorescein (CDCF), lucifer yellow (LY), and benzbromarone were purchased from Sigma-Aldrich (St. Louis, MO, USA). Nicotinamide adenine dinucleotide phosphate sodium salt ($NADP^+$), and glucose-6-phosphate barium salt (G6P) were from Reanal (Budapest, Hungary). S-mephenytoin, 4-hydroxymephenytoin, dextromethorphan, and dextrorphan were obtained from Carbosynth (Berkshire, UK). Isorhamnetin (IR) and Ko143 were purchased from Extrasynthese (Genay Cedex, France) and Tocris Bioscience (Bristol, UK), respectively. Quercetin-3'-sulfate (Q3'S), quercetin-3-glucuronide (Q3G), and isorhamnetin-3 -glucuronide (I3G) were synthetized as described previously [46].

2.2. CYP Assays

The in vitro inhibitory effects of Q and its conjugates on CYP enzymes were tested, using CypExpress™ Cytochrome P450 human kits (Sigma-Aldrich, St. Louis, MO, USA). Each experiment included solvent controls (DMSO did not exceed 0.6 *v*/*v*%). In CYP2C19, 2D6, and 3A4 assays, Food and Drug Administration (FDA)-recommended substrates (S-mephenytoin, dextromethorphan, and testosterone, respectively) and positive controls (ticlopidine, quinidine, and ketoconazole, respectively) were employed.

Inhibition of CYP2C19 [47], 3A4 [48], and 2D6 [49] by Q and its conjugates was tested based on our previously reported methods, without modifications.

2.3. HPLC Analyses

Substrates and the formed metabolites were analyzed by a HPLC system built up from a Waters 510 pump (Milford, MA, USA), a Rheodyne 7125 injector with a 20-µL sample loop (Berkeley, CA, USA), and a Waters 486 UV-detector (Milford, MA, USA). Data were evaluated employing a Waters Millennium Chromatography Manager (Milford, MA, USA).

S-mephenytoin and 4-hydroxymephenytoin (CYP2C19 assay), testosterone and 6β-hydroxytestosterone (CYP3A4 assay), as well as dextromethorphan and dextrorphan (CYP2D6 assay) were quantified using the previously described methods [47–49], with minor modifications. Representative chromatograms are demonstrated in Figure S1.

In CYP2C19 assay, the mobile phase contained acetonitrile, methanol (VWR), and sodium phosphate buffer (10 mM, pH 4.55) (17:10:73 *v*/*v*%). Samples were driven through a guard column (Phenomenex Security Guard C8, 4.0 × 3.0 mm) linked to an analytical column (Phenomenex C8 100 × 4.6 mm; 2.6 µm), with a 1 mL/min flow rate, at room temperature. After the isocratic elution, S-mephenytoin and 4-hydroxymephenytoin were detected at 230 nm.

In the CYP3A4 assay, samples were driven through a guard column (Security Guard™ Catridge C18 4.0 × 3.0 mm; Phenomenex, Torrance, CA, USA) linked to an analytical column (Kinetex C18 150 × 4.6 mm; 5 µm; Phenomenex, Torrance, CA, USA), with a 1.2 mL/min flow rate, at room temperature. The mobile phase contained methanol (VWR, Budapest, Hungary), water, and acetic acid (53:46:1 *v*/*v*%). After the isocratic elution, testosterone and 6β-hydroxytestosterone were detected at 240 nm.

In the CYP2D6 assay, samples were driven through a guard column (Security Guard C8, 4.0 × 3.0 mm; Phenomenex, Torrance, CA, USA) linked to an analytical column (Mediterranea Sea8 C8 150 × 4.6 mm; 5 µm; Teknokroma, Barcelona, Spain). The isocratic elution was performed with 1 mL/min flow rate at room temperature, the mobile phase contained acetonitrile and 6.9 mM sodium-acetate buffer (pH 4.0) (31:69 *v*/*v*%). Dextromethorphan and dextrorphan were detected at 280 nm.

2.4. OATP Overexpressing Cell Lines and OATP Interaction Tests

A431 cells overexpressing human OATPs, 1A2 (BC042452, HsCD00333163), 1B1 (Gene ID: AB026257), 1B3 (BC141525, HsCD00348132) or 2B1 (BC041095.1, HsCD00378878), or their mock transfected controls, were generated as previously described [50,51]. Cells were cultured in Dulbecco's Modified Eagle Medium (DMEM; Thermo Fischer Scientific, Waltham, MA, USA) supplemented with 10% fetal bovine serum, 2 mM L-glutamine, 100 units/mL penicillin and 100 µg/mL streptomycin, at 37 °C with 5% CO_2.

The interaction between flavonoids and OATPs was investigated in an indirect assay [50] employing the fluorescent dye substrates, pyranine and sulforhodamine 101 [51,52]. Briefly, A431 cell overexpressing OATPs, 1A2, 1B1, 1B3 or 2B1, or their mock transfected controls [50,51], were seeded on 96-well plates in a density of $8x10^4$ cells/well in 200 µL DMEM one day prior to the transport measurements. The next day, the medium was removed, then cells were washed three times with 200 µL

phosphate-buffered saline (PBS, pH 7.4) and pre-incubated with 50 µL uptake buffer (125 mM NaCl, 4.8 mM KCl, 1.2 mM $CaCl_2$, 1.2 mM KH_2PO_4, 12 mM $MgSO_4$, 25 mM MES (2-(N-morpholino)ethanesulfonic acid), and 5.6 mM glucose, pH 5.5) with or without increasing concentrations of the flavonoids at 37°C. Each test compound was dissolved in DMSO (that did not exceed 0.5 *v*/*v*% in samples), and solvent controls were also applied. The reaction was started by the addition of 50 µL uptake buffer containing pyranine in a final concentration of 10 µM (OATP1B1) or 20 µM (OATP1B3 and OATP2B1), or 0.5 µM sulforhodamine 101 (OATP1A2). Thereafter, cells were incubated at 37°C for 15 min (OATP1B1 and OATP2B1), 10 min (OATP1A2), or 30 min (OATP1B3). The reactions were stopped by removing the supernatants, then the cells were washed three times with ice-cold PBS. Fluorescence (in 200 µL PBS/well) was determined employing an Enspire plate reader (Perkin Elmer, Waltham, MA) ex/em: 403/517 nm (pyranine) or 586/605 nm (sulforhodamine 101). OATP-dependent transport was calculated by extracting fluorescence measured in mock transfected cells. Transport activity was calculated based on the fluorescence signal in the absence (100%) of flavonoids. Experiments were repeated at least in three biological replicates. IC_{50} values were calculated by Hill1 fit, using the Origin Pro8.6 software (GraphPad, La Jolla, CA, USA).

2.5. Transport Activity Measurements for MRP2 and BCRP Transporters

Experiments were performed in insect membrane vesicles, as describe previously [53–57]. Human BCRP and MRP2 were expressed in Sf9 insect cells by baculoviruses. At the third day of infection, cells were collected and membrane vesicles were obtained by mechanical disruption and differential centrifugation. To get full activity for BCRP, the cholesterol levels of the vesicles were adjusted to the level of mammalian membranes [57]. Vesicles were stored at -80°C, total protein content of preparations was measured by the Lowry method (used as a reference of the quantity). Membrane vesicles (50 µg protein/sample) were incubated at 37 °C for 10 min (without or with 4 mM of Mg-ATP) in 50 µL volume, in the presence of transporter specific fluorescent substrates (10 µM lucifer yellow (LY) for BCRP and 5 µM 5(6)-Carboxy-2′,7′-dichlorofluorescein (CDCF) for MRP2). Quality of membrane vesicles was confirmed applying known reference inhibitors (benzbromarone and Ko143). ATP dependent uptake of fluorescent substrates was examined in the presence of flavonoids (up to 50–200 µM). Each compound was dissolved in DMSO and solvent controls were applied in all experiments. Under the applied conditions (DMSO did not exceed 2 *v*/*v*% final concentration), it did not affect the measurements. After incubation, samples were rapidly filtered and washed on filter plate (MSFBN6B10, Millipore, Burlington, MA, USA). Accumulated substrates in vesicles were solved back from the filter by 100 µL of 10% sodium dodecyl sulfate and centrifuged into another plate. A 100-µL volume of fluorescence stabilizer was added to the samples (DMSO for LY, and 0.1 M NaOH for CDCF). Fluorescence of samples was measured by a plate reader (Victor X3 Perkin-Elmer, Waltham, MA, USA) at appropriate wavelengths (filters were λ_{ex} = 405 nm and λ_{em} = 535 nm for LY as well as λ_{ex} = 492 nm and λ_{em} = 635 nm for CDCF). ABC related transport was calculated by subtracting passive uptake measured without Mg-ATP (with Mg-AMP the same background was detected) from values measured in the presence of Mg-ATP. Under the applied circumstances, we did not observe considerable quenching effects of flavonoids.

2.6. ATPase Activity Assays for BCRP Transporter Interaction

ATPase activity was measured on Sf9 membrane vesicles containing human BCRP prepared as described in 2.5. Appropriate amounts of vesicles (10 µg/50 µL) were used in the assays. Experimental parameters were the same as it has been earlier reported [53–57]. Membrane vesicles were incubated with 3 mM of Mg-ATP for 25 min at 37 °C. Effects of flavonoids were investigated up to 50 µM. Solvent controls were applied in each experiment (DMSO concentration was 2 *v*/*v*% in all samples, which did not modify basal activity). ABC transporter function was determined as vanadate sensitive ATPase activity. Liberated inorganic phosphate was measured by a colorimetric reaction as described [53]. Absorbance of samples was measured after 25 min at 660 nm.

2.7. Statistics

Data represent means ± standard error of the mean (SEM) values. Statistical analyses were performed employing one-way ANOVA ($p < 0.01$) with a Tukey's post-hoc test (IBM SPSS Statistics, Armonk, NY, USA).

3. Results

3.1. Inhibition of CYP Enzymes by Q and Its Conjugates

The effects of flavonoids (and positive controls) on CYP enzymes are summarized in Figure 2. Each compound tested induced concentration-dependent inhibition of CYP2C19 and 3A4 activity. Q conjugates proved to be similarly strong inhibitors of these enzymes to the parent compound, while their inhibitory effects were considerably weaker compared to the positive controls. Flavonoids showed significant ($p < 0.01$) inhibitory effects on CYP2C19 and 3A4 at 5 to 20 μM concentrations (one- to four-fold concentration vs. The substrates). In the presence of 30 μM flavonoid concentrations, approximately 25% to 35% and 30% to 45% decreases in metabolite formation were observed in CYP2C19 (Figure 2A) and CYP3A4 (Figure 2B) assays, respectively. Thus, under the applied conditions, Q and its metabolites failed to induce 50% or larger inhibitory effects on CYP2C19 and 3A4. The interaction of Q and its conjugates with CYP2D6 was also tested; however, no significant inhibition was noticed, even in the presence of 30 μM flavonoid concentrations (Figure 2C).

3.2. Inhibition of OATP Activity by Q and Its Conjugates

Inhibitory effects of flavonoids on OATP-mediated dye uptake are summarized in Figure 3. Each flavonoid examined induced a concentration dependent inhibition of OATP1A2 activity: Q3'S and Q showed the strongest impacts (IC_{50} values were 4.9 and 10.1 μM, respectively), while other Q metabolites (Q3G, IR, and I3G) proved to be weak inhibitors of this transporter (Figure 3A). We observed a potent inhibition of OATP1B1 by each flavonoid (Figure 3B), showing low micromolar (Q, Q3G, IR, and I3G) or even nanomolar (Q3'S) IC_{50} values (Table 1). Q conjugates were similarly strong inhibitors of OATP1B3 to the parent compound, each flavonoid caused a 50% decrease in transport activity at low micromolar concentrations (Figure 3C). The IC_{50} values of Q, Q3'S, and IR were in the submicromolar range for OATP2B1 (Table 1). Furthermore, glucuronides (Q3G and I3G) were also strong inhibitors of OATP2B1, with approximately 4 to 5 μM IC_{50} (Figure 3D). Generally, Q3'S was the most potent and glucuronides (Q3G/I3G) were the least effective inhibitors of the OATPs tested (Table 1). Nevertheless, the IC_{50} values of Q3G and I3G were close to 5 μM regarding OATPs 1B1, 1B3, and/or 2B1.

Table 1. IC_{50} values of flavonoids for CYP2C19, CYP3A4, OATPs, BCRP, and MRP2.

Proteins	Q	Q3'S	Q3G	IR	I3G
	IC_{50} (μM)	IC_{50} (μM)	IC_{50} (μM)	IC_{50} (μM)	IC_{50} (μM)
CYP2C19	>30.0	>30.0	>30.0	>30.0	>30.0
CYP3A4	>30.0	>30.0	>30.0	>30.0	>30.0
OATP1A2	10.1	4.92	>30.0	>30.0	>30.0
OATP1B1	1.55	0.33	4.05	3.12	5.63
OATP1B3	3.22	2.50	5.71	3.10	9.62
OATP2B1	0.34	0.43	4.85	0.82	4.14
BCRP	0.13	3.20	13.5	0.06	>30
MRP2	>30.0	19.6	24.2	>30.0	14.9

Data were calculated based on measurements demonstrated in Figures 2–4. Q, quercetin; Q3'S, quercetin-3'-sulfate; Q3G, quercetin-3-glucuronide; IR, isorhamnetin; I3G, isorhamnetin-3-glucuronide.

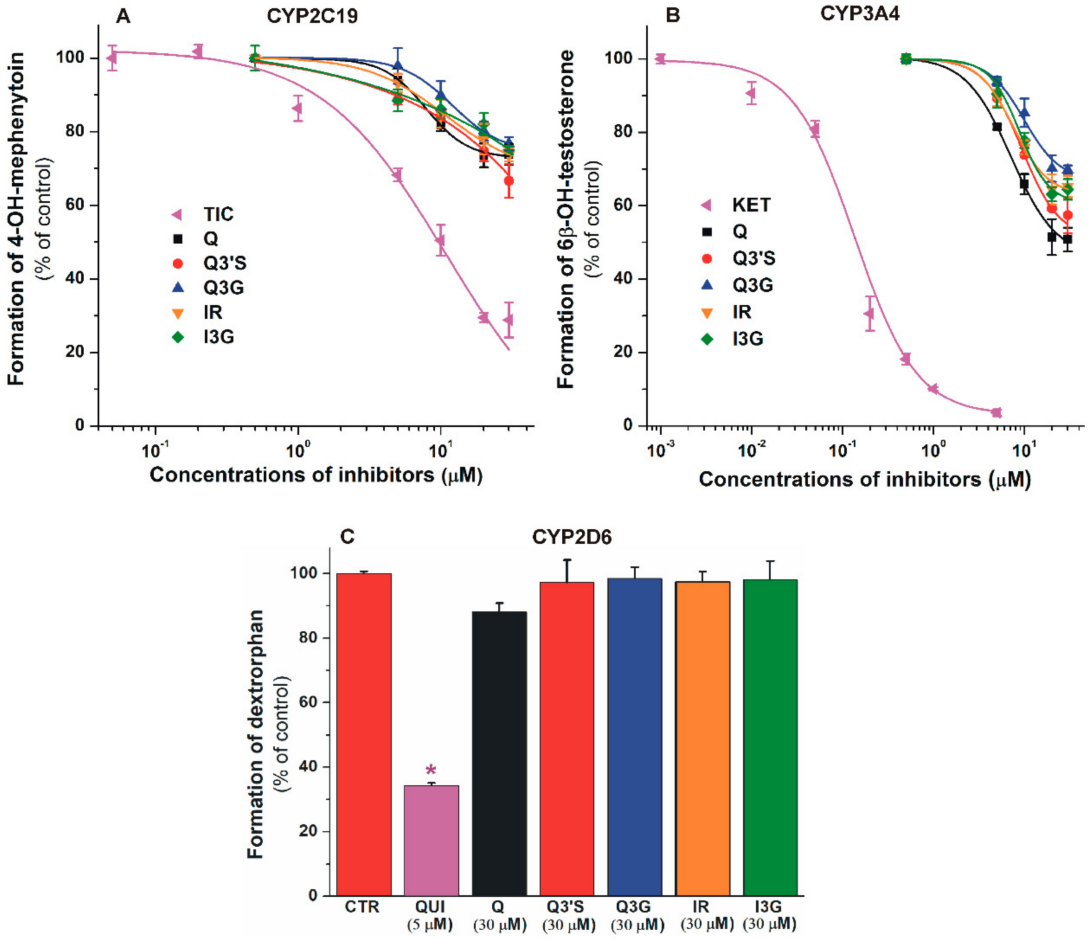

Figure 2. Inhibitory effects of Q, Q3'S, Q3G, IR, I3G, and positive controls on cytochrome P450 (CYP)2C19 (**A**), 3A4 (**B**), and 2D6 ((**C**); * $p < 0.01$) enzymes. Inhibition of CYP2C19-catalyzed S-mephenytoin hydroxylation (positive control: ticlopidine, TIC; IC_{50} = 4.3 μM), CYP3A4-catalyzed testosterone hydroxylation (positive control: ketoconazole, KET; IC_{50} = 0.2 μM), and CYP2D6-catalyzed dextromethorphan *O*-demethylation (positive control: quinidine, QUI; IC_{50} = 0.2 μM) by flavonoids (substrate concentrations: 5 μM in each assay). CYP2C19: statistically significant ($p < 0.01$) decrease in metabolite formation was induced by 5 μM of TIC, 10 μM of Q, and 20 μM of Q3'S, Q3G, IR, and I3G. CYP3A4: statistically significant ($p < 0.01$) decrease in metabolite formation was induced by 0.05 μM of KET, 5 μM of Q, 20 μM of Q3G, and 10 μM of Q3'S, IR, and I3G (Q, quercetin; Q3'S, quercetin-3'-sulfate; Q3G, quercetin-3-glucuronide; IR, isorhamnetin; I3G, isorhamnetin-3-glucuronide).

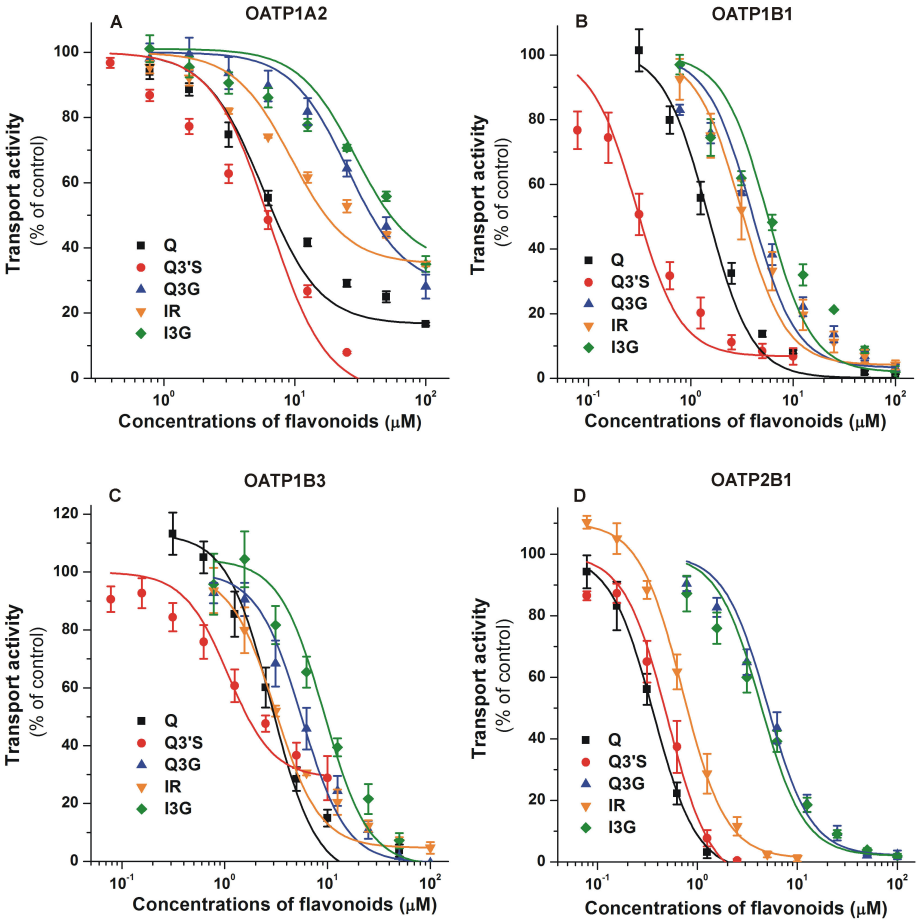

Figure 3. Concentration-dependent inhibitory effects of Q, Q3′S, Q3G, IR, and I3G on the transporter functions of organic anion-transporting polypeptides: OATP1A2 (**A**), OATP1B1 (**B**), OATP1B3 (**C**), and OATP2B1 (**D**). Uptake of pyranine (10 μM for OATP1B1, and 20 μM for OATP1B3 and OATP2B1) or 0.5 μM sulforhodamine 101 (OATP1A2) was measured in A431 cells overexpressing OATPs 1A2, 1B1, 1B3, or 2B1 in the presence of increasing concentrations of the flavonoids for 10 (OATP1A2), 15 (OATP1B1 and OATP2B1), or 30 min (OATP1B3). Fluorescence measured in mock transfected controls was subtracted from the values measured in A431-OATP cells. Fluorescence determined in the absence of the flavonoids was set as 100 %. Mean ± standard error of the mean (SEM) values were obtained from three biological replicates. Regarding Q3′S, we did not use concentrations above 20 μM, since higher levels of Q3′S exhibited fluorescence that interfered with the signal of the test substrate pyranine. The effects of bromosulfophthalein (positive control) on OATPs in the same experimental models have been previously reported [49,51]. OATP1A2: statistically significant ($p < 0.01$) inhibition was caused by 3.1 μM of Q, 0.8 μM of Q3′S, 25 μM of Q3G, 3.1 μM of IR, and 12.5 μM of I3G. OATP1B1: statistically significant ($p < 0.01$) inhibition was induced by 1.3 μM of Q, 0.3 μM of Q3′S, 1.6 μM of Q3G, 3.1 μM of IR, and 1.6 μM of I3G. OATP1B3: statistically significant ($p < 0.01$) inhibition was caused by 2.5 μM of Q, 1.3 μM of Q3′S, 3.1 μM of Q3G, 3.1 μM of IR, and 6.3 μM of I3G. OATP2B1: statistically significant ($p < 0.01$) inhibition was induced by 0.3 μM of Q, 0.3 μM of Q3′S, 3.1 μM of Q3G, 0.6 μM of IR, and 1.6 μM of I3G (Q, quercetin; Q3′S, quercetin-3′-sulfate; Q3G, quercetin-3-glucuronide; IR, isorhamnetin; I3G, isorhamnetin-3-glucuronide).

3.3. *Effects of Q and Its Conjugates on ABC Transporters*

To test the influence of Q and its conjugates on the transport activity of BCRP and MRP2, vesicular uptake measurements were performed with the fluorescent substrates LY (BCRP) and CDCF (MRP2). The inhibitory effects of flavonoids are demonstrated in Figure 4. The specificity of transports were confirmed employing reference inhibitors, namely benzbromarone for MRP2 and Ko143 for BCRP (data

not shown). Since we observed a small background during CDCF transport (MRP2) measurements, mock membrane data for Q3G are also presented (Figure 4B; data for the other compounds were identical, and are not shown). Both BCRP- and MRP2-mediated transport activities were significantly inhibited by the flavonoids tested. Q and IR proved to be potent inhibitors of BCRP, followed by Q3'S which also showed strong inhibition, whereas glucuronides (Q3G and I3G) can be classified as weak inhibitors (Figure 4A). In contrast, MRP2 showed the strongest interactions with glucuronide and sulfate conjugates, while Q and IR were less effective inhibitors (Figure 4B).

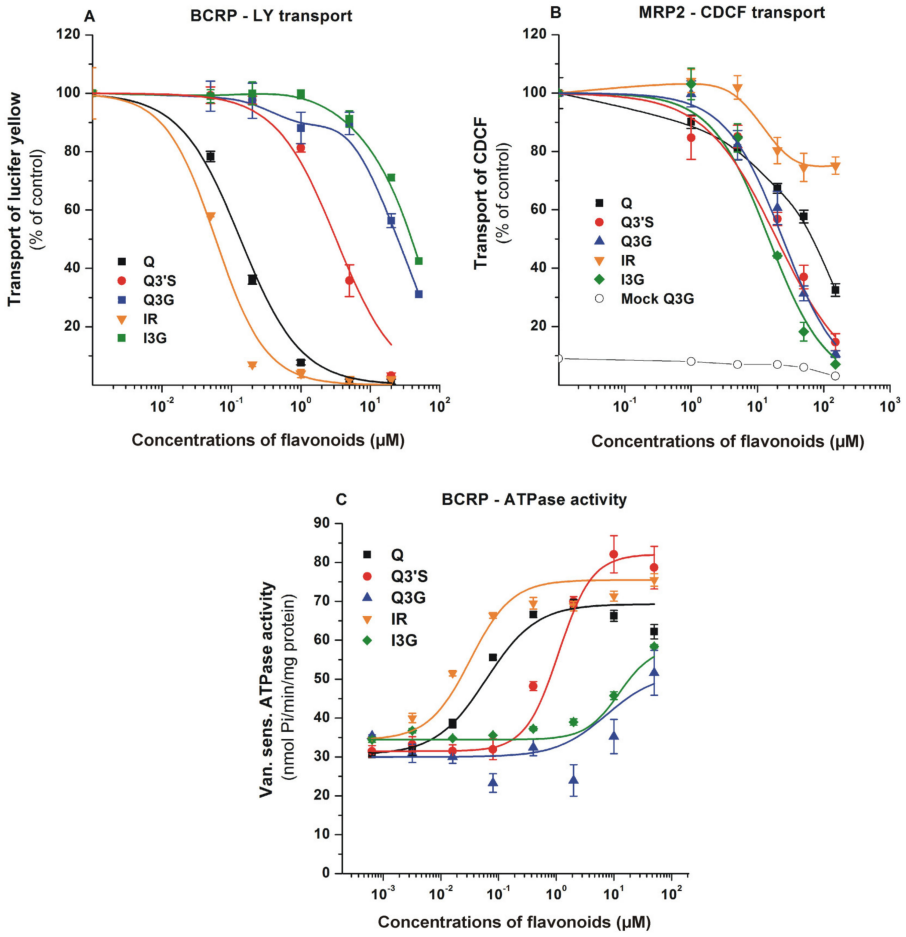

Figure 4. Effects of Q and its metabolites on BCRP and MRP2. BCRP transporter function was measured in human transporters containing inverted insect cell membrane vesicles. Transport activity was characterized by vesicular uptake of a specific fluorescent substrate (lucifer yellow (LY) for ABCG2 and 5(6)-carboxy-2′,7′-dichlorofluorescein (CDCF) for MRP2), where the transport by the ABC transporter is defined as ATP dependent uptake of the substrate into the vesicles. Vanadate sensitive ATPase activity of BCRP was measured by detecting inorganic, deliberated phosphate in a colorimetric reaction. (**A**) Effects of flavonoids on the transport of LY by BCRP. Statistically significant ($p < 0.01$) decrease in transport was induced by 0.05 μM of Q, 0.2 μM of Q3'S, 1.0 μM of Q3G, 0.05 μM of IR, and 20 μM of I3G. (**B**) Effects of flavonoids on the transport of CDCF by MRP2. Flavonoid-induced impacts were tested on mock membranes as well, data in the presence of Q3G are demonstrated (data for other flavonoids were identical). Statistically significant ($p < 0.01$) decrease in transport was caused by 20 μM of each flavonoid. (**C**) Changes in the ATPase activity of BCRP in the presence of flavonoids. Statistically significant ($p < 0.01$) increase in ATPase activity was induced by 0.08 μM of Q, 0.4 μM of Q3'S, 50 μM of Q3G, 0.02 μM of IR, and 10 μM of I3G. Mean ± SEM values were obtained from three biological replicates (Q, quercetin; Q3'S, quercetin-3'-sulfate; Q3G, quercetin-3-glucuronide; IR, isorhamnetin; I3G, isorhamnetin-3-glucuronide).

Since Q and some of its metabolites were potent inhibitors of BCRP, we also examined BCRP ATPase activity in the presence of flavonoids. BCRP ATPase activity was stimulated by Q and its metabolites (Figure 4C), suggesting that these flavonoids can be substrates and not only inhibitors of the transporter. In good accordance with the transport assay, highest affinity was observed with IR and Q (K_m = 0.03 and 0.13 μM, respectively). However, glucuronides showed activation only at high concentrations (100 μM). Based on these observations, both BCRP and MRP2 interact with the Q metabolites investigated.

4. Discussion

Based on previously reported positive effects of Q (as an anti-oxidant, anti-inflammatory, and cardioprotective agent), Q-containing dietary supplements are widely marketed through the Internet, and high intake of Q may interfere with drug therapy [2,3,13]. Therefore, there is an urgent need for the deeper understanding of drug interactions regarding Q and its metabolites. In human studies, the pharmacokinetics of certain medications was not affected by Q, while other reports demonstrated that even a single dose of Q can alter the bioavailability of several drugs [2]. As a result of the oral administration of high doses of Q (1500 mg daily for a week) to human subjects, C_{max} and $AUC_{0-\infty}$ values of midazolam were declined [58], likely due to the increased CYP3A4-catalyzed elimination of the drug. Furthermore, after seven days treatment with 500 mg Q daily, the oral bioavailability of fexofenadine was significantly increased [59], presumably because of the inhibition of P-gp. However, both single and repeated treatment with Q (1500 mg/day) reduced C_{max} and $AUC_{0-\infty}$ values of talinolol in human volunteers [60]. Authors suggested the interactions of Q with both efflux (e.g., P-gp) and uptake (e.g., OATP) transporters; thus, the inhibition of OATP-mediated absorption of talinolol seems to be the dominant mechanism.

The inhibitory effect of Q on CYP enzymes has been reported in several studies, however, some of these results are inconsistent. Previous reports suggest strong [11] or weak [61,62] inhibitory effects of Q on the CYP2C19-catalyzed S-mephenytoin hydroxylation. Furthermore, the significant inhibitory action of Q on CYP3A4-catalyzed midazolam [11] and testosterone [16] hydroxylation has also been demonstrated. In agreement with our current results (Figure 2C), moderate or negligible effects of Q on CYP2D6-mediated bufuralol hydroxylation [11,61] and dextromethorphan *O*-demethylation [62] have been described. In HEK293 cells (overexpressing the respective CYP enzyme), Q inhibited CYP1A1 and 1B1 enzymes, while it did not show relevant inhibition on CYP3A4 and 2D6 [63]. In a few studies, the effects of IR on CYP enzymes have also been examined. Previous in vitro studies regarding CYP3A4 showed controversial results: IR inhibited testosterone hydroxylation (recombinant, human CYP3A4) [16] and 7-benzyloxy-4-trifluoromethylcoumarin *O*-dealkylation (in hepatic microsomes from male and female pigs) [64], while it did not affect 7-benzyloxy-4-trifluoromethylcoumarin *O*-demethylation (tested with both recombinant CYP3A4 and human liver microsomes) [65]. In a recent study, IR did not show an inhibitory effect on the CYP2D6-catalyzed *O*-demethylation of dextromethorphan in vitro [66]. Based on our results, Q and its conjugates are weak inhibitors of CYP2C19 and 3A4, while they did not affect the CYP2D6 enzyme (Figure 2). Therefore, it does not seem likely that Q strongly influences the biotransformation of drugs eliminated via CYP2C19, 3A4, and/or 2D6 enzymes. Nevertheless, a milder inhibition regarding CYP2C19- and/or CYP3A4-mediated elimination of certain drugs cannot be excluded, since not only Q but its metabolites can also exert moderate inhibition on these enzymes. This hypothesis is supported by the report of Bedada and Neerati [67] where the administered Q (500 mg twice daily for 10 days) significantly decreased the CYP2C9-mediated elimination of diclofenac in healthy human subjects, despite the observations in a previous in vitro study that Q and some of its conjugates (Q3'S, IR, and tamarixetin) were only weak inhibitors of the enzyme and glucuronides (Q3G and I3G) did not affect CYP2C9 activity [14]. Previous studies showed the similar or stronger interactions of methyl and sulfate metabolites of Q with xanthine oxidase enzyme [68] and human serum albumin [14,69]

compared to the parent compound. Furthermore, Q sulfates and glucuronides showed potent inhibitory effects on organic anion transporters (OAT1 and OAT3) [70].

Transporters of the ABC and OATP family are key participants in the absorption, distribution and elimination of a wide array of chemically diverse compounds. OATP2B1 and OATP1A2 (expressed in enterocytes) may be involved in the absorption of orally consumed/administered flavonoids. Indeed, Duan and colleagues showed transcellular transport of IR, which was inhibited by estrone-3-sulfate (a known substrate of OATPs) [30]. Some other studies suggest the involvement of OATP2B1 and/or other OATPs (1B1/1B3) in the uptake of Q into Caco-2 and HepG2 cells, respectively [43,71]. In addition, Glaeser and colleagues demonstrated direct cellular uptake of radiolabeled Q into HEK-293 cells overexpressing OATPs 1A2, 2A1, 2B1, 1B1, 1B3, 3A1, and 5A1 [29]. Based on these data, OATPs 1B1, 1B3, and 2B1 may contribute to the hepatic uptake then elimination of flavonoids and their conjugates. Furthermore, OATPs 1A2 and 2B1 may also influence the penetration of flavonoids through the blood–brain barrier [25]. A previous study failed to confirm the involvement of OATPs in the uptake of quercetin-7-glucuronide and Q3G into HepG2 cells [72]; however, in this study, the expression of OATPs in HepG2 cells was not confirmed. Wong and colleagues described the OATP4C1-mediated uptake of Q metabolites, including Q3G and Q3'S, into HepG2 cells [70]; nevertheless, this transporter is not a typical OATP in the liver. Therefore, the role of OATPs in the cellular uptake of Q metabolites is not clearly understood yet. Certain food components can influence the function of OATPs and are able to alter the pharmacokinetics of OATP substrate drugs. As a matter of fact, apple, grapefruit, and orange juices are potent inhibitors of intestinal OATP2B1 and OATP1A2, and cause clinically relevant food–drug interactions [19]. In vivo data also show that Q influences the pharmacokinetics of the OATP substrate pravastatin [73]. Herein, we demonstrated that Q and its conjugates can inhibit multispecific OATPs (1B1, 1B3, and 2B1) at submicromolar or low micromolar concentrations (Table 1). Furthermore, Q3'S is a potent inhibitor of OATPs 1B1 and 2B1, because its nanomolar concentrations can strongly decrease transport activities. Similarly, submicromolar IC_{50} values of Q and IR were noticed for OATP2B1. The only exception among OATPs was OATP1A2, which is weakly inhibited by Q, Q3G, IR, and I3G. This latter observation is in good agreement with our recent study, showing that chrysin and its sulfate/glucuronide metabolites are weak inhibitors of OATP1A2, while chrysin conjugates proved to be strong inhibitors of OATPs 1B1, 1B3, and 2B1 [49]. In addition, our data confirm the previous findings obtained with [^{3}H]-bromosulfophthalein, [^{3}H]-estrone-3-sulfate, and atorvastatin as test substrates [20,73]. On the other hand, these are the first results which demonstrate that sulfate and glucuronic acid conjugates of Q and/or IR can strongly inhibit OATP-mediated transport. Based on previous clinical studies, Q3'S, Q3G, and I3G can achieve high nanomolar or even micromolar concentrations in human circulation [6–8], suggesting that these metabolites may be able to induce a relevant inhibition of OATP-mediated uptake of certain compounds from the blood into tissues (e.g., liver and/or brain). Furthermore, some Q conjugates seem to be excreted to the intestinal lumen by ABC transporters from enterocytes and/or through bile [1]; therefore, both the parent compound and its metabolites may appear in the intestinal lumen, and consequently may be able to interfere with the OATP-driven absorption of other compounds. Considering the above-listed data, high intake of Q may affect the OATP-mediated transport (e.g., absorption, hepatic uptake, or blood-brain barrier penetration) of certain drugs. On the other hand, some toxins (e.g., alpha-amanitin and ochratoxin A) are also taken up by OATP transporters into hepatocytes [21,22]; therefore, it is reasonable to hypothesize that circulating Q conjugates may decrease the hepatic uptake of these toxins.

ABC multidrug transporters are responsible for extrusion of drugs and metabolites at the apical surface of cells in important tissue barriers. Studies on the transport of fluorescent or radioactive probe substrates in polarized epithelial cells and transporter overexpressing cell lines showed that P-gp-, BCRP-, and MRP2-related transports are inhibited by Q. In monolayers, selective inhibitors were applied to show the protein specified inhibitions [38,40,74]. Based on blood–brain barrier penetration and monolayer cell experiments, Q seems to be transported by BCRP and MRP2 [40,41,43,74,75]. Although the interactions of certain Q conjugates with BCRP and MRP2 have

been reported [27,30,42,44,72,76,77], the characterization of inhibition/transport is far from complete. In the current study, the comparison of IC_{50} values of Q and its metabolites in vesicular transport assay was suitable to reveal the differences in the strength of interactions between ABC transporters and Q derivatives. Both BCRP- and MRP2-mediated transport activities were significantly inhibited by each Q metabolite tested; however, the order of their inhibitory potency were different for these ABC transporters. Q and IR proved to be the most potent inhibitors of BCRP with nanomolar IC_{50} values, and Q3'S also showed strong inhibitory effect at low micromolar concentrations (Table 1). Similarly, the transport-coupled ATPase activity of BCRP was significantly stimulated by low concentrations of Q, IR, and Q3'S (Figure 4C). The same trends and similar concentration dependence were observed in ATPase and transport assays, suggesting that not only Q but its conjugates may be substrates of BCRP. However, direct transport measurements are necessary to confirm this hypothesis. For MRP2, IC_{50} data are higher by an order of magnitude than for BCRP. This difference is generally observed with many other substrates [40,78]. MRP2 is known to expel glucuronide and sulfate conjugates from the cells, whereas hydrophobic compounds are less effectively transported by MRP2. Our current results are in harmony with these previous observations. We found weaker interactions of Q and IR with MRP2 compared to glucuronide and sulfate conjugates. Considering the strong inhibition of BCRP by Q, IR, and Q3'S, it is reasonable to hypothesize that the simultaneous administration of Q may affect the BCRP-mediated transport of some drugs.

In summary, the current study underlines the potent interactions of Q conjugates with pharmacologically important proteins. Considering the above-listed data, Q and/or its metabolites may cause clinically relevant interactions with certain biotransformation enzymes and drug transporters. Therefore, the simultaneous administration of high dose Q-containing dietary supplements with drugs should be carefully considered.

Supplementary Materials: The following are available online at http://www.mdpi.com/2072-6643/12/8/2306/s1, Figure S1: Representative chromatograms of S-mephenytoin and 4-hydroxymephenytoin (CYP2C19 assay), dextromethorphan and dextrorphan (CYP2D6 assay) as well as testosterone and 6β-hydroxytestosterone (CYP3A4 assay) (each 2.5 μM).

Author Contributions: M.P., C.Ö.-L., and Á.T. conceived the study. M.P., V.M., C.Ö.-L., and Á.T. wrote the paper. V.M. performed CYP assays, E.F.-N. carried out HPLC analyses. O.U. examined the effects of flavonoids on OATP activity, K.K. tested the influence of quercetin and its metabolites on ABC transporters. Sulfate and glucuronide metabolites of quercetin were synthetized by P.W.N. and P.A.K. All authors have read and agreed to the published version of the manuscript.

Funding: The project has been supported by the European Union, co-financed by the European Social Fund (EFOP-3.6.1.-16-2016-00004; M.P., V.M., and E.F.-N.), by the ÚNKP-19-3-IV-PTE-164 New National Excellence Program of the Ministry for Innovation and Technology (E.F.-N.), and by the National Research, Development and Innovation Office (OTKA FK 128751; Cs.Ö-L). P.A.K. and P.W.N. gratefully acknowledge the support of the Biotechnology and Biological Sciences Research Council (BBSRC) and the funding of the Institute Strategic Programme Food Innovation and Health BB/R012512/1 and its constituent projects BBS/E/F/000PR10346 and BBS/E/F/000PR10347.

Acknowledgments: The authors thank to Katalin Fábián for her excellent assistance in the experimental work. The work of Cs.Ö-L. was supported by the János Bolyai Research Scholarship of the Hungarian Academy of Sciences.

Conflicts of Interest: The authors declare no conflict of interest.

References

1. Guo, Y.; Bruno, R.S. Endogenous and Exogenous Mediators of Quercetin Bioavailability. *J. Nutr. Biochem.* **2015**, *26*, 201–210. [CrossRef]
2. Andres, S.; Pevny, S.; Ziegenhagen, R.; Bakhiya, N.; Schäfer, B.; Hirsh-Ernst, K.I.; Lampen, A. Safety Aspects of the Use of Quercetin as a Dietary Supplement. *Mol. Nutr. Food Res.* **2018**, *62*, 1700447. [CrossRef] [PubMed]

3. Vida, R.G.; Fittler, A.; Somogyi-Végh, A.; Poór, M. Dietary quercetin supplements: Assessment of online product informations and quantitation of quercetin in the products by high-performance liquid chromatography. *Phytother. Res.* **2019**, *33*, 1912–1920. [CrossRef] [PubMed]
4. Egert, S.; Wolffram, S.; Bosy-Westphal, A.; Boesch-Saadatmandi, C.; Wagner, A.E.; Frank, J.; Rimbach, G.; Mueller, M.J. Daily quercetin supplementation dose-dependently increases plasma quercetin concentrations in healthy humans. *J. Nutr.* **2008**, *138*, 1615–1621. [CrossRef] [PubMed]
5. Conquer, J.A.; Maiani, G.; Azzini, E.; Raguzzini, A.; Holub, B.J. Supplementation with quercetin markedly increases plasma quercetin concentration without effect on selected risk factors for heart disease in healthy subjects. *J. Nutr.* **1998**, *128*, 593–597. [CrossRef] [PubMed]
6. Day, A.J.; Mellon, F.; Barron, D.; Sarrazin, G.; Morgan, M.R.; Williamson, G. Human metabolism of dietary flavonoids: Identification of plasma metabolites of quercetin. *Free Radic. Res.* **2001**, *35*, 941–952. [CrossRef]
7. Mullen, W.; Edwards, C.A.; Crozier, A. Absorption, excretion and metabolite profiling of methyl-, glucuronyl-, glucosyl- and sulpho-conjugates of quercetin in human plasma and urine after ingestion of onions. *Br. J. Nutr.* **2006**, *96*, 107–116. [CrossRef]
8. Cialdella-Kam, L.; Nieman, D.C.; Sha, W.; Meaney, M.P.; Knab, A.M.; Shanely, R.A. Dose–response to 3 months of quercetin-containing supplements on metabolite and quercetin conjugate profile in adults. *Br. J. Nutr.* **2012**, *109*, 1923–1933. [CrossRef]
9. Kaushik, D.; O'Fallon, K.; Clarkson, P.M.; Dunne, C.P.; Conca, K.R.; Michniak-Kohn, B. Comparison of Quercetin Pharmacokinetics Following Oral Supplementation in Humans. *J. Food Sci.* **2012**, *77*, H231–H238. [CrossRef] [PubMed]
10. McDonnell, A.M.; Dang, C.H. Basic Review of the Cytochrome P450 System. *J. Adv. Pract. Oncol.* **2013**, *4*, 263–268. [CrossRef] [PubMed]
11. Rastogi, H.; Jana, S. Evaluation of Inhibitory Effects of Caffeic acid and Quercetin on Human Liver Cytochrome P450 Activities. *Phytother. Res.* **2014**, *28*, 1873–1878. [CrossRef] [PubMed]
12. Korobkova, E.A. Effect of Natural Polyphenols on CYP Metabolism: Implications for Diseases. *Chem. Res. Toxicol.* **2015**, *28*, 1359–1390. [CrossRef] [PubMed]
13. Miron, A.; Aprotosoaie, A.C.; Trifan, A.; Xiao, J. Flavonoids as modulators of metabolic enzymes and drug transporters. *Ann. N. Y. Acad. Sci.* **2017**, *1398*, 152–167. [CrossRef] [PubMed]
14. Poór, M.; Boda, G.; Needs, P.W.; Kroon, P.A.; Lemli, B.; Bencsik, T. Interaction of Quercetin and Its Metabolites with Warfarin: Displacement of Warfarin from Serum Albumin and Inhibition of CYP2C9 Enzyme. *Biomed. Pharmacother.* **2017**, *88*, 574–581. [CrossRef]
15. Chang, T.K.H.; Chen, J.; Yeung, E.Y.H. Effect of Ginkgo Biloba Extract on Procarcinogen-Bioactivating Human CYP1 Enzymes: Identification of Isorhamnetin, Kaempferol, and Quercetin as Potent Inhibitors of CYP1B1. *Toxicol. Appl. Pharmacol.* **2006**, *213*, 18–26. [CrossRef]
16. Kimura, Y.; Ito, H.; Ohnishi, R.; Hatano, T. Inhibitory effects of polyphenols on human cytochrome P450 3A4 and 2C9 activity. *Food Chem. Toxicol.* **2010**, *48*, 429–435. [CrossRef]
17. Takemura, H.; Itoh, T.; Yamamoto, K.; Sakakibara, H.; Shimoi, K. Selective Inhibition of Methoxyflavonoids on Human CYP1B1 Activity. *Bioorgan. Med. Chem.* **2010**, *18*, 6310–6315. [CrossRef]
18. Johnson, E.J.; Won, C.S.; Köck, K.; Paine, M.F. Prioritizing pharmacokinetic drug interaction precipitants innatural products: Application to OATP inhibitors in grapefruitjuice. *Biopharm. Drug Dispos.* **2017**, *38*, 251–259. [CrossRef]
19. Yu, J.; Zhou, Z.; Tay-Sontheimer, J.; Levy, R.H.; Ragueneau-Majlessi, I. Intestinal Drug Interactions Mediated by OATPs: A Systematic Review of Preclinical and Clinical Findings. *J. Pharm. Sci.* **2017**, *106*, 2312–2325. [CrossRef]
20. Mandery, K.; Balk, B.; Bujok, K.; Schmidt, I.; Fromm, M.F.; Glaeser, H. Inhibition of hepatic uptake transporters by flavonoids. *Eur. J. Pharm. Sci.* **2012**, *46*, 79–85. [CrossRef]
21. Letschert, K.; Faulstich, H.; Keller, D.; Keppler, D. Molecular characterization and inhibition of amanitin uptake into human hepatocytes. *Toxicol. Sci.* **2006**, *91*, 140–149. [CrossRef] [PubMed]
22. Wang, J.; Gan, C.; Qi, X.; Lebre, M.C.; Schinkel, A.H. Human Organic Anion Transporting Polypeptide (OATP) 1B3 and Mouse OATP1A/1B Affect Liver Accumulation of Ochratoxin A in Mice. *Toxicol. Appl. Pharmacol.* **2020**, *401*, 115072. [CrossRef]

23. König, J.; Cui, Y.; Nies, A.T.; Keppler, D. A Novel Human Organic Anion Transporting Polypeptide Localized to the Basolateral Hepatocyte Membrane. *Am. J. Physiol. Gastrointest. Liver Physiol.* **2000**, *278*, G156–G164. [CrossRef] [PubMed]
24. Nakanishi, T.; Tamai, I. Genetic Polymorphisms of OATP Transporters and Their Impact on Intestinal Absorption and Hepatic Disposition of Drugs. *Drug Metab. Pharmacokinet.* **2012**, *27*, 106–121. [CrossRef] [PubMed]
25. Urquhart, B.L.; Kim, R.B. Blood-brain Barrier Transporters and Response to CNS active Drugs. *Eur. J. Clin. Pharmacol.* **2009**, *65*, 1063–1070. [CrossRef]
26. Shitara, Y.; Maeda, K.; Ikejiri, K.; Yoshida, K.; Horie, T.; Sugiyama, Y. Clinical Significance of Organic Anion Transporting Polypeptides (OATPs) in Drug Disposition: Their Roles in Hepatic Clearance and Intestinal Absorption. *Biopharm. Drug Dispos.* **2013**, *34*, 45–78. [CrossRef]
27. Wu, L.-X.; Guo, C.-X.; Qu, Q.; Yu, J.; Chen, W.-Q.; Wang, G.; Fan, L.; Li, Q.; Zhang, W.; Zhou, H.-H. Effects of natural products on the function of human organic anion transporting polypeptide 1B1. *Xenobiotica* **2011**, *42*, 339–348. [CrossRef]
28. Mandery, K.; Bujok, K.; Schmidt, I.; Keiser, M.; Siegmund, W.; Balk, B.; König, J.; Fromma, M.F.; Glaeser, H. Influence of the flavonoids apigenin, kaempferol, and quercetin on the function of organic anion transporting polypeptides 1A2 and 2B1. *Biochem. Pharmacol.* **2010**, *80*, 1746–1753. [CrossRef]
29. Glaeser, H.; Bujok, K.; Schmidt, I.; Fromm, M.F.; Mandery, K. Organic anion transporting polypeptides and organic cation transporter 1 contribute to the cellular uptake of the flavonoid quercetin. *Naunyn Schmiedebergs Arch. Pharmacol.* **2014**, *387*, 883–891. [CrossRef]
30. Duan, J.; Xie, Y.; Luo, H.; Li, G.; Wu, T.; Zhang, T. Transport characteristics of isorhamnetin across intestinal Caco-2 cell monolayers and the effects of transporters on it. *Food Chem. Toxicol.* **2014**, *66*, 313–320. [CrossRef]
31. Fuchikami, H.; Satoh, H.; Tsujimoto, M.; Ohdo, S.; Ohtani, H.; Sawada, Y. Effects of Herbal Extracts on the Function of Human Organic Anion-Transporting Polypeptide OATP-B. *Drug Metab. Dispos.* **2006**, *34*, 577–582. [CrossRef] [PubMed]
32. Roth, M.; Araya, J.J.; Timmermann, B.N.; Hagenbuch, B. Isolation of Modulators of the Liver-Specific Organic Anion-Transporting Polypeptides (OATPs) 1B1 and 1B3 From Rollinia Emarginata Schlecht (Annonaceae). *J. Pharmacol. Exp. Ther.* **2011**, *339*, 624–632. [CrossRef] [PubMed]
33. Szakács, G.; Váradi, A.; Ozvegy-Laczka, C.; Sarkadi, B. The Role of ABC Transporters in Drug Absorption, Distribution, Metabolism, Excretion and Toxicity (ADME-Tox). *Drug Discov. Today* **2008**, *13*, 379–393. [CrossRef] [PubMed]
34. Sarkadi, B.; Homolya, L.; Szakács, G.; Váradi, A. Human Multidrug Resistance ABCB and ABCG Transporters: Participation in a Chemoimmunity Defense System. *Physiol. Rev.* **2006**, *86*, 1179–1236. [CrossRef] [PubMed]
35. Jetter, A.; Kullak-Ublic, G.A. Drugs and hepatic transporters: A review. *Pharmacol. Res.* **2020**, *154*, 104234. [CrossRef] [PubMed]
36. Marquez, B.; Van Bambeke, F. ABC Multidrug Transporters: Target for Modulation of Drug Pharmacokinetics and Drug-Drug Interactions. *Curr. Drug Targets* **2011**, *12*, 600–620. [CrossRef]
37. Wlcek, K.; Stieger, B. ATP-binding Cassette Transporters in Liver. *Biofactors* **2013**, *40*, 188–198. [CrossRef]
38. Alvarez, A.I.; Real, R.; Pérez, M.; Mendoza, G.; Prieto, J.G.; Merino, G. Modulation of the Activity of ABC Transporters (P-glycoprotein, MRP2, BCRP) by Flavonoids and Drug Response. *J. Pharm. Sci.* **2010**, *99*, 598–617. [CrossRef]
39. Ahmed-Belkacem, A.; Pozza, A.; Muñoz-Martínez, F.; Bates, S.E.; Castanys, S.; Gamarro, F.; Di Pietro, A.; Pérez-Victoria, J.M. Flavonoid Structure-Activity Studies Identify 6-prenylchrysin and Tectochrysin as Potent and Specific Inhibitors of Breast Cancer Resistance Protein ABCG2. *Cancer Res.* **2005**, *65*, 4852–4860. [CrossRef]
40. Morris, M.E.; Zhang, S. Flavonoid-drug Interactions: Effects of Flavonoids on ABC Transporters. *Life Sci.* **2006**, *78*, 2116–2130. [CrossRef]
41. An, G.; Gallegos, J.; Morris, M.E. The Bioflavonoid Kaempferol Is an Abcg2 Substrate and Inhibits Abcg2-mediated Quercetin Efflux. *Drug Metab. Dispos.* **2011**, *39*, 426–432. [CrossRef] [PubMed]
42. Sesink, A.L.A.; Arts, I.C.W.; De Boer, V.C.J.; Breedveld, P.; Schellens, J.H.M.; Hollman, P.C.H.; Russel, F.G.M. Breast Cancer Resistance Protein (Bcrp1/Abcg2) Limits Net Intestinal Uptake of Quercetin in Rats by Facilitating Apical Efflux of Glucuronides. *Mol. Pharmacol.* **2005**, *67*, 1999–2006. [CrossRef] [PubMed]

43. Chabane, M.N.; Al Ahmad, A.; Peluso, J.; Muller, C.D.; Ubeaud-Séquier, G. Quercetin and naringenin transport across human intestinal Caco-2 cells. *J. Pharm. Pharmacol.* **2009**, *61*, 1473–1483. [CrossRef]
44. Van Zanden, J.J.; Van der Woude, H.; Vaessen, J.; Usta, M.; Wortelboer, H.M.; Cnubben, N.H.P.; Rietjens, I.M.C.M. The Effect of Quercetin Phase II Metabolism on Its MRP1 and MRP2 Inhibiting Potential. *Biochem. Pharmacol.* **2007**, *15*, 345–351. [CrossRef]
45. Moon, Y.J.; Morris, M.E. Pharmacokinetics and Bioavailability of the Bioflavonoid Biochanin A: Effects of Quercetin and EGCG on Biochanin A Disposition in Rats. *Mol. Pharm.* **2007**, *4*, 865–872. [CrossRef]
46. Needs, P.W.; Kroon, P.A. Convenient synthesis of metabolically important glucuronides and sulfates. *Tetrahedron* **2006**, *62*, 6862–6868. [CrossRef]
47. Fliszár-Nyúl, E.; Mohos, V.; Bencsik, T.; Lemli, B.; Kunsági-Máté, S.; Poór, M. Interactions of 7,8-Dihydroxyflavone with Serum Albumin as well as with CYP2C9, CYP2C19, CYP3A4, and Xanthine Oxidase Biotransformation Enzymes. *Biomolecules* **2019**, *9*, 655. [CrossRef]
48. Mohos, V.; Bencsik, T.; Boda, G.; Fliszár-Nyúl, E.; Lemli, B.; Kunsági-Máté, S.; Poór, M. Interactions of casticin, ipriflavone, and resveratrol with serum albumin and their inhibitory effects on CYP2C9 and CYP3A4 enzymes. *Biomed. Pharmacother.* **2018**, *107*, 777–784. [CrossRef]
49. Mohos, V.; Fliszár-Nyúl, E.; Ungvári, O.; Bakos, É.; Kuffa, K.; Bencsik, T.; Zsidó, B.Z.; Hetényi, C.; Telbisz, Á.; Özvegy-Laczka, C.; et al. Effects of chrysin and its major conjugated metabolites chrysin-7-sulfate and chrysin-7-glucuronide on cytochrome P450 enzymes, and on OATP, P-gp, BCRP and MRP2 transporters. *Drug Metab. Dispos.* **2020**. accepted. [CrossRef]
50. Patik, I.; Székely, V.; Német, O.; Szepesi, Á.; Kucsma, N.; Várady, G.; Szakács, G.; Bakos, É.; Özvegy-Laczka, C. Identification of Novel Cell-Impermeant Fluorescent Substrates for Testing the Function and Drug Interaction of Organic Anion Transporting Polypeptides, OATP1B1/1B3 and 2B1. *Sci. Rep.* **2018**, *8*, 2630. [CrossRef]
51. Bakos, É.; Német, O.; Patik, I.; Kucsma, N.; Várady, G.; Szakács, G.; Özvegy-Laczka, C. A Novel Fluorescence-Based Functional Assay for Human OATP1A2 and OATP1C1 Identifies Interaction between Third-Generation P-gp Inhibitors and OATP1A2. *FEBS J.* **2020**, *287*, 2468–2485. [CrossRef] [PubMed]
52. Székely, V.; Patik, I.; Ungvári, O.; Telbisz, Á.; Szakács, G.; Bakos, É.; Özvegy-Laczka, C. Fluorescent Probes for the Dual Investigation of MRP2 and OATP1B1 Function and Drug Interactions. *Eur. J. Pharm. Sci.* **2020**, *151*, 105395. [CrossRef] [PubMed]
53. Sarkadi, B.; Price, E.M.; Boucher, R.C.; Germann, U.A.; Scarborough, G.A. Expression of the Human Multidrug Resistance cDNA in Insect Cells Generates a High Activity Drug-Stimulated Membrane ATPase. *J. Biol. Chem.* **1992**, *267*, 4854–4858. [PubMed]
54. Bodó, A.; Bakos, E.; Szeri, F.; Váradi, A.; Sarkadi, B. The Role of Multidrug Transporters in Drug Availability, Metabolism and Toxicity. *Toxicol. Lett.* **2003**, *140*, 133–143. [CrossRef]
55. Ozvegy, C.; Litman, T.; Szakács, G.; Nagy, Z.; Bates, S.; Váradi, A.; Sarkadi, B. Functional Characterization of the Human Multidrug Transporter, ABCG2, Expressed in Insect Cells. *Biochem. Biophys. Res. Commun.* **2001**, *285*, 111–117. [CrossRef]
56. Ozvegy, C.; Váradi, A.; Sarkadi, B. Characterization of Drug Transport, ATP Hydrolysis, and Nucleotide Trapping by the Human ABCG2 Multidrug Transporter. Modulation of Substrate Specificity by a Point Mutation. *J. Biol. Chem.* **2002**, *277*, 47980–47990. [CrossRef]
57. Telbisz, A.; Müller, M.; Ozvegy-Laczka, C.; Homolya, L.; Szente, L.; Váradi, A.; Sarkadi, B. Membrane Cholesterol Selectively Modulates the Activity of the Human ABCG2 Multidrug Transporter. *Biochim. Biophys. Acta* **2007**, *1768*, 2698–2713. [CrossRef]
58. Nguyen, M.A.; Staubach, P.; Wolffram, S.; Langguth, P. The Influence of Single-Dose and Short-Term Administration of Quercetin on the Pharmacokinetics of Midazolam in Humans. *J. Pharm. Sci.* **2015**, *104*, 3199–3207. [CrossRef]
59. Kim, K.-A.; Park, P.-W.; Park, J.-Y. Short-term Effect of Quercetin on the Pharmacokinetics of Fexofenadine, a Substrate of P-glycoprotein, in Healthy Volunteers. *Eur. J. Clin. Pharmacol.* **2009**, *65*, 609–614. [CrossRef]
60. Nguyen, M.A.; Staubach, P.; Wolffram, S.; Langguth, P. Effect of single-dose and short-term administration of quercetin on the pharmacokinetics of talinolol in humans-Implications for the evaluation of transporter-mediated flavonoid-drug interactions. *Eur. J. Pharm. Sci.* **2014**, *61*, 54–60. [CrossRef]
61. He, N.; Xie, H.-G.; Collins, X.; Edeki, T.; Yan, Z. Effects of individual ginsenosides, ginkgolides and flavonoids on cyp2c19 and cyp2d6 activity in human liver microsomes. *Clin. Exp. Pharmacol. Physiol.* **2006**, *33*, 813–815. [CrossRef] [PubMed]

62. Cao, L.; Kwara, A.; Greenblatt, D.J. Metabolic interactions between acetaminophen (paracetamol) and two flavonoids, luteolin and quercetin, through in-vitro inhibition studies. *J. Pharm. Pharmacol.* **2017**, *69*, 1762–1772. [CrossRef] [PubMed]
63. Sharma, R.; Gatchie, L.; Williams, I.S.; Jain, S.K.; Vishwakarma, R.A.; Chaudhuri, B.; Bharate, S.B. Glycyrrhiza glabra extract and quercetin reverses cisplatin resistance in triple-negative MDA-MB-468 breast cancer cells via inhibition of cytochrome P450 1B1 enzyme. *Bioorg. Med. Chem. Lett.* **2017**, *27*, 5400–5403. [CrossRef]
64. Ekstrand, B.; Rasmussen, M.K.; Woll, F.; Zlabek, V.; Zamaratskaia, G. In Vitro Gender-Dependent Inhibition of Porcine Cytochrome P450 Activity by Selected Flavonoids and Phenolic Acids. *BioMed Res. Int.* **2015**, *2015*, 387918. [CrossRef]
65. Östlund, J.; Zlabek, V.; Zamaratskaia, G. In vitro inhibition of human CYP2E1 and CYP3A by quercetin and myricetin in hepatic microsomes is not gender dependent. *Toxicology* **2017**, *381*, 10–18. [CrossRef] [PubMed]
66. Bojic, M.; Kondža, M.; Rimac, H.; Benkovic, G.; Maleš, Ž. The Effect of Flavonoid Aglycones on the CYP1A2, CYP2A6, CYP2C8 and CYP2D6 Enzymes Activity. *Molecules* **2019**, *24*, 3174. [CrossRef] [PubMed]
67. Bedada, S.K.; Neerati, P. Evaluation of the Effect of Quercetin Treatment on CYP2C9 Enzyme Activity of Diclofenac in Healthy Human Volunteers. *Phytother. Res.* **2018**, *32*, 305–311. [CrossRef]
68. Mohos, V.; Pánovics, A.; Fliszár-Nyúl, E.; Schilli, G.; Hetényi, C.; Mladěnka, P.; Needs, P.W.; Kroon, P.A.; Pethő, G.; Poór, M. Inhibitory Effects of Quercetin and Its Human and Microbial Metabolites on Xanthine Oxidase Enzyme. *Int. J. Mol. Sci.* **2019**, *20*, 2681. [CrossRef]
69. Janisch, K.M.; Williamson, G.; Needs, P.; Plumb, G.W. Properties of Quercetin Conjugates: Modulation of LDL Oxidation and Binding to Human Serum Albumin. *Free Radic. Res.* **2004**, *38*, 877–884. [CrossRef]
70. Wong, C.C.; Akiyama, Y.; Abe, T.; Lippiat, J.D.; Orfila, C.; Williamson, G. Carrier-mediated transport of quercetin conjugates: Involvement of organic anion transporters and organic anion transporting polypeptides. *Biochem. Pharmac.* **2012**, *84*, 564–570. [CrossRef]
71. Notas, G.; Nifli, A.-P.; Kampa, M.; Pelekanou, V.; Alexaki, V.-I.; Theodoropoulos, P.; Vercauteren, J.; Castanas, E. Quercetin accumulates in nuclear structures and triggers specific gene expression in epithelial cells. *J. Nutr. Biochem.* **2012**, *23*, 656–666. [CrossRef] [PubMed]
72. O'Leary, K.A.; Day, A.J.; Needs, P.W.; Mellon, F.A.; O'Brien, N.M.; Williamson, G. Metabolism of quercetin-7- and quercetin-3-glucuronides by an in vitro hepatic model: The role of human β-glucuronidase, sulfotransferase, catechol-O-methyltransferase and multi-resistant protein 2 (MRP2) in flavonoid metabolism. *Biochem. Pharmacol.* **2003**, *65*, 479–491. [CrossRef]
73. Wu, L.-X.; Guo, C.-X.; Chen, W.-Q.; Yu, J.; Qu, Q.; Chen, Y.; Tan, Z.-R.; Wang, G.; Fan, L.; Li, Q.; et al. Inhibition of the organic anion-transporting polypeptide 1B1 by quercetin: An in vitro and in vivo assessment. *Br. J. Clin. Pharmacol.* **2011**, *73*, 750–757. [CrossRef] [PubMed]
74. Chen, C.; Zhou, J.; Ji, C. Quercetin: A Potential Drug to Reverse Multidrug Resistance. *Life Sci.* **2010**, *87*, 333–338. [CrossRef] [PubMed]
75. Rozanski, M.; Studzian, M.; Pulaski, L. Direct Measurement of Kinetic Parameters of ABCG2-Dependent Transport of Natural Flavonoids Using a Fluorogenic Substrate. *J. Pharmacol. Exp. Ther.* **2019**, *371*, 309–319. [CrossRef] [PubMed]
76. Williamson, G.; Aeberli, I.; Miguet, L.; Zhang, Z.; Sanchez, M.-B.; Crespy, V.; Barron, D.; Needs, P.; Kroon, P.A.; Glavinas, H.; et al. Interaction of Positional Isomers of Quercetin Glucuronides With the Transporter ABCC2 (cMOAT, MRP2). *Drug Metab. Dispos.* **2007**, *35*, 1262–1268. [CrossRef]
77. Youdim, K.A.; Qaiser, M.Z.; Begley, D.J.; Rice-Evans, C.A.; Abbott, N.J. Flavonoid Permeability Across an in Situ Model of the Blood-Brain Barrier. *Free Radic. Biol. Med.* **2004**, *36*, 592–604. [CrossRef]
78. Zhang, S.; Yang, X.; Morris, M.E. Flavonoids Are Inhibitors of Breast Cancer Resistance Protein (ABCG2)-mediated Transport. *Mol. Pharmacol.* **2004**, *65*, 1208–1216. [CrossRef]